AD NUMBER

AD834262

NEW LIMITATION CHANGE

TO

Approved for public release, distribution unlimited

FROM

Distribution authorized to U.S. Gov't. agencies and their contractors; Critical Technology; FEB 1968. Other requests shall be referred to Naval Air Systems Command, Arlington, VA.

AUTHORITY

NAVAIR ltr, 12 Apr 1976

[redacted]

BOEING

VERTOL DIVISION

D8-0911

A PARAMETRIC STUDY OF SWIRL INLET PARTICLE SEPARATORS

Final Report

February 1968

by

Richard Darling

Prepared under Contract NOw 66-0562c for the Naval Air Systems Command, Department of the Navy, by The Boeing Company, Vertol Division, Philadelphia, Pennsylvania

SUMMARY

The Boeing Company, Vertol Division, conducted a parametric study of particle separators for gas-turbine-powered VTOL aircraft. This report, presenting the results of that study, includes a brief review of the present state of separator technology, together with an examination of the factors affecting inlet separator design. The factors considered are: types of foreign object damage associated with gas turbines; design features incorporated or possible to avoid engine damage; effect on foreign object ingestion of the engine location relative to the airflow pattern around the aircraft; and effect of the engine drive arrangement on possible particle separator configurations.

Extensive analytical work was carried out in determining the characteristics of the Boeing inertial (swirl) separator. Airflow data were obtained from two-dimensional electrical analog plots and fed into a digital computer program which calculated the trajectories of typical particles entering the inlet. A large number of these trajectories (almost 4000) were calculated, representing data for seven inlet configurations and several basic inlet types. By modifying the inlet contours, two optimized inlets were achieved for #70 sand ingested at the maximum airflow for the G.E. T58 engine. One of these inlets was optimized for downwash, the other for no-downwash conditions.

The separation efficiencies of the various inlet configurations were estimated for various particle sizes and size distributions at both design and off-design airflow conditions by counting the number of particles separated from the ingested particles. These data were compared with experimental (bench test) separation data for similar inlets; agreement was good.

Based on the computed particle trajectories, the effects of several parameters on particles entering the inertial separator were determined. The parameters considered were: percent trap airflow; total airflow; individual particle specific gravity; presence or absence of downwash; particle diameter; particle/wall resilience; and particle initial position and velocity. The effects of these parameters on future inertial separator design were also discussed, and special consideration was given to their effects on aircraft designed for ASW or desert operations.

Recommendation is made for three future courses of action: (1) to obtain a larger quantity of both experimental and analytical data on geometrically similar inlets, so that accurate comparison can be made between these two methods of gathering data, (2) to use the present analytical methods to gather data on a larger variety of basic inlet types, the method being

applicable, in principle, to any inertial separator which does not utilize large amounts of swirl, and (3) to modify the present analytical method to create a rapid and efficient design method for future inlet development.

TABLE OF CONTENTS

LIST OF ILLUSTRATIONS

LIST OF TABLES

LIST OF SYMBOLS

A - area square feet or square inches

d - particle diameter, inches

F - force (drag, inertial, etc.)

k - proportionality constant

K - coefficient of restitution for particle wall collisions

m - mass flow, pounds per second

r - radial coordinate of a point in the inlet (r = 0 at centerline), inches

t - time, seconds

u - axial velocity component, feet per second

v - radial velocity component, feet per second

V - total velocity, feet per second

x - axial coordinate, inches (x = 0 at inlet throat)

α - velocity scale factor to convert electrical analog data to actual inlet velocities

Δ - an increment in some variable (as in $\Delta t = t_2 - t_1$)

∇ - differential operator

ε - bounce parameter, inches

θ - circumferential coordinate, radians

μ - microns

ρ - density

ϕ - electrical potential, volts

ψ - stream function

INTRODUCTION

NATURE OF THE PARTICLE SEPARATION PROBLEM

A particle separation problem is generally encountered whenever a gas-turbine-powered helicopter or VTOL aircraft is operated near the ground or water. Debris, dirt, dust, water, and the like are kicked up by downwash from the rotors or fans and recirculated throughout the airflow pattern surrounding the vehicle. Some of this foreign material will enter the inlets, continue into the engine, and eventually cause damage of some significant severity. The amount of material ingested depends on many factors among which are the engine location; the inlet design; the engine airflow; the presence of other aircraft in the vicinity the amount and severity of damage are, again, functions of several variables among which are: type of engine; type of foreign material; time during which material is ingested; and the local operating conditions. Damage may be due to direct impact of foreign objects on engine structure, airflow blockage, thermal distortion of the compressor due to water, compressor corrosion due to saltcarrying sprays, compressor fouling, or compressor erosion. The materials causing this damage include birds, nuts, bolts, stones, ice, grass, water, saltwater, oil, soot, dust, and sand. The degree of damage ranges from the negligible coating or polishing of the compressor blades to the immediate failure of the engine from wedging of some large foreign object between rotor and stator, or from severe impact damage to an early compressor stage. Prolonged hover over sand appears to be the worst flight condition. The damage in this case occurs through erosion of the compressor blades and stators. In general, the worst flight conditions (hover, low-altitude, low-speed flight, landing on unimproved fields), in terms of foreign object damage (FOD) to the engine are exactly those in which the helicopter and VTOL aircraft are clearly superior to the conventional aircraft. To take advantage of this superiority, adequate means must be found to protect engines and other propulsion components from damage caused by the airborne foreign objects inherent in these environments. Engines must be protected from large flying debris, and methods must be provided for separating smaller debris, dirt, dust, and the like from the inlet air stream.

PRESENT SEPARATION METHODS

Two basic types of particle separators are being used to protect helicopter gas-turbine engines. The barrier type is basically a simple filter of the wet or dry type, similar to that most commonly used on reciprocating engines. These provide very good protection (nearly 100 percent) over a wide range of particle sizes, and, when clean, have good pressure

loss characteristics (99 percent pressure recovery).

Development work on this type filter is very advanced at present. There are substantial disadvantages inherent in the barrier filter when applied to helicopter gas turbines. Perhaps the most important of these is the fact that the barrier filter is not a self-cleaning device. In addition, an alternate, open-door inlet must usually be provided for use in icing or emergency conditions.

The other basic type of separator currently under development for helicopters is the inertial type. The operation of this separator is based on the principle that solid particles will tend to travel in a straight line when the airstream in which they are carried is turned suddenly. The particles tend to concentrate in the outer portion of the turning airstream and can then be skimmed off by appropriate scoops or traps. Three different types of inertial separators have been considered by the gas-turbine helicopter industry. The first of these sends the air around a sharp turn as it enters the inlet, skims off the particle-laden portion of air, and cleans it by passing it through a labyrinth and filter. The cleaned air then returns to the main airstream. The ~~Donaldson~~ second separator consists of a large number of vortex tubes mounted axially in the airstream. As the air enters these tubes it is swirled, and any solid particles are thus forced to the outside of each vortex where they are skimmed off by a scavenging system. The clean vortex core air passes straight through to the engine inlet. The tubes range from 3 to 6 inches in length and large banks are needed to clean the air for the typical gas turbine. The third is similar to the second except that it uses only one vortex tube through which all the engine airflow must pass.

A third type of inertial separator, with which this report will be most concerned, is the Boeing inertial (or swirl) separator. In this separator particles are accelerated as they pass through the inlet throat so that they will tend to follow a straight line, while the air is turned suddenly to pass around a centerbody a short distance downstream of the throat. The centerbody (or trap) is cup-shaped with the open end facing upstream, and is scavenged by a blower. Five to ten percent of the total airflow is removed in the trap. In the optimized separator of this type, all particles entering the inlet would be either bounced or aerodynamically forced into the trap.

The separation efficiency of the inertial separators (all types mentioned) is in the range 80 to 95 percent, depending to some extent on particle size, while the pressure recovery

is typically 97 to 99 percent. All types mentioned can be made self-cleaning. The use of scavenge air in the Boeing and other inertial separators requires additional ducting and additional power for a blower, but these requirements do not appear to be critical in terms of payload or power loss.

SCOPE OF PRESENT STUDY

The analytical work described in this report is limited to the Boeing-type inertial separator. The study was designed to fulfill the requirements of the subject contract by providing information leading to more efficient separator design. The approach, as outlined in the contract, was to determine the effects on particle separation of several parametric changes in both the inlet and the incident particles. Several of these effects were isolated and are described in later sections. Included are considerations of: percent of secondary flow; presence or absence of a bounce plate; variations in throat diameter; particle resiliency; particle size; presence or absence of downwash; primary flow area; and total airflow.

In addition to the parametric information, this study also provides information on the nature of the particle separation problem itself. Discussion covers such topics as: the difficulty in separating heavy particles by aerodynamic means alone; difficulty in separating light dust by inertial means alone; and the importance of downwash as a factor in separator design. These are general considerations which must be taken into account in the choice or design of a separator for a given mission and, as such, are relevant to the subject contract.

The report also presents in detail a description of the methods used to carry out the parametric inlet study. It discusses the advantages and disadvantages of these methods and the estimated accuracy of the answers obtained, and suggests improvements for future uses of the same basic method.

FACTORS AFFECTING INLET SEPARATOR DESIGN

A study of the factors affecting inlet separator design was presented in the second Quarterly Progress Report[1]. Significant items from this report are included in the following paragraphs.

Engine resistance to FOD is directly related to several factors. Included are: engine airflow rate per unit of frontal area, compressor tip speed, and compressor blade thickness, shape, and material. For engines of similar technology, ingesting the same size particles will have a more pronounced effect on smaller engines.

EFFECT OF FOREIGN OBJECTS ON ENGINE OPERATION

The effects of FOD on a turbine engine are characterized as follows:

1. Direct Impact Damage - Direct impact damage is usually inflicted upon the front frame, inlet guide vanes, and/or first-stage compressor rotor blades. This damage is caused by large hard objects such as birds, hardware, stones, ice, and so forth. Further damage in later stages may also occur from these objects. Direct impact damage is likely to cause engine surge or stall, particularly in the smaller helicopter turbine engines.

2. Induction Airflow Blockage - Blockage can be caused by grass accumulation, ice buildup, etc. Compressor blade stall due to severe flow directional changes through the inlet ducting may result. In the less severe condition, the blockage will result in increased duct losses and engine power loss.

3. Compressor Mechanical Distortion - Compressor thermal distortion resulting in compressor rubbing can be caused by the ingestion of large quantities of water. In addition, compressor surge or engine flameout can occur during water ingestion.

4. Component Corrosion - Corrosion can result through ingestion of salt water and spray.

5. Compressor Fouling - Fouling may result from the ingestion of adhering types of foreign material such as oil, soot, smoke, dust, and/or other fine matter.

6. Compressor Erosion - Erosion by sand and dust in the compressor stages will cause engine power deterioriation and may result in sudden engine stall.

DESIGN FEATURES TO AVOID DAMAGE

Turbine engine design features which reduce the effects of FOD are discussed as follows:

1. Direct Impact Damage - Induction air ducting to the compressor may provide some protection from impact damage, particularly where the ducting causes the air to turn (Figure 1). The use of an annular inlet is advisable because the inner hub causes deflection of foreign bodies. The annular inlet with large hub-to-inside-diameter ratio limits the size of ingested objects. Figure 1 also illustrates a rear inlet engine. This type of engine inlet has an inherent capability to separate foreign particles by turning the airflow into the inlet.

   Inlet guide vanes provide the next stage of impact protection. The guide vanes can block direct entry into the compressor by large objects and will absorb the impact energy of smaller objects. Foreign objects may break upon striking the guide vanes. Inlet guide vanes should be strong and ductile to absorb energy; compressor blades should be capable of absorbing impact from small foreign objects.

   Because of the deflection of the blades during foreign object ingestion, adequate spacing between stages is an important design feature for FOD prevention. Clearance between inlet guide vanes and the first stage rotor is also important in preventing wedging damage from objects which pass through the guide vanes.

   Shrouding of compressor blades is an additional engine characteristic which is helpful in providing mechanical integrity.

2. Induction Airflow Blockage - Blockage of induction airflow by materials such as grass and ice should be prevented. The engine inlet ducting should contain a system (screens, guard, etc.) designed to prevent material accumulation.

3. Mechanical Distortion - Mechanical distortion such as that resulting in vane case rubbing can be prevented by increasing rotor tip clearances (with some loss in compressor efficiency) or by stopping the foreign material before it reaches the compressor.

4. Compressor Corrosion - The ingestion of salt water and salt spray can be reduced by use of a particle separator designed to remove water. Corrosion effects on the compressor can be reduced by using corrosion-resistant

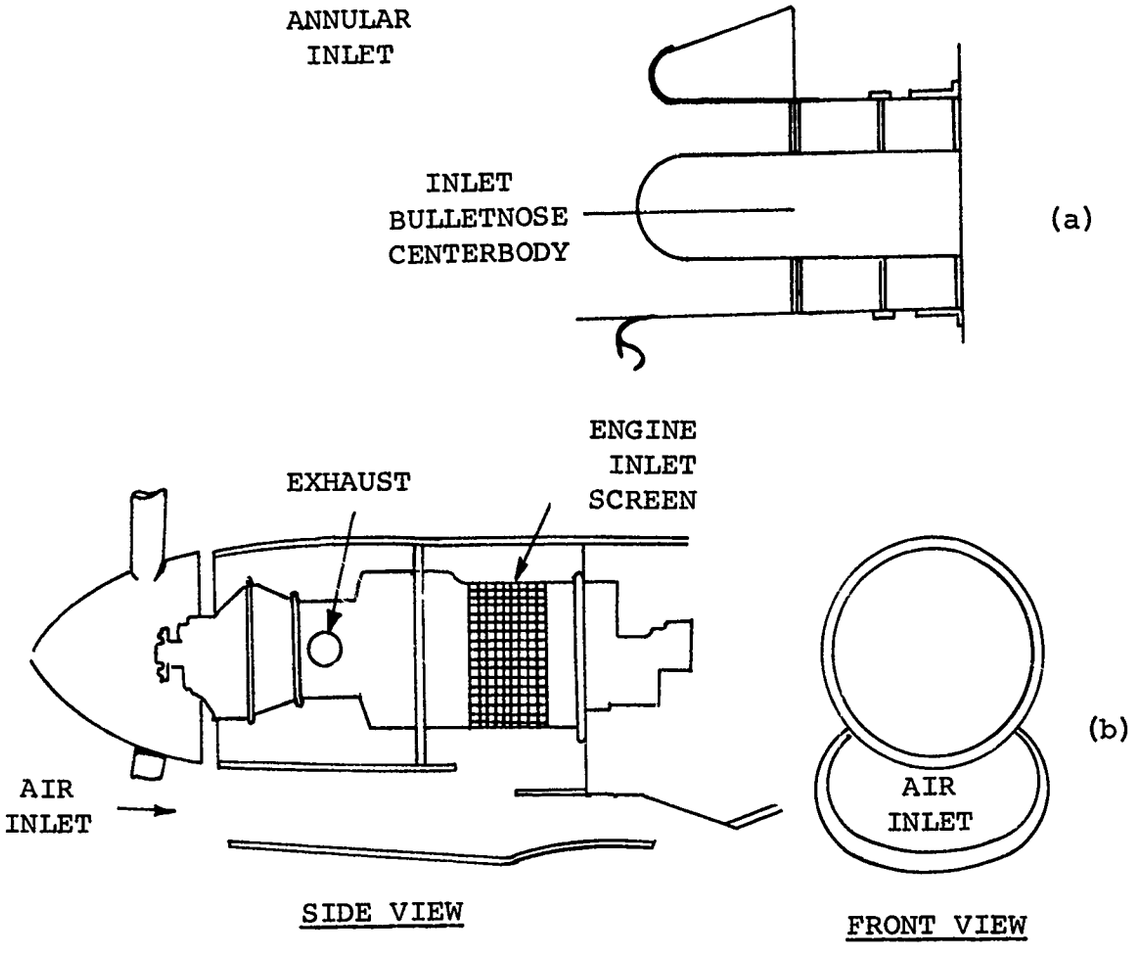

Figure 1. Typical Engine Inlet Characteristics

materials or phenolic coatings. Water washing of the engines followed by the application of corrosion preventive is also important.

5. Compressor Fouling - Compressor fouling is difficult to prevent by engine design or by the use of separators due to the fine nature of the materials which cause fouling. Water washing and the use of mild abrasives are helpful in keeping the compressor clean.

6. Compressor Erosion - Compressor erosion caused by sand and dust results in power loss and engine compressor stall. Engine design aspects for the prevention of such erosion include blade and vane construction and basic design and construction of the compressor. Larger and thicker blades tend to have greater life because of the greater mass of blade material. Blade erosion most often appears on the leading edges of the forward rotor stages and on the trailing edges of the later stage vanes. Strengthening of these components would improve resistance to FOD in most engines. An important aspect of erosion involves the centrifugal effect of the compressor on sand particles. Blade erosion at the blade tips is greater in the later stages. Performance degradation is accentuated by the smaller size of later stage rotor and stator vanes. Centrifugal compressors generally withstand greater amounts of erosion because of heavier construction and lower blade speeds.

EFFECT OF ENGINE LOCATION RELATIVE TO EXTERNAL AIRFLOW CHARACTERISTICS

Figure 2 illustrates Navy experience[2] with single-rotor helicopters hovering over water. The effect of wind on particle ingestion is important. With 8-knot winds, recirculation of rotor downwash carries sea salt into the engines. An interesting aspect of this condition is the path of the rotor blade tip vortexes. These vortexes move downward and outward with the outermost portion of the rotor wash. During hover with an 8-knot wind, the vortexes continue downward to the surface of the ocean entraining additional moisture. Hovering into 20-knot winds results in no recirculation of the downwash; rotor downwash and spray are carried aft.

Little information is presently available concerning optimum inlet location. Pod-mounted engines appear to ingest less foreign matter. This is believed to be the result of a tendency for particles to be swept past the inlets due to the rotor wash. Fuselage-mounted engines seem to be exposed to greater quantities of foreign particles from the interaction of the fuselage with the downwash. Locations for engine inlets for a

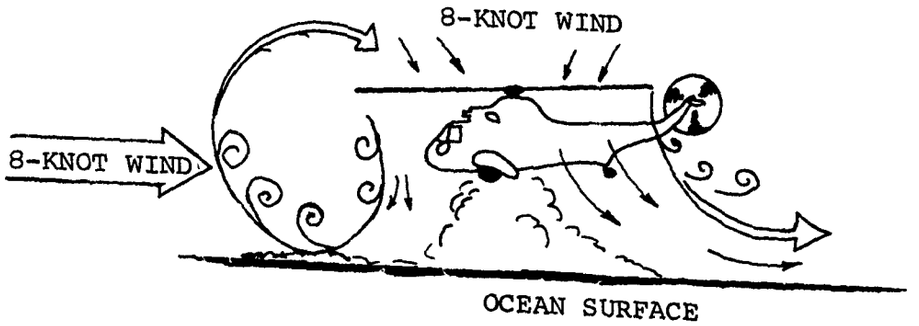

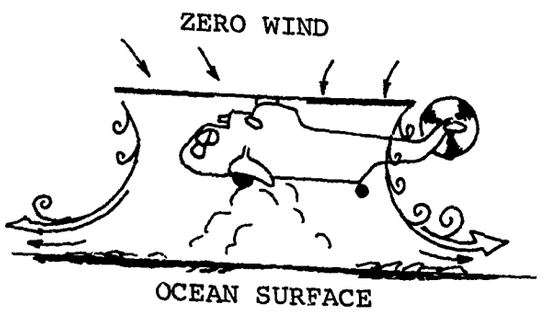

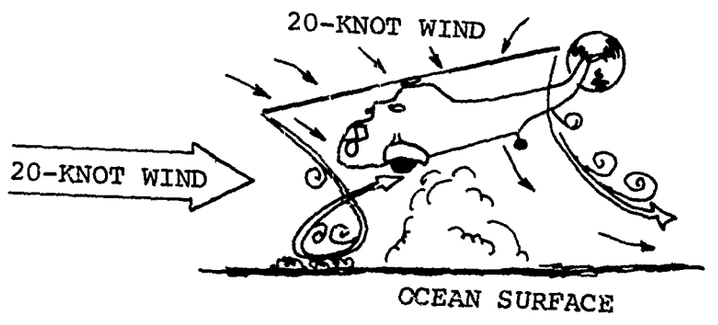

Figure 2. Typical Airflow Surrounding a Helicopter

ducted-propeller aircraft have been studied by the Kellett Aircraft Corporation[3]. Six potential inlet locations for the X-22 aircraft were studied for ingestion characteristics from the downwash patterns near the fuselage (Figures 3 and 4). The results of this investigation show the general advisability of fuselage-mounted inlets under the nose of the aircraft. Although this location may have been optimum for the aircraft studied, it does not necessarily apply to other configurations.

EFFECT OF ENGINE DRIVE ARRANGEMENT ON SEPARATOR CONFIGURATION

Engine drive arrangement has been studied with regard to the characteristics of a foreign particle separator. Figure 5 illustrates a separator configuration for a front-drive engine[4]. The inlet has been placed ahead of the transmission. Length and shape of this type of separator make the attainment of good pressure-drop characteristics difficult. This arrangement also incurs penalties with respect to weight and anti-icing design. A separator of this type has been tested in an environment with no downwash. Good separation and fair pressure-drop characteristics were obtained. Current trends in effective separator design with downwash involve increased inlet velocity and improved bounce-plate design. Since high inlet velocities require more exacting duct design, low pressure drop and high separation efficiency with this separator would be more difficult to obtain.

Figure 6 shows a separator arrangement for rear-drive engines. Rear drive permits more freedom in separator design, because there are no design restraints due to shafting and transmissions. Figure 7 shows another arrangement for front-drive engines which has been proposed for a Boeing STOL vehicle. The duct arrangement in this type of design is critical, since it influences separator frontal area and increases the primary airflow cross section. Redirection of the inlet airflow in this arrangement makes the duct design more difficult than for the separators illustrated in Figures 5 and 6.

Figure 8 depicts other separators which are used on front- and rear-drive engines. Scheme 3 and scheme 4 represent separators that are applicable to all engines. Both separators rotate the airflow. Scheme 3 employs a motor-driven rotating screen. The Scheme 3 separator employs rotation of the inlet airflow to cause particle separation. This rotation, as in the scheme 4 separator, centrifuges sand and dust to the outside of the separator. A scavenging airflow drawn from the tube wall extracts the airflow carrying the sand. The scheme 5 separators, which are small, individual units, are assembled into banks in order to supply the engines with adequate airflow.

The scheme 6 separator[5] uses a sharp turn to the inlet airflow with a skimmer on the outside wall to carry away the foreign objects. This separator can be front- or rear-drive mounted.

It is evident from this brief study that duct loss factors allow better separator designs when the engine inlet is separate from the engine drive. Forward-facing engine inlets are advantageous for the same reason.

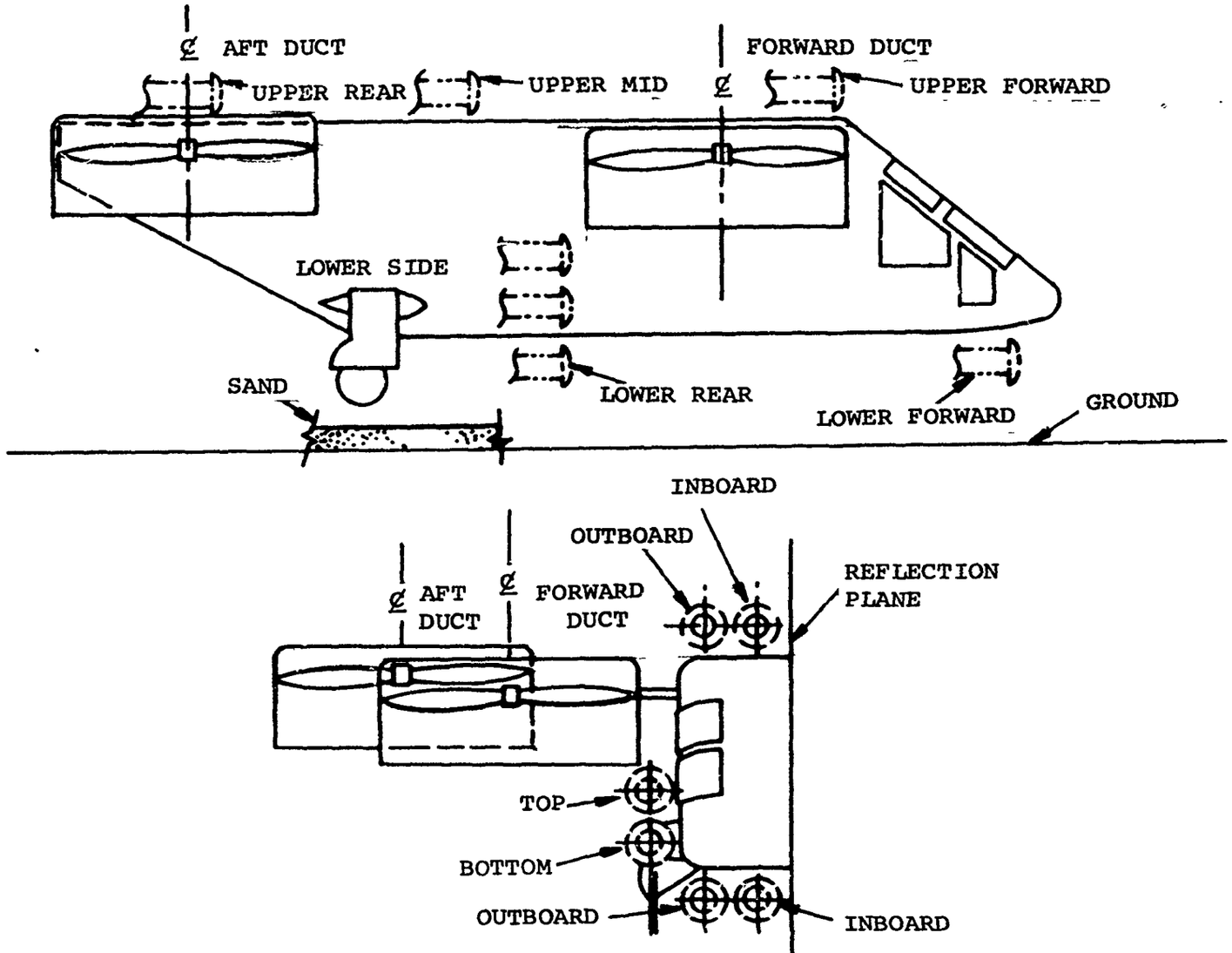

Figure 3. Possible Engine Inlet Locations on a Ducted-Propeller Aircraft

DISC LOADING
50 POUNDS PER SQUARE FOOT

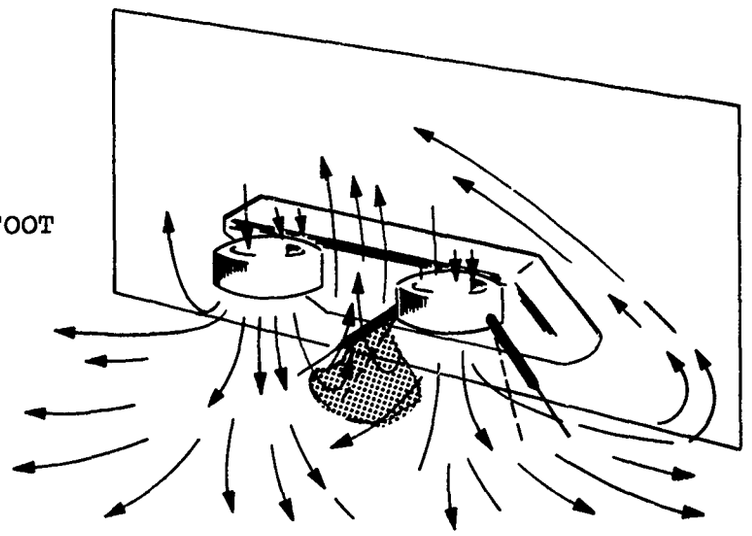

DISC LOADING
40 POUNDS PER SQUARE FOOT

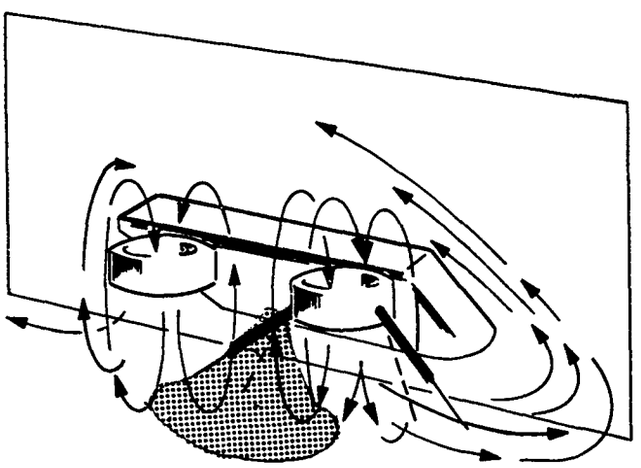

DISC LOADING
20 POUNDS PER SQUARE FOOT

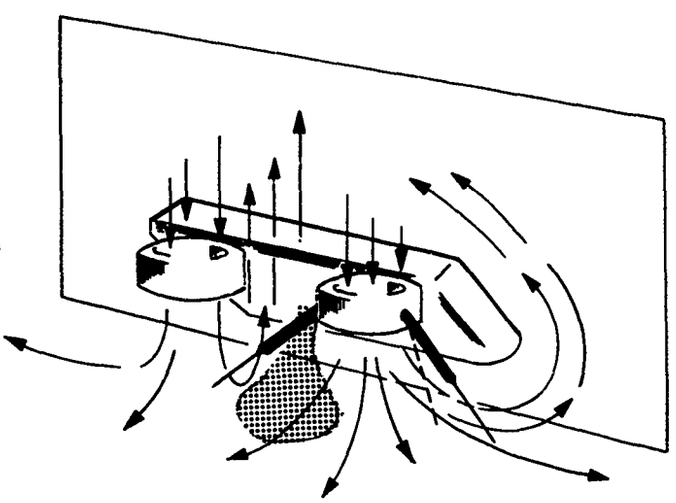

Figure 4. Downwash Patterns of a Ducted-Propeller Aircraft

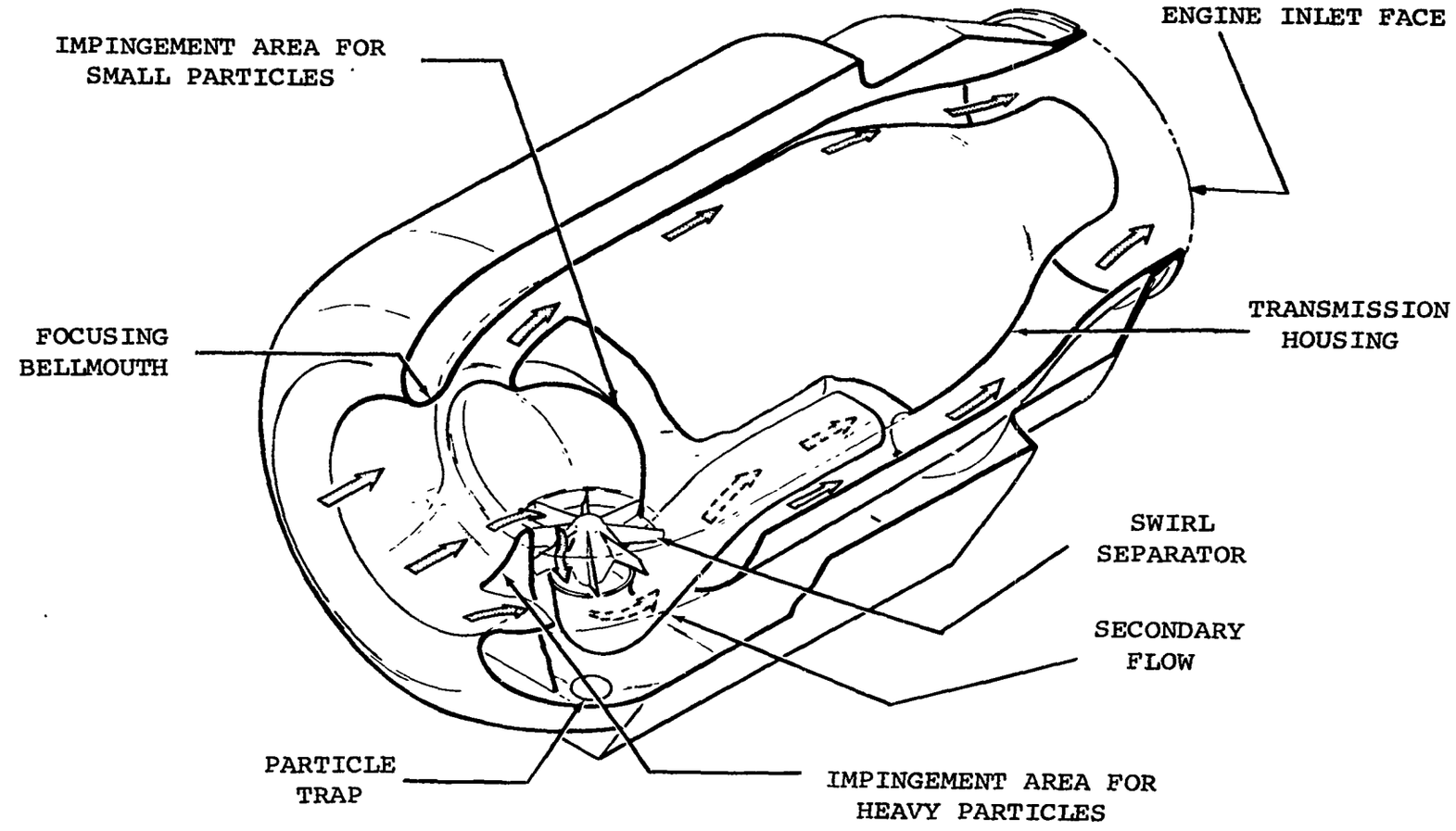

Figure 5. Particle Separator for a Front-Drive Turboshaft Engine with Integral Transmission

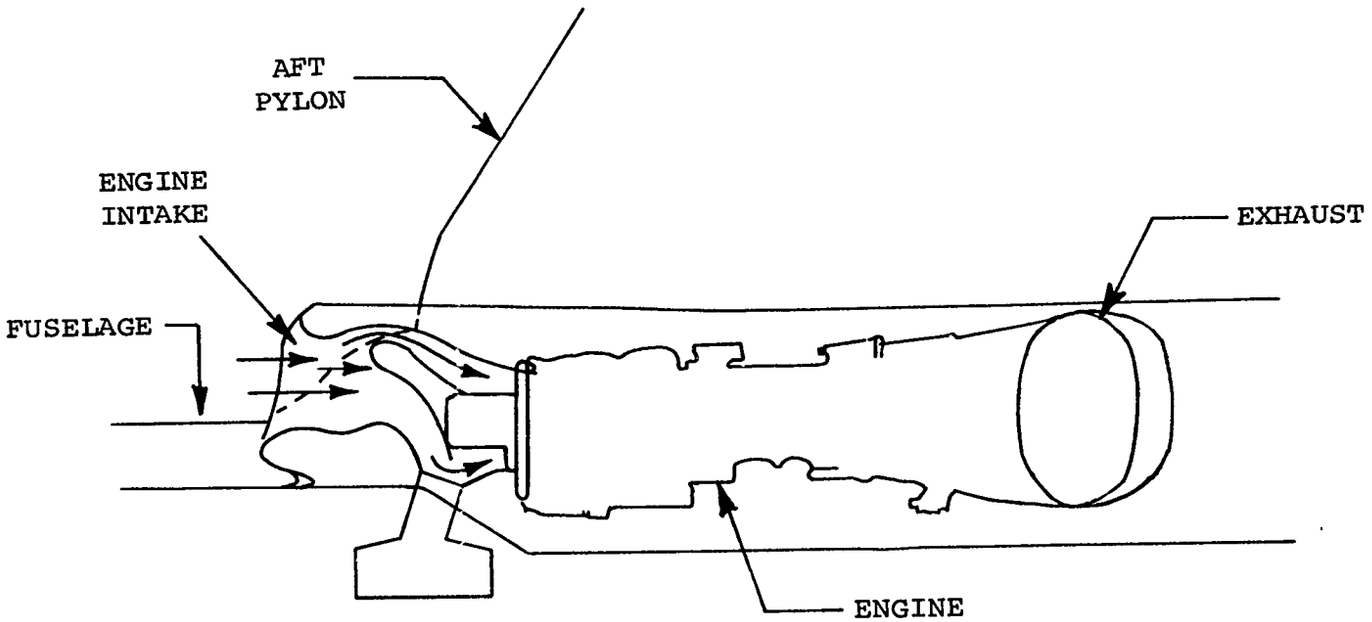

Figure 6. Particle Separator for a Rear-Drive Turboshaft Engine

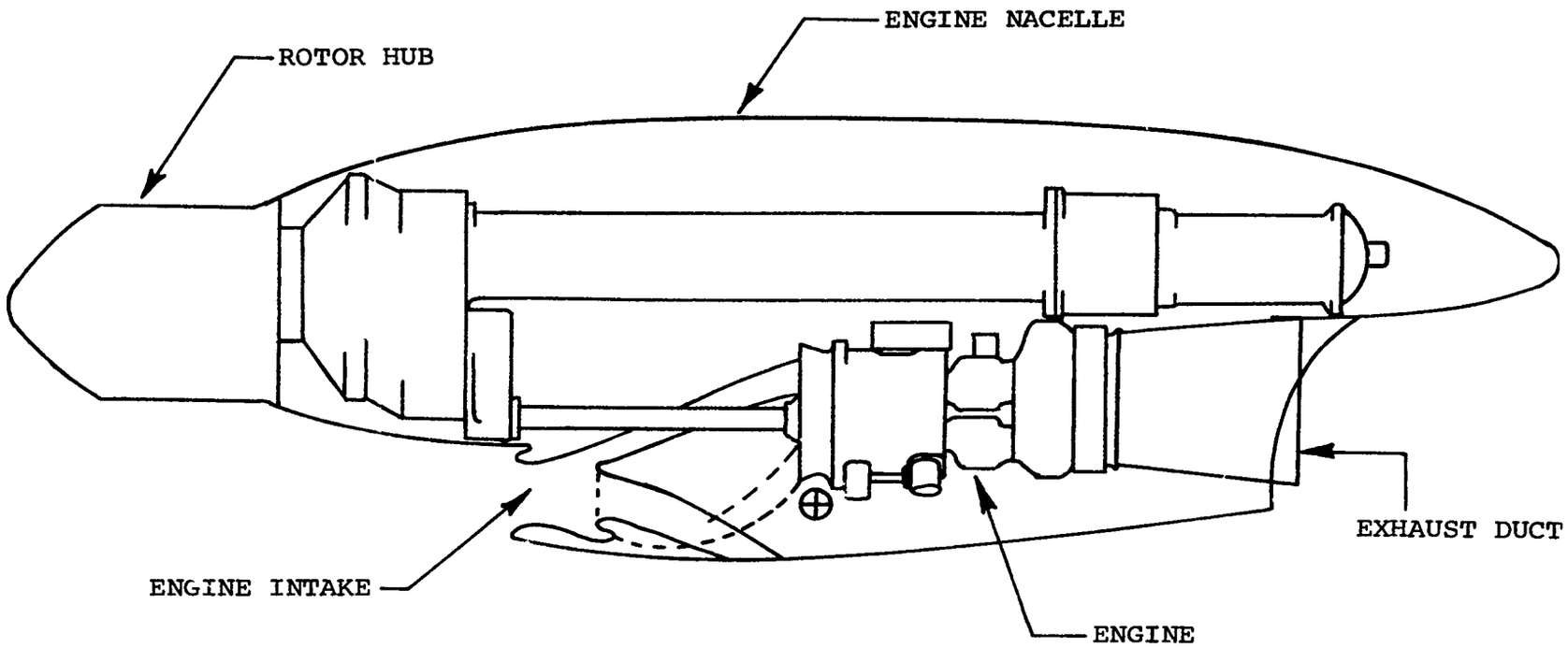

Figure 7. Particle Separator for a Front-Drive Turboshaft Engine

SCHEME 1

FULL BARRIER FILTER

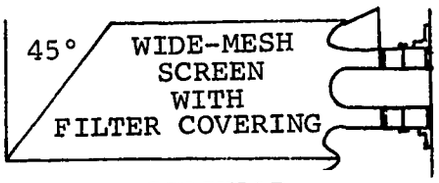

CIRCULAR
CROSS SECTION

SCHEME 2

BOEING INERTIAL SEPARATOR

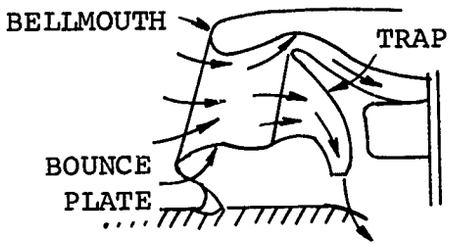

SECONDARY FLOW
DUMPED OVERBOARD

SCHEME 3

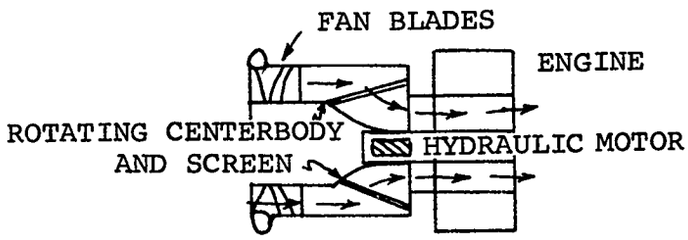

SCHEME 4

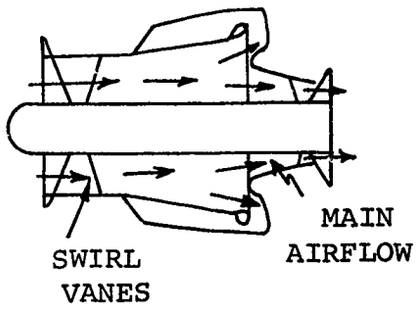

SCHEME 5

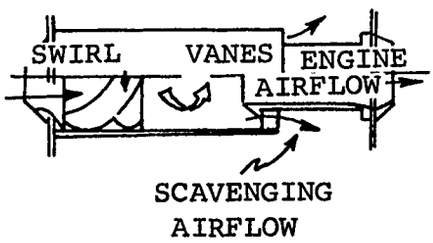

SCHEME 6

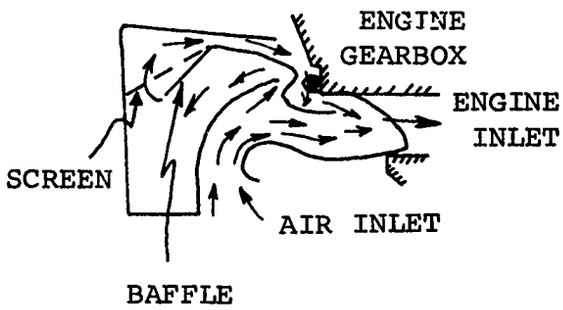

Figure 8. Particle Separator Designs in Current Use

PARAMETRIC STUDY OF TWO-DIMENSIONAL SEPARATORS AT DESIGN AND OFF-DESIGN CONDITIONS

DEFINITION OF PROBLEM

This portion of the contract called for a study in which two-dimensional electrical analog and digital computer data would be used to determine the trajectories of particles entering the separator inlet. These data were then to be used to determine the effects of several varying parameters on particle separation, and for the optimization of several inlet designs. The inlet parameters to be considered specifically were:

1. Inlet shape
2. Inlet length
3. Trap shape and location
4. Airflow through the trap

Additional parameters which were considered by the contractor were:

1. Total airflow (primary plus secondary)
2. Particle wall collision resiliency
3. Particle density (specific gravity)
4. Presence or absence of bounce plate
5. Presence or absence of downwash

In addition, the following parameters were varied as a matter of procedure in determining particle separation efficiencies:

1. Particle diameter
2. Particle initial position
3. Particle initial velocity

The separation efficiencies were determined from data obtained by varying each of the latter three parameters and by combining these data in a way considered to be representative of the particle distribution approaching an actual aircraft inlet. In the course of this study three specific problem areas were identified for further investigation:

1. Determination of airflow patterns through the inlet configurations.
2. Computation of particle trajectories for each of these airflow patterns.
3. Reduction of the computer data to produce useful information on separation efficiency.

EQUIPMENT AND METHODS

Airflow data were obtained for the case of two-dimensional, incompressible, potential flow for each inlet configuration by means of an electrical resistive analog. This apparatus produced plots of the potential flow streamlines through the inlet. The streamline data were converted manually to air velocity versus position data and fed in this form into a digital computer programmed to compute particle trajectories. Additional information, such as position of bounce surfaces, scale factor for velocity, air viscosity and density, was also included in the program input. The digital computer output consisted of printed lists of x and r coordinates which represented points on the particle trajectories. These were plotted manually, the characteristics of the trajectories were noted, and the results were evaluated in the light of the known behavior of actual inlets. Particle size distributions of several types (MIL-E-5007C, #70 sand, #140 silica flour, MIL-A-13488B AC coarse sand) were used to compute typical weight percent separation estimates, in conjunction with the computer trajectory data for the appropriately sized particles.

ELECTRICAL ANALOG LAYOUTS

The analog field plotter used (Sunshine Scientific Model 241A) consists of a thin sheet of electrically conductive paper (0.004 inch thick) in which an electrical current flow pattern is set up by means of suitably attached and energized electrodes. The resultant potential-drop pattern is detected and plotted directly on the paper by means of a searching stylus in conjunction with a high-sensitivity detecting instrument. The current and potential patterns established in the plotting sheet sheet are chosen to be analogous to the corresponding flux and potential functions of the actual fluid flow field being studied. Due to the thinness of the plotting paper the electrical field is effectively two-dimensional, and is thus a simulation of a two-dimensional rather than a three-dimensional flow field. This limits theoretical studies to two-dimensional inlet ducts (i.e., slots) and the results must be extrapolated to apply to three dimensional, axisymmetrical ducts.

In this study, the inlet cross section to be studied was outlined on the sheet of analog paper using highly conductive wire fastened to the paper with silver paint and tape. The paint provided an excellent contact between the paper and the outline electrodes. In cases where downwash was to be studied, the electrodes were extended upstream of the inlet in the outline of a typical downwash streamtube (see Figure 9). In these cases a nickel-chromium resistance wire was stretched across the upstream end of the streamtube and fastened to the paper with paint and tape, to provide a linear voltage drop between the upper and lower outline electrodes at this station. This

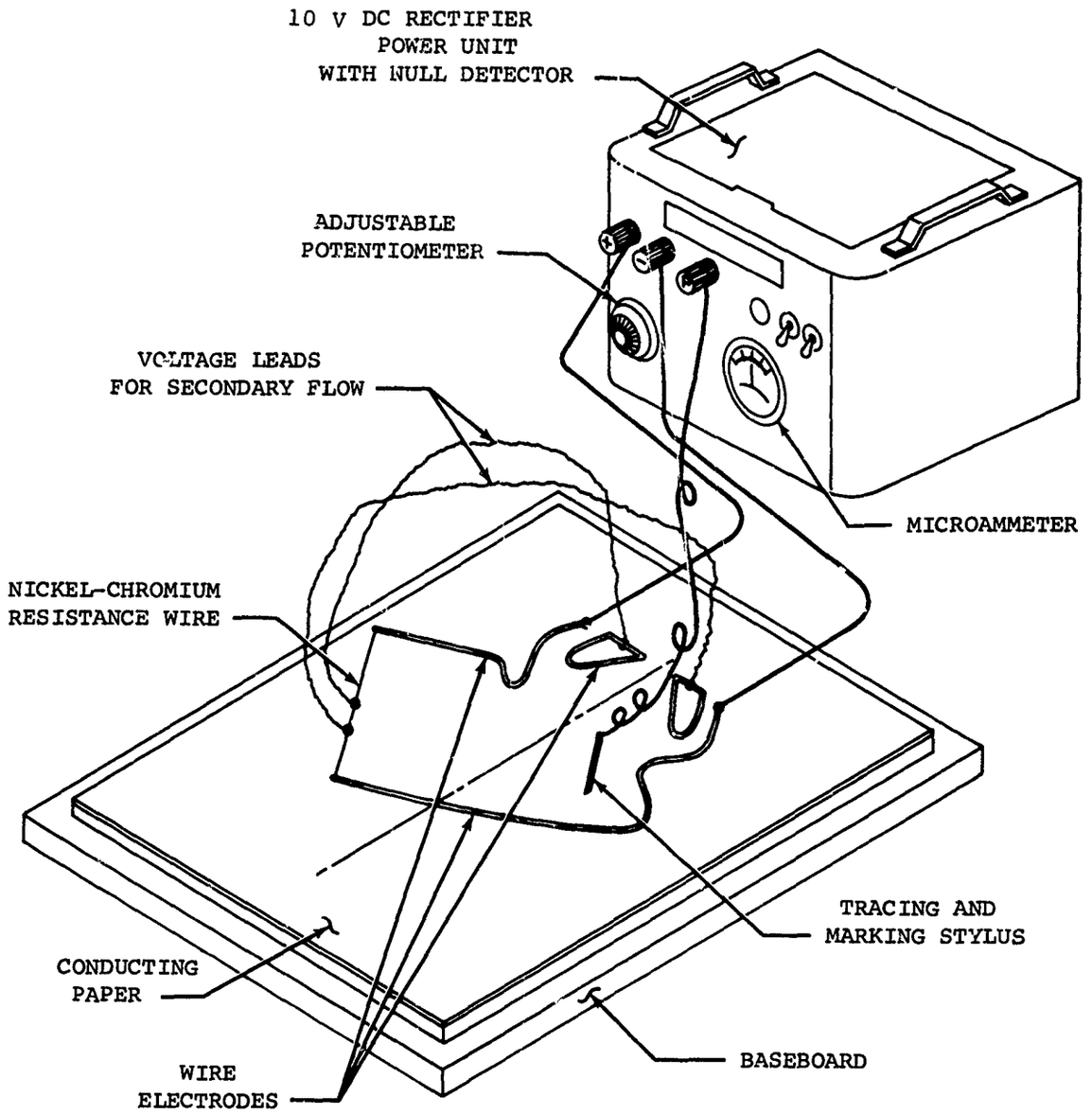

Figure 9. Analog Field Plotter Set Up For Inlet With Downwash

simulates
a uniform fluid flow in the streamtube. To simulate the secondary flow (for example, at 5 percent of total flow), voltage taps would be made at the 47.5 percent and 52.5 percent points on the resistance wire to excite the electrodes representing the upper and lower trap surfaces with the appropriate voltages.

In cases without downwash the upstream resistance wire was fastened in an approximately circular arc upstream of the inlet bellmouth, the ends of the arc connecting with the upper and lower inlet surface electrodes. The constant-voltage lines in this arrangement simulate flow approaching the inlet along radial lines. Again, in this situation, leads would be connected from the electrodes representing the upper and lower trap surfaces to the points on the upstream resistance wire at which the percentages of total voltage drop were appropriate to the percent secondary flow being simulated. It should be noted here that these leads from the upstream resistance wire to the trap surface electrodes in all cases were kept well away from the plotting surface, so that their presence would have a negligible effect on the potential field being plotted.

Voltage was applied to the upper and lower inlet surface electrodes by connecting them to the terminals of the regulated dc power supply. The power supply includes a null indicator circuit which was used to plot the lines of constant electrical potential within the inlet cross section on the plotting board. As stated before, the lines of constant electrical potential are representative of the fluid streamlines in the actual flow situation. The null detector indicates to the operator whether a given point on the plotting surface is at the voltage level of the desired equipotential line. The voltage level of the equipotential being plotted is selected by an adjustable potentiometer, which has a range from 0 to 100 percent of the total voltage being applied to the power supply terminals and an accuracy of approximately ± 0.5 percent. A probe is connected to the middle terminal of the adjustable potentiometer through a protective diode circuit and a microammeter.

When the probe tip is brought into contact with a point on the plotting surface which is at the same potential as the setting of the potentiometer, there is no voltage difference across the terminals of the microammeter and a null reading is indicated. This enables the operator to mark the point as one lying on the equipotential line of interest. Bringing the probe tip in contact with the paper at a point of different potential results in a finite reading on the microammeter, indicating to the operator that the point is not one lying on the equipotential line being plotted. The marking of equipotential points in this study was done by pressing the probe tip against the paper, leaving a small indentation which was then emphasized with a small pencil mark. This method of

marking is not considered to affect appreciably the characteristics of the potential field. The various instrumentation and experimental accuracies combine to give an estimated accuracy in point location of ± 0.010 inch under average reading conditions[6].

Using this methodology, equipotential lines were plotted for the configurations discussed under the heading, "Description of Configurations and Range of Parameters Studied." These inlet configurations are described later. In general, equipotential lines were plotted for 0 to 100 percent total voltage drop, in 10 percent increments, with additional lines being plotted near the center of the duct to describe more accurately the flow into the trap. Figures 10 and 11 show two typical plots.

As was stated before, the equipotential lines obtained through the above process represent the fluid flow streamlines, or, in other words, lines across which there is no mass flow of fluid (air). To obtain velocity data from these plots, it was necessary to utilize the formula

$$m = \rho V A \tag{1}$$

where m = mass flow
ρ = density
A = area of flow,

and V is the velocity desired. If the density and the total mass flow are assumed to be unity, the velocity at any point between two streamlines (equipotentials) is given by

$$V = \Delta\phi/A \ , \tag{2}$$

where $\Delta\phi$ is the potential difference between the two lines (given as a decimal; 10 percent = 0.1) and A is the flow area represented by the distance between the streamlines. In a three-dimensional, axisymmetrical inlet this area is a function both of the distance between the streamlines, ΔR, and the mean radial distance, R, of the streamlines from the duct centerline. Thus the velocity V in an axisymmetrical duct is

$$V = \Delta\phi/\pi \left[\left(R + \frac{\Delta R}{2}\right)^2 - \left(R - \frac{\Delta R}{2}\right)^2\right] = \Delta\phi/2\pi R\Delta R. \tag{3}$$

In a two-dimensional inlet, the area A is a function only of the distance between the streamlines (and the width of the inlet, in this case assumed equal to unity), and thus the velocity is given by

$$V = \Delta\phi/\Delta R. \tag{4}$$

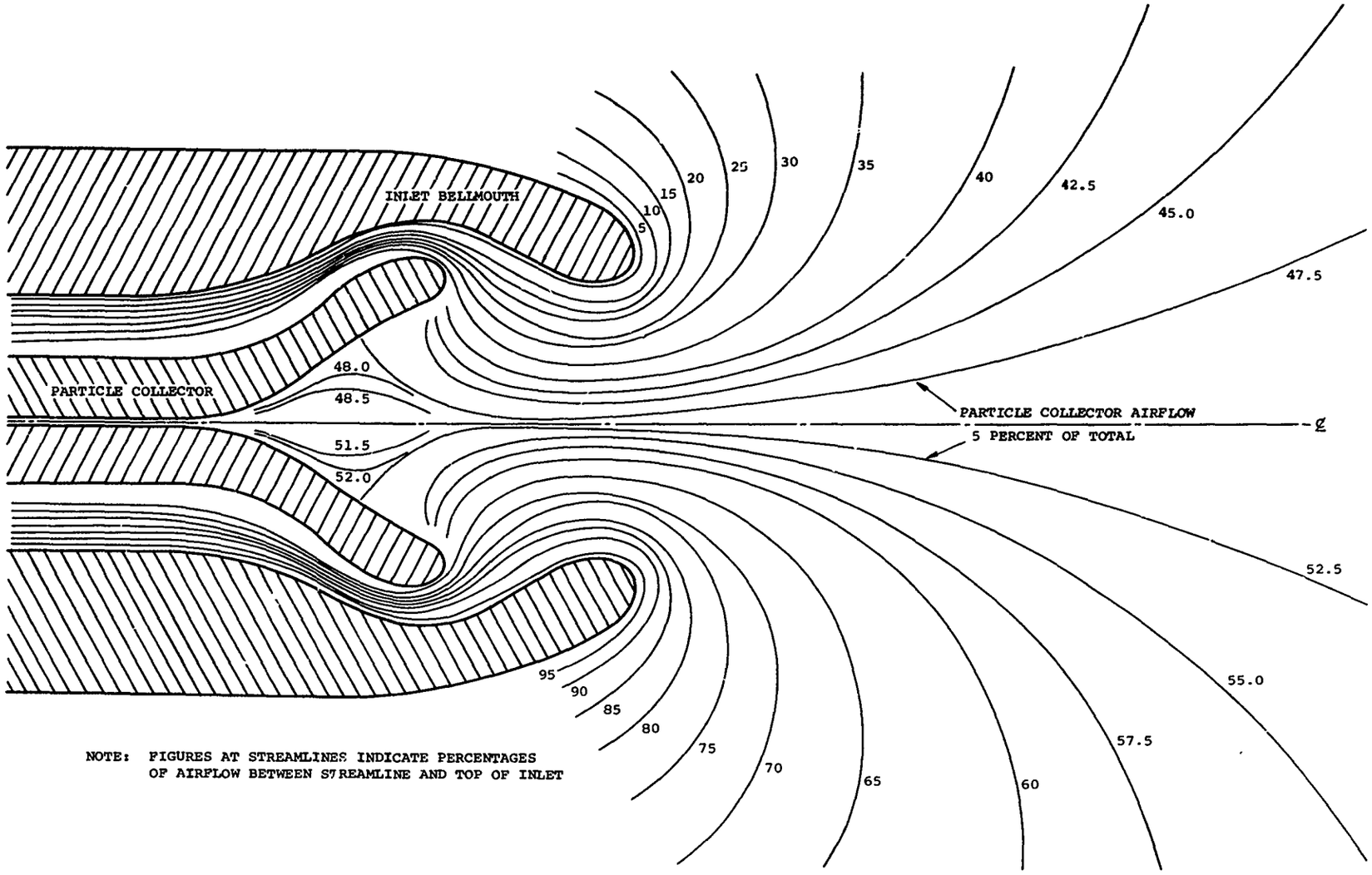

Figure 10. Engine Inlet Airflow Streamlines for Typical Inlet With No Downwash

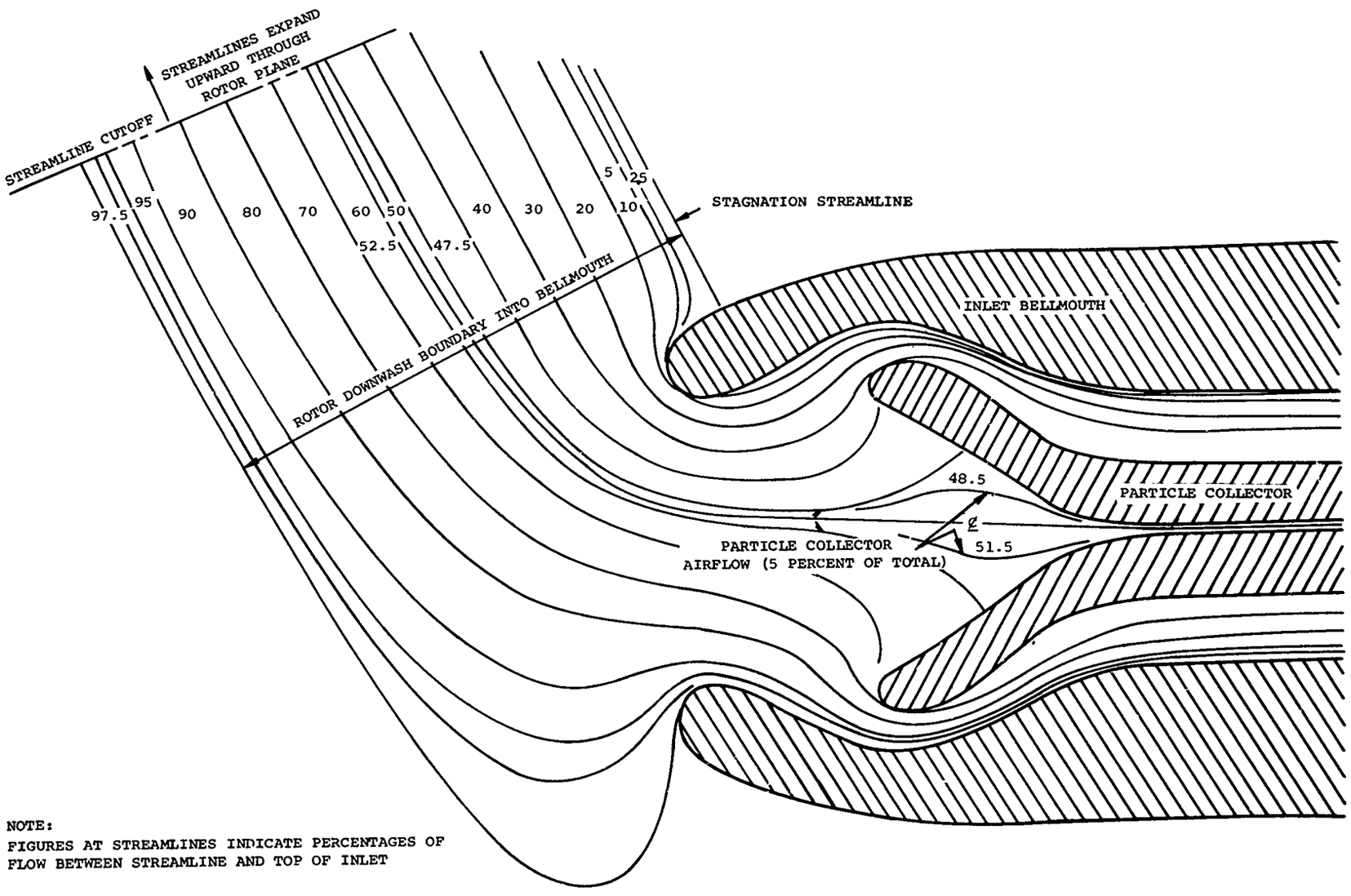

Figure 11. Engine Inlet Airflow Streamlines for Typical Inlet With Simulated Rotor Downwash

The difference between equations (3) and (4) is important and will be discussed in a latter section. As this study was to be concerned only with the two-dimensional case, the latter of the foregoing equations was utilized to determine a velocity table for each inlet configuration. These tables were computed manually from the analog data for approximately 25 points in the flow field at each of approximately 18 axial stations, a total of 450 points. For each of these points the two bracketing streamlines were examined to determine the direction and velocity of the flow at the point. The results were tabulated in a form such that two-dimensional linear interpolation could be used to approximate the direction and magnitude of the air velocity at any intermediate point in the flow field.

COMPUTATION OF PARTICLE TRAJECTORIES

An IBM Model 360 digital computer was used to compute particle trajectories through the inlet configurations. Inputs to the program were punched cards; printed sheets formed the output. The running time per trajectory was approximately 3 seconds, and an unlimited number of trajectories could be computed consecutively in one computer run.

Trajectory calculations were based on a summing of forces operating on the particle in the x and r directions and a calculation of the particle acceleration in a given time increment due to these forces. The program flow chart, Figure 12, describes these calculations, as well as the routines set up to handle bounces of the particle from the duct walls. In general, the procedure used is as follows:

1. Given initial particle coordinates and velocity components in the x and r directions, a new particle position after a given small time, Δt, was computed by using the initial velocity components only; this was called a tentative path increment.

2. At the midpoint of this tentative path increment, the air velocity components were then determined, the velocity difference between air and particle was computed, and the drag coefficient for the effective particle Reynolds number was determined from a table (7).

3. Using this information, the tentative particle acceleration during the time Δt was calculated (based on drag force and gravitational force) and the new velocity after the time increment was compared to the velocity assumed in calculating the tentative path increment.

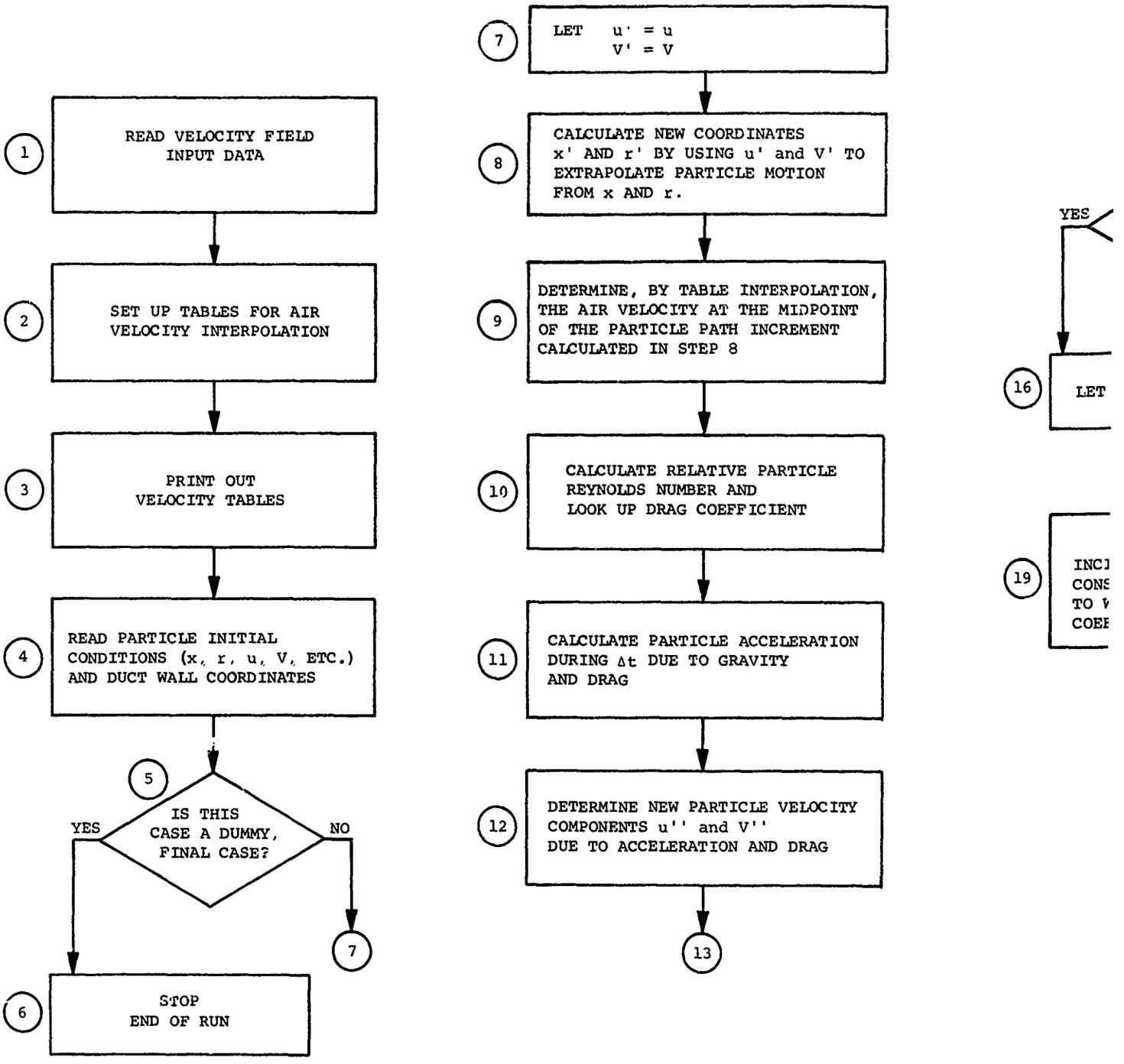

Figure 12. Trajectory Progr

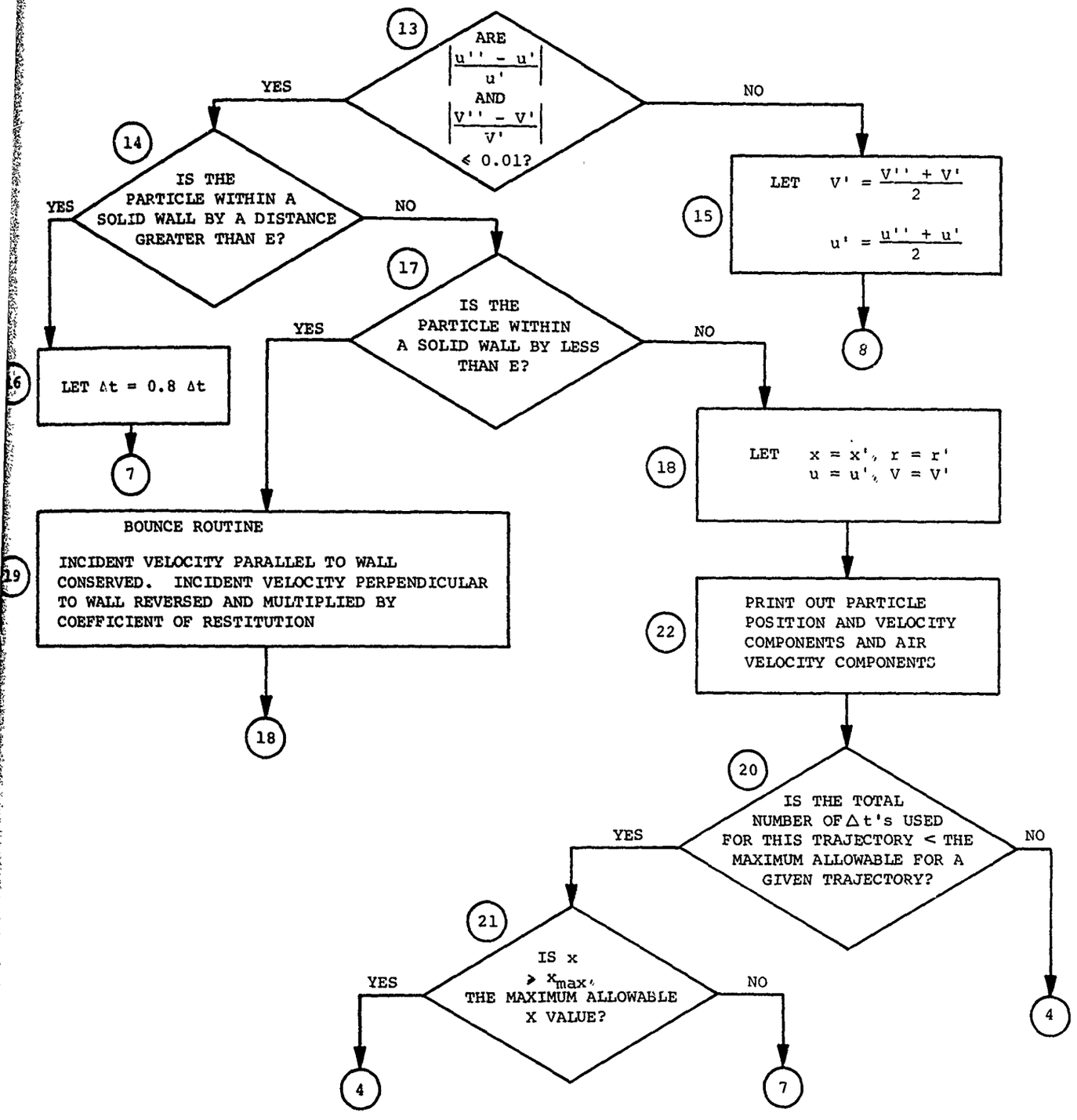

y Program Flow Chart

4. If the assumed and calculated velocities agreed to within 1 percent the tentative path increment was considered to be good, and the new x and r coordinates, as well as the average of the assumed and calculated velocities, were taken as the particle conditions for a point of the trajectory being calculated (except as described in step 6). Calculation then proceeded to step 6.

5. If the assumed and calculated velocities did not agree to within 1 percent, they were averaged and the average was used to calculate a new tentative path increment, using the initial position of step 1. Beginning with step 2, this process was then repeated until the criterion in step 4 was satisfied. If more than 40 (an arbitrary number) different tentative path increments had been computed for the given initial position without satisfying step 4, processing moved to the next input particle.

6. The particle coordinates from step 4 were checked against the known wall coordinates to determine whether the particle had penetrated a duct wall in its first path increment. If it had penetrated a wall by more than a given input distance, ε, the entire procedure was repeated starting with step 1. Using the original initial conditions and a reduced Δt, and the path increment was recalculated.

7. If the particle had penetrated the duct wall by a distance less than ε, it was considered to have ricocheted from the surface. The x and r coordinates of step 4 were considered to be the new particle coordinates, but the particle velocity components calculated in step 4 were modified as follows: the component of velocity parallel to the duct surface was preserved intact, while the component of velocity perpendicular to the surface was reversed in sign and then reduced by the resilience factor, K. Computation then proceeded back to step 1, using the new particle conditions as the initial conditions for a new path increment.

8. If the particle had not penetrated the duct wall, computation proceeded back to step 1 using the particle conditions from step 4 as the initial conditions for a new path increment.

9. Computation proceeded as above until a given number (an input value) of path increments had been calculated, or until the particle x coordinate exceeded an input x limit.

Air velocities within the program were obtained by two-dimensional linear interpolation in a mesh of approximately 450 velocity points (points at which coordinates, air velocity, and direction had been input). The four velocity points lying closest to the particle position in question were used in this interpolation procedure.

The inputs for the duct wall coordinates were independent of the air velocity inputs, and, as far as the computer was concerned, the two sets of inputs did not have to be consistent with each other. Thus, in regions in which the airflow was known not to influence the particle trajectories critically, it was possible to input an arbitrary wall shape for examination of bounce characteristics, without necessarily having to prepare (and reduce the data from) an entirely new analog velocity plot. This procedure was followed in this study during optimization of the inlet bounce plate.

In addition to the duct coordinates and the air velocity point data, the following inputs were necessary for each trajectory:

1. Axial and radial velocities
2. Axial and radial coordinates of initial position
3. Angular coordinate and angular velocity (always equal to zero in this study)
4. Time increment, Δt
5. Velocity scale factor by which analog data are multiplied to yield full-scale inlet velocities
6. Particle diameter and density
7. Air velocity and density
8. Bounce parameters: penetration constant (ε), time increment reduction factor, resiliency constant (K)
9. Number of trajectories to be calculated and the number of path increments to calculate per case
10. The maximum x coordinate for trajectory calculation.

The computer output sheets provided the following information:

1. At the head of the printout:
   a. A listing of the input data
   b. A listing of the input velocity points after they had been arranged for interpolation
2. At the beginning of each trajectory printout:
   a. A listing of the particle initial conditions and properties
   b. A listing of the duct and trap wall coordinates for the bounce calculations

3. For each path increment on a given trajectory:

   a. Particle x and r coordinates
   b. Particle x and r velocity components
   c. Air x and r velocity components
   d. Warning statements if the edges of the velocity point mesh were being approached

4. At the end of each trajectory the reason for termination is printed out.

REDUCTION AND EVALUATION OF COMPUTER DATA

Due to the vast quantity of data involved, several different methods were applied to the evaluation of the particle trajectory information obtained from the computer. Initially, all trajectory data were plotted manually over the outlines of the appropriate inlet cross sections. After a learning process had taken place during which the various particle distributions (see Figure 16) were judged for their ability to produce realistic and significant trajectory patterns, much of the data was evaluated with only abbreviated plots. In general, an experienced person could obtain directly from the coordinate listings such simple information as whether or not the given particle had been trapped. For more complex questions, such as the degree to which the resiliency of the walls affected the trajectories, more completely plotted data were used for visual evaluation. In many cases (approximately 10 percent of the total number) only fragmentary trajectories were calculated. This was due to several factors such as choice of a Δt too small for the path increments to add up to a trajectory of the desired length in the allowed time. Also, on occasion, a sudden change in the direction of airflow made convergence on a new position impossible for some particular particle with the Δt input. In as many instances as possible these cases were rerun with appropriate changes to yield complete trajectories; however, the large number of initial runs to be completed often made such reruns impractical. In these situations the incomplete trajectories were either discarded or extrapolated visually. These extrapolations were carried out with careful consideration being given to all similar cases for which complete trajectories were available. The abundance and consistency of such cases led to a great deal of confidence in the accuracy of the extrapolations. No extrapolated data were used in the evaluation of parametric effects on particle trajectories; the use of such data was limited to evaluation of the separation efficiency of the various inlets.

In many other cases, completely computed trajectories were only partially plotted. This was done deliberately as a timesaving device, with great care being taken that the essential part of each trajectory was plotted. Usually only the upstream end of the trajectory ($X<0.0$) was discarded.

The following assumptions were made during the evaluation of the computed trajectories:

1. Particles within the trap, and in motion downstream of the stagnation point and apparently not in a position to collide with a wall, were considered trapped.

2. Particles reaching x = 12.8 within the trap (or x = 16.0 in configuration 5) were considered trapped.

3. Particles directly approaching the annular engine inlets shown in the trajectory plots were considered ingested by the engine with no possibility of rebound.

4. Particles bouncing from an inlet surface in such a way that they passed out of the inlet velocity field (this could only happen upstream of the inlet throat) were considered to be beyond the reach of the engine and were not counted as either trapped or ingested.

5. Collisions between particles were ignored.

DIFFICULTIES AND ADVANTAGES ASSOCIATED WITH THE TWO-DIMENSIONAL METHODS

The use of a two-dimensional analysis to describe what is actually a three-dimensional flow field leads to several difficulties or possible sources of error. In particular, one theoretical problem and one practical problem of substantial magnitude arise.

The theoretical problem is caused by the difference between the three-dimensional and the two-dimensional potential flow (Laplace) equations. The two-dimensional equation is simply

$$\nabla^2 \psi = 0 \quad \text{(two-dimensional)} \tag{5}$$

or, expanded,

$$\frac{\delta^2 \psi}{\delta x^2} + \frac{\delta^2 \psi}{\delta r^2} = 0 \ , \tag{6}$$

while the three-dimensional equation is

$$\nabla^2 \psi = 0 \quad \text{(three-dimensional)} \tag{7}$$

or, expanded,

$$\frac{\delta^2 \psi}{\delta x^2} + \frac{\delta^2 \psi}{\delta r^2} + \frac{1}{r}\frac{\delta \psi}{\delta r} + \frac{1}{\theta^2}\frac{\delta^2 \psi}{\delta \theta^2} = 0. \tag{8}$$

If, as in this study, circumferential variations are ignored, the three-dimensional equation becomes

$$\frac{\delta^2 \psi}{\delta x^2} + \frac{\delta^2 \psi}{\delta r^2} + \boxed{\frac{1}{r}\frac{\delta \psi}{\delta r}} = 0, \qquad (9)$$

which differs from the two-dimensional equation [6] by the term in the box. Comparing equation (6) and (9) there is no reason to expect that the streamlines (lines of constant ψ) in the two-dimensional case are necessarily similar to those for the three-dimensional case. A very simple example is the case of uniform flow in a straight channel (two-dimensional) compared to uniform flow in a straight pipe (axisymmetrical three-dimensional). In the latter case the streamlines must obviously be closer together as they get farther from the pipe axis, while in the former case they would be uniformly spaced, as shown in Figure 13. It can be seen easily, however, that if a two-dimensional analog plot, such as one representing the two-dimensional channel in Figure 13 were treated as two-dimensional throughout the process of calculating velocity from the streamline spacing, the correct velocity distribution (uniform) for the three-dimensional case would be obtained. In other words, although the streamlines are spaced differently for the two-dimensional case, the correct three-dimensional velocity distribution can be obtained from the two-dimensional case if the data are consistently treated as two-dimensional. This is not necessarily true for any case but the straight ducts described above, but it is the justification for the consistent two-dimensional treatment given the analog data.

The practical problem is caused by the fact that two-dimensional areas vary as the character width while three-dimensional areas vary as the square of the diameter. In the incompressible flow studied here, area changes are inversely proportionall to average velocity changes. Therefore, if the inlet cross section studied on the analog plotter is the actual cross section of a three-dimensional inlet, the average velocity will vary on the two-dimensional plot in a way not necessarily similar to the flow in the actual inlet. On the other hand, if attempts are made to distort the two-dimensional analog outline so that the average velocities obtained from the analog approximate those known to exist in the actual the surface slopes and positions on the plot will have changed so that particle-bounce calculations will be incorrect. In addition, the regions of turning in the airflow will have been displaced and modified so that particle inertial forces will not have the proper relationship to aerodynamic forces. Thus, two sources of error will have been substituted for one, and, for this reason, no attempt was made to modify the inlet cross sections used on the analog plotter to provide realistic, three-dimensional, average air velocities at all axial stations.

STREAMLINES
EVENLY SPACED

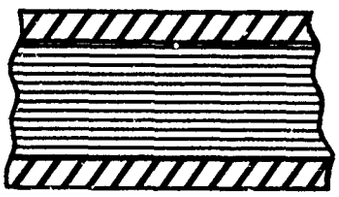

(a)

TWO-DIMENSIONAL
CHANNEL

STREAMLINES CLOSER
TOGETHER NEAR WALLS

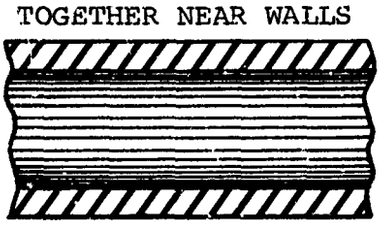

(b)

AXISYMMETRICAL
PIPE

Figure 13. Fluid Streamlines in Two-Dimensional and Three-Dimensional Flow

In all cases, the air at the inlet throat (x = 0.0) was given an average velocity appropriate to the airflow being considered, and all other average velocities then depended on the ratio of the local duct area to the throat area. This did result in unrealistically high air velocities in some areas, particularly upstream of the throat in the configurations which had downwash. For this reason, particles used for the finalized data were those which had been given initial positions close enough to the inlet throat so that they did not reach unrealistically high velocities before entering the inlet.

It must be recognized from the above discussion that although the two-dimensional airflow analysis has shortcomings with respect to a three-dimensional analysis, certain benefits can also be realized. One particular advantage isthe ability to describe a skewed airflow (such as the downwash entering the inlet) with the two-dimensional analysis. Neither of the two commonly used methods of analyzing three-dimensional potential flow (the electrical analog tank and the method of seeking solutions of the three-dimensional Laplace equation) is able to describe this flow situation. This advantage applies equally to asymetrical ducts, such as the inertial inlet with bounce plate, configuration 4.

A second advantage of the two-dimensional over the three-dimensional analog plots is the rapidity and ease with which the former can be produced. This puts the two-dimensional analog at a substantial advantage when an optimization study is being conducted. Furthermore, the two-dimensional analysis gives excellent correlation with actual experimental data in the areas of particle separation and the prediction of typical trajectories for inlets of the type being studied here. This will be shown in subsequent sections of this report.

In light of the previous discussion it can be concluded that the two-dimensional airflow analysis, as used, is quite appropriate for the type of study being conducted. Given a knowledge of the various inaccuracies inherent in the method, it is not too difficult to evaluate the data in such a way that good correlation with experimental results can be obtained, and predictions based on the two-dimensional results can be treated with a high degree of confidence.

DESCRIPTION OF CONFIGURATIONS AND RANGE OF PARAMETERS STUDIED

Seven inlet configurations were defined for this study (Figure 14). Some are merely modifications of, or different cross sections of, the same basic inlet. There are, however, four substantially different designs represented. Configurations 1, 2, 6, and 7 represent type A, the basic symmetrical inlet with nc centerbody. Configuration 3 represents type B, the basic symmetrical inlet with a centerbody to

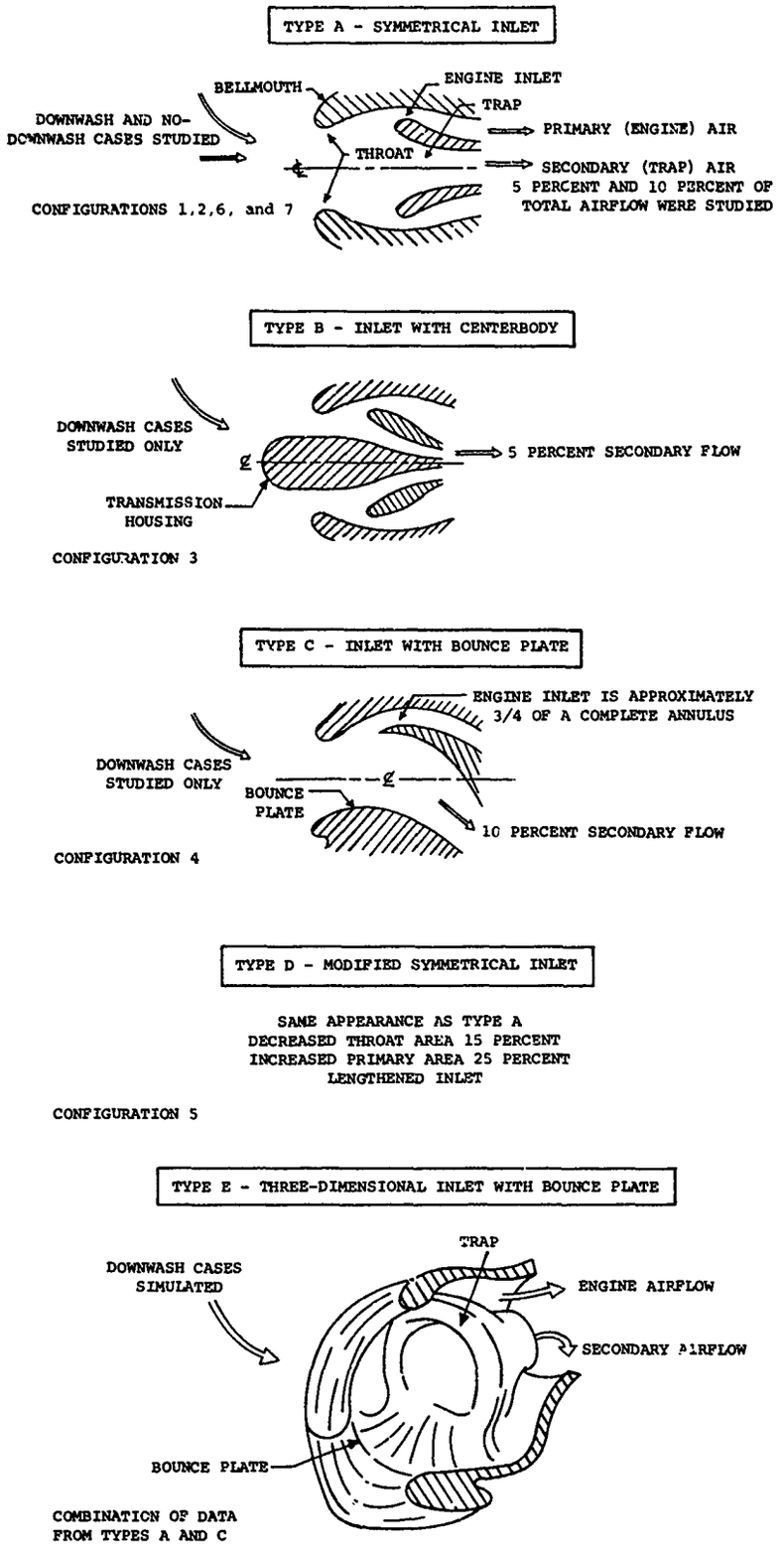

Figure 14. Inlet Configurations Studied

contain a transmission, starter motor, etc. Configuration 4 represents type C, the two-dimensional inlet with a bounce plate. Configuration 5 represents type D, a symmetrical inlet with increased aerodynamic focusing action. A fifth basic inlet type, type E, was generated by combining data from configurations 2 and 4 to simulate a three-dimensional inlet, with a bounce plate filling the lower quarter of the engine inlet annulus.

The inlet configurations studied are described in the following paragraph.

Configuration 1, Type A

This design is the basic inlet shape; it is an approximation of the cross section of an actual developmental inlet. The inlet has a 5 percent secondary flow and the air enters with a downwash component. The throat diameter is 12.4 inches.

Configuration 2, Type A

This is essentially the same as configuration 1 with the following exceptions: 10 percent secondary flow, trap contour modified for flatter inner surface, and sharper leading edge (extended leading edge tends to move stagnation point upstream). The throat diameter is 11.6 inches.

Configuration 3, Type B

This is a front-drive engine inlet with a trap located downstream of the transmission housing, The trap design is basically the same as configuration 2, and has 10 percent secondary flow. The air has downwash components. The transmission case diameter is 6.6 inches and the throat diameter (including the transmission case) is 14 inches.

Configuration 4, Type C

This configuration uses the cross section of configuration 2 modified to approximate more closely a current experimental inlet. It represents the actual inlet cross section in the vertical plane which contains the inlet axis. The upper trap inner surface is more curved (concave) than that of configuration 2, and the lower trap surface is replaced by a bounce plate of arbitrary shape. Secondary flow is 10 percent; flow upstream of the throat includes downwash and is identical with the flow of configuration 2. Approximately 45 percent of the inlet air flows around to the sides of the bounce plate between $x = 0$ and $x = 4$ inches. The throat diameter is 10.6 inches.

Configuration 5, Type D

This configuration has the same basic design as configuration 1 but with a 25 percent increase in primary flow area and a 15 percent decrease in throat area (based on three-dimensional calculation). It has 5 percent secondary flow and the same downwash pattern as configuration 1. The throat diameter is 11.0 inches.

Configuration 6, Type A

This inlet is the same as configuration 1 but the inlet is considered stationary in a no-downwash flow. Airflow downstream of the throat is the same as for configuration 1.

Configuration 7, Type A

This design is the same as configuration 4 but in this case the inlet is considered symmetrical with no bounce plate. The flow upstream of the throat is the same as that of configuration 6 (stationary inlet, no downwash) and the secondary flow is 10 percent. Configuration 7 represents an approximation of the flow in the actual inlet in the horizontal plane containing the inlet axis. The throat diameter is 11.6 inches.

Standard airflow was considered to be 12.8 pounds per second, and the scale factor, α, was chosen to produce an average velocity at the throat of about 210 feet per second for this airflow. Particle density used was 0.0833 pound per cubic inch for sand and 0.0361 pound per cubic inch for water. All particles were considered to be spherical. The assumed coefficient of restitution for particle wall collisions was 0.8. Downwash was represented by a streamtube at an angle approximately 30 degrees from the vertical and with a cross-sectional area (for the three-dimensional case) approximately four times that of the inlet throat. This would represent an upstream velocity of about 60 feet per second for the actual inlet.

Figure 15 illustrates the various combinations of particle initial positions and velocities used. Most of the data used in this report are based on the N distribution described in this figure. Extensive data were also obtained for the other distributions. Particles of the A distribution usually approached the inlet too rapidly to provide realistic data, but a distribution data were in the evaluation of separation efficiency when they appeared reasonable.

LEGEND			
SYMBOL	DISTRIBUTION NAME	AXIAL VELOCITY (U) fps	RADIAL VELOCITY (V) fps
○	A	90.0	-170.0
□	J	0.0	0.0
□	J	40.0	0.0
□	J	80.0	0.0
◇	M	0.0	0.0
◇	M	40.0	- 40.0
	N (COMBINED M AND J)		

NOTES: 1. IN DISTRIBUTION J AND M THE SOLID SYMBOLS REPRESENT PARTICLE INITIAL POSITIONS WHICH WERE RUN FOR EACH PARTICLE DIAMETER. THE OPEN SYMBOLS REPRESENT PARTICLES WHICH WERE NOT ALWAYS RUN.

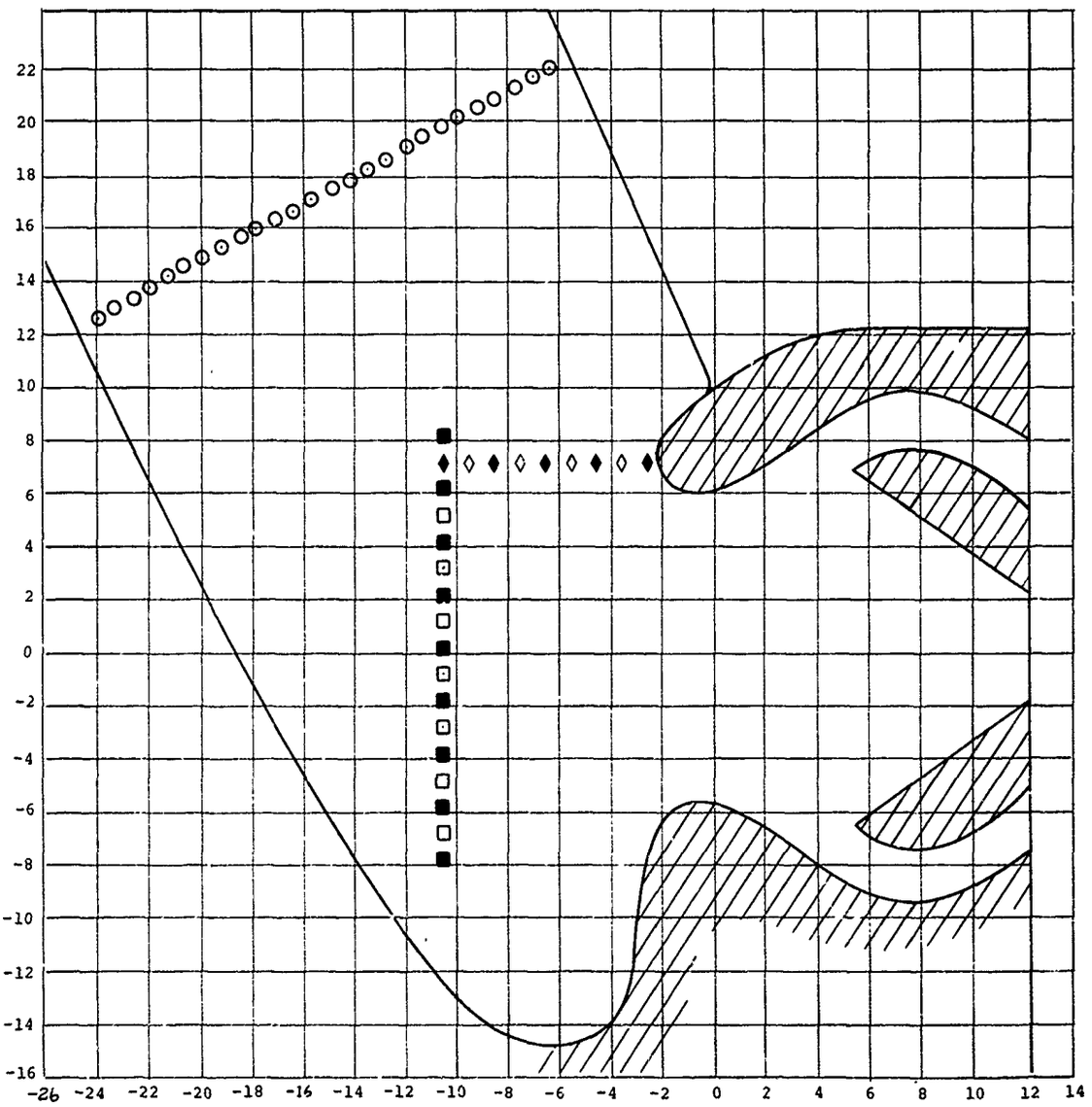

Figure 15. Particle Initial Position Distributions

PARTICLE SEPARATION EFFICIENCY - RESULTS AND DISCUSSION

GENERAL

Six of the configurations were analyzed to determine the separation efficiency. The type B inlet, configuration 3, was not covered in this part of the study since the initial trajectory plots for the configuration proved to be too unrealistic to expect reasonable results. Due to the presence of the transmission housing in the center of the type B inlet, the two-dimensional flow at the throat is not a reasonably accurate representation of the flow in the three-dimensional case. This means that when the velocity scale factor is adjusted to obtain the proper throat velocity, the velocities upstream of the throat are significantly too low. This airflow field then produces unrealistic particle trajectories when used in the trajectory program. The centerbody case evidently requires a more sophisticated method of determining air velocities than the method used here. Figure 16 gives an example of the trajectories obtained for configuration 3.

The separation efficiency of the other six configurations, types A, C, and D, was determined for several sand particle diameters at standard airflow. Separation efficiency was also determined for configuration 4 (type C) and configuration 7 (type A) for salt water spray and supercooled water droplets. The object of these studies was to optimize the separator design for #70 sand and standard airflow, based on the present airflow requirements of the CH-46 helicopter with the T58 engine. Both of these factors (the particle size and the airflow) were chosen largely for ease of comparison with experimental data, but they are also typical of present helicopter design. The Lycoming T53 used in the UH-1B, for instance, operates at about the same airflow as the T58.

In order to determine the effect of varying airflow in the inlets, configurations 2, 4, and 7 were also evaluated at 50 percent and 150 percent of the standard value of 12.8 pounds per second. In addition, the results of the separation studies of configurations 4 and 7 were combined to obtain an estimate of the performance of a type E separator as a function of airflow.

The most commonly used distributions of particle initial positions for this part of the study were distributions N, M, and J (see Figure 15). In determining the separation efficiency for a given particle size and airflow, the total number of particles of the given size in the relevant distributions was divided into the number trapped by the separator, as determined from the plots by count. When the separation efficiency for a given type of particle (e.g., #70 sand) was to be determined,

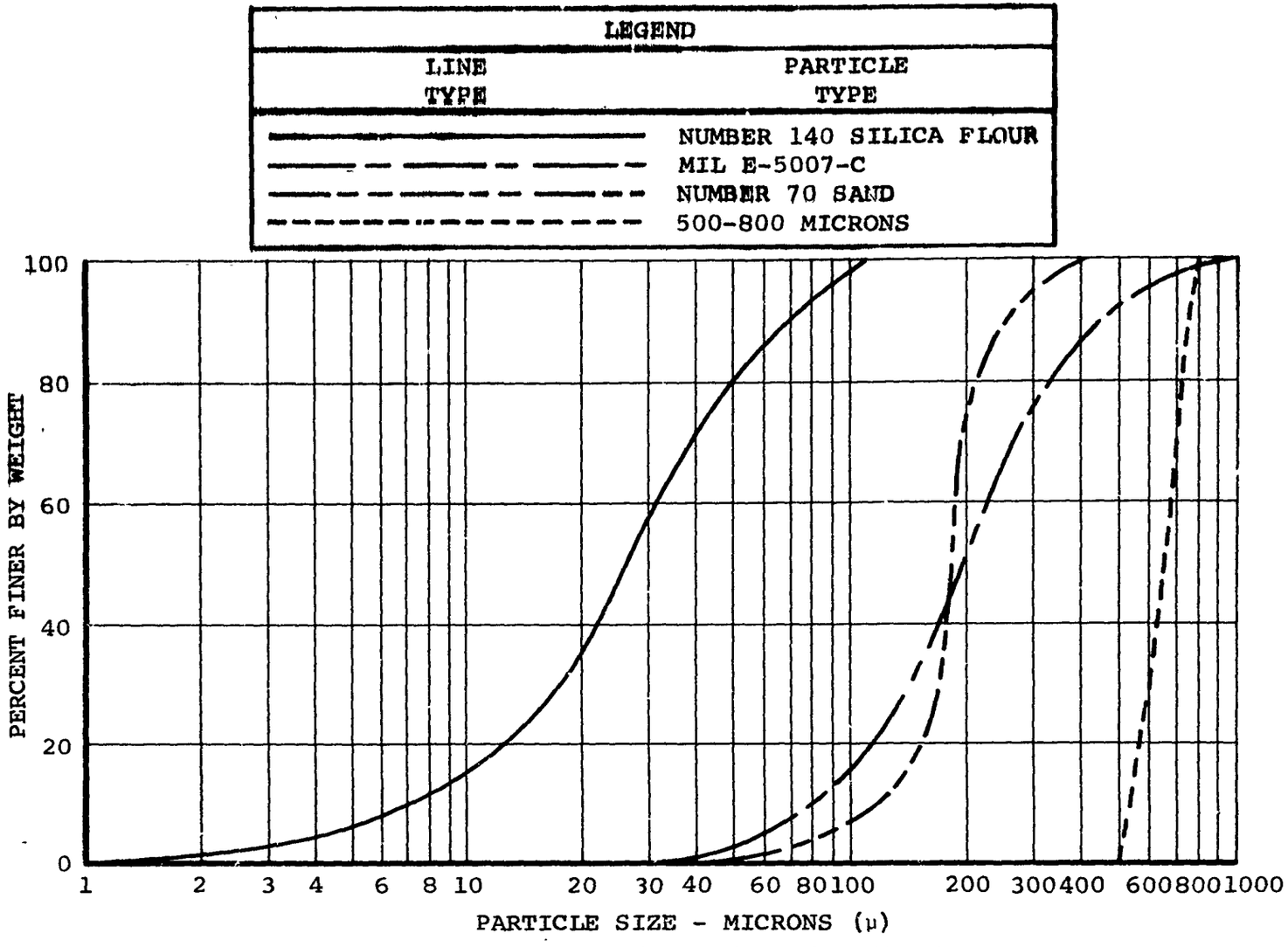

Figure 16. Sand Particle Size Distribution

the separation efficiencies of all relevant particle sizes for which data were available were combined and weighted according to the particle size distribution defined for that particle. Figure 16 shows the size distributions for the four types of sand and dust investigated.

The standard particle size distributions were divided into size increments for this study. The behavior of any particle in a given increment was considered to be characterized by the behavior of a particle with the mean diameter for the increment. The increments were chosen so that these mean diameters corresponded closely with the particle diameters for which computer data were available (i.e., 10, 70, 180, 500, and 800 microns). In several of the standard size distributions, the entire distribution is characterized by the behavior of particles of only one or two diameters.

An alternate method of combining the computed separation data with the standard size distributions consisted of using the curves of Figure 17 to determine the separation efficiency at particle sizes of 50, 150, 250, 350, 450, 550, 650, and 750 microns. The total weight per 100 pounds of particles between 0 and 100 microns, 100 and 200, 200 and 300, and so forth, was then determined from the relevant standard size distribution and multiplied by the appropriate separation efficiency to give a weight of particles separated in the given size increment for 100 pounds of sand. The sum of these values for all size increments then gave the separation efficiency of the inlet for the given standard sand size distribution.

This method was tried on several cases but did not yield results appreciably different from those obtained by the preceding, simpler method, The simpler method was, therefore, the one chosen in practice.

The separation efficiencies represent the weight of particles trapped per 100 pounds of particles actually entering the inlet. Particles missing the inlet altogether are not considered in the efficiency determination. In addition, no consideration is given to the tendency of the rotor downwash to lift lighter, smaller particles rather than heavy ones, or, in other words, to the tendency of a #70 sand distribution on the ground to be something different at the inlet. The sand distributions for which data are presented, then, are distributions as seen by the inlet.

PRESENTATION OF THE SEPARATION RESULTS

Tables II through XIII present the separation data obtained for each particle size, airflow, and sand or dust size distribution. The same results are combined and shown graphically in Figures 17 through 20. Table XIV summarizes the separation efficiency results.

Figures 21 through 58 present typical trajectory data obtained from the computer program. One series of cases for each particle size and inlet configuration is show, with additional cases being shown for the 10-micron particles in configuration 2, the 70- and 800-micron particles in configuration 4, and the 180-micron particles in configuration 7. In configurations 3, 4, and 5, cases are also shown where particles approach the inlets with the very high downwash velocities which are reached by the particles when they are started far upstream in the downwash streamtube. In most of the plots shown, alternate trajectories were deleted for clarity. In most cases, the behavior of the deleted particles can be easily inferred from the plotted trajectories. The plots shown, about one-sixth of the total number of trajectories plotted during this study, are representative of the total results obtained.

DISCUSSION OF SEPARATION RESULTS

Figure 17 is a plot of weight percent separation versus particle size at standard airflow (approximately 12.8 pounds per second) for all configurations except configuration 3. The effects of secondary flow variation, presence or absence of downwash, throat size variation, inlet shape variation, and addition of a bounce plate are all evident in this figure.

The best separation efficiency attained was 100 percent for configuration 4 with 70- and 180-micron particles. The worst efficiency was 3 percent for configuration 1 with 10-micron particles.

For all configurations the separation efficiency increases quite rapidly as particle size increases from 10 microns to 70 microns. For the three inlets with downwash (1, 2, 5), this rapid increase continues to about 180 microns, after which the curves begin to level off as they do in the other three configurations (4, 6, 7) upon reaching 70 microns. The three symmetrical inlets with downwash (1, 2, 5) show very similar curves, none of which rise higher than 51 percent (configuration 5 at 500 microns), and all of which lie between 35 and 51 percent for particles 180 microns or larger. In fact, except for configuration 2 at 70 microns, these three inlets lie within 20 percent of each other in separation efficiency throughout the entire size range of 0 to 800 microns. It is evident from this that minor design changes in the symmetrical

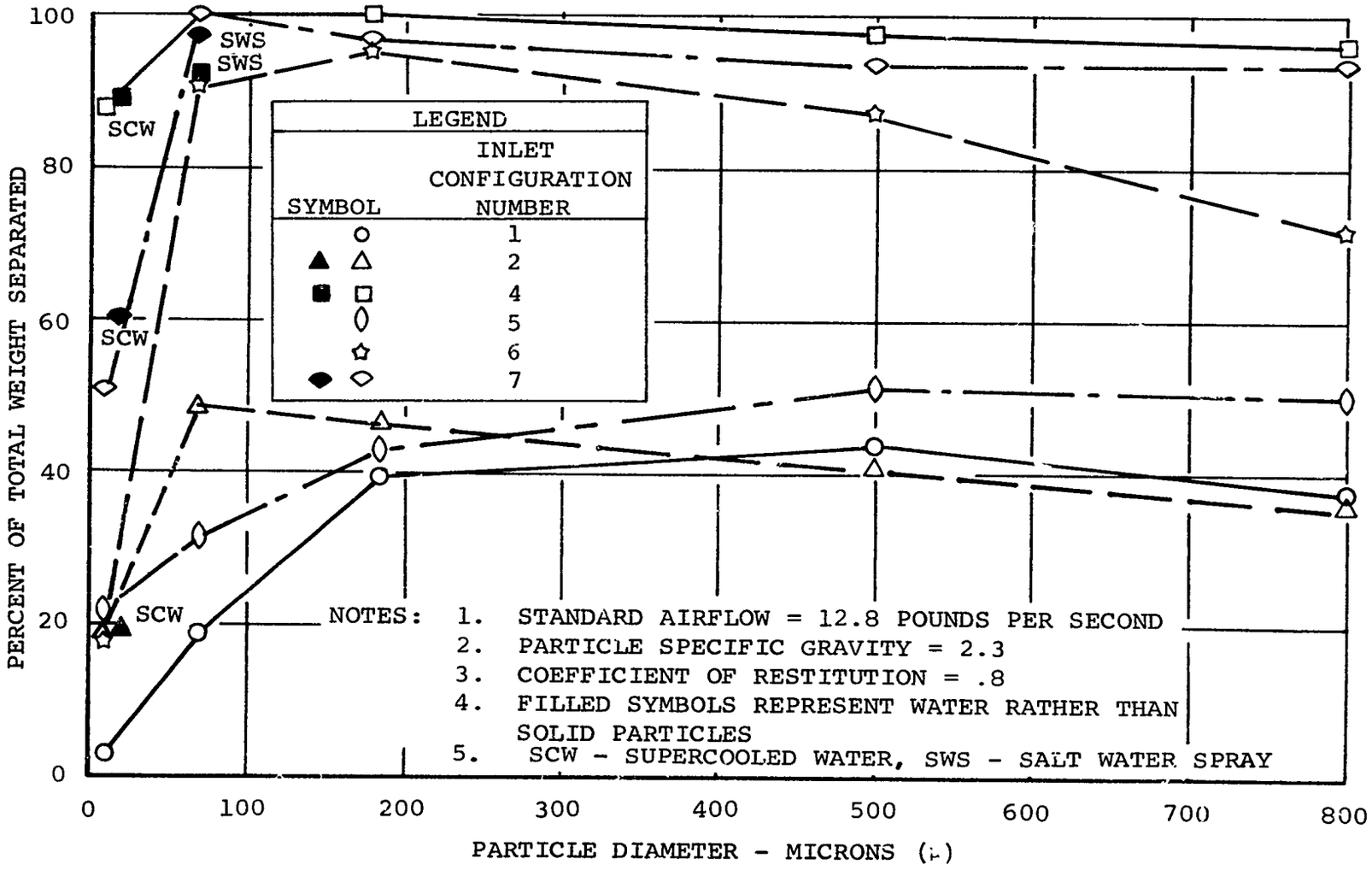

Figure 17. Separation Efficiency As a Function of Particle Diameter

inlet will produce only mild changes in separation efficiency when operating in a downwash environment. This is reasonable since the dominant factor in this situation is the air downwash which drives many particles directly into the lower half of the engine inlet annulus. Little can be done to improve this situation without design changes which would block off the lower half of the annulus.

One factor which does show consistent effects of a reasonable magnitude, however, is the percentage of the total flow which is used for secondary airflow. Configurations 1 and 2 have the same basic shape, differing only in that the former has 5 percent secondary flow while the latter has 10 percent. It can be seen that there is a consistent improvement in separation efficiency from configuration 1 to configuration 2 for the smaller particles, and virtually no difference for the larger particles. The magnitude of the improvement averages about 18 percent for particles 180 microns or smaller. This again demonstrates the dominance of the downwash in determining the performance of a type A or type D inlet in a downwash velocity field. The larger particles are driven downward so strongly as they enter the inlet that a relatively minor change in the velocity field within the inlet does not appreciably affect their behavior. The lighter particles are more strongly influenced by the flow field within the inlet and some improvement in the separation of these particles may be obtained by modifying this field.

An interesting contrast to the foregoing behavior is seen when configurations 6 and 7 are compared. These are identical to configurations 1 and 2, respectively, but are studied in a no-downwash velocity field. In this case there is, again, substantial improvement in small particle separation when going from 5 to 10 percent secondary flow, but now the improvement is lowest at 180 microns, and increases again for the larger particles. This behavior is indicative of the fact that, in a symmetrical flow field, the symmetrical inlet tends to focus the incident particles on some area of the trap. This focusing behavior, for the type A inlet, is optimum for particles of 180-micron diameter; the bellmouth flow field causes virtually all of these to converge on the center of the trap, and they are thus little affected by changes in the secondary flow. They are, to all intents and purposes, trapped from the moment they enter the bellmouth. The lighter, smaller particles, on the other hand, tend to follow the airflow in their immediate vicinity quite closely. They are thus not very much affected by the focusing action of the bellmouth, but are affected by the interior flow field of the inlet. A change in the interior flow field of the inlet tending to draw more air into the trap will, therefore, also tend to draw more of the light particles into the trap. In this light it is noteworthy that an approximate doubling of the secondary airflow more than doubles the

separation efficiency for 10-micron particles; configuration 6 shows 17 percent while configuration 7 shows 51 percent efficiency.

Heavier particles greater than 180 microns in diameter, because of their high inertia, are not focused ideally by the bellmouth. They do tend to converge on some point in the inlet, but the point of convergence is much farther downstream and the particles enter the inlet in a wide band, striking the sides of the trap over a much wider area than that impinged upon by the 180-micron particles. Figures 53 and 55 illustrate this behavior. The improvement in separation efficiency due to the increase in secondary flow for these heavier particles may thus be attributed to the higher secondary flow which produces better control of these particles when they rebound. The fact that there are rebounds, however, tends to decrease efficiency, and this is the reason that both configuration 6 and configuration 7 show declining efficiencies at the higher particle sizes.

Figure 17 shows a definite improvement in separation efficiency with an increase in secondary flow. The improvement, however, is dependent on particle size, and, in the case of a symmetrical inlet with downwash, the improvement is almost meaningless since the flow situation makes a high efficiency impossible.

The effect of downwash is shown clearly in Figure 17. Choosing a particle size of 180 microns as an example, it can be seen that configuration 6, with no downwash, has a separation efficiency of 95 percent, while configuration 1, the same inlet with downwash, has an efficiency of only 40 percent. Configuration 7, with no downwash, has an efficiency of 97 percent at 180 microns, while configuration 2, the same inlet with downwash, has an efficiency of only 46 percent. This decrease in separation efficiency caused by downwash is nearly the same magnitude (50 to 60 percent) for all particle sizes except 10 microns. It has already been pointed out that particles this small tend to follow the air very closely, and thus they will follow very similar paths inside the inlet no matter what happens to the flow field upstream of the bellmouth.

In summary, downwash causes a drastic drop in the separation efficiency of a symmetrical inlet for all particle sizes. The efficiency drop is less for smaller particles (10 microns or smaller), but efficiencies for these particles even in no-downwash conditions are so low that they make the symmetrical separator of questionable utility in collecting them.

Figure 17 also shows separation efficiency for configuration 5, type D, which, as has been previously defined, is a change in basic inlet shape from type A. The data are plotted for 5 percent secondary flow in a downwash flow field, so that the

most relevant comparison is with configuration 1. Configuration 5 shows substantial improvement in efficiency, particularly at the upper and lower ends of the particle size range. It will be recalled that configuration 5 has a smaller throat and a larger primary flow area than configuration 1. Thus, particles will be accelerated more as they enter the bellmouth, and, once inside, there will be less of a tendency for them to be drawn into the engine by the primary airflow. The greater focusing tendency of configuration 5 improves trapping efficiency for the heavier particles, while the decelerated primary airflow improves trapping efficiency for the smaller and lighter particles. The disadvantage of this type design lies in the greater redirection experienced by the air, leading to a tendency for boundary layer separation and pressure losses in the actual, nonpotential flow situation.

The greatest separation efficiency for all particle sizes is shown by configuration 4. This is the type C inlet with a bounce plate covering the lower engine intake. The only particle size for which the separation drops below 95 percent in this inlet is the smallest, 10 microns. It should be noted that these efficiencies for configuration 4 are in a downwash flow situation, which is the most difficult condition for the other inlets to handle.

Trapping of particles in this inlet is done almost exclusively by bouncing them off the lower surface (bounce plate) and into the trap. This design is optimum for this process at a particle size of 70 to 180 microns. The lower efficiency at 10 microns is due to the smaller particles being ingested immediately as they enter near the inlet upper lip. The decreasing efficiency for particles larger than 180 microns is due to poor control of their postcollision trajectories by the secondary airflow.

Separation efficiency was also calculated for salt water spray (70-micron diameter assumed) and supercooled water (20-micron diameter assumed) in configurations 2, 4, and 7. Configuration 2 had an efficiency of 19 percent for supercooled water. Configuration 4 had efficiencies of 89 percent for supercooled water and 92 percent for salt water spray, while configuration 7 had efficiencies of 60 percent for supercooled water and 97 percent for salt water spray. These points are illustrated in Figure 17 which shows that they lie quite close to the sand separation curves for the inlets involved. The change in particle specific gravity between sand and water has little effect on the separation.

Figures 18 and 19 show the separation efficiency of configurations 2, 4, and 7 as functions of the total airflow for various sand types. The configuration 4 curves are essentially flat, showing no airflow effect. The configuration 7 curves,

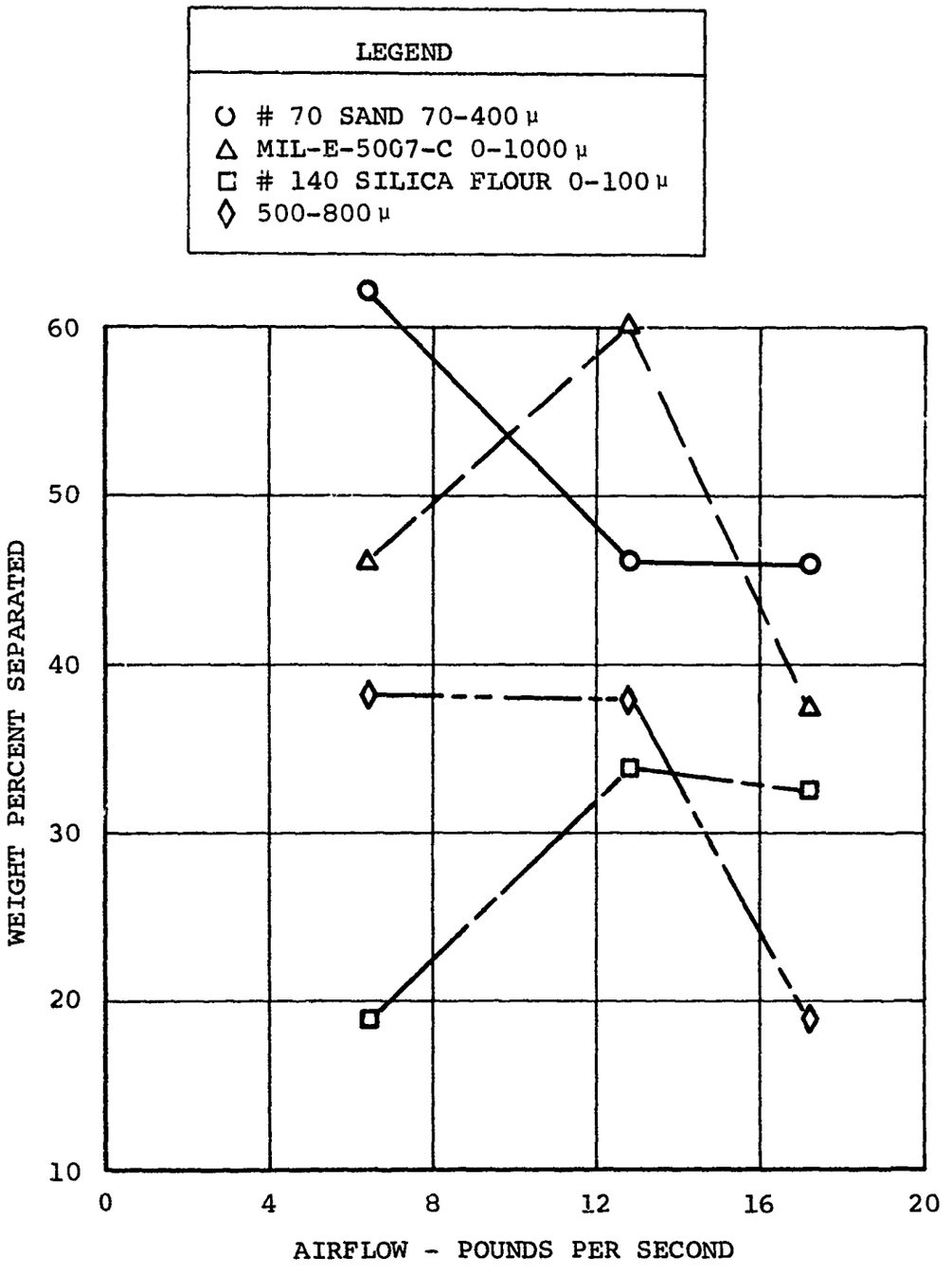

Figure 18. Separation Efficiency as a Function of Airflow for Configuration 2

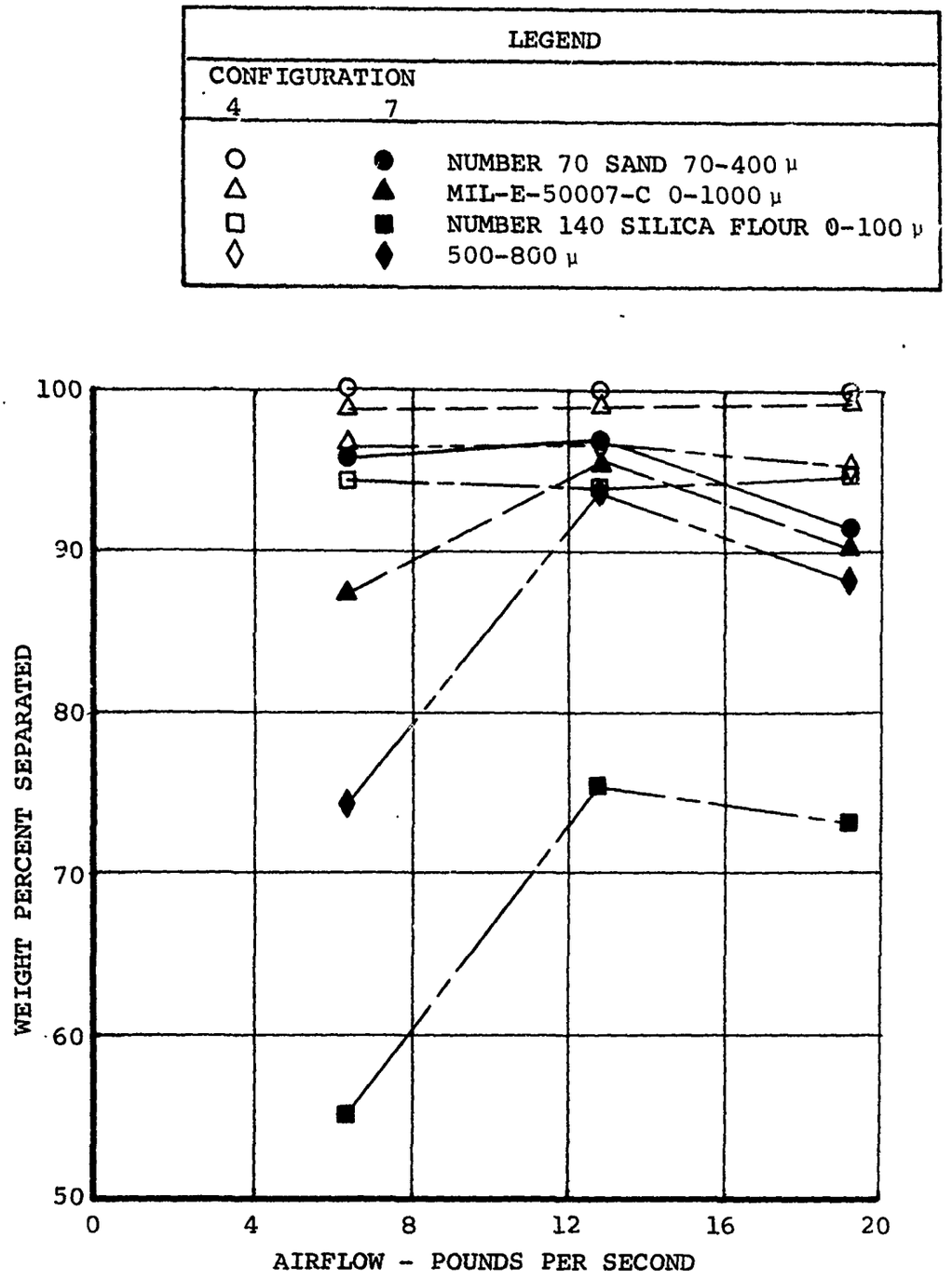

Figure 19. Separation Efficiency as a Function of Airflow For Configurations 4 and 7

conversely, show higher efficiency at the standard airflow, 12.8 pounds per second, indicating optimization at this airflow. For both configurations, the #70 sand is separated most efficiently, again indicating optimization for this type of sand. It is interesting to note that the MIL-E-5007C-type sand produces separation curves very similar to those for the #70 sand but with a somewhat lower (by 2 to 10 percent) efficiency indicated throughout. The variation is due to the differences in the particle size distributions between the two types of sand. The MIL-E-5007C sand has a more uniform size distribution and thus has more particles at the extreme size ranges than does the #70 sand. The size distribution for #70 sand is very much biased toward particles approximately 180 microns in diameter, which is the optimum particle size for these separators.

The variation in separation efficiency with airflow can be easily explained by considering two effects previously noted. As airflow increases from a low value, the focusing effect of the bellmouth increases. The high axial component of velocity imparted to the particles by the accelerating airflow in the bellmouth is the means by which this focusing mechanism works, and, as the airflow increases, the mechanism works more efficiently. However, above some optimum airflow the high velocity imparted to the incoming particles increases the probability that many of the heavier particles will collide with the inner trap surfaces. The faster the incident particles are moving, the more energetic these collisions will be. This increases the probability that the particles will bounce back upstream into the region where they may again be caught by the primary airstream and ingested by the engine. This bouncing process may appear too complex and improbable to have any significant or consistent effect on the separation efficiency of the inlet. However, many examples of the frequency with which the process does occur can be seen in Figures 21 through 98.

In order to simulate the behavior of an asymmetrical three-dimensional inlet, the particle separation data from configurations 4 and 7 were combined and averaged. The data from the two configurations were weighted equally in the averaging process. The principle behind this procedure was the assumption that approximately 50 percent of the particles approaching the inlet are moving in axial planes lying within 45 degrees of the vertical, and that the other 50 percent are moving in axial planes lying within 45 degrees of the horizontal (an axial plane contains the duct axis). Therefore, if the bounce plate in the actual inlet is assumed to fill approximately the lower quadrant of the engine intake annulus, the particle trajectories of configurations 4 and 7 each will approximate the trajectories of 50 percent of the incident particles. This reasoning involves the assumption that all particles

approach the inlet along radial lines, which is obviously not the case in the actual inlet flow field. However, the present approach appears to be the only reasonable one if the velocity fields are to be limited to two dimensions.

Figure 20, showing the separation efficiency for the type E inlet, again indicates an inlet optimized for #70 sand at standard airflow. The inlet shows moderate sensitivity to airflow and to particle size. The separation efficiency for #70 sand drops from 90 percent at standard airflow to 96 percent at 1.5 times standard airflow. At standard airflow the separation efficiency ranges from 90 percent for #70 sand to 85 percent for #140 silica flour and to 75 percent for supercooled water droplets.

The range of experimental data for inertial separators with bounce plate, bench tested in downwash conditions at Boeing, is also shown in Figure 20. These experimental data are primarily for #70 sand. The analytical approximation for #70 sand separation lies about 6 percent higher than the mean of the experimental range. This is quite good agreement when the approximations which were involved in deriving the analytical results are considered. Furthermore, the discrepancy is in the expected direction, inasmuch as the two major effects which were ignored in the analysis (particles approaching in nonradial planes and the presence of swirl components in the airflow) would both operate to decrease separation efficiency. In general, it must be expected that the experimental data will fall somewhat below the analytical data for separation efficiency, and allowance must be made for this in the evaluation of separator designs.

Results for salt water spray and supercooled water were also calculated for the type E inlet at standard airflow. Separation efficiencies of 94.6 and 74.3 percent, respectively, were obtained as shown in Figure 20.

Table XIII summarized the separation efficiencies obtained for the various inlet configurations for standard airflow and the particle types specified in the contract. Low (50-percent design) and high (150-percent design) airflow results are also given for configurations 2, 4, and 7. Some of the data given differ from that presented in the Sixth Quarterly Progress Report[9] since more data became available after the preparation of that report. Table XIV also presents experimental data for an inlet type E for comparison.

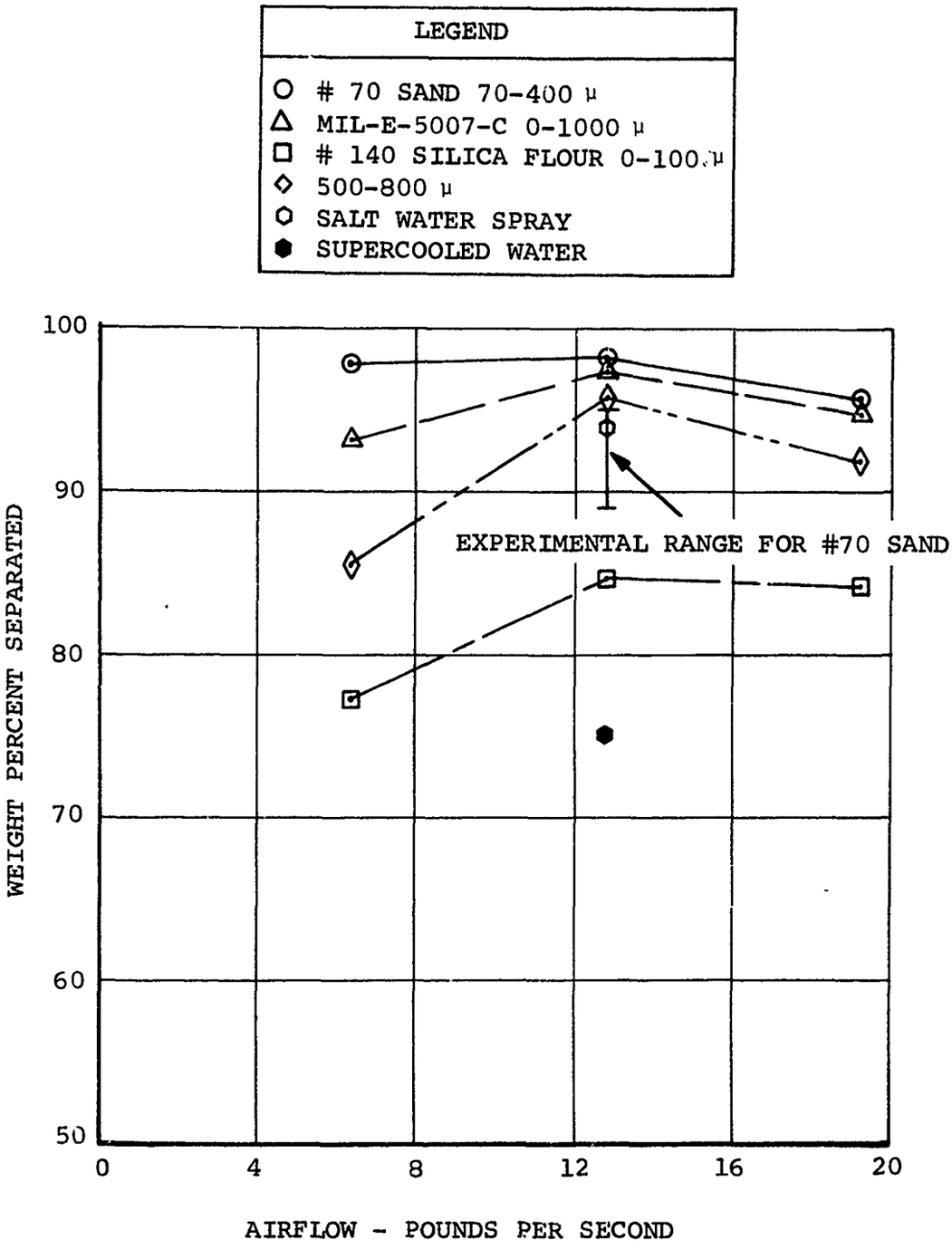

Figure 20. Separation Efficiency as a Function of Airflow for Inlet Type E

TABLE I
CODE LETTER IDENTIFICATION FOR TABLES II THROUGH XIII

Code Letter	A	B	C	D	E	F
Particle Distribution	M	M	J	J	J	M
Initial Velocity u, Feet per Second	0.0	40.0	0.0	40.0	80.0	0.0
Initial Velocity v, Feet per Second	0.0	-40.0	0.0	0.0	0.0	-40.0

TABLE II
PERFORMANCE FACTORS FOR INLET CONFIGURATION 1 WITH STANDARD AIRFLOW

Computed Separation Data								Separation Efficiency for Standard Particle Size Distribution							
								#70 Sand 70-400 Microns		MIL-E-5007-C 0-1000 Microns		#140 Silica Flour 0-100 Microns		500-800 Microns	
Particle Diameter (d) in Microns	Number of Particles Trapped / Number of Particles						(Total Trapped) /(Total Particles)	Separation Efficiency for Particles of Diameter d - %	Pounds Per Hundred in Size Range Characterized by Diameter d	Pounds Per Hundred Separated in This Size Range	Pounds Per Hundred in Size Range Characterized by Diameter d	Pounds Per Hundred Separated in This Size Range	Pounds Per Hundred in Size Range Characterized by Diameter d	Pounds Per Hundred Separated in This Size Range	Pounds Per Hundred in Size Range Characterized by Diameter d	Pounds Per Hundred Separated in This Size Range
	A	B	C	D	E	F										
10		1/5	0/9	0/9	0/9		1/32	3.1			2	0.6	50	1.5		
70		3/5	1/9	1/9	1/9		6/32	18.8			26	4.5	50	9.4		
180		4/9	3/14	1/9	9/15		17/43	39.5	100	39.5	42	10.6				
500		2/5	0/9	6/9	6/9		14/32	43.8			25	10.9			50	21.8
800		0/5	0/9	6/9	6/9		12/32	37.5			5	1.9			50	19.0
Separation Efficiency (Total Pounds Separated per Hundred Pounds of Sand)									39.5		34.5		10.9		40.8	

TABLE III
PERFORMANCE FACTORS FOR
INLET CONFIGURATION 2 WITH LOW AIRFLOW

Computed Separation Data									Separation Efficiency for Standard Particle Size Distribution							
									#70 Sand 70-400 Microns		MIL-E-5007-C 0-1000 Microns		#140 Silica Flour 0-100 Microns		500-800 Microns	
Particle Diameter (d) in Microns	Number of Particles Trapped / Number of Particles						(Total Trapped) /(Total Particles)	Separation Efficiency for Particles of Diameter d - %	Pounds Per Hundred in Size Range Characterized by Diameter d	Pounds Per Hundred Separated in This Size Range	Pounds Per Hundred in Size Range Characterized by Diameter d	Pounds Per Hundred Separated in This Size Range	Pounds Per Hundred in Size Range Characterized by Diameter d	Pounds Per Hundred Separated in This Size Range	Pounds Per Hundred in Size Range Characterized by Diameter d	Pounds Per Hundred Separated in This Size Range
	A	B	C	D	E	F										
10	-	2/5	1/9	2/9	2/9		6/32	18.8			2	3.6	50	9.4		
70	-	2/5	1/9	2/9	2/9		6/32	18.8*			26	4.9	50	9.4		
180	3/5	3/5	5/9	4/9	8/9		23/37	62.2	100	62.2	42	26.2				
500	0/5	0/5	2/9	5/8	6/7		13/34	38.3			25	9.6			50	19.1
800	0/5	0/5	2/9	5/8	6/7		13/34	38.3*			5	1.9			50	19.1
Separation Efficiency (Total Pounds Separated per Hundred Pounds of Sand)									62.2		46.2		18.8		38.2	

*Indicates Extrapolated Data

TABLE IV
PERFORMANCE FACTORS FOR
INLET CONFIGURATION 2 WITH STANDARD AIRFLOW

Computed Separation Data									Separation Efficiency for Standard Particle Size Distribution							
									#70 Sand 70-400 Microns		MIL-E-5007-C 0-1000 Microns		#140 Silica Flour 0-100 Microns		500-800 Microns	
Particle Diameter (d) in Microns	Number of Particles Trapped / Number of Particles						(Total Trapped) /(Total Particles)	Separation Efficiency for Particles of Diameter d - %	Pounds Per Hundred in Size Range Characterized by Diameter d	Pounds Per Hundred Separated in This Size Range	Pounds Per Hundred in Size Range Characterized by Diameter d	Pounds Per Hundred Separated in This Size Range	Pounds Per Hundred in Size Range Characterized by Diameter d	Pounds Per Hundred Separated in This Size Range	Pounds Per Hundred in Size Range Characterized by Diameter d	Pounds Per Hundred Separated in This Size Range
	A	B	C	D	E	F										
10	2/5	2/5	1/9	1/9	1/9		7/37	18.9			2	0.4	50	9.5		
70	3/5	3/5	3/9	3/9	6/9		18/37	48.7			26	12.6	50	24.3		
180		2/9		5/8	5/9		12/26	46.2	100	46.2	42	19.4				
500	1/5	1/5	3/9	2/9	8/9		15/37	40.5			25	10.1			50	20.3
800	1/5	2/5	1/7	2/9	6/8		12/34	35.3			5	17.7			50	17.6
Separation Efficiency (Total Pounds Separated per Hundred Pounds of Sand)									46.2		60.2		33.8		37.9	

TABLE V
PERFORMANCE FACTORS FOR
INLET CONFIGURATION 2 WITH HIGH AIRFLOW

Computed Separation Data									Separation Efficiency for Standard Particle Size Distribution							
									#70 Sand 170-400 Microns		MIL-E-5007-C 0-1000 Microns		#140 Silica Flour 0-100 Microns		500-800 Microns	
Particle Diameter (d) in Microns	Number of Particles Trapped / Number of Particles						(Total Trapped) / (Total Particles)	Separation Efficiency for Particles of Diameter d - %	Pounds Per Hundred in Size Range Characterized by Diameter d	Pounds Per Hundred Separated in This Size Range	Pounds Per Hundred in Size Range Characterized by Diameter d	Pounds Per Hundred Separated in This Size Range	Pounds Per Hundred in Size Range Characterized by Diameter d	Pounds Per Hundred Separated in This Size Range	Pounds Per Hundred in Size Range Characterized by Diameter d	Pounds Per Hundred Separated in This Size Range
	A	B	C	D	E	F										
10	2/5	2/5	1/9	1/9	1/9		7/37	18.9			2	0.4	50	9.5		
70	3/5	2/5	6/9	2/9	4/9		17/37	46.0*			26	12.0	50	23.0		
180	3/5	2/5	6/9	2/9	4/9		17/37	46.0	100	46.0	42	19.3				
500	0/5	1/5	0/6	0/8	5/8		6/32	18.7*			25	4.7			50	9.4
800	0/5	1/5	0/6	0/8	5/8		6/32	18.7			5	0.9			50	9.4
Separation Efficiency (Total Pounds Separated per Hundred Pounds of Sand)									46.0		37.3		32.5		18.8	

*Indicates Extrapolated Data

TABLE VI
PERFORMANCE FACTORS FOR
INLET CONFIGURATION 4 WITH LOW AIRFLOW

Computed Separation Data									Separation Efficiency for Standard Particle Size Distribution							
									#70 Sand 70-400 Microns		MIL-E-5007-C 0-1000 Microns		#140 Silica Flour 0-100 Microns		500-800 Microns	
Particle Diameter (d) in Microns	Number of Particles Trapped / Number of Particles						(Total Trapped) / (Total Particles)	Separation Efficiency for Particles of Diameter d - %	Pounds Per Hundred in Size Range Characterized by Diameter d	Pounds Per Hundred Separated in This Size Range	Pounds Per Hundred in Size Range Characterized by Diameter d	Pounds Per Hundred Separated in This Size Range	Pounds Per Hundred in Size Range Characterized by Diameter d	Pounds Per Hundred Separated in This Size Range	Pounds Per Hundred in Size Range Characterized by Diameter d	Pounds Per Hundred Separated in This Size Range
	A	B	C	D	E	F										
10	3/5	3/5	9/9	9/9	9/9		33/37	89.0			2	1.8	50	44.4		
70	5/5	5/5	9/9	9/9	9/9		37/37	100.0*			26	26.0	50	50.0		
180	5/5	5/5	9/9	9/9	9/9		37/37	100.0	100	100	42	42.0				
500	4/4	5/5	8/8	7/8	9/9		33/34	97.0*			25	24.2			50	48.5
800	4/4		8/8	7/8	9/9		28/29	96.8			5	4.8			50	48.0
Separation Efficiency (Total Pounds Separated per Hundred Pounds of Sand)									100		98.8		94.4		96.5	

*Indicates Extrapolated Data

TABLE VII
PERFORMANCE FACTORS FOR
INLET CONFIGURATION 4 WITH STANDARD AIRFLOW

Computed Separation Data									Separation Efficiency for Standard Particle Size Distribution							
									#70 Sand 70-400 Microns		MIL-E-5007-C 0-1000 Microns		#140 Silica Flour 0-100 Microns		500-800 Microns	
Particle Diameter (d) in Microns	Number of Particles Trapped / Number of Particles						(Total Trapped) / (Total Particles)	Separation Efficiency for Particles of Diameter d - %	Pounds Per Hundred in Size Range Characterized by Diameter d	Pounds Per Hundred Separated in This Size Range	Pounds Per Hundred in Size Range Characterized by Diameter d	Pounds Per Hundred Separated in This Size Range	Pounds Per Hundred in Size Range Characterized by Diameter d	Pounds Per Hundred Separated in This Size Range	Pounds Per Hundred in Size Range Characterized by Diameter d	Pounds Per Hundred Separated in This Size Range
	A	B	C	D	E	F										
10	2/4	2/4	8/8	8/8	9/9		29/33	87.8			2	1.8	50	44		
70	5/5	5/5	9/9	9/9	9/9		37/37	100.0			26	26.0	50	50		
180			8/8	8/8	8/8	9/9	34/34	100.0	100	100	42	42.0				
500	5/5	5/5	8/9	9/9	9/9		36/37	97.4			25	24.4			50	48.7
800	4/4	4/4		9/9	8/9		25/26	96.0			5	4.8			50	48.0
Separation Efficiency (Total Pounds Separated per Hundred Pounds of Sand)									100		99.0		94.0		96.7	

TABLE VIII
PERFORMANCE FACTORS FOR
INLET CONFIGURATION 4 WITH HIGH AIRFLOW

Computed Separation Data									Separation Efficiency for Standard Particle Size Distribution							
									#70 Sand 70-400 Microns		MIL-E-5007-C 0-1000 Microns		#140 Silica Flour 0-100 Microns		500-800 Microns	
Particle Diameter (d) in Microns	Number of Particles Trapped / Number of Particles						(Total Trapped) /(Total Particles)	Separation Efficiency for Particles of Diameter d - %	Pounds Per Hundred in Size Range Characterized by Diameter d	Pounds Per Hundred Separated in This Size Range	Pounds Per Hundred in Size Range Characterized by Diameter d	Pounds Per Hundred Separated in This Size Range	Pounds Per Hundred in Size Range Characterized by Diameter d	Pounds Per Hundred Separated in This Size Range	Pounds Per Hundred in Size Range Characterized by Diameter d	Pounds Per Hundred Separated in This Size Range
	A	B	C	D	E	F										
10	3/5	3/5	9/9	9/9	9/9		33/37	89.2			2	1.8	50	44.8		
70	5/5	5/5	9/9	9/9	9/9		37/37	100.0*			26	26.0	50	50.0		
180	5/5	5/5	9/9	9/9	9/9		37/37	100.0	100	100	42	42.0				
500	4/5	5/5	8/9	9/9	9/9		35/37	94.8*			25	24.7			50	47.4
800	4/5	5/5	7/9	9/9	9/9		34/37	96.0			5	4.8			50	48.0
Separation Efficiency (Total Pounds Separated per Hundred Pounds of Sand)									100		99.3		94.8		95.4	

*Indicates Extrapolated Data

TABLE IX
PERFORMANCE FACTORS FOR
INLET CONFIGURATION 5 WITH STANDARD AIRFLOW

Computed Separation Data									Separation Efficiency for Standard Particle Size Distribution							
									#70 Sand 70-400 Microns		MIL-E-5007-C 0-1000 Microns		#140 Silica Flour 0-100 Microns		500-800 Microns	
Particle Diameter (d) in Microns	Number of Particles Trapped / Number of Particles						(Total Trapped) /(Total Particles)	Separation Efficiency for Particles of Diameter d - %	Pounds Per Hundred in Size Range Characterized by Diameter d	Pounds Per Hundred Separated in This Size Range	Pounds Per Hundred in Size Range Characterized by Diameter d	Pounds Per Hundred Separated in This Size Range	Pounds Per Hundred in Size Range Characterized by Diameter d	Pounds Per Hundred Separated in This Size Range	Pounds Per Hundred in Size Range Characterized by Diameter d	Pounds Per Hundred Separated in This Size Range
	A	B	C	D	E	F										
10		2/5	1/9	2/9	2/9		7/32	21.8			2	0.4	50	10.9		
70	2/4	2/4	2/9	2/9	3/9		11/35	31.4			26	8.2	50	15.7		
180	1/4	3/5	1/8	3/9	7/9		15/35	42.8	100	42.8	42	18.0				
500	1/4	3/5	1/6	5/8	6/8		16/31	51.6			25	12.9			50	25.8
800	1/4	2/5	0/5	4/8	8/8		15/30	50.0			5	2.5			50	25.0
Separation Efficiency (Total Pounds Separated per Hundred Pounds of Sand)									42.8		42.0		26.6		50.8	

TABLE X
PERFORMANCE FACTORS FOR
INLET CONFIGURATION 6 WITH STANDARD AIRFLOW

Computed Separation Data									Separation Efficiency for Standard Particle Size Distribution							
									#70 Sand 70-400 Microns		MIL-E-5007-C 0-1000 Microns		#140 Silica Flour 0-100 Microns		500-800 Microns	
Particle Diameter (d) in Microns	Number of Particles Trapped / Number of Particles						(Total Trapped) /(Total Particles)	Separation Efficiency for Particles of Diameter d - %	Pounds Per Hundred in Size Range Characterized by Diameter d	Pounds Per Hundred Separated in This Size Range	Pounds Per Hundred in Size Range Characterized by Diameter d	Pounds Per Hundred Separated in This Size Range	Pounds Per Hundred in Size Range Characterized by Diameter d	Pounds Per Hundred Separated in This Size Range	Pounds Per Hundred in Size Range Characterized by Diameter d	Pounds Per Hundred Separated in This Size Range
	A	B	C	D	E	F										
10	0/10	0/10	3/9	3/8	2/9		8/46	17.4			2	0.4	50	8.7		
70	6/8	8/10	8/8	8/8	8/8		38/42	90.5			26	23.5	50	45.3		
180	6/8	8/8	8/8	8/8	8/8		38/40	95.0	100	95	42	39.8				
500	10/10	6/10	9/9	9/9	7/9		41/47	87.2			25	21.8			50	43.6
800	8/10	2/10	8/9	8/9	7/8		33/46	71.8			5	3.6			50	35.9
Separation Efficiency (Total Pounds Separated per Hundred Pounds of Sand)									95.0		89.1		54.0		79.5	

TABLE XI
PERFORMANCE FACTORS FOR
INLET CONFIGURATION 7 WITH LOW AIRFLOW

Computed Separation Data									Separation Efficiency for Standard Particle Size Distribution							
									#70 Sand 70-400 Microns		MIL-E-5007-C 0-1000 Microns		#140 Silica Flour 0-100 Microns		500-800 Microns	
Particle Diameter (d) in Microns	Number of Particles Trapped / Number of Particles						(Total Trapped) /(Total Particles)	Separation Efficiency for Particles of Diameter d - %	Pounds Per Hundred in Size Range Characterized by Diameter d	Pounds Per Hundred Separated in This Size Range	Pounds Per Hundred in Size Range Characterized by Diameter d	Pounds Per Hundred Separated in This Size Range	Pounds Per Hundred in Size Range Characterized by Diameter d	Pounds Per Hundred Separated in This Size Range	Pounds Per Hundred in Size Range Characterized by Diameter d	Pounds Per Hundred Separated in This Size Range
	A	B	C	D	E	F										
10	0/10	0/10	3/9	2/9	2/9		7/47	14.8			2	0.3	50	7.4		
70	8/10	10/10	9/9	9/9	9/9		45/47	95.8*			26	24.8	50	47.9		
180	8/10	10/10	9/9	9/9	9/9		45/47	95.8	100	95.8	42	40.1				
500	8/10	6/10	5/7	5/7	5/5		29/39	74.3*			25	18.6			50	37.2
800	8/10	6/10	5/7	5/7	5/5		29/39	74.3			5	3.7			50	37.2
Separation Efficiency (Total Pounds Separated per Hundred Pounds of Sand)									95.8		87.5		55.3		74.4	

*Indicates Extrapolated Data

TABLE XII
PERFORMANCE FACTORS FOR
INLET CONFIGURATION 7 WITH STANDARD AIRFLOW

Computed Separation Data									Separation Efficiency for Standard Particle Size Distribution							
									#70 Sand 70-400 Microns		MIL-E-5007-C 0-1000 Microns		#140 Silica Flour 0-100 Microns		500-800 Microns	
Particle Diameter (d) in Microns	Number of Particles Trapped / Number of Particles						(Total Trapped) /(Total Particles)	Separation Efficiency for Particles of Diameter d - %	Pounds Per Hundred in Size Range Characterized by Diameter d	Pounds Per Hundred Separated in This Size Range	Pounds Per Hundred in Size Range Characterized by Diameter d	Pounds Per Hundred Separated in This Size Range	Pounds Per Hundred in Size Range Characterized by Diameter d	Pounds Per Hundred Separated in This Size Range	Pounds Per Hundred in Size Range Characterized by Diameter d	Pounds Per Hundred Separated in This Size Range
	A	B	C	D	E	F										
10	2/10	4/10	6/9	6/9	6/9		24/47	51.0			2	1.0	50	25.5		
70	10/10	10/10	9/9	9/9	9/9		47/47	100.0			26	26.0	50	50.0		
180		16/18	17/17	17/17	9/9		59/61	96.8	100	96.8	42	40.6				
500	10/10	8/10	9/9	9/9	7/8		43/46	93.5			25	23.4			50	46.8
800	10/10	8/10	9/9	9/9	7/8		43/46	93.5			5	4.7			50	46.8
Separation Efficiency (Total Pounds Separated per Hundred Pounds of Sand)									96.8		95.7		75.5		93.6	

TABLE XIII
PERFORMANCE FACTORS FOR
INLET CONFIGURATION 7 WITH HIGH AIRFLOW

Computed Separation Data									Separation Efficiency for Standard Particle Size Distribution							
									#70 Sand 70-400 Microns		MIL-E-5007-C 0-1000 Microns		#140 Silica Flour 0-100 Microns		500-800 Microns	
Particle Diameter (d) in Microns	Number of Particles Trapped / Number of Particles						(Total Trapped) /(Total Particles)	Separation Efficiency for Particles of Diameter d - %	Pounds Per Hundred in Size Range Characterized by Diameter d	Pounds Per Hundred Separated in This Size Range	Pounds Per Hundred in Size Range Characterized by Diameter d	Pounds Per Hundred Separated in This Size Range	Pounds Per Hundred in Size Range Characterized by Diameter d	Pounds Per Hundred Separated in This Size Range	Pounds Per Hundred in Size Range Characterized by Diameter d	Pounds Per Hundred Separated in This Size Range
	A	B	C	D	E	F										
10	4/10	4/10	6/9	6/9	6/9		26/47	55.3			2	1.1	50	27.7		
70	8/10	8/10	9/9	9/9	9/9		43/47	91.5*			26	23.6	50	45.7		
180	8/10	8/10	9/9	9/9	9/9		43/47	91.5	100	91.5	42	38.4				
500	6/6	8/10	9/9	9/9	6/8		38/42	90.5*			25	22.6			50	45.2
800	6/6	8/10		9/9	6/8		29/33	88.0			5	4.4			50	44.0
Separation Efficiency (Total Pounds Separated per Hundred Pounds of Sand)									91.5		90.3		73.4		88.2	

*Indicates Extrapolated Data

TABLE XIV
SUMMARY OF PARTICLE SEPARATION EFFICIENCIES BY PERCENT SEPARATED BY WEIGHT

Inlet Type	A									C			D	E			Experimental
Configuration	1	2			6	7				4			5	4 and 7			
Description	Basic Symmetrical Inlet, Downwash, 5% Secondary Flow	Basic Symmetrical Inlet, Downwash, 10% Secondary Flow			Basic Symmetrical Inlet, No Downwash, 5% Secondary Flow	Optimized Basic Symmetrical Inlet, No Downwash, 10% Secondary Flow				Optimized Inlet With Bounce Plate, Downwash, 10% Secondary Flow			Modified Symmetrical Inlet, Downwash, 5% Secondary Flow	Simulated 3D Asymmetrical Inlet With Bounce Plate, Downwash, 10% Secondary Flow			Bench Test Data, Downwash, Apprcx 10% Secondary Flow
Particle Sizes in Microns / Airflow	Std	50% Std	Std	150% Std	Std	50% Std	Std	150% Std		50% Std	Std	150% Std	Std	50% Std	Std	150% Std	Varied
0 to 100	11	19	34	33	54	55	76	73		94	94	95	27	77	85	84	
70 to 400	40	62	46	46	95	96	97	92		100	100	100	43	98	98	96	90 to 95
500 to 800	41	38	38	19	80	74	94	88		97	97	95	51	85	96	92	
Salt Water Spray							97				92				94		
Supercooled Water			19				60				89				75		

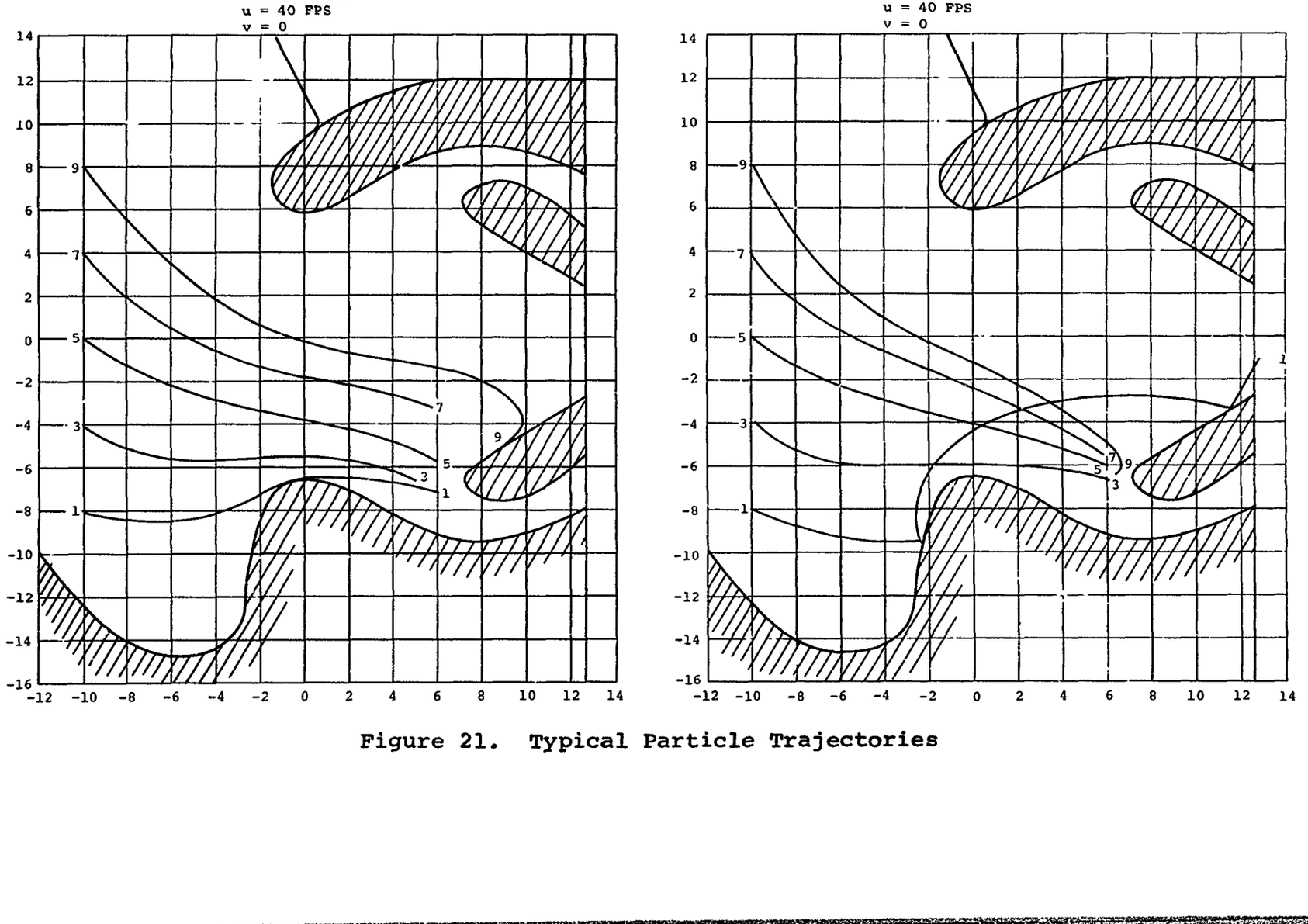

Figure 21. Typical Particle Trajectories

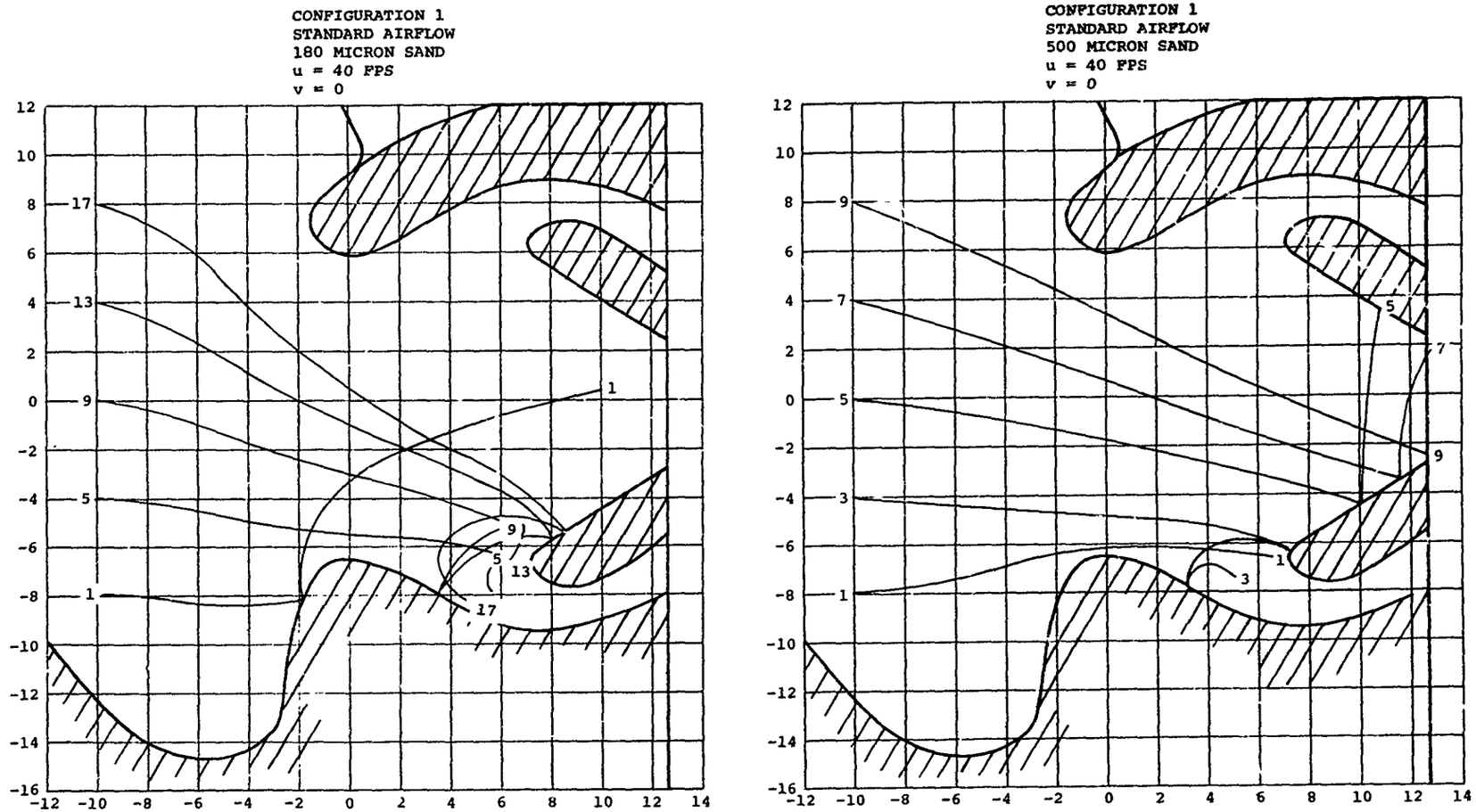

Figure 22. Typical Particle Trajectories

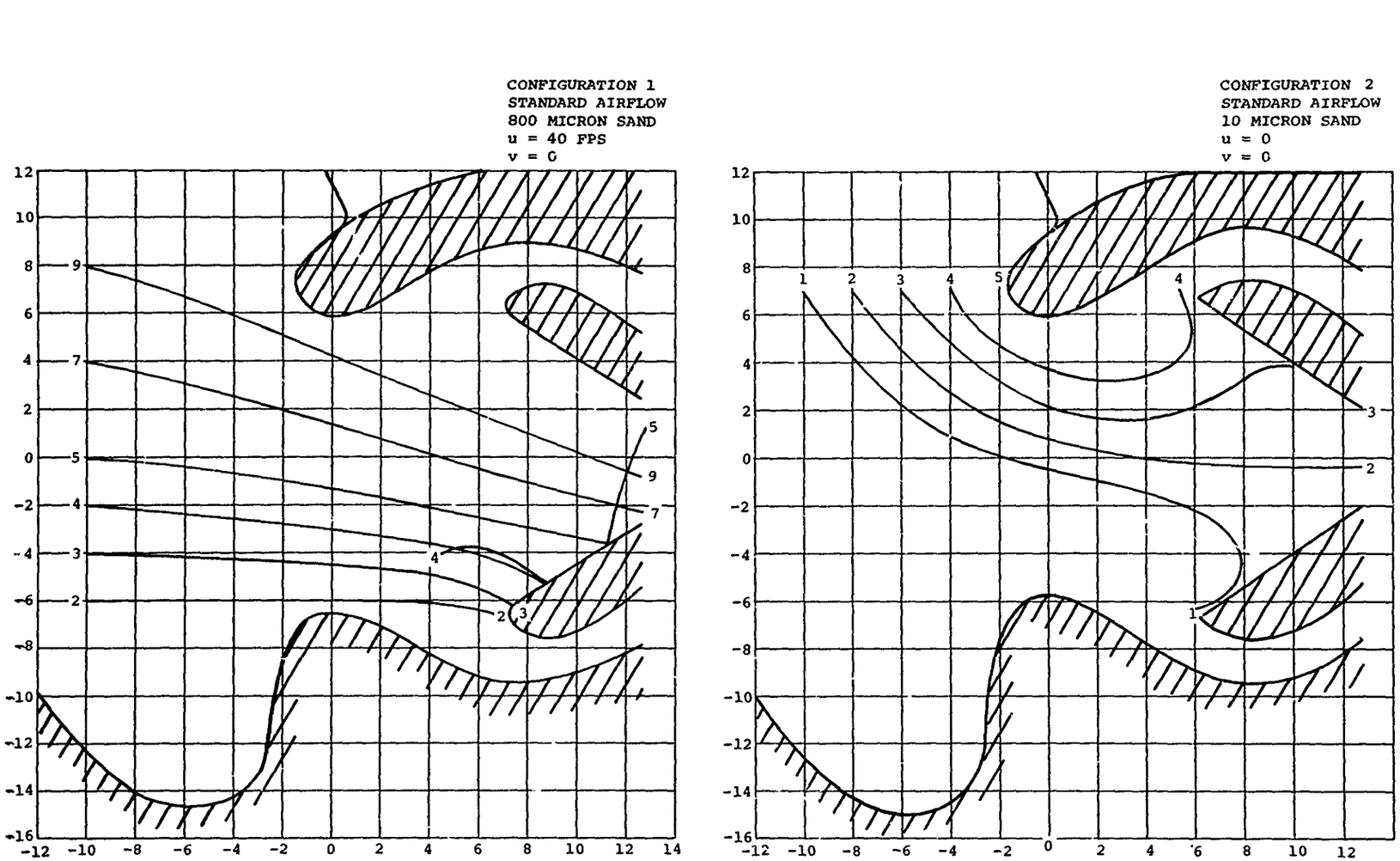

Figure 23. Typical Particle Trajectories

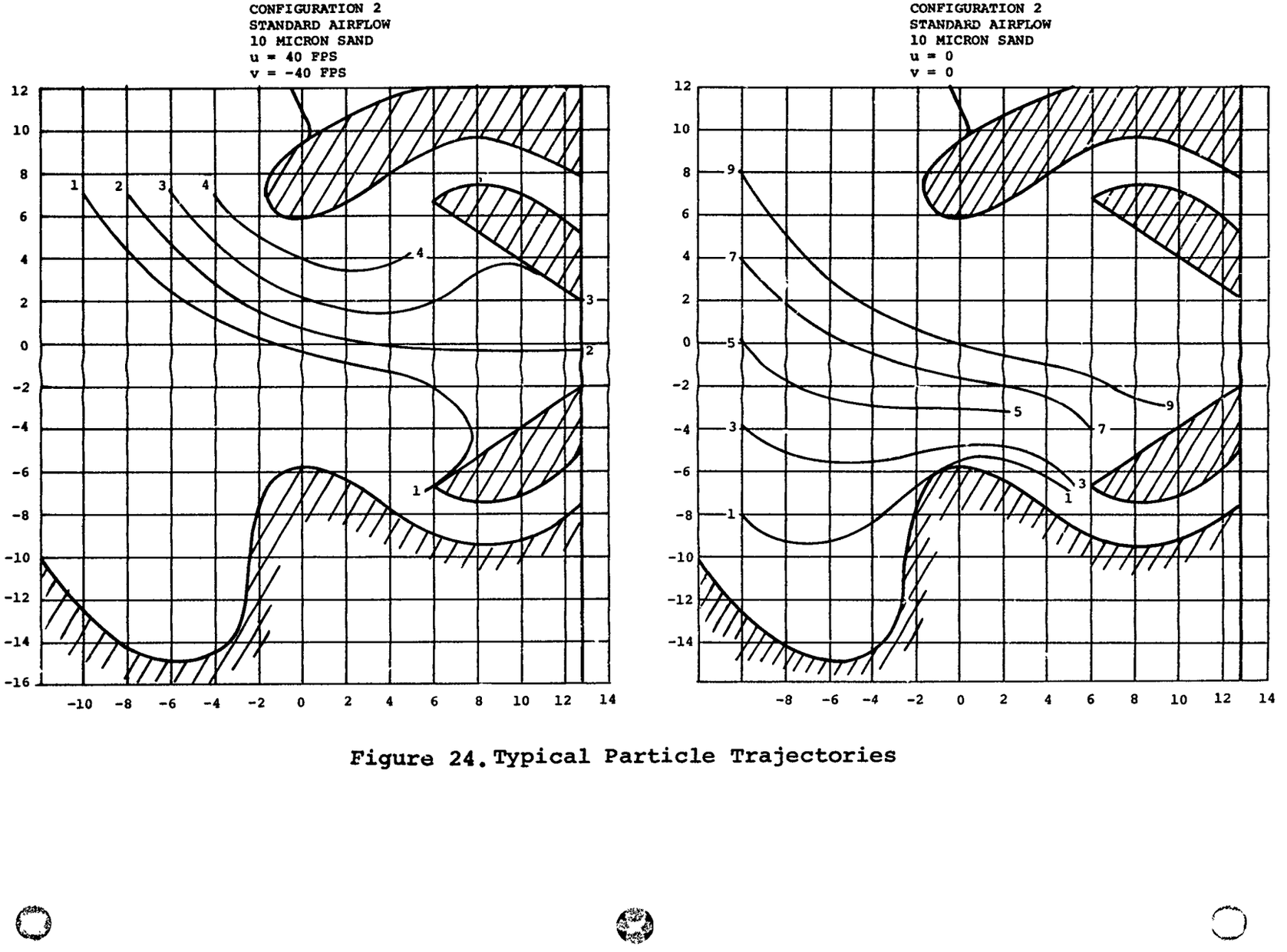

Figure 24. Typical Particle Trajectories

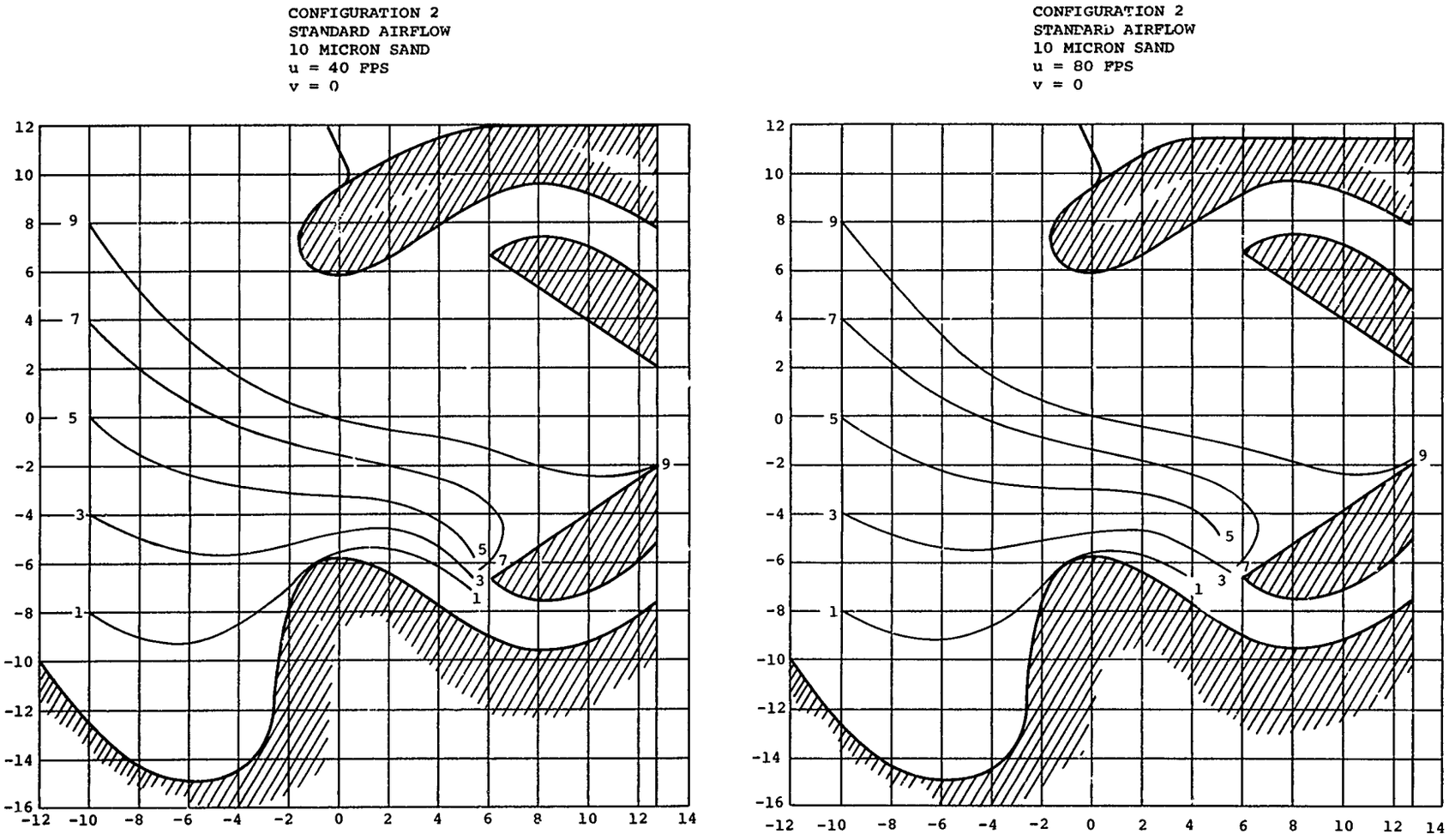

Figure 25. Typical Particle Trajectories

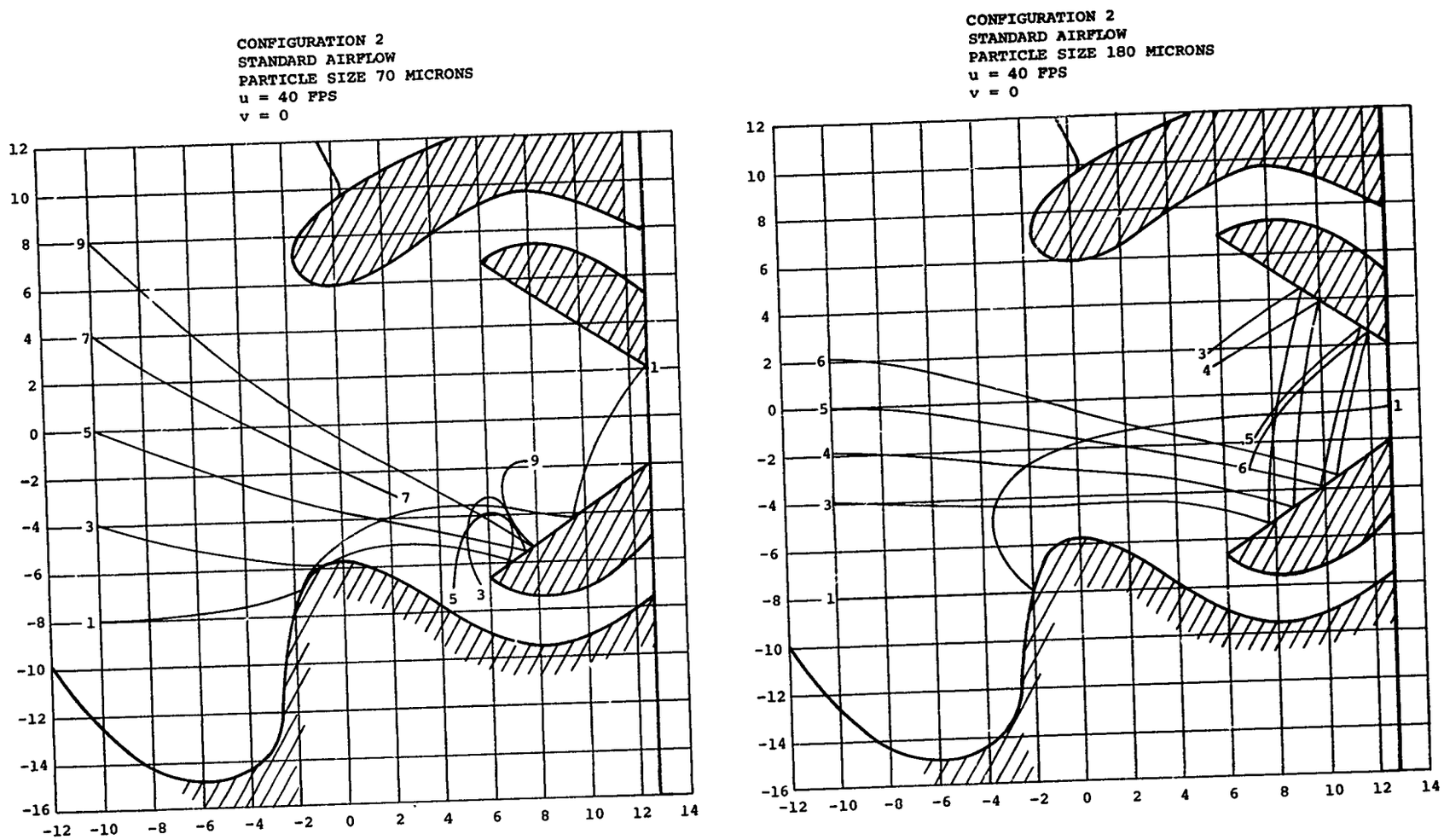

Figure 26. Typical Particle Trajectories

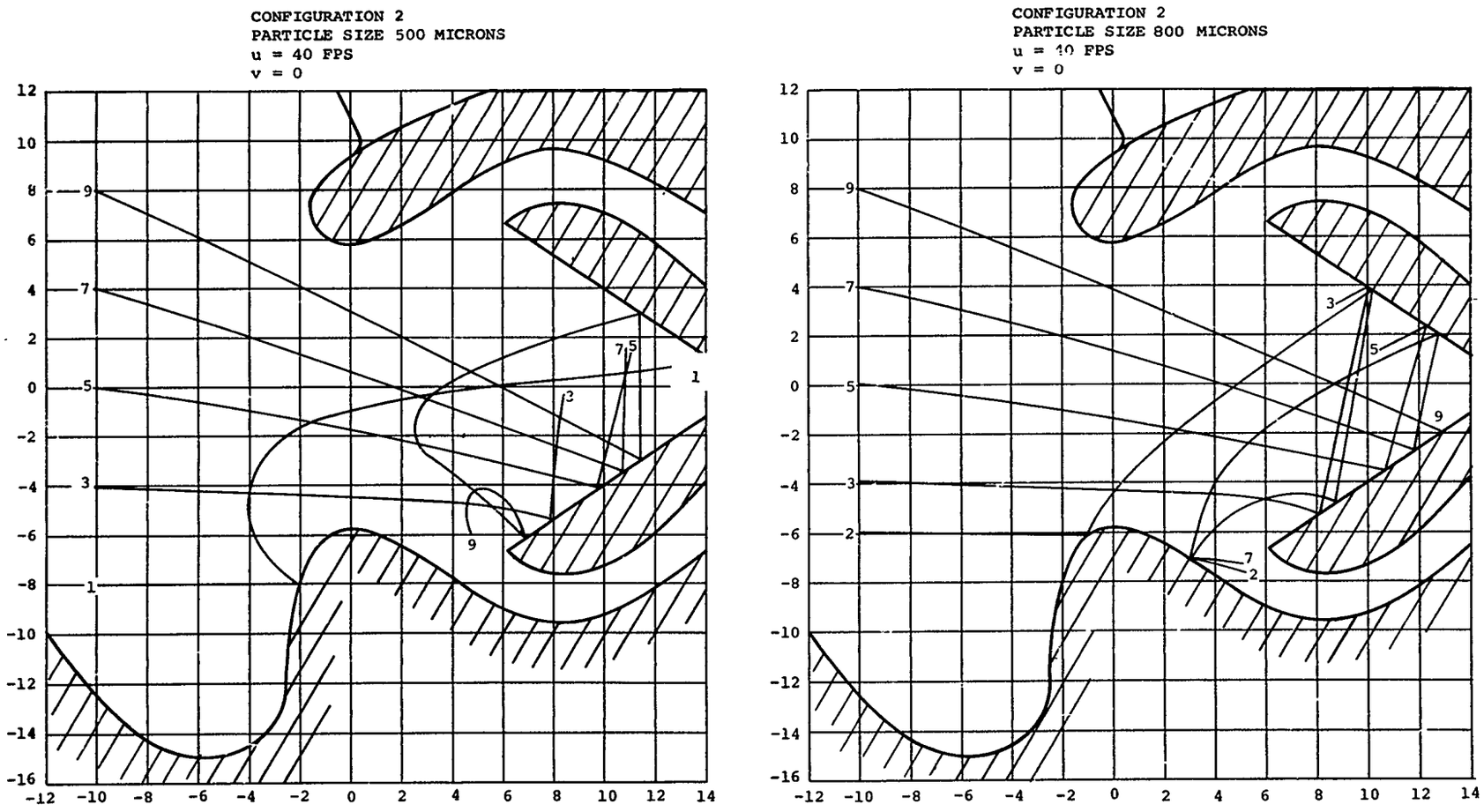

Figure 27. Typical Particle Trajectories

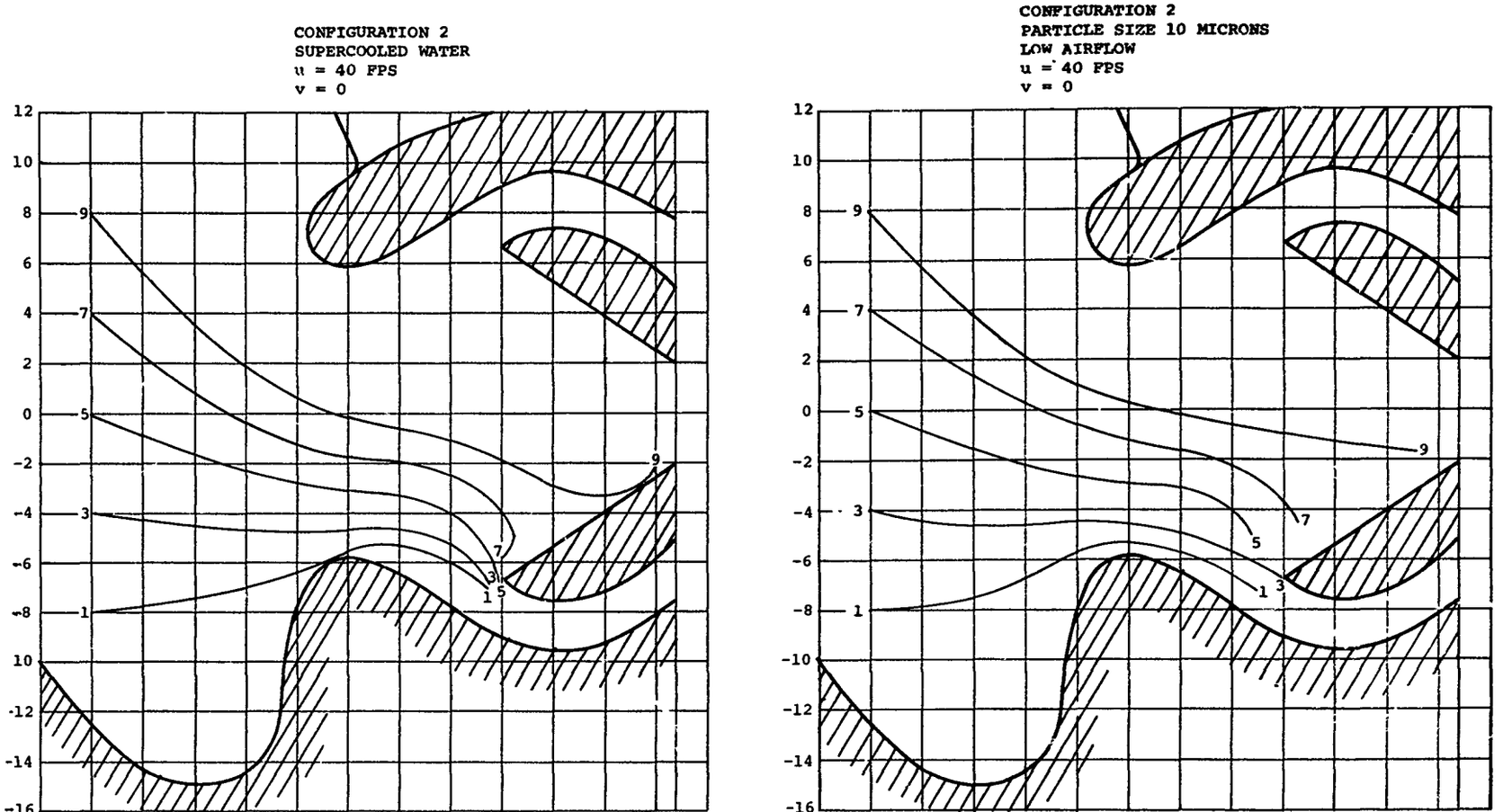

Figure 28. Typical Particle Trajectories

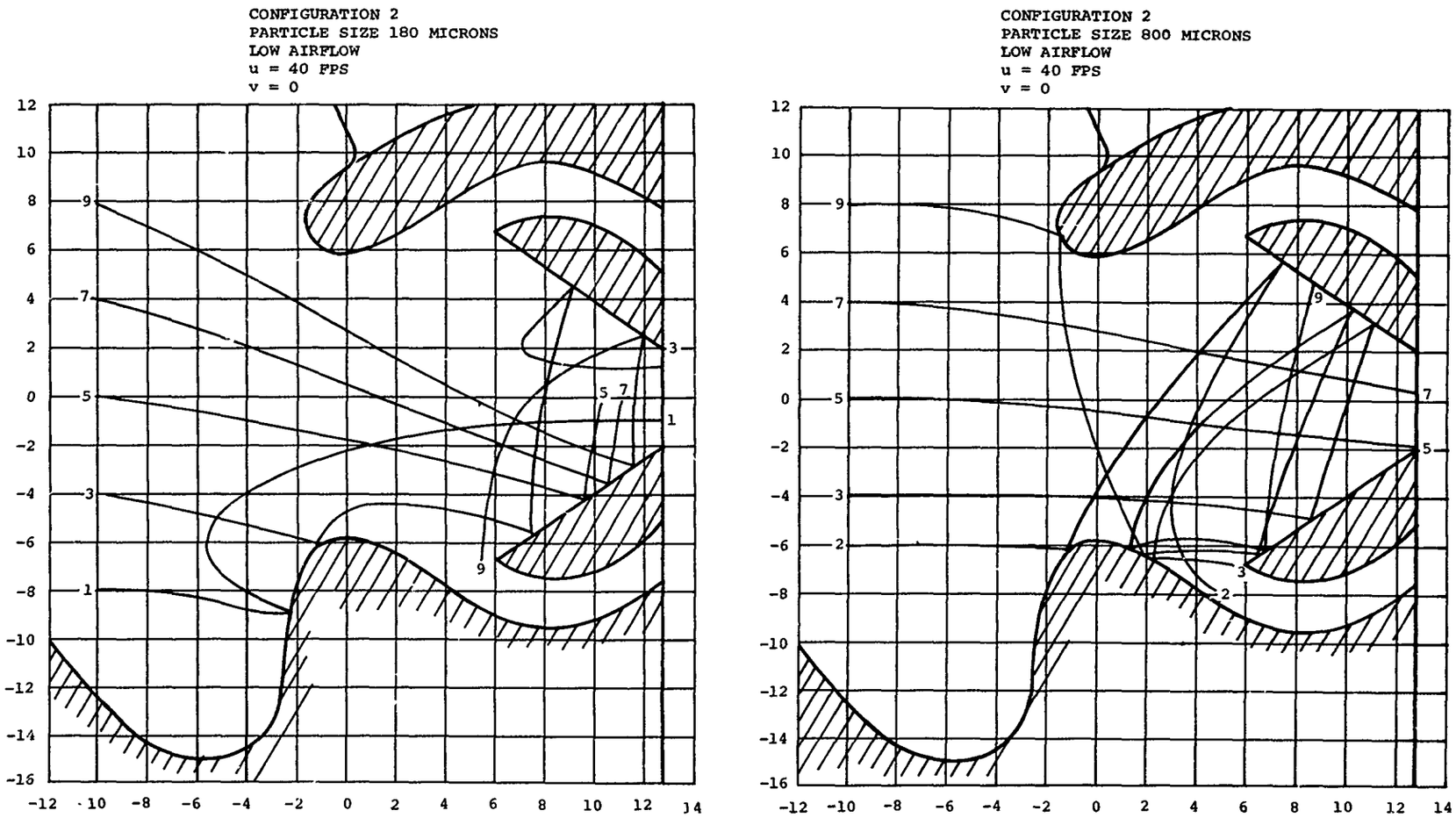

Figure 29. Typical Particle Trajectories

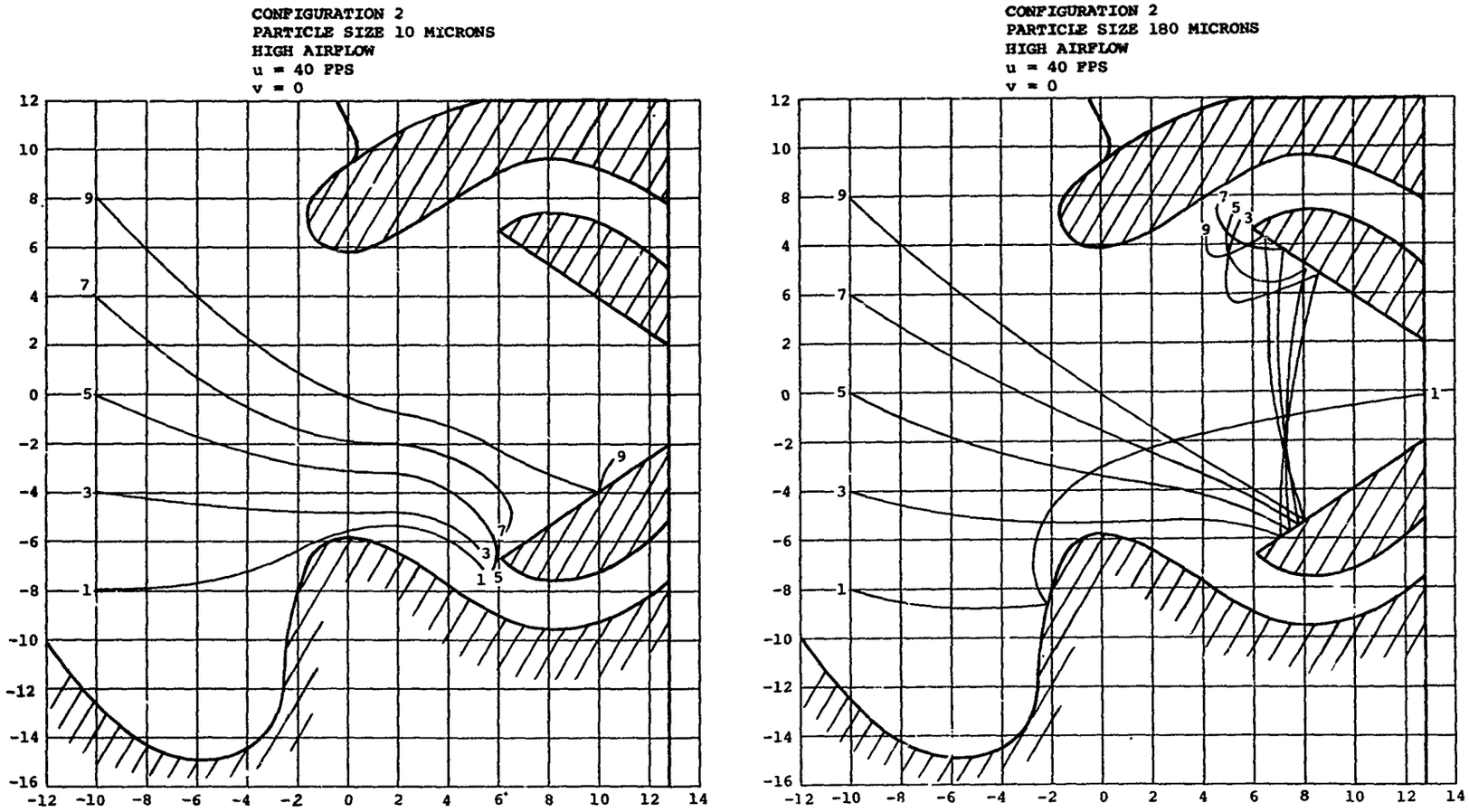

Figure 30. Typical Particle Trajectories

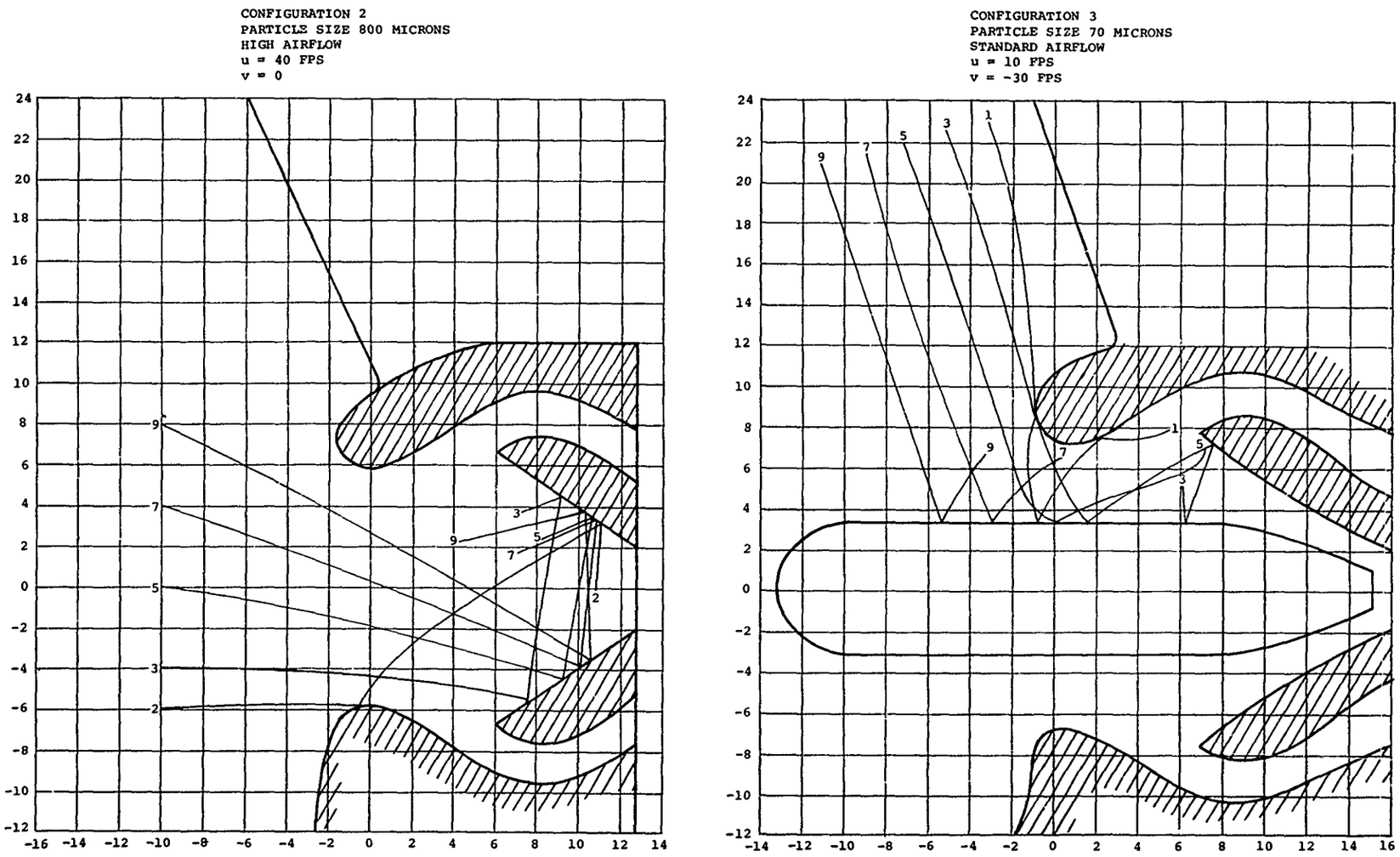

Figure 31. Typical Particle Trajectories

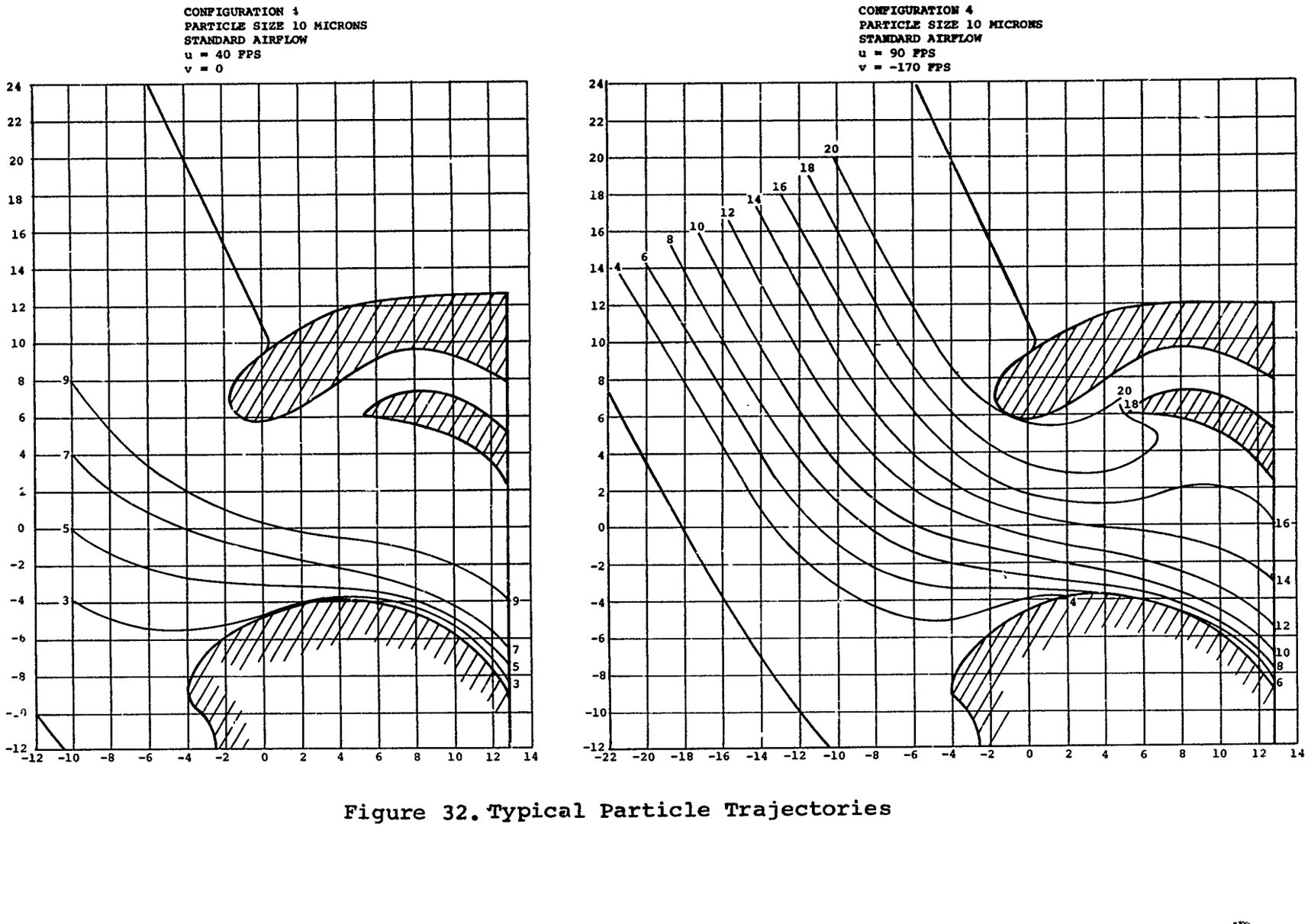

Figure 32. Typical Particle Trajectories

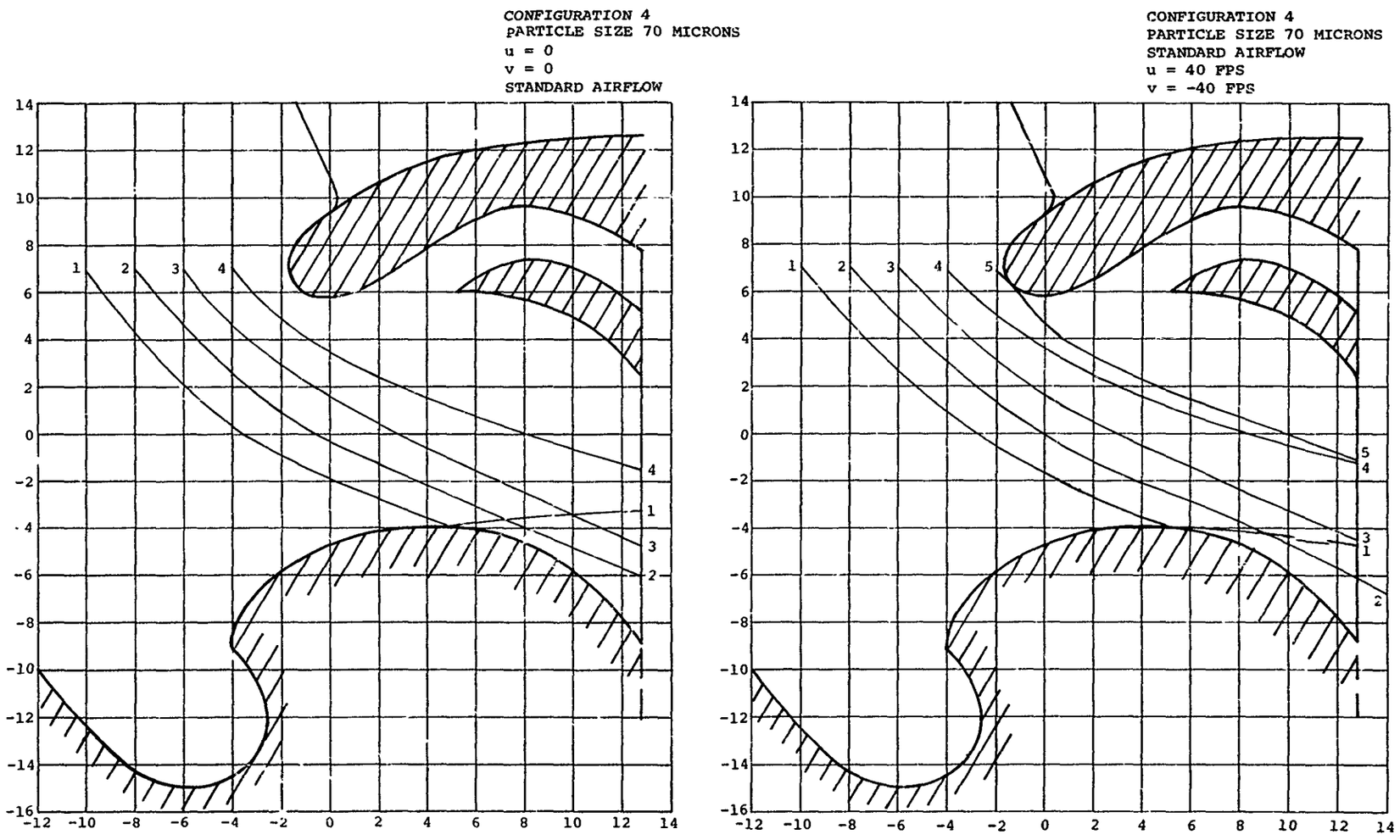

Figure 33. Typical Particle Trajectories

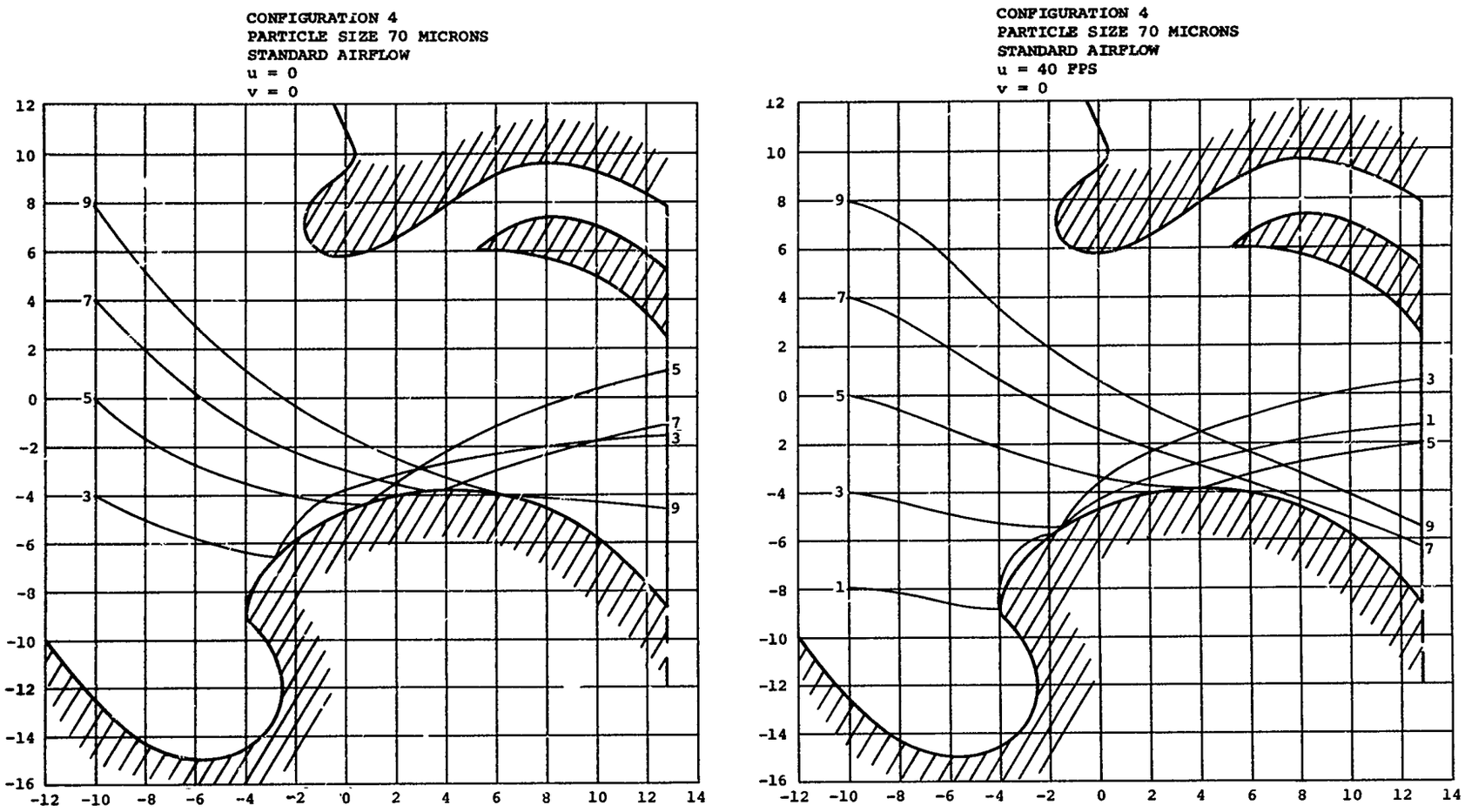

Figure 34. Typical Particle Trajectories

CONFIGURATION 4
PARTICLE SIZE 70 MICRONS
STANDARD AIRFLOW
u = 80 FPS
v = 0

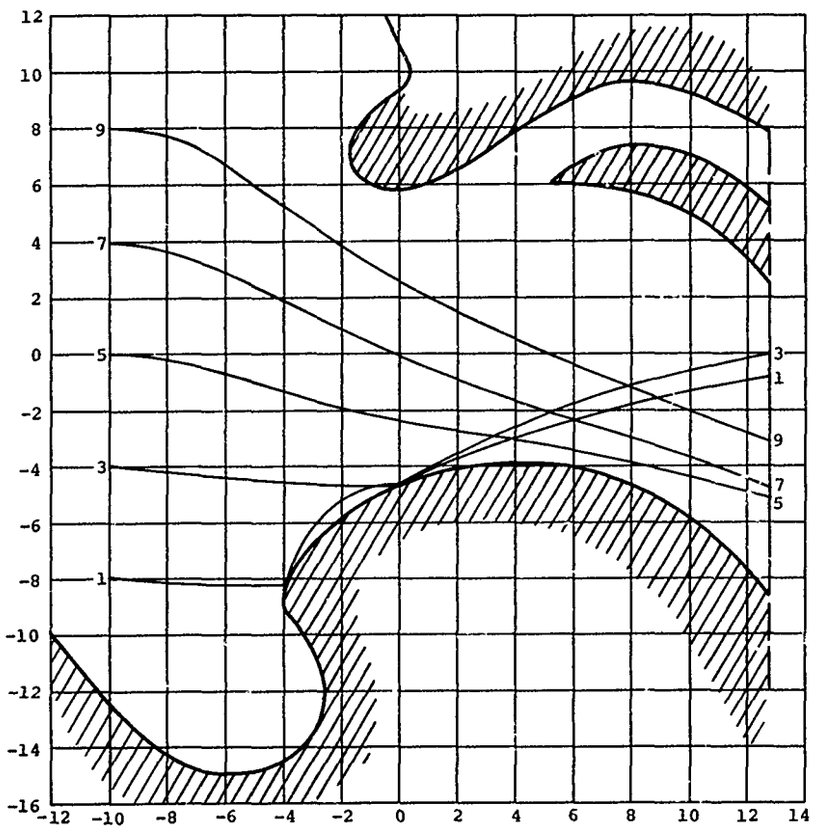

CONFIGURATION 4
PARTICLE SIZE 180 MICRONS
STANDARD AIRFLOW
u = 40 FPS
v = 0

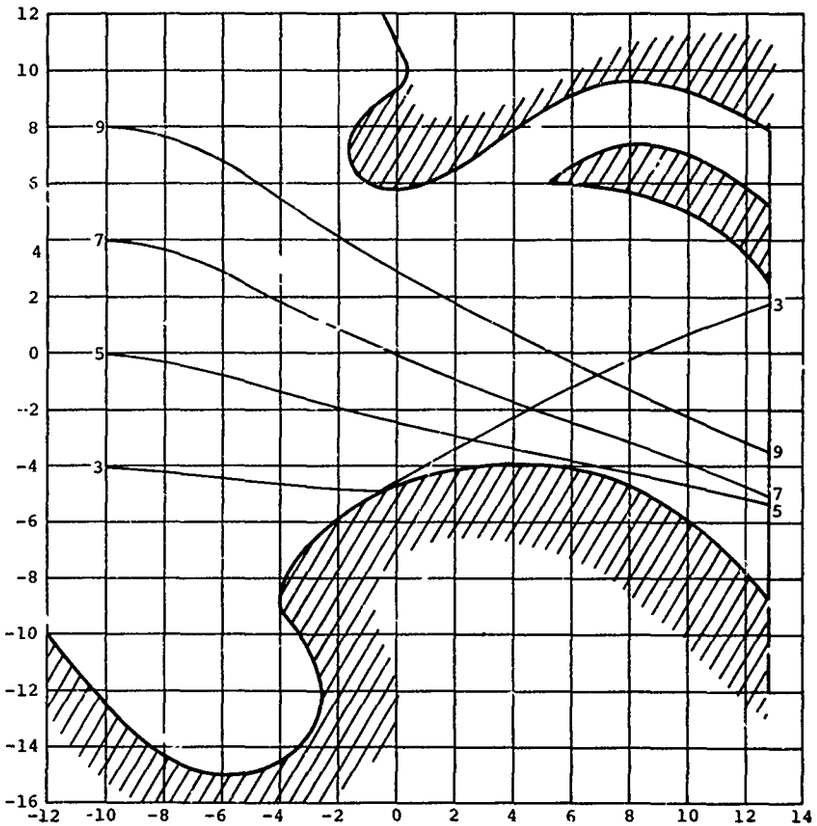

Figure 35. Typical Particle Trajectories

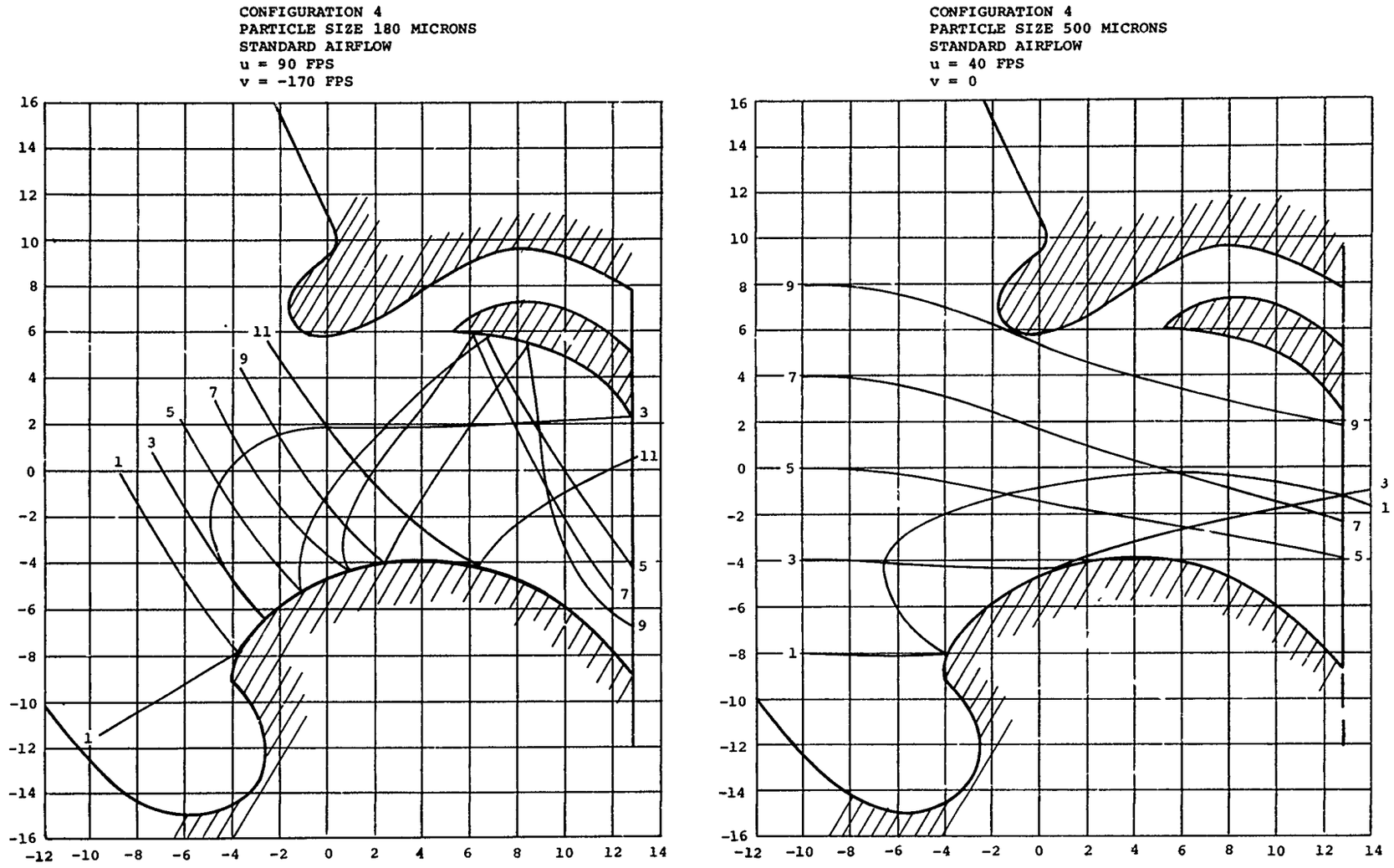

Figure 36. Typical Particle Trajectories

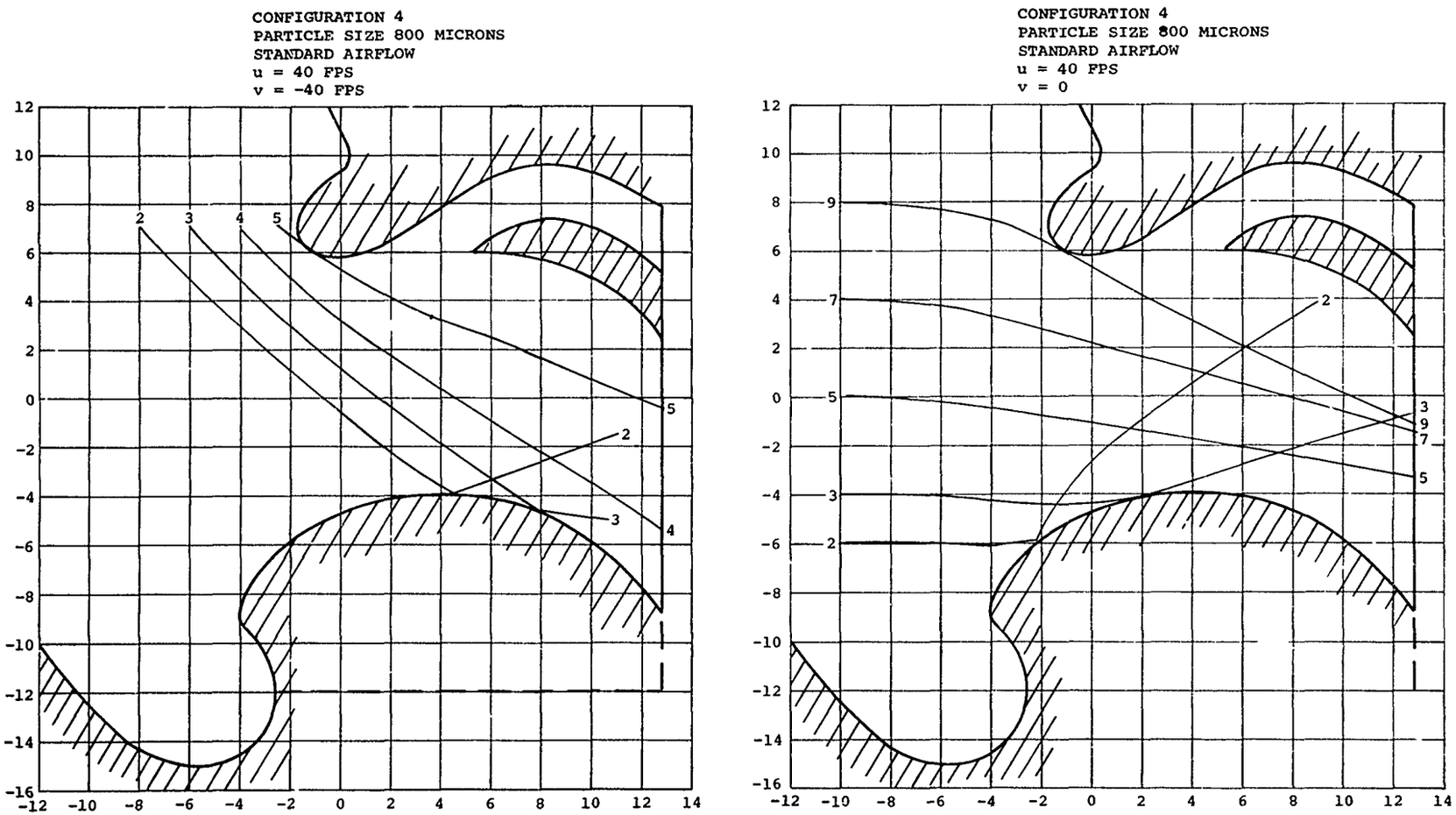

Figure 37. Typical Particle Trajectories

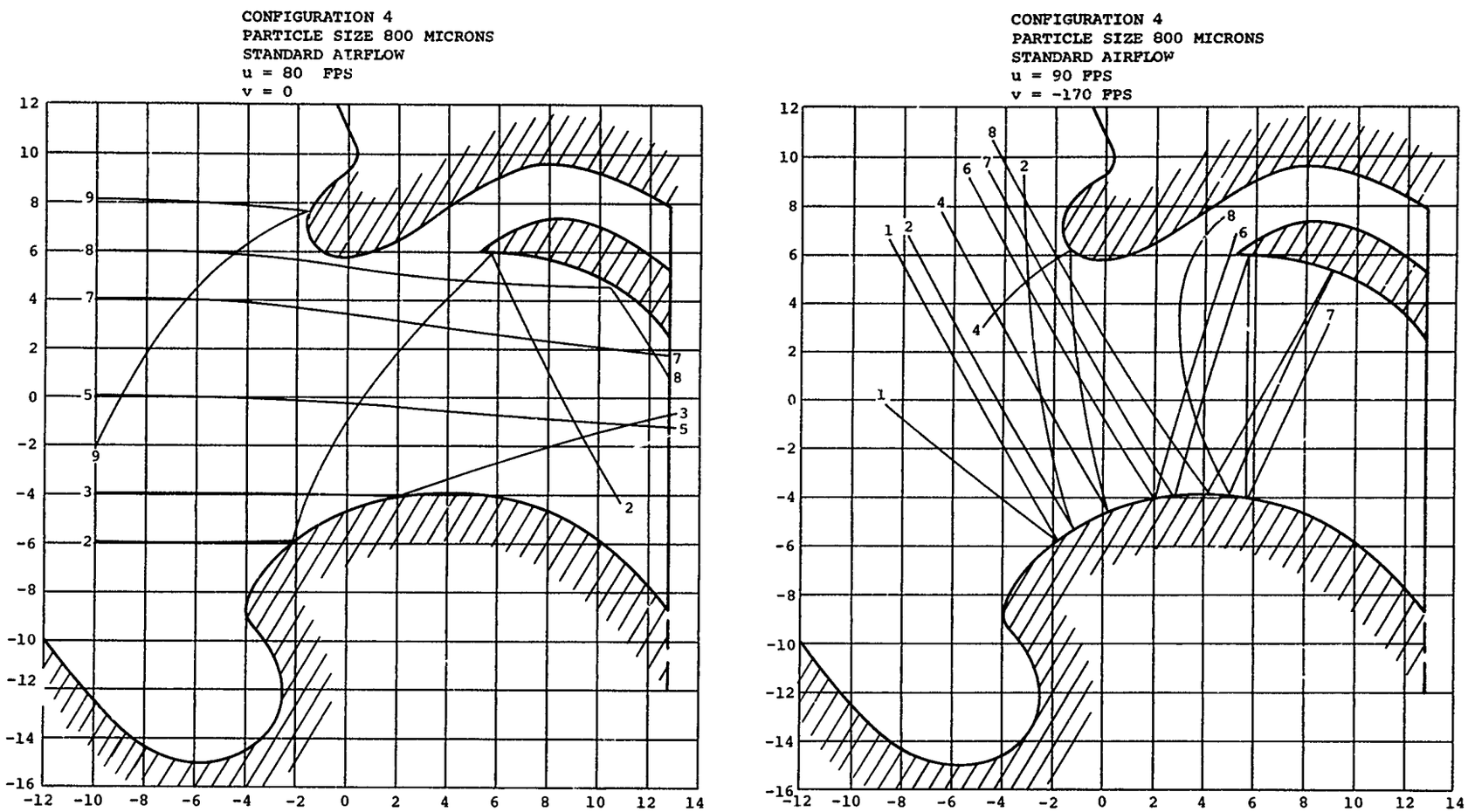

Figure 38.Typical Particle Trajectories

CONFIGURATION 4

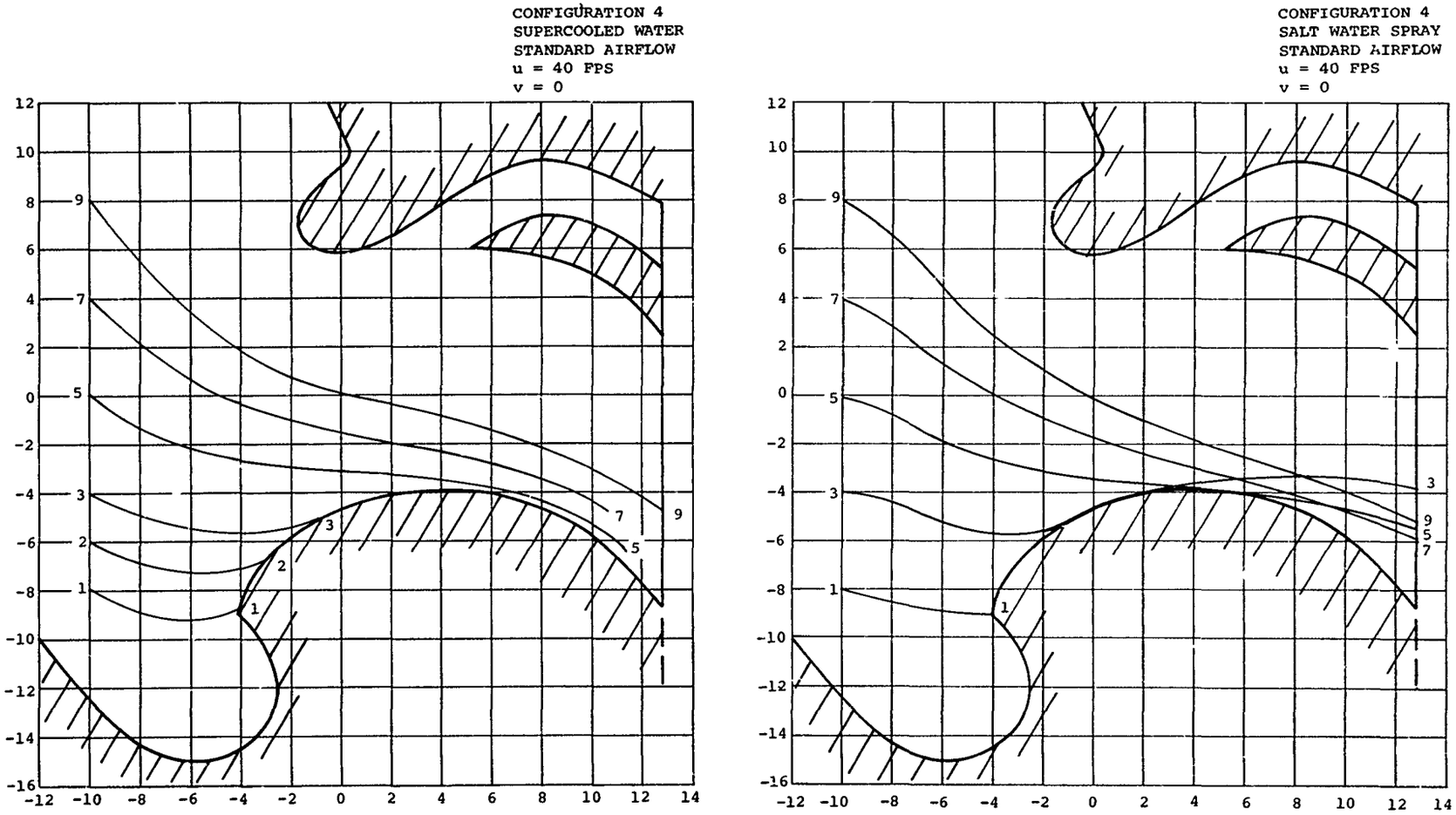

Figure 39. Typical Particle Trajectories

CONFIGURATION 4
PARTICLE SIZE 10 MICRONS
LOW AIRFLOW
u = 40 FPS
v = 0

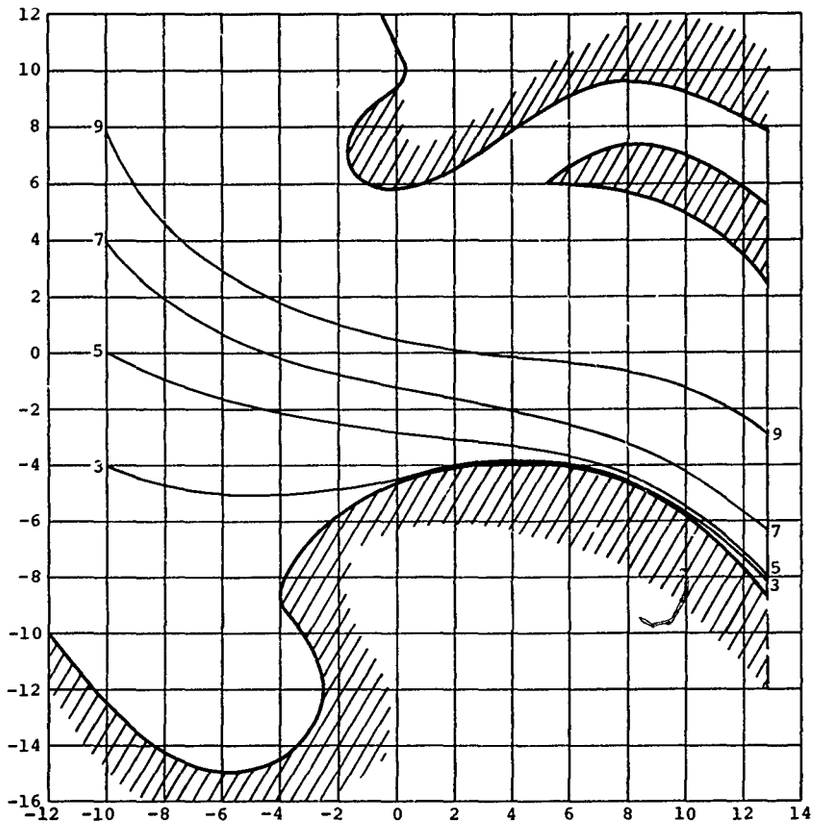

CONFIGURATION 4
PARTICLE SIZE 180 MICRONS
LOW AIRFLOW
u = 40 FPS
v = 0

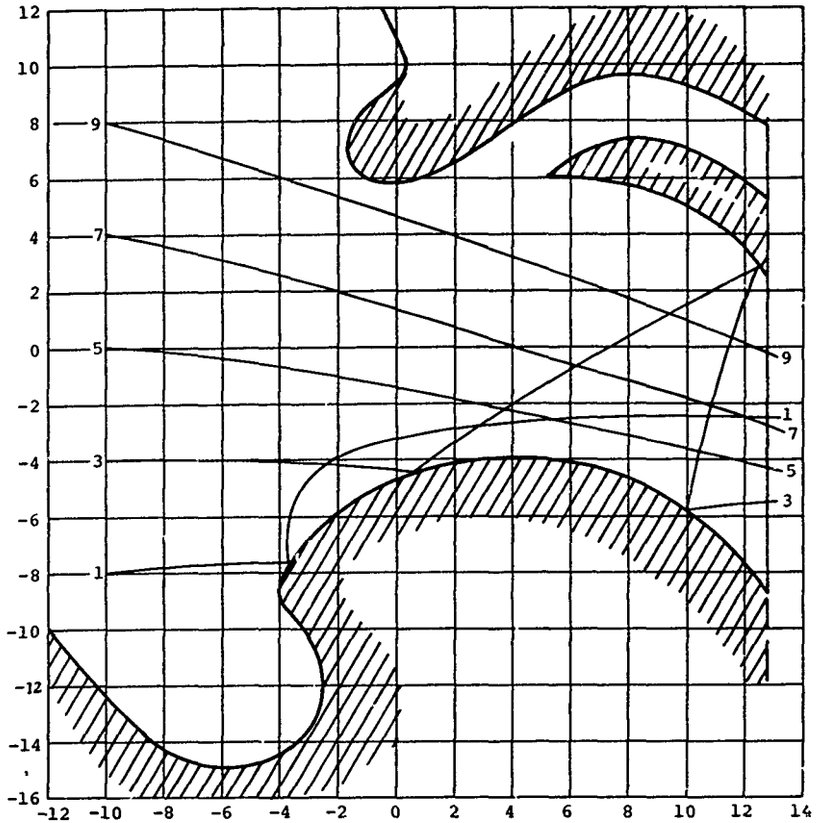

Figure 40. Typical Particle Trajectories

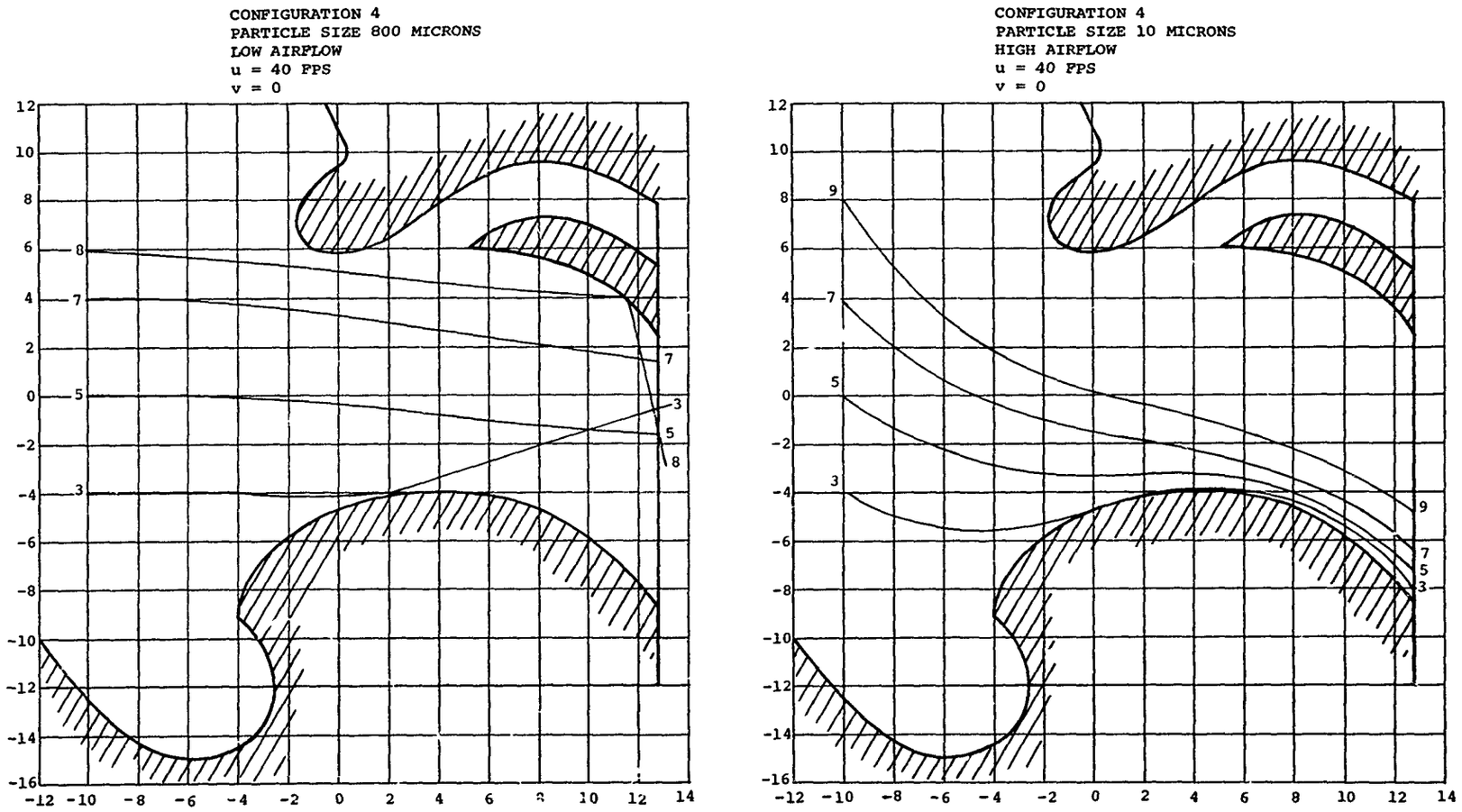

Figure 41. Typical Particle Trajectories

CONFIGURATION 4
PARTICLE SIZE 180 MICRONS
HIGH AIRFLOW
u = 40 FPS
v = 0

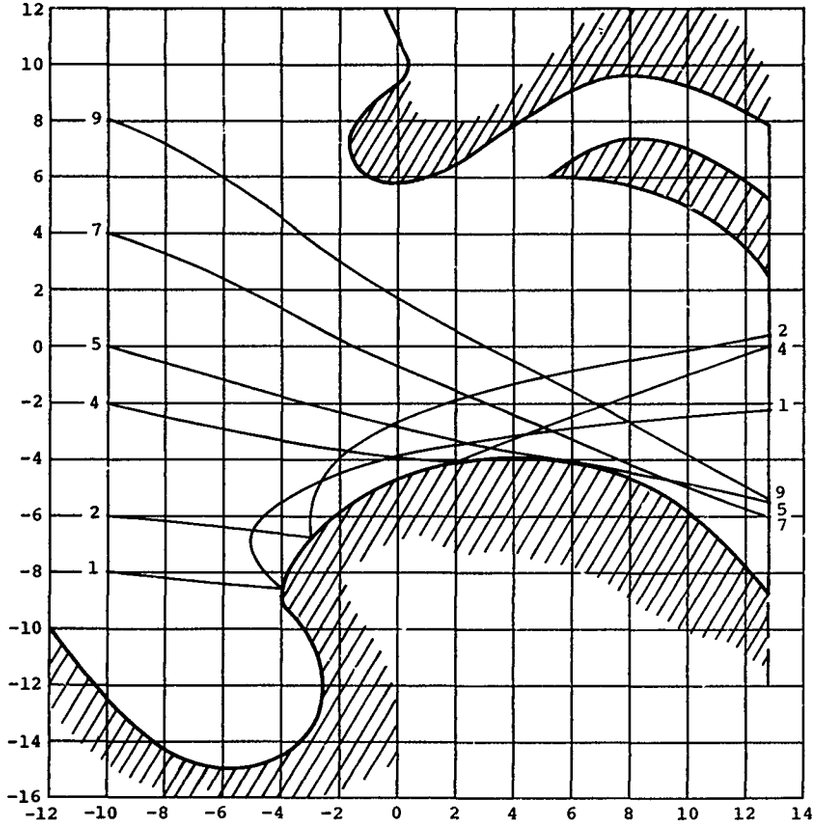

CONFIGURATION 4
PARTICLE SIZE 800 MICRONS
HIGH AIRFLOW
u = 40 FPS
v = 0

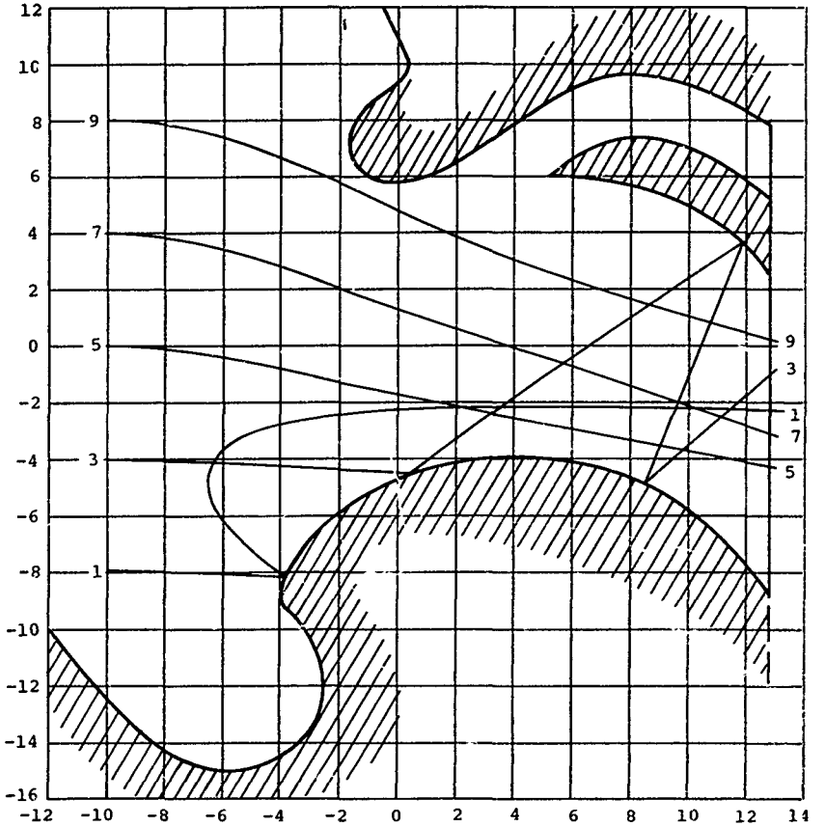

Figure 42. Typical Particle Trajectories

CONFIGURATION 5
PARTICLE SIZE 10 MICRONS
STANDARD AIRFLOW
u = 40 FPS
v = -40 FPS

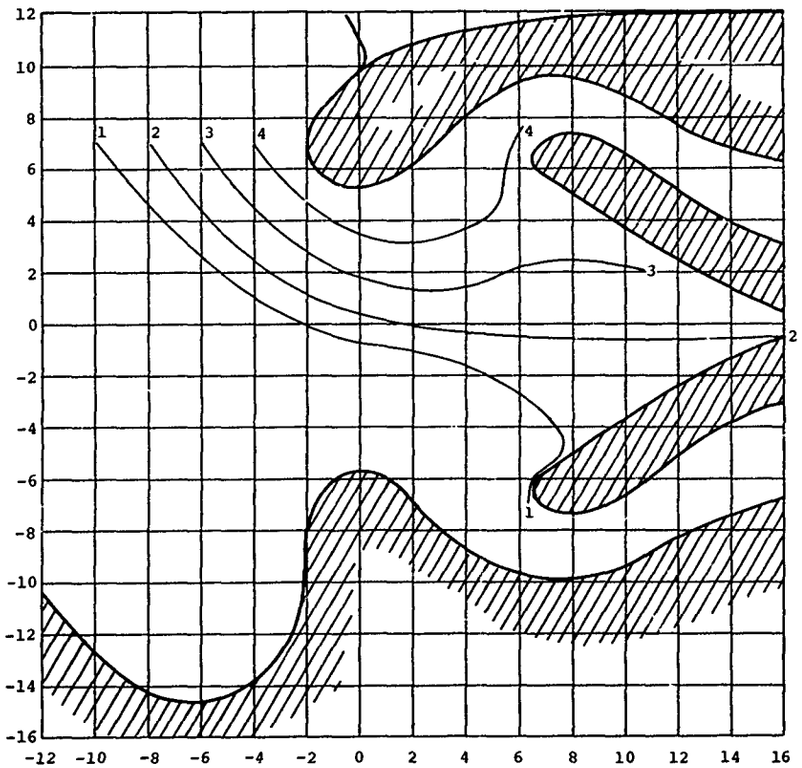

CONFIGURATION 5
PARTICLE SIZE 10 MICRONS
STANDARD AIRFLOW
u = 40 FPS
v = 0

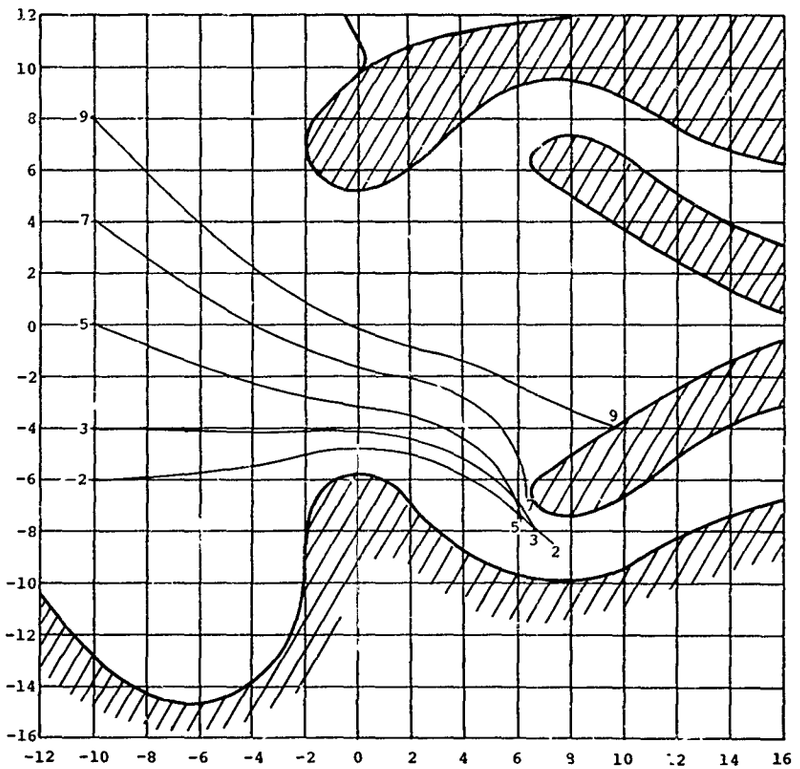

Figure 43. Typical Particle Trajectories

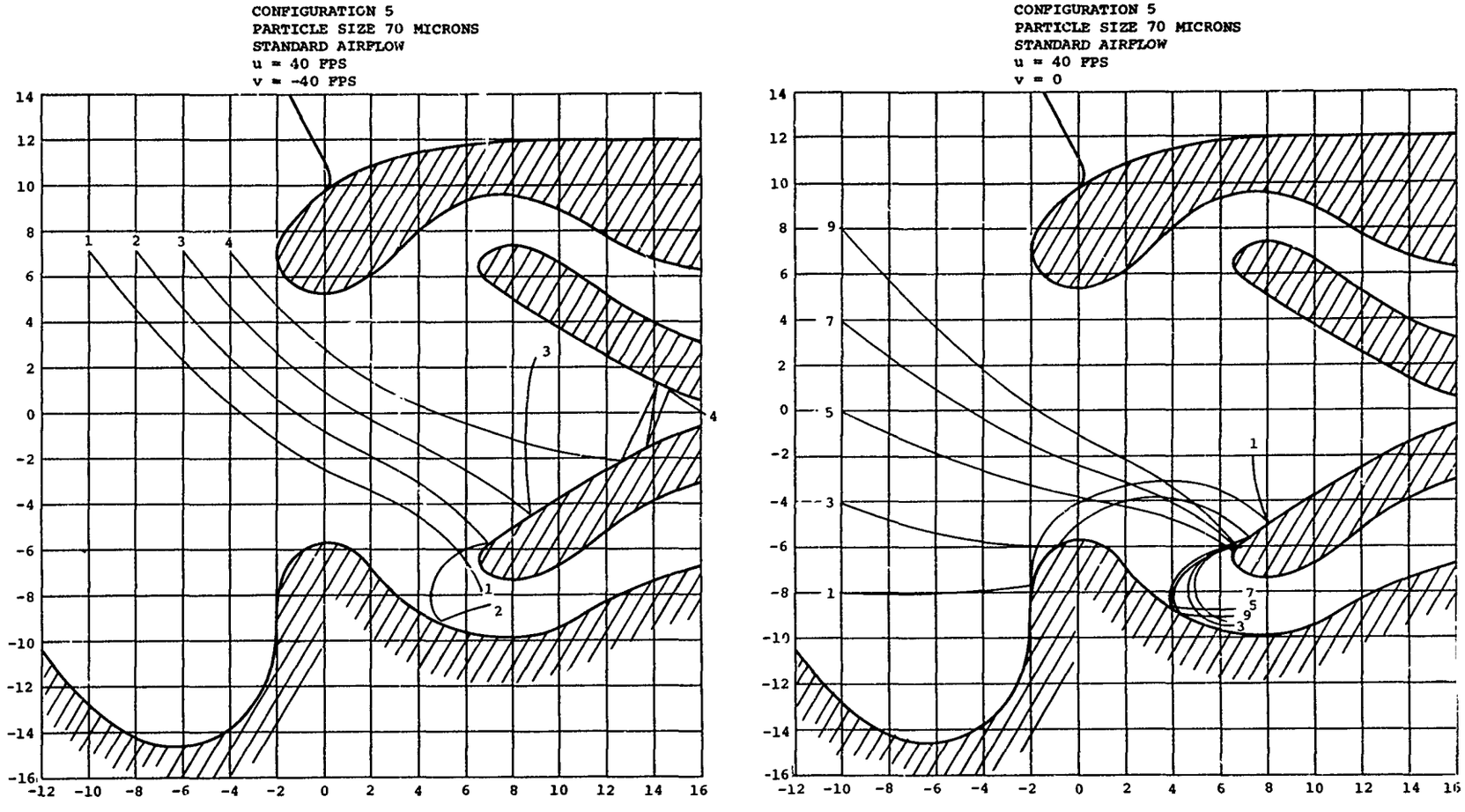

Figure 44. Typical Particle Trajectories

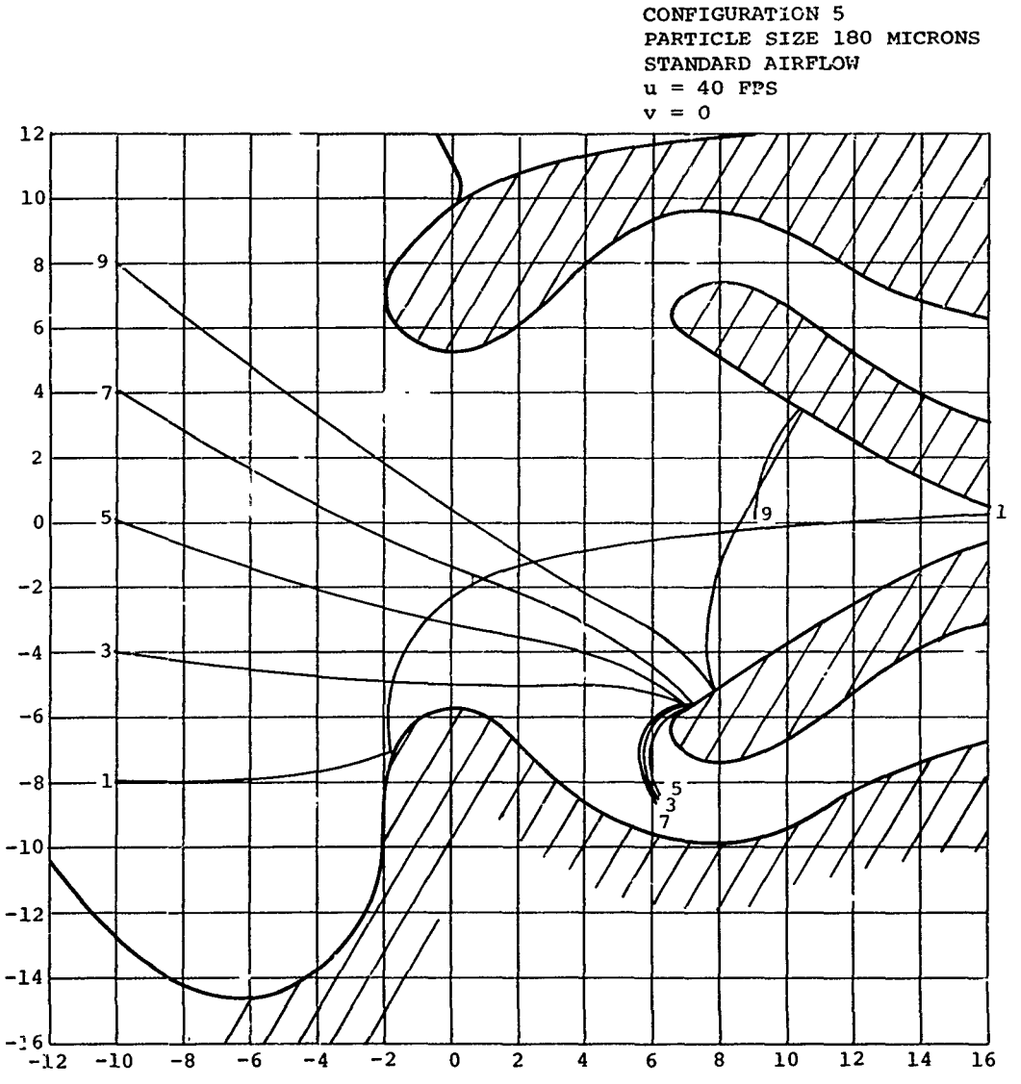

Figure 45. Typical Particle Trajectories

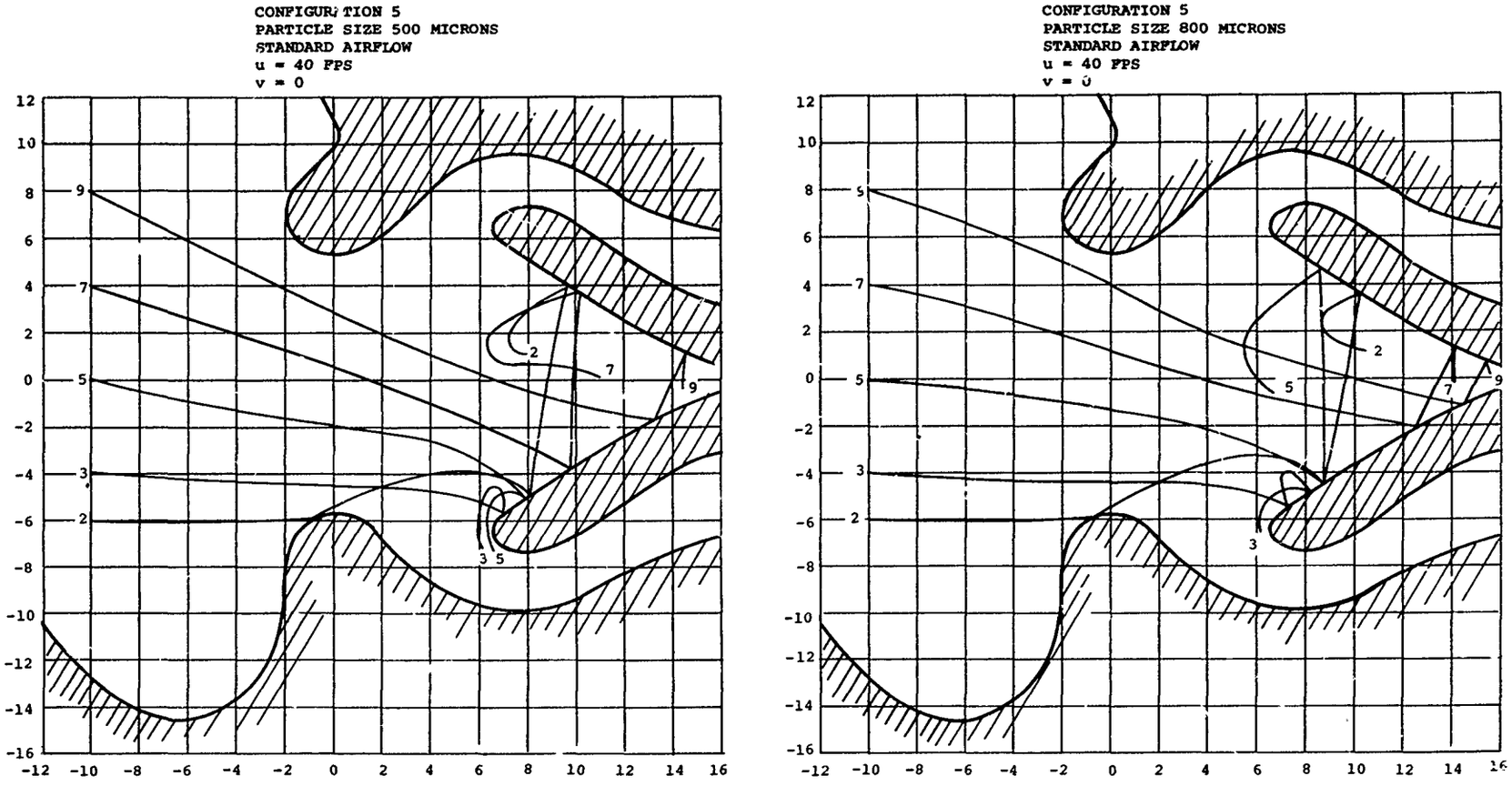

Figure 46. Typical Particle Trajectories

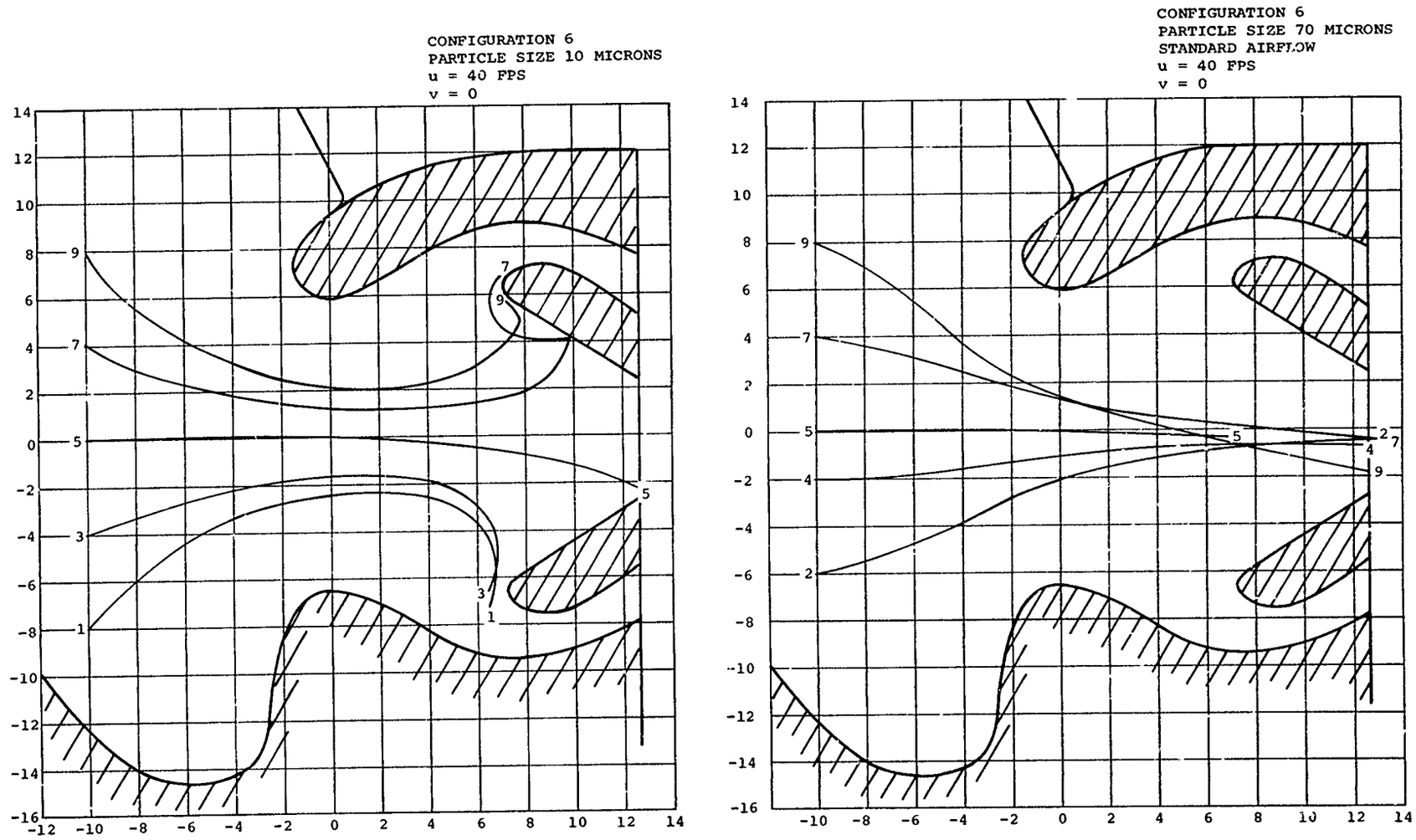

Figure 47. Typical Particle Trajectories

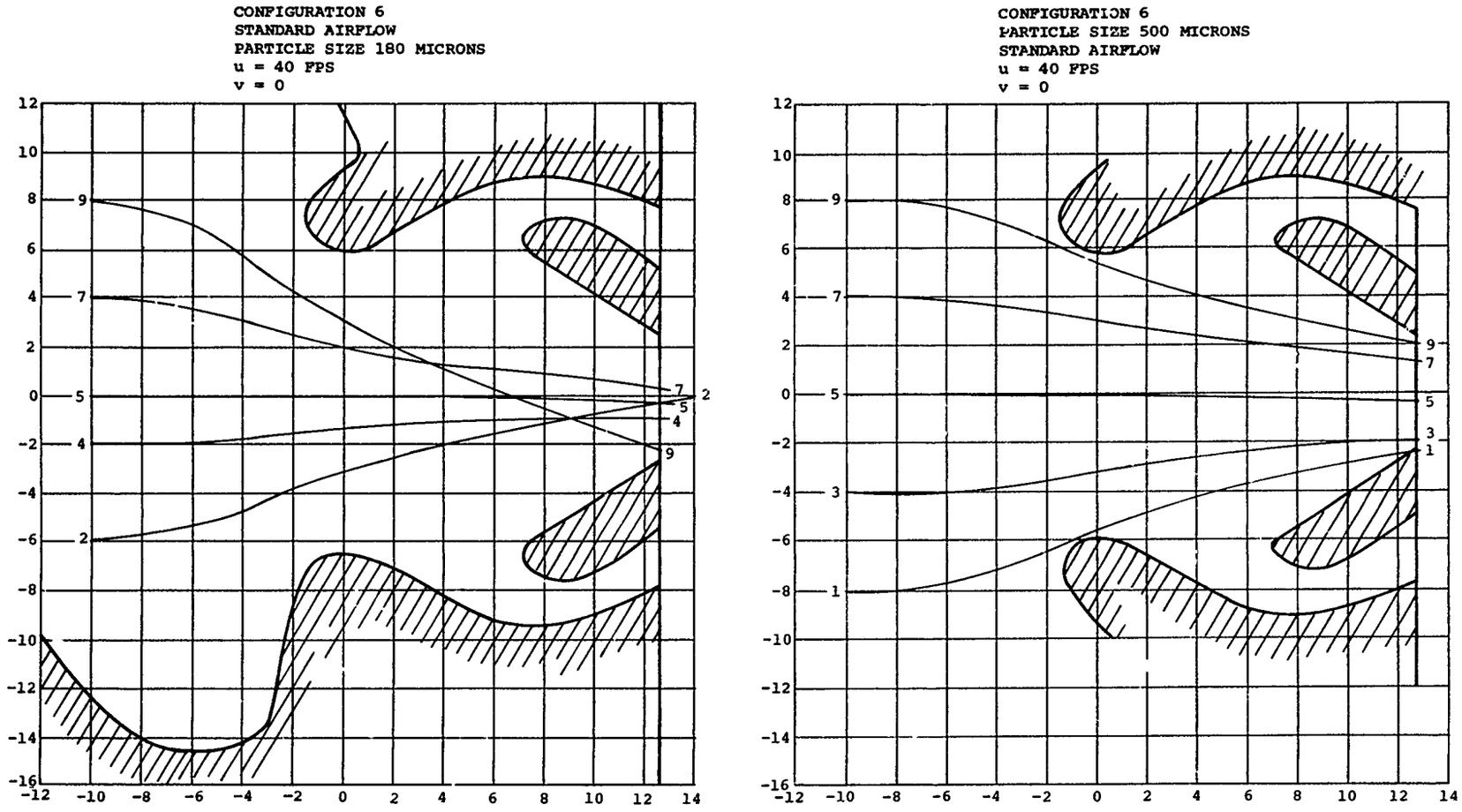

Figure 48. Typical Particle Trajectories

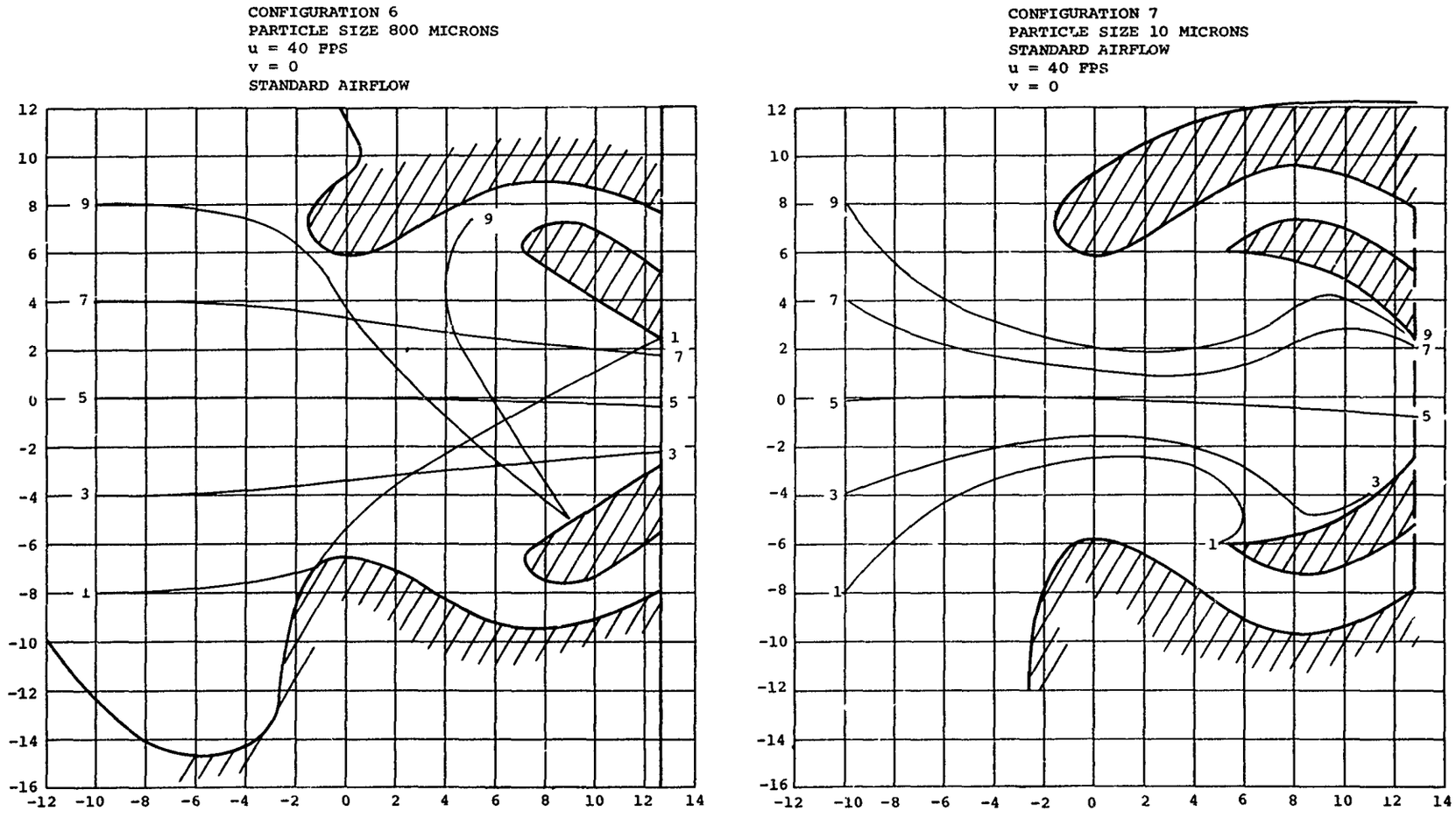

Figure 49. Typical Particle Trajectories

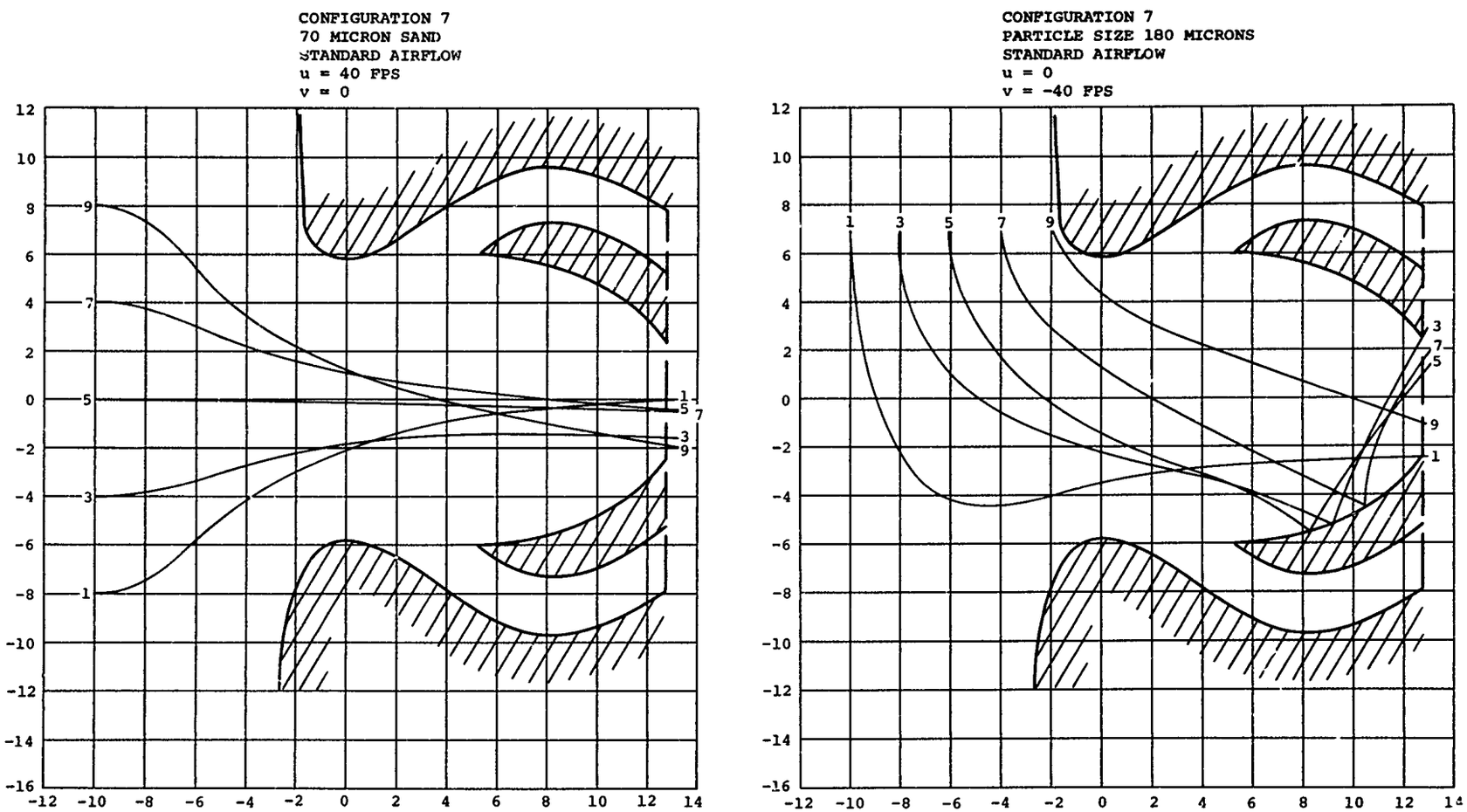

Figure 50. Typical Particle Trajectories

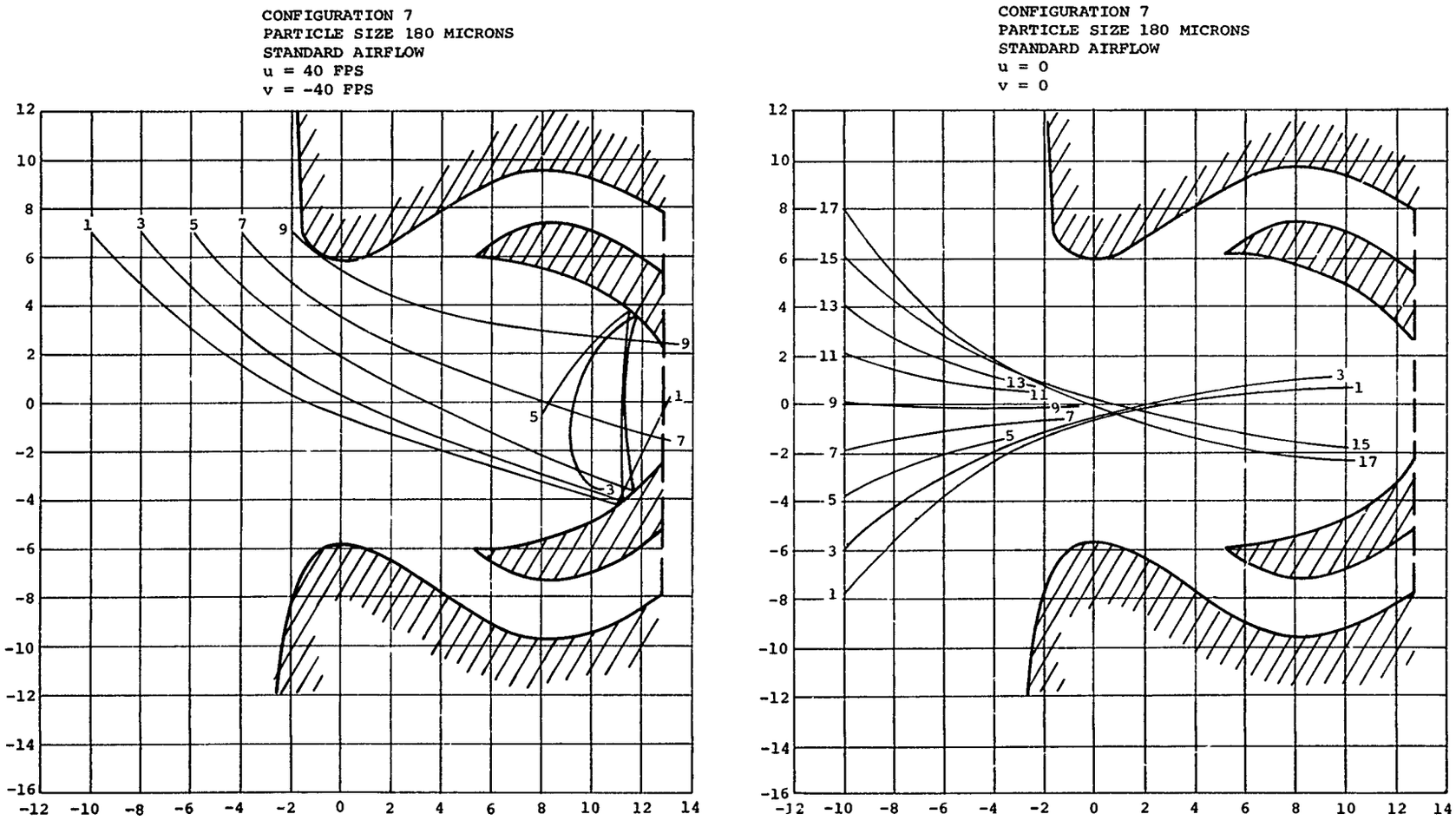

Figure 51. Typical Particle Trajectories

CONFIGURATION 7
PARTICLE SIZE 180 MICRONS
STANDARD AIRFLOW
u = 40 FPS
v = 0

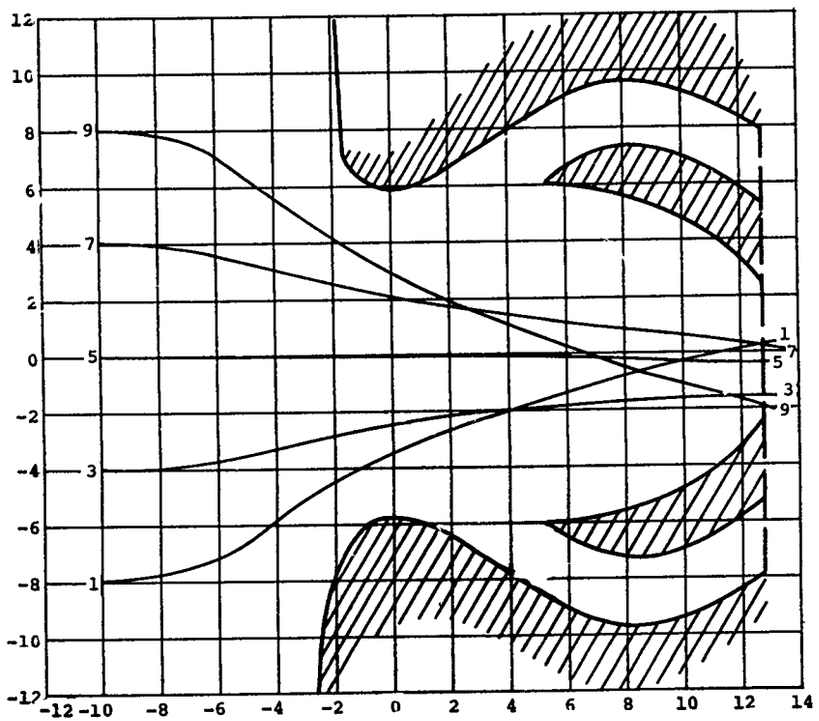

CONFIGURATION 7
PARTICLE SIZE 180 MICRONS
STANDARD AIRFLOW
u = 80 FPS
v = 0

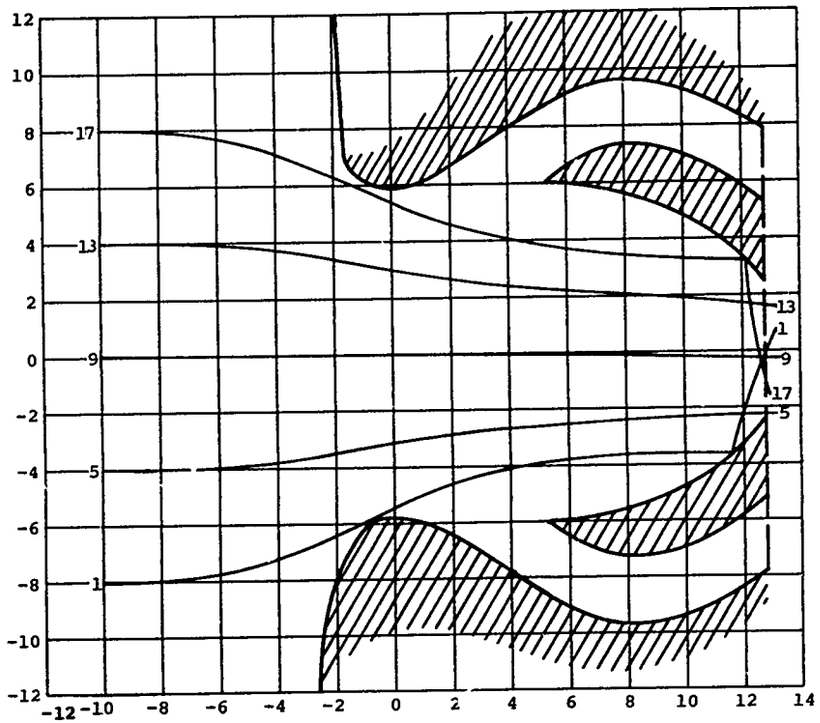

Figure 52. Typical Particle Trajectories

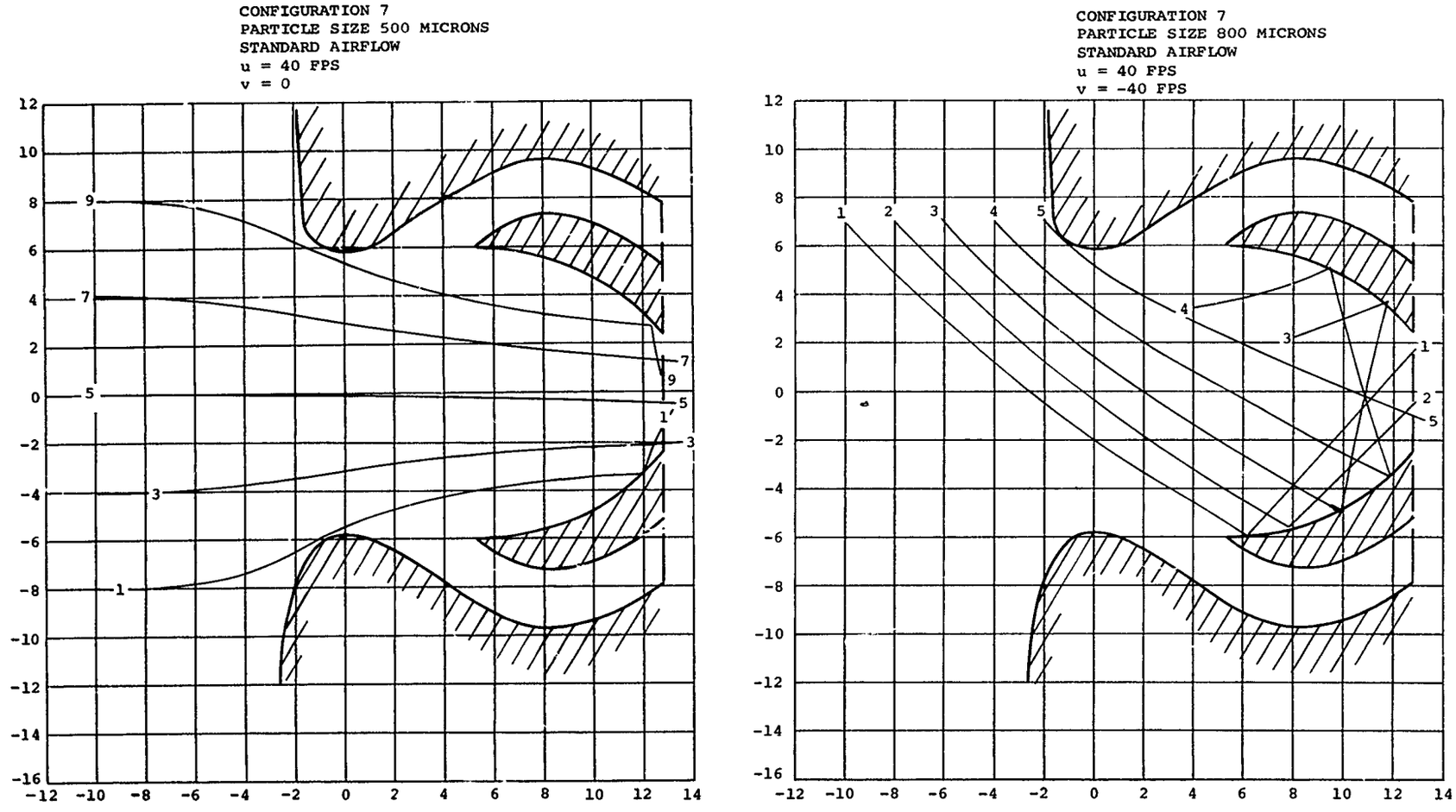

Figure 53. Typical Particle Trajectories

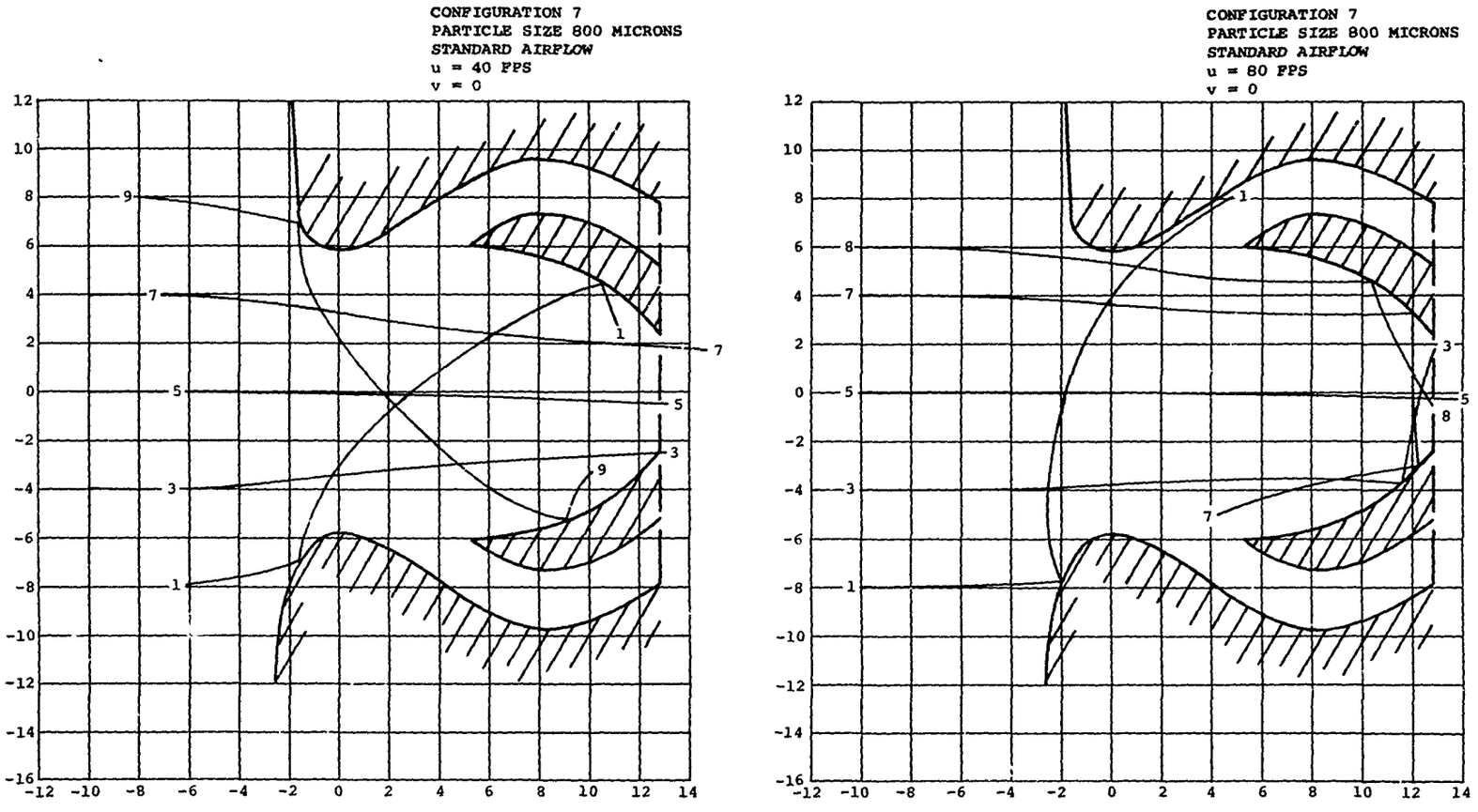

Figure 54. Typical Particle Trajectories

CONFIGURATION 7
SUPERCOOLED WATER
STANDARD AIRFLOW
u = 40 FPS
v = 0

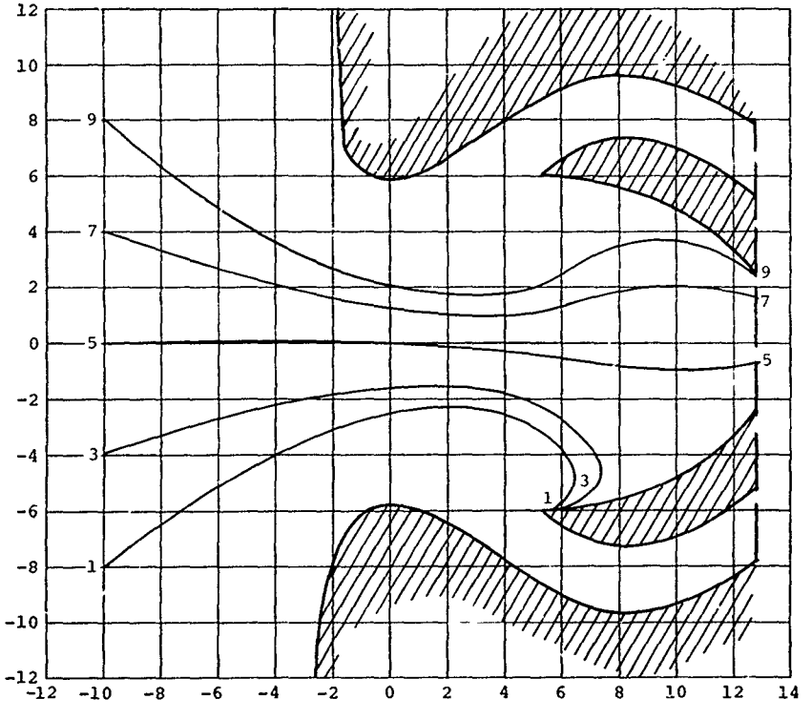

CONFIGURATION 7
SALT WATER SPRAY
STANDARD AIRFLOW
u = 40 FPS
v = 0

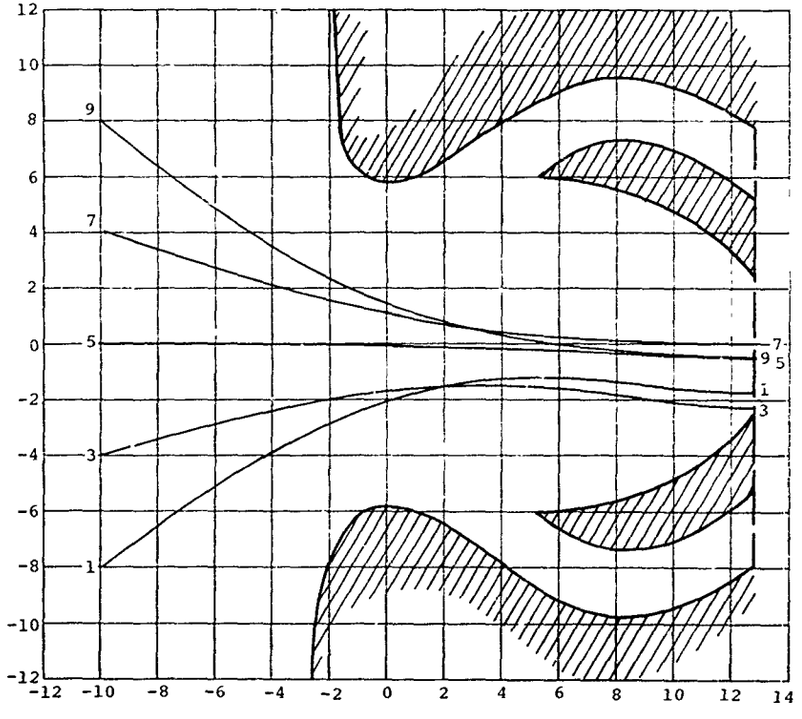

Figure 55. Typical Particle Trajectories

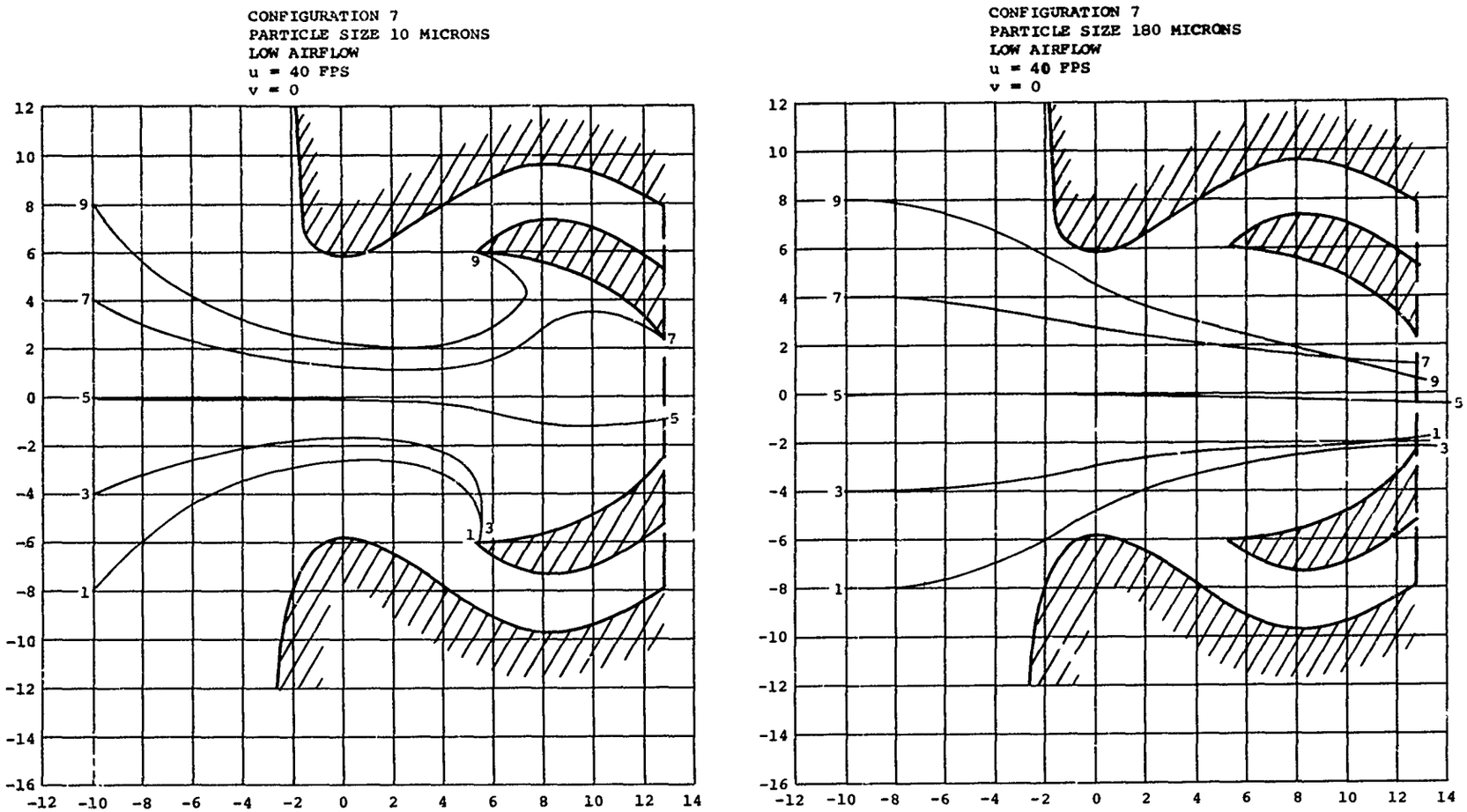

Figure 56. Typical Partical Trajectories

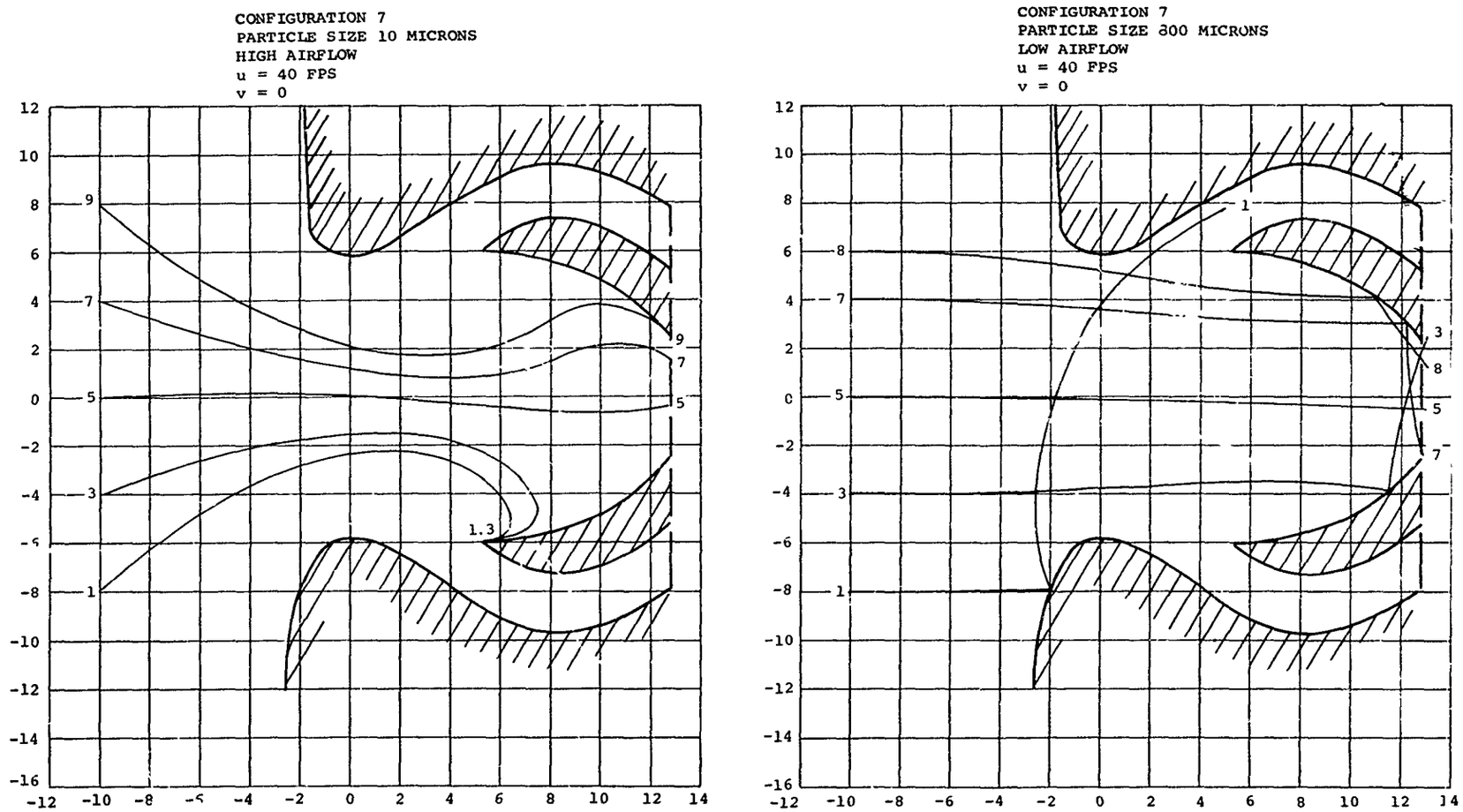

Figure 57. Typical Particle Trajectories

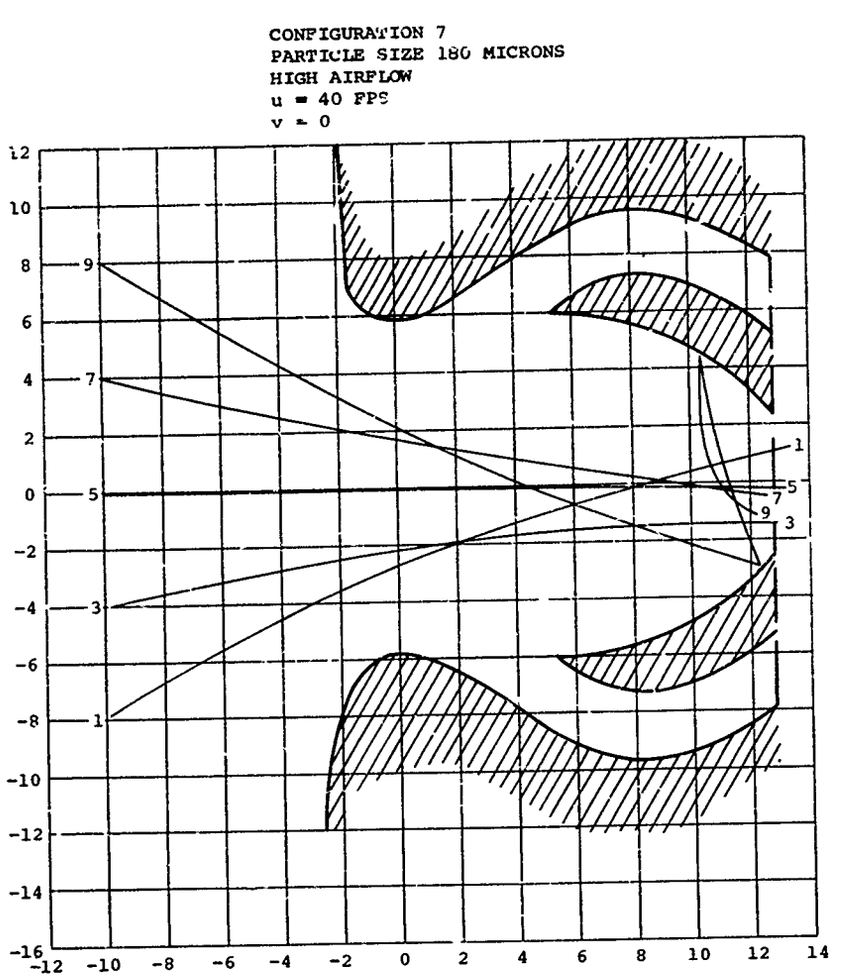

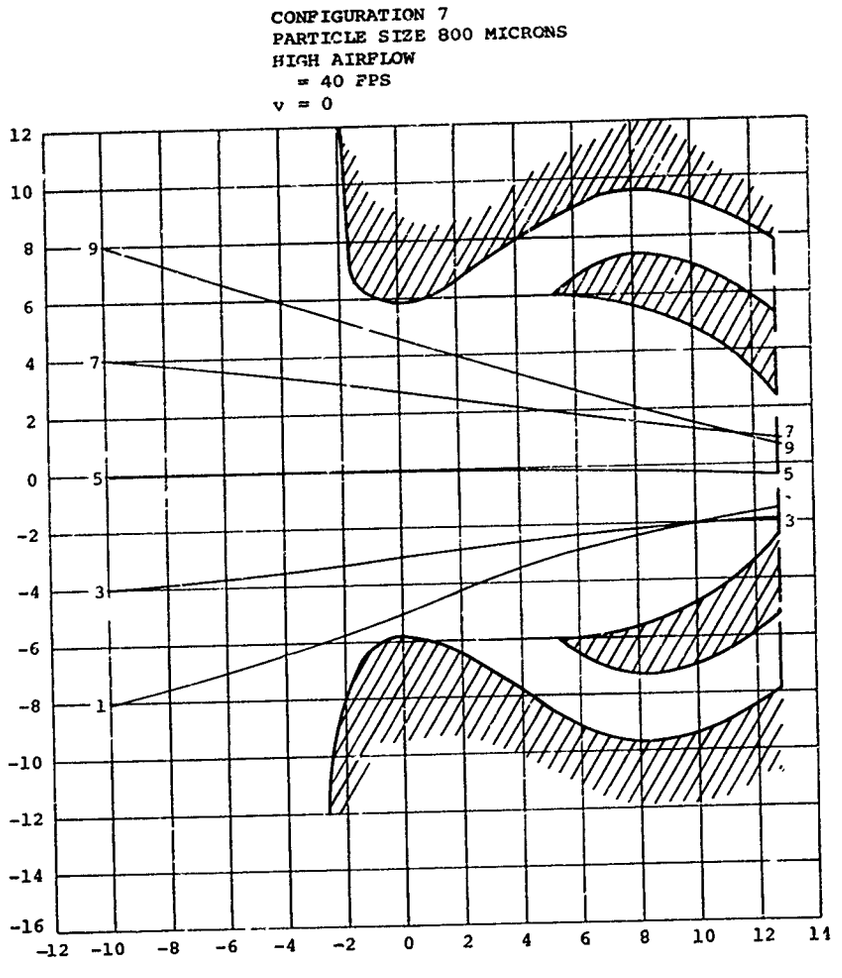

Figure 58. Typical Particle Trajectories

PARAMETRIC EFFECTS ON PARTICLE TRAJECTORIES - RESULTS AND DISCUSSION

PARTICLE DIAMETER EFFECTS

Figures 59 and 60, which illustrate the effect of particle diameter at constant density and airflow, are of considerable interest. It can be seen that the larger, heavier particles follow much straighter trajectories than the light particles. This difference is sometimes desirable, particularly when the purpose of the design is to sort out one size of particle. This could often be the case; since engine deterioration tends to be largely a function of the total weight of foreign material ingested, separation of only the larger components of the entering dust cloud can result in significant improvements in engine life. The most useful separator, however, is able to work efficiently with a wide variety of particle sizes, and this means that the whole range of possible trajectories must be considered. In many cases this is relatively easy. Configuration 7, Figure 60, is typical of one such case. The trajectories of the various size particles form a regular fan, and if the characteristics of the two extreme trajectories are known, the intermediate trajectories can be easily predicted.

This case, however, is a very simple one (a symmetrical inlet with no downwash), and the situation becomes more complicated when the same basic inlet is run in a flow field with downwash (Figure 59). In the case of particles numbered 1, the fan formed by the trajectories is now much narrower than that formed by the same particles in Figure 60. The effect of diameter here is still quite simple; the light particles follow the air streamlines while the heavy particles generally move in straight lines. The particles numbered 2 in Figure 59 provide an indication of a much more complex effect, as evidenced by the trajectory of the 70-micron particle which lies midway between those for the 180- and 500-micron particles. The 180-, 500-, and 800-micron trajectories occur in exactly the inverse of the sequence expected from the plots in Figure 60. The heavier particles end up higher in the inlet than the lighter ones. It should be noted that the amount of curvature in the trajectories is, however, exactly as expected. The heavier particles have straighter paths than the lighter ones. The explanation for the inverse sequence of these particles is not too complex, but it will demonstrate the difficulty of designing an inertial separator to take into account all contingencies. What has happened is that the four particles, initially given velocity components (u = 40 feet per second, V = -40 feet per second) at 45 degrees with respect to the vertical, are in a flow field that is moving nearly vertically

LEGEND	
LINE TYPE	PARTICLE SIZE IN MICRONS
————	10
—·—·—	70
—··—··	180
— — — —	500
—— —— —	800

NOTES: 1. CONFIGURATION 2

U = 40 FPS

V = -40 FPS

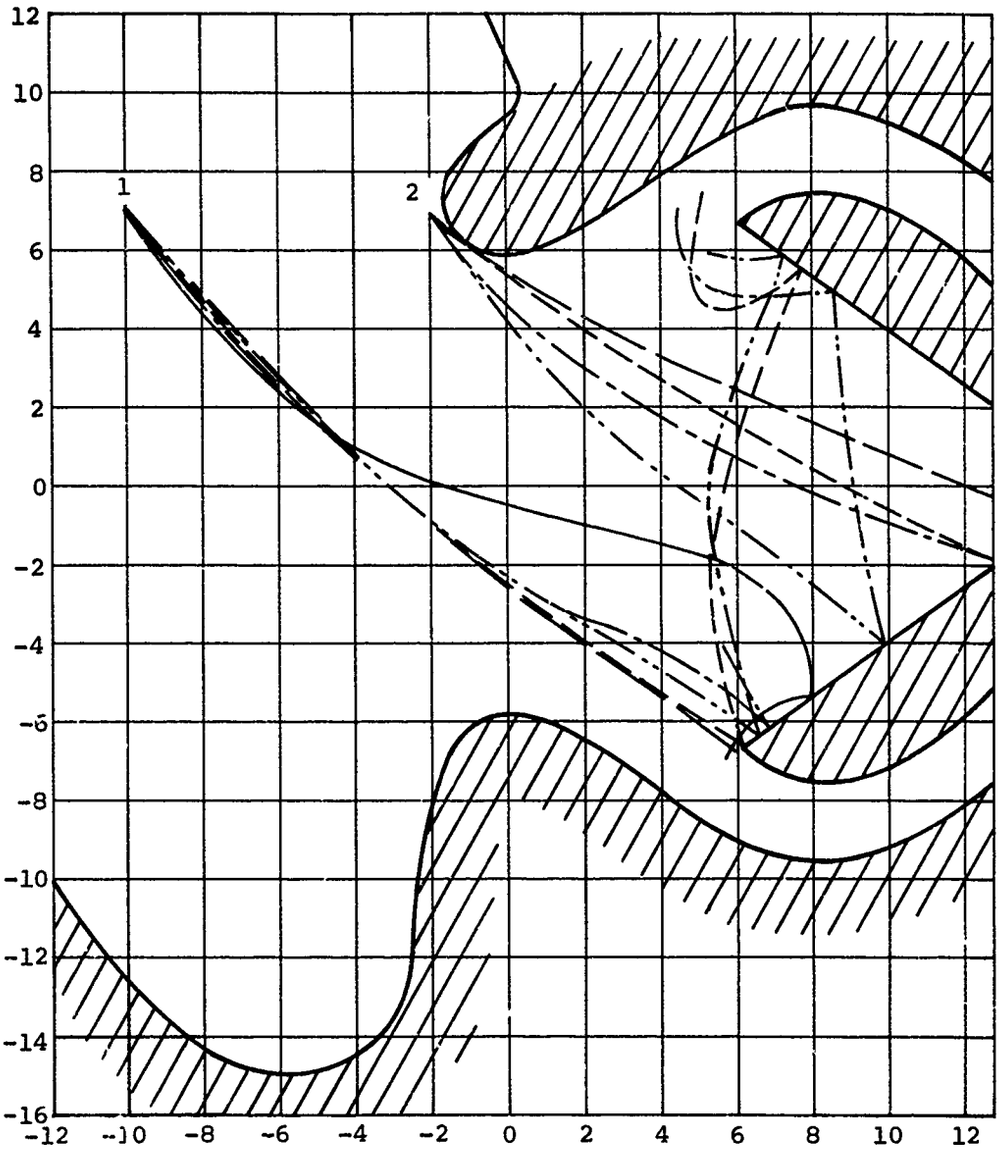

Figure 59. Effect of Particle Diameter in Configuration 2

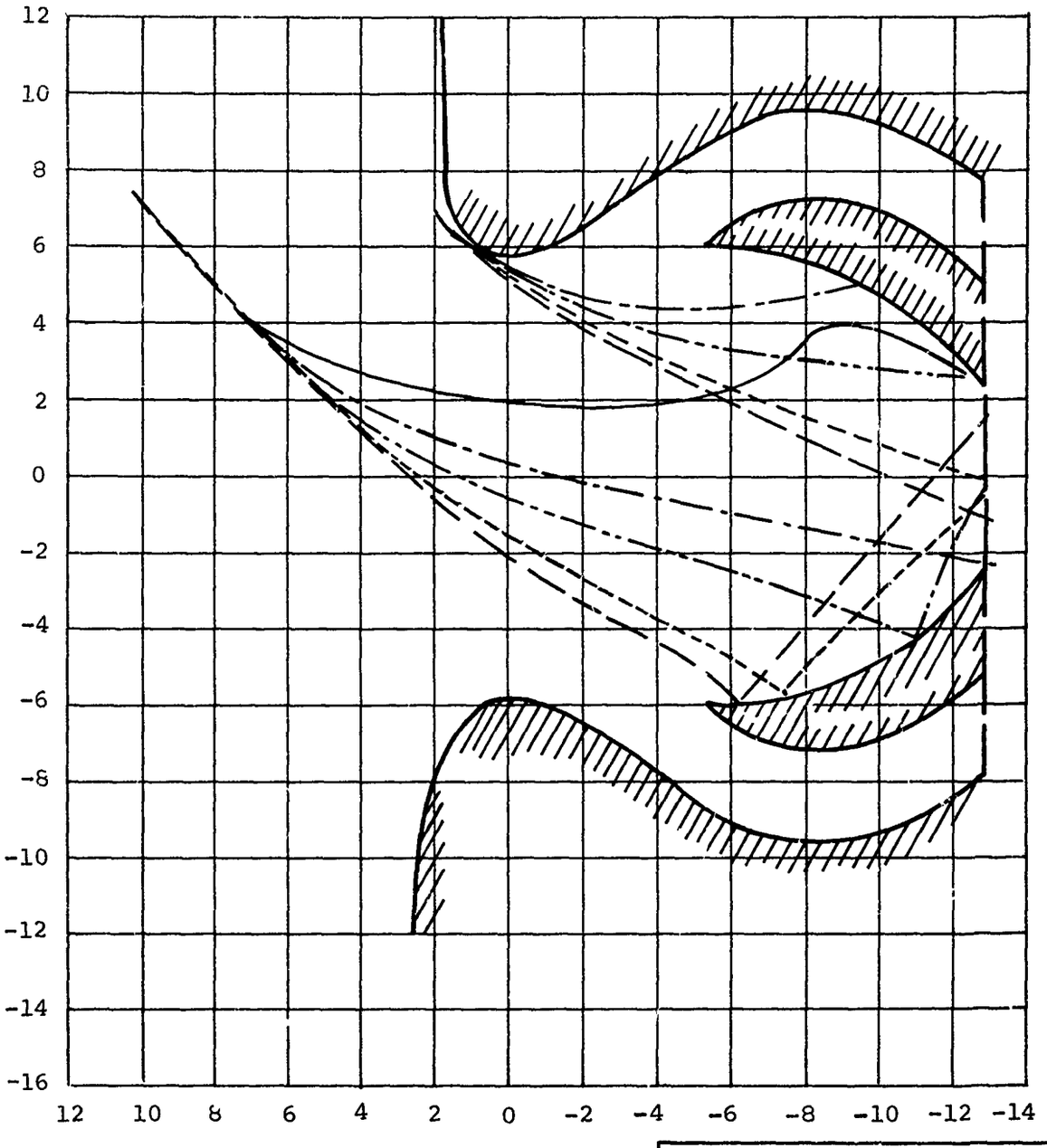

NOTES: 1. CONFIGURATION 7
2. u = 480 IPS
3. V = 480 IPS

LEGEND	
LINE TYPE	PARTICLE SIZE IN MICRONS
———	10
— — —	70
—·—·—	180
— — — —	500
— — —	800

Figure 60. Effect of Particle Diameter in Configuration 7

in a downward direction. Before the particles enter the bellmouth they are carried downward by this flow a distance inversely proportional to their size. As they enter the bellmouth they are then turned toward the horizontal, again by an amount almost inversely proportional to their size. The 70-micron particle, which entered the bellmouth below the 180-micron particle but which, in following the airflow, changed its direction significantly within the bellmouth, then ends up higher in the trap. The larger 180-, 500-, and 800-micron particles, none of which have been turned significantly by the bellmouth, end up at relative radial positions in the trap reflecting the relative radial positions at which they entered the bellmouth. Using this reasoning, it is not difficult to predict that a 10-micron particle would end up higher in the trap than the 70-micron, and could easily end up higher than the 800-micron particle. This is not an isolated case of this complex behavior. This study has shown that it is very difficult to predict the trajectories of particles entering near the upper or lower lips of the bellmouth.

Another factor that is affected very much by the particle diameter is the degree to which ricocheted particles can be controlled by the airflow within the trap. Note that in Figures 59 and 60 particles of 180 microns or more are easily able to rebound from surfaces in directions which are entirely contrary to the airflow in the immediate vicinity and which are determined only by the orientation of the surface. In contrast to this, the 10-micron particle in Figure 60 is turned parallel to the upper trap surface by the airflow and thus never collides with it, and the 10-micron particle in Figure 59 rebounds in a direction determined largely by the airflow after colliding with the lower trap surface.

The task of the designer, in allowing for particle size variation, is to consider two objectives. The first is to move the lightest particles downstream of the stagnation point on the trap surface as quickly as possible. As long as they are upstream of this point they may be easily sucked in by the primary airflow, but once past this point they are almost certainly trapped by the secondary air. This objective must be achieved by control of the airflow alone, specifically by moving the air stagration point upstream on the trap surface. The second objective is to turn the heavy particles sufficiently upon entering the inlet so that they enter the trap with few additional bounces. Additional bounces inside the trap have the tendency to result in undesirable upstream motion of the particle. The initial turning of these heavy particles may be accomplished either by aerodynamic (high throat velocity) or by ricochet (bounce plate) methods.

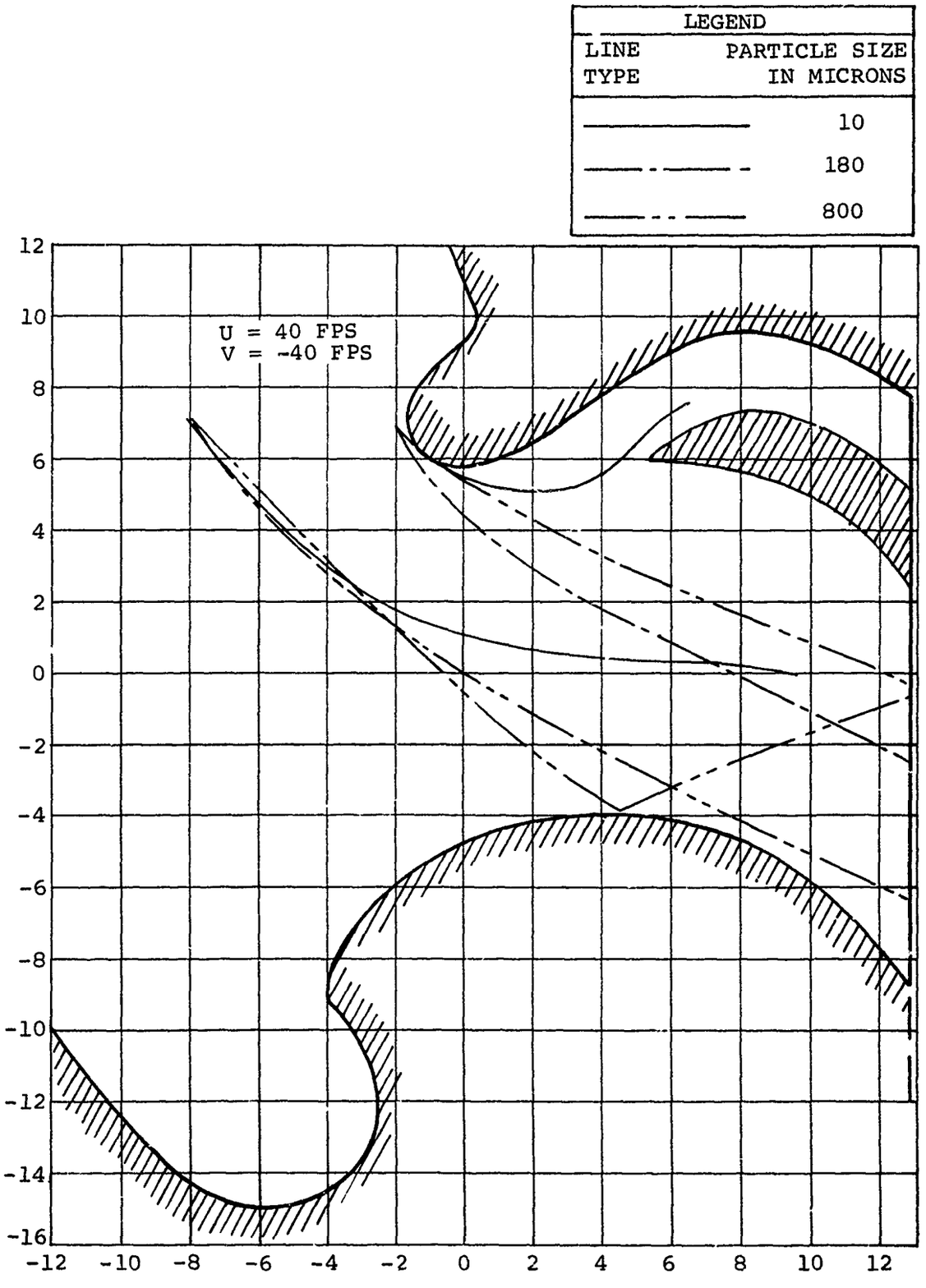

Figure 61. Effect of Particle Diameter in Configuration 4

SECONDARY FLOW EFFECTS

Figures 62 through 66 illustrate the effect of varying the percentage of the total flow which is used as secondary (trap) flow. The expected effects of increasing secondary flow are: (1) more particles entering the trap, and (2) better control of the particles once they have entered the trap. Three of the figures (62 through 64) demonstrate that these effects are not very predictable in a symmetrical inlet operating in downwash. Much of this inconsistency is caused by the fact that the surface contours of configuration 1 and configuration 2 were not quite identical. However, any substantial secondary flow effect should appear quite consistently in spite of this variation. A case which illustrates the type of effect referred to is the case of the 10-micron particle numbered 4 in Figure 62. Here the 5- and 10-percent secondary flow inlets produce virtually identical trajectories up to the region of the stagnation point on the upper trap surface. At this point the 5-percent flow inlet draws the particle toward the engine intake where it will be ingested. The 10-percent flow inlet, on the other hand, draws the particle downstream, deeper into the trap.

The complete trajectory plots for these two configurations confirmed that the secondary flow effect is not very strong in the downwash cases illustrated. This is also confirmed by Figure 17 which shows that separation of all but the smallest particles is not improved to an acceptable point in the downwash, symmetrical inlet case by increasing the secondary flow from 5 to 10 percent.

Figures 65 and 66 illustrate the much more consistent secondary flow effect obtained for the same basic inlets in a no-downwash flow field. The two particles numbered 4 and 5 in Figure 65 should be noted. In both of these cases, although the 5-percent secondary flow particle travels a good distance into the trap, it is eventually turned around and ingested by the engine, while the 10-percent flow particle continues downstream and is trapped. It should also be noted that there is no inconsistency in the trap surface contours between configurations 6 and 7, and hence the possible masking of the secondary flow effect is not present in Figures 65 and 66.

Figure 66 demonstrates that the variation in secondary flow above 5 percent has little effect on particles of 180 microns or more, in a no-downwash symmetrical inlet. The particles are controlled and focused so well by the bellmouth flow that there is little left for the secondary flow to do, except to accelerate the trapping process very slightly in the 10-percent secondary flow case.

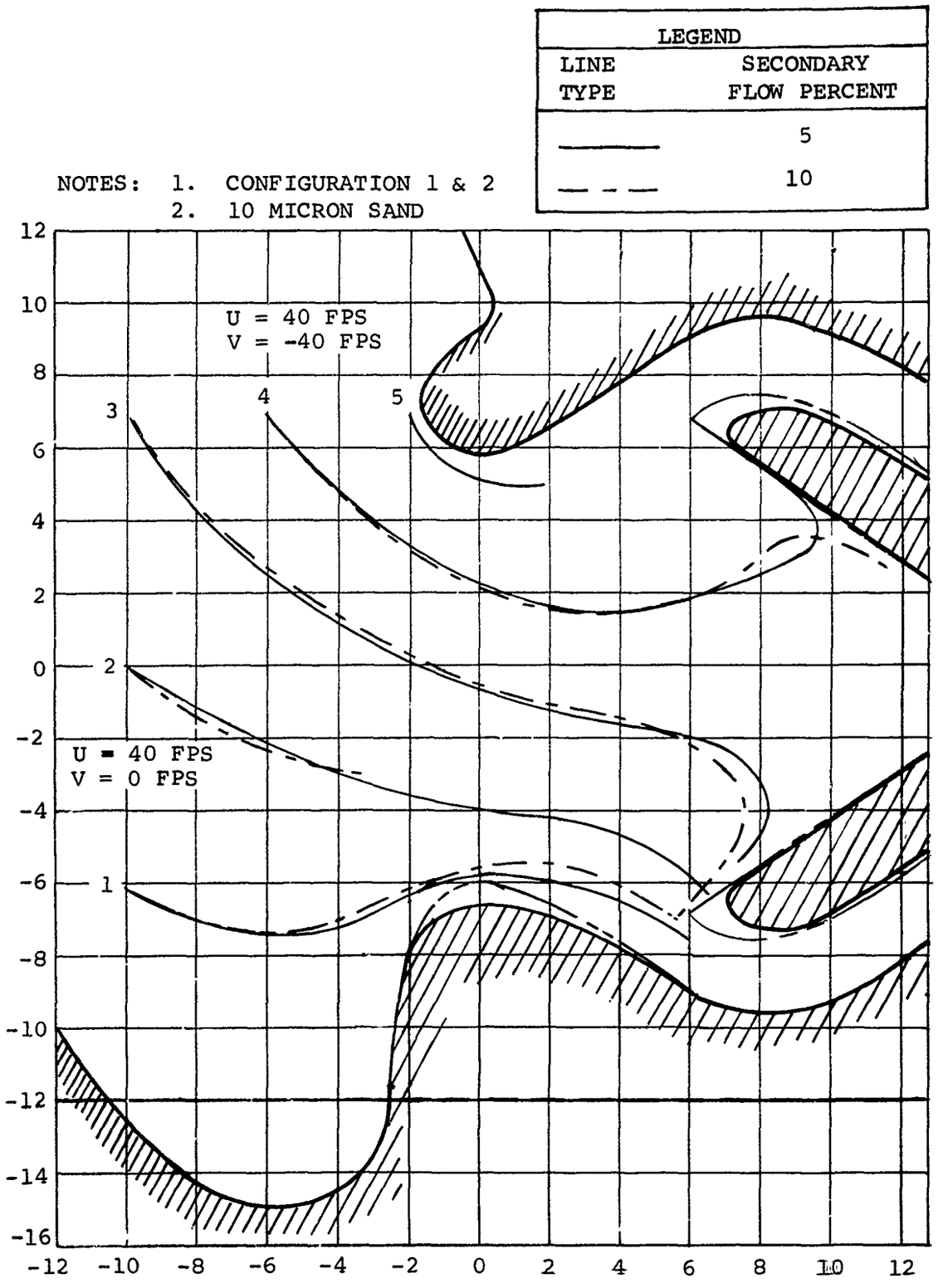

Figure 62. Effect of Varying Secondary Flow on 10-Micron Particles - With Downwash

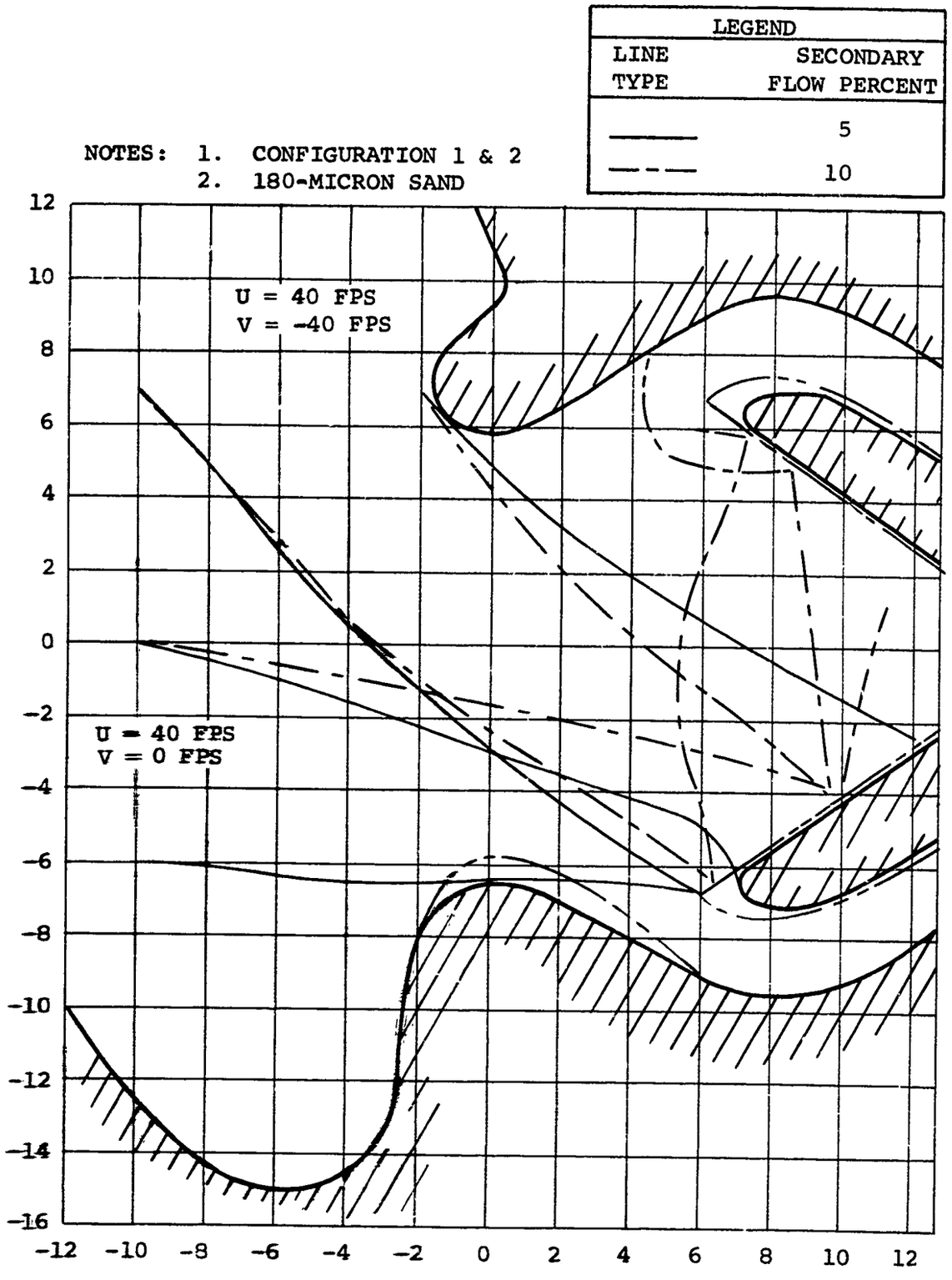

Figure 63. Effect of Varying Secondary Flow on 180-Micron Particles - With Downwash

NOTES: 1. CONFIGURATION 1 & 2
2. 800-MICRON SAND

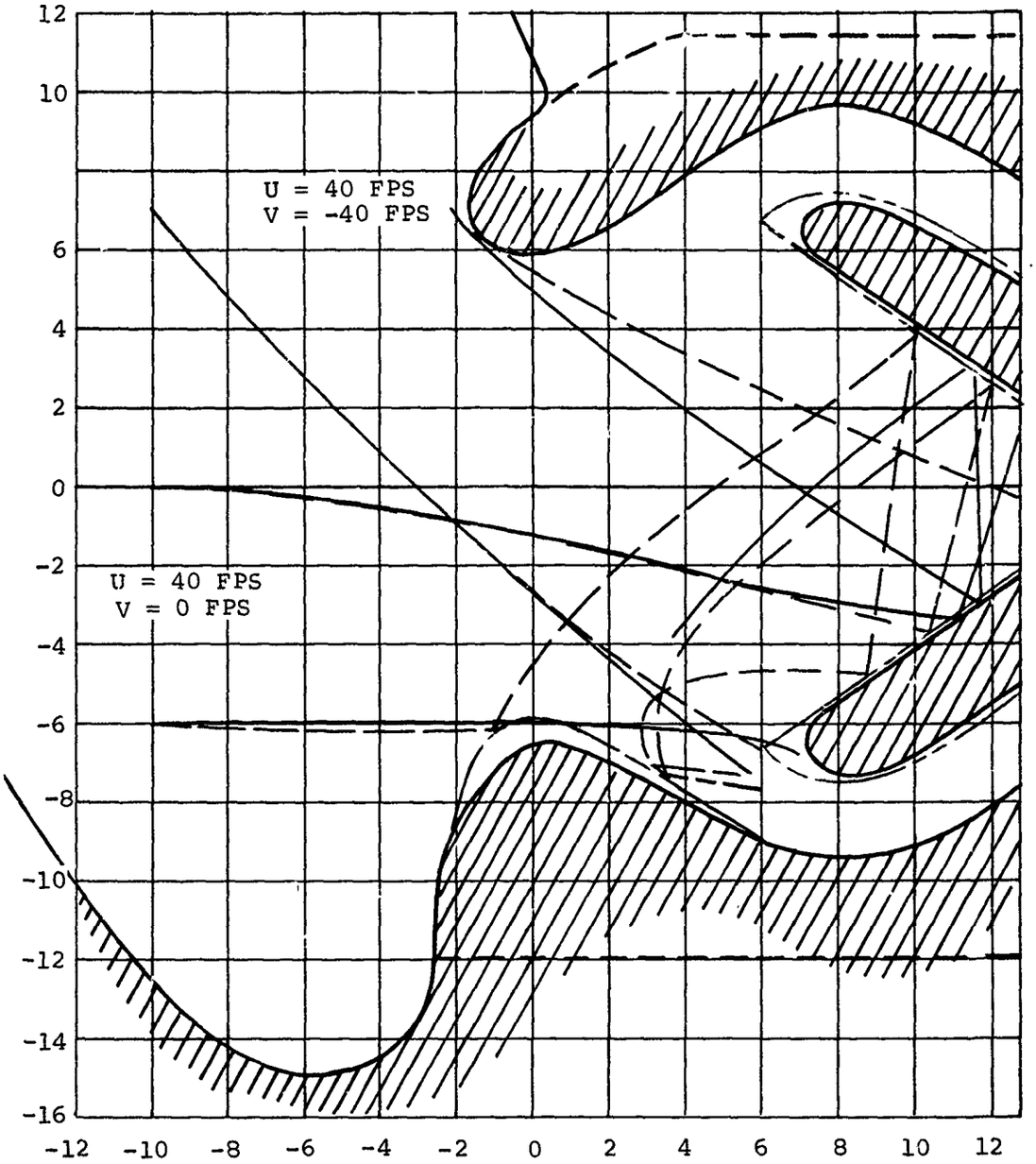

LEGEND	
LINE TYPE	SECONDARY FLOW PERCENT
———	5
— — —	10

Figure 64. Effect of Varying Secondary Flow on 800-Micron Particles - With Downwash

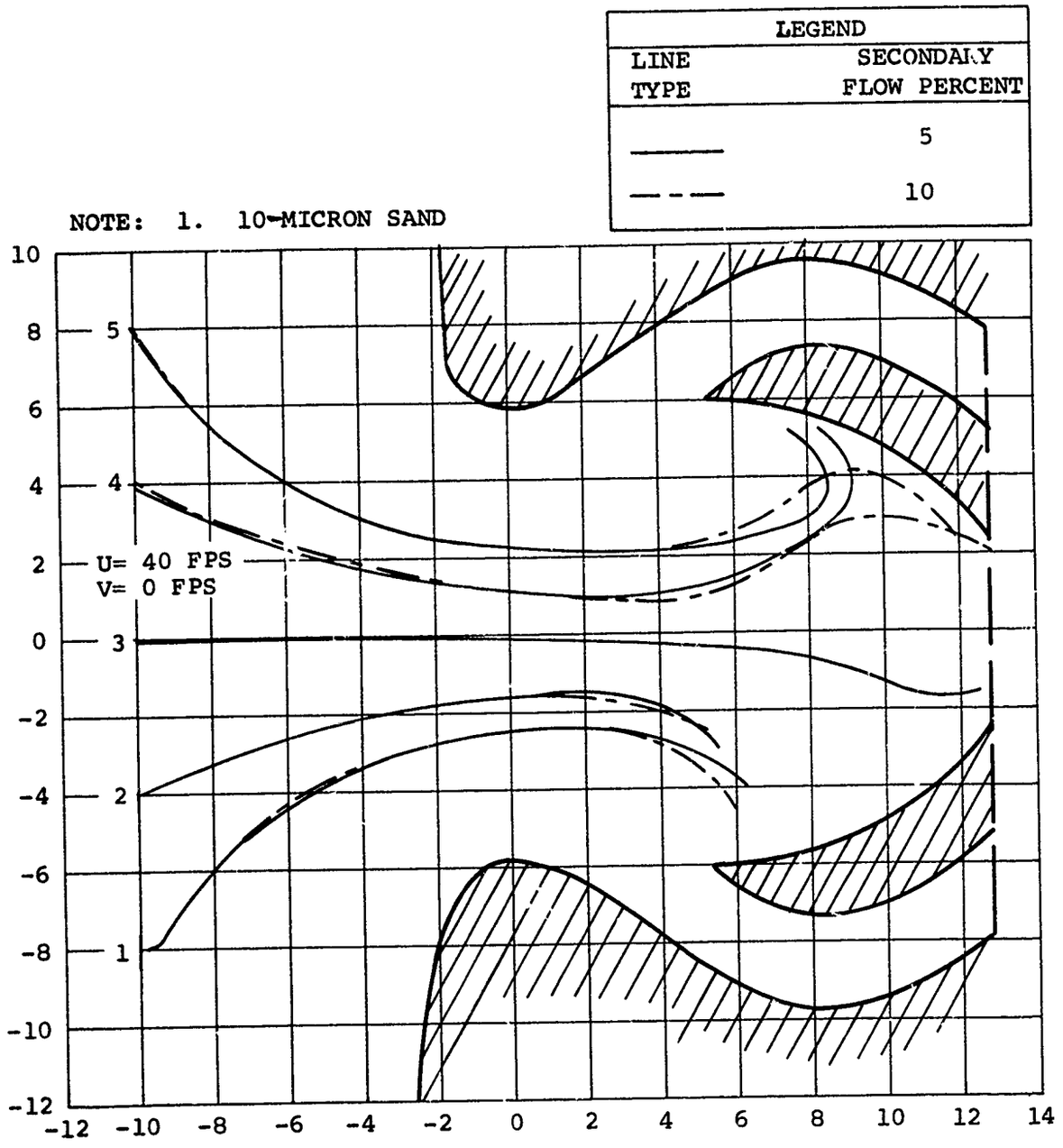

Figure 65. Effect of Varying Secondary Flow on 10-Micron Particles - Without Downwash

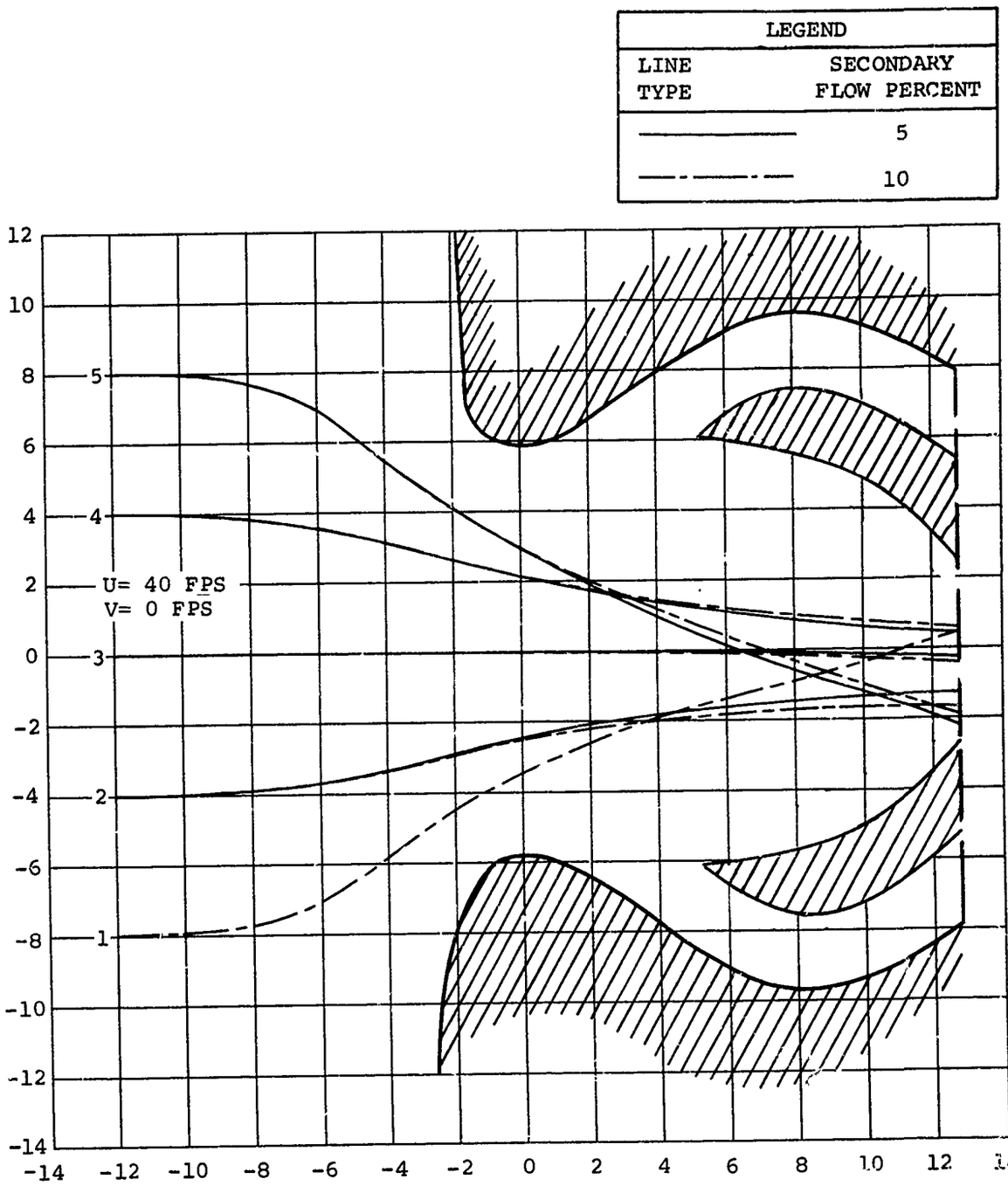

Figure 66. Effect of Varying Secondary Flow on 180-Micron Particles - Without Downwash

Although a figure similar to Figure 65 and 66 is not presented for the heavier particles, it is notable that 10-percent secondary flow does provide a slight improvement in separation as the particles get larger than 200 microns. This is because these larger particles tend to bounce, and increasing the secondary flow provides better control of the rebounding particles.

Data for secondary flow of less than 5 percent are not presented here, but this does not imply that there is no variation in the particle trajectories below this flow. On the contrary, bench tests have shown a drastic dropoff in separation efficiency in actual inlets as the secondary flow is decreased below 5 percent. Indeed, this is the chief reason why flows lower than 5 percent were not considered in this study; it was not believed that a practical inlet of the type under consideration could be designed with a very low secondary flow.

If we consider the percentage of the total flow drawn through the trap as a design variable, then, the objective is to have this percentage as high as possible consistent with power consumption, inlet size, blower weight, and so forth. A lower limit, for inlets of the type studied here, is about 5 percent. Twice this amount gives a substantial improvement in the separation of light particles and is, therefore, highly desirable. Increasing the secondary flow beyond 10 percent improves the separation efficiency. However, for each given increment of secondary airflow beyond 10 percent, the rate of separation efficiency does not increase in a linear fashion; it tends, rather, to level off. This performance should be weighed carefully against such disadvantages as weight, power consumption, and other factors.

TOTAL AIRFLOW EFFECTS

Figures 67 through 75 illustrate the effect of varying the total airflow in the inlet. Two inlet types are represented here, A and C, as well as three particle sizes, 10, 180, and 800 microns. As can be seen from Figures 21 through 58, two of the particle sizes considered, 70 and 500 microns, behave very similarly to the 180- and 800-micron particles, respectively. Therefore, Figures 67 through 75 use 10-, 180-, and 800-micron particles to represent the behavior of virtually all particles in the 0- to 800-micron range.

The figures show only a small airflow effect on the light (10-micron) particles. The only significant deviation in a light particle trajectory due to a change in total airflow occurs in Figure 69, configuration 7, where the particle numbered 1 is trapped at high and standard airflows but is ingested by the engine at low airflow. Configuration 4 shows virtually no variation in the trajectories of the light particles as the airflow is varied; the same is true of

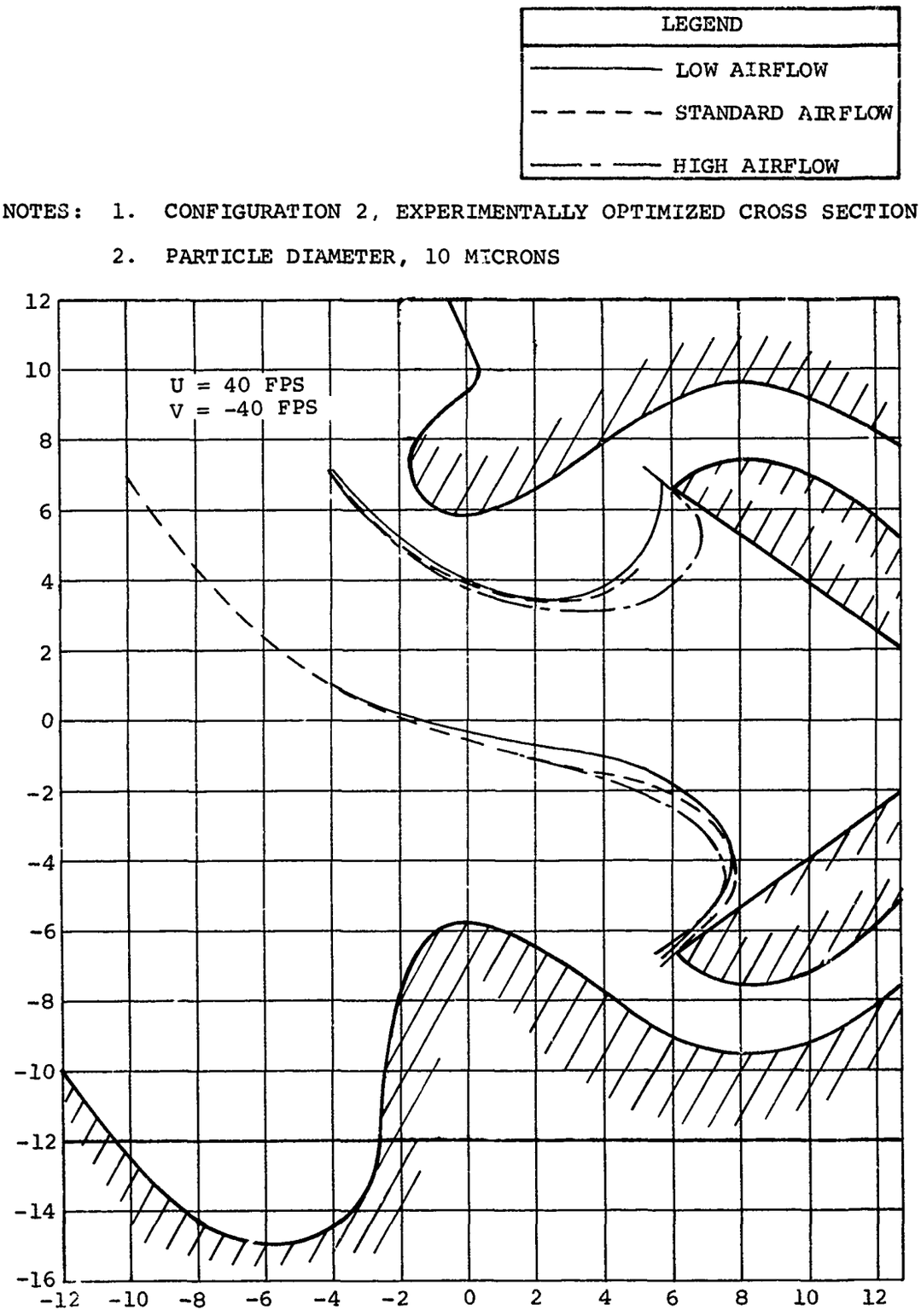

NOTES: 1. CONFIGURATION 2, EXPERIMENTALLY OPTIMIZED CROSS SECTION

2. PARTICLE DIAMETER, 10 MICRONS

Figure 67. Effect of Varying Total Airflow 10-Micron Particles with Downwash

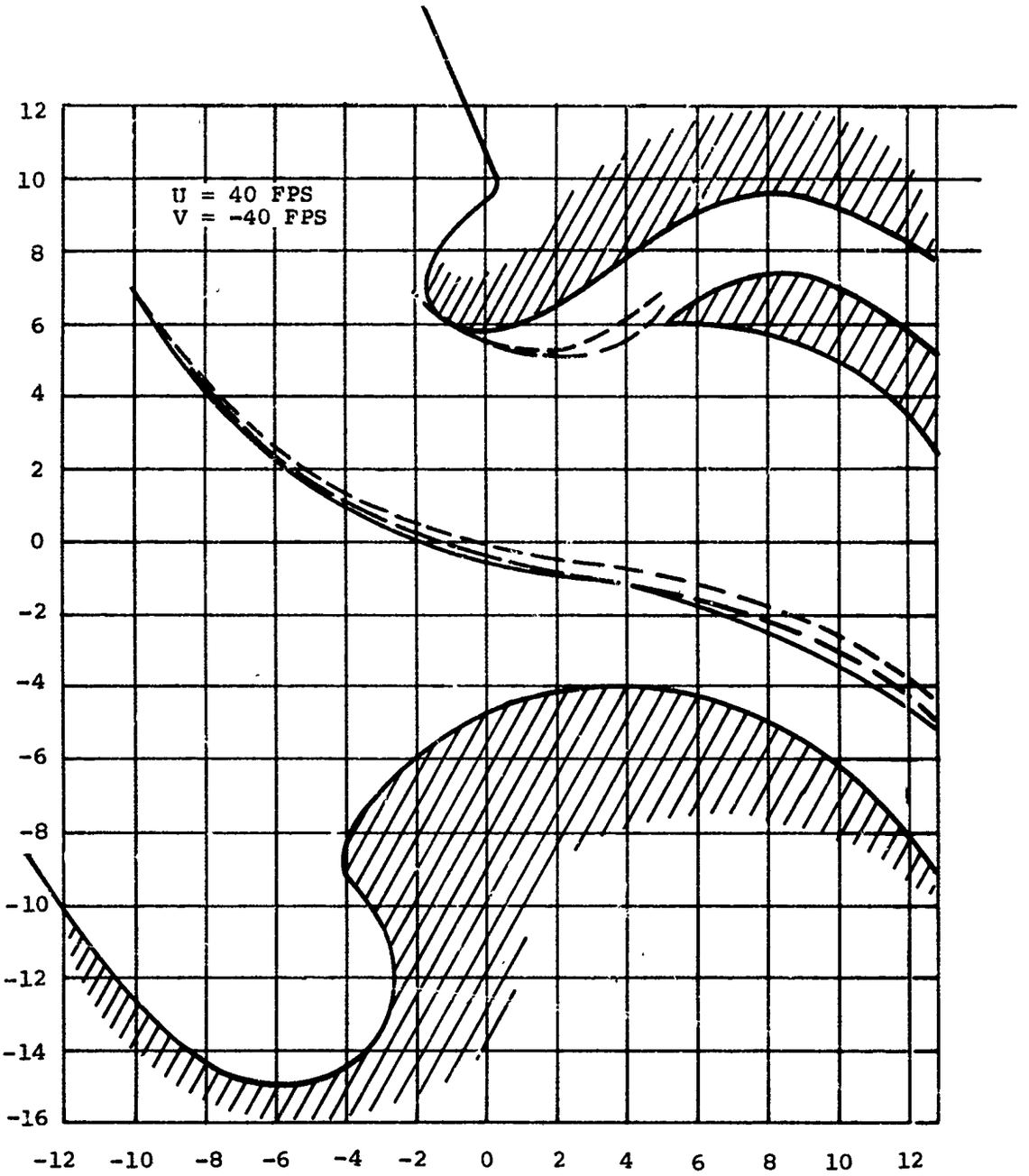

NOTES: 1. CONFIGURATION 4, EXPERIMENTALLY OPTIMIZED CROSS-SECTION MODIFIED TO INCLUDE BOUNCE PLATE

2. PARTICLE DIAMETER, 10 MICRONS

LEGEND	
— — — —	LOW AIRFLOW
- - - - - - - -	NORMAL AIRFLOW
————	HIGH AIRFLOW

Figure 68. Effect of Varying Total Airflow on 10-Micron Particles with Downwash and Bounce Plate

NOTES: 1. INLET CONFIGURATION 7

2. 10 PERCENT SECONDARY FLOW

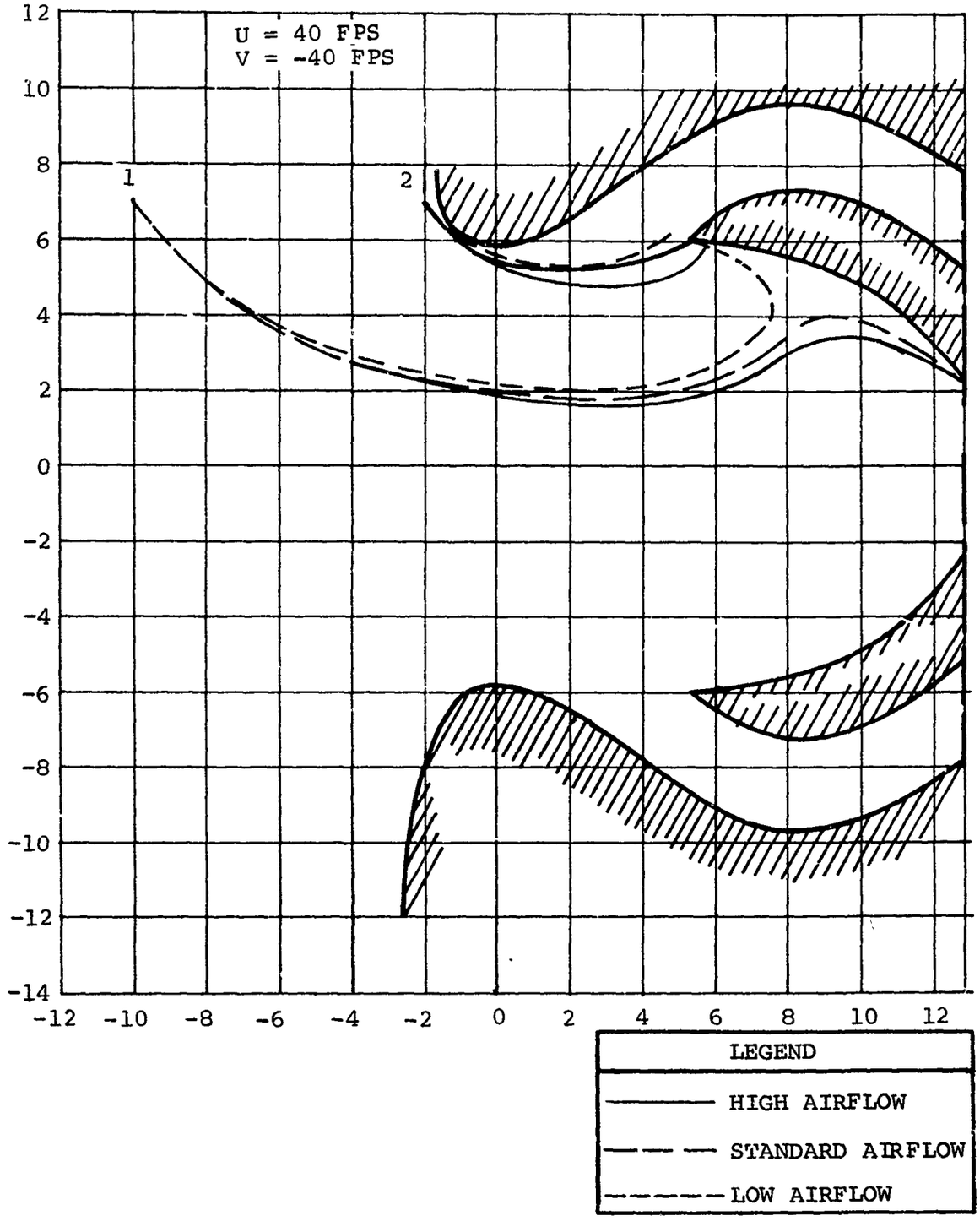

Figure 69. Effect of Varying Total Airflow on 10-Micron Particles With No Downwash

configuration 2. This insensitivity of the light particles to airflow is apparently due to their ability to accelerate almost instantaneously to the local air velocity, and then to follow the streamlines almost exactly. The streamlines do not change as the airflow is changed in potential flow, and hence the particle trajectories do not deviate.

Figures 70 through 72 illustrate the effect of total airflow on particles of 180-micron diameter. Trajectories in configuration 2 show little change as airflow varies. The downwash velocity is high enough here so that even these heavier particles are in equilibrium with the air as they pass through the bellmouth (i.e., they are following streamlines), and there is little redirection of the particles by the air until they reach the region of the trap. Even doubling the air velocity within the trap does not change its absolute magnitude appreciably with respect to the particle velocity, and therefore, raising the airflow does not materially increase the amount of particle redirection in the trap.

The foregoing observation may be rephrased as a principle: varying the air velocity in a region of a given inlet will affect the trajectory of a given size particle in that region only if it is a region in which high aerodynamic forces are active on the particle. Figures 73 through 75 illustrate this principle further by showing the effects of airflow on 800-micron particles. Here, again, the varying airflow causes changes in the trajectories only in regions in which the air would normally be turning, or trying to turn, the particles.

A designer must then consider several factors if he expects the total airflow through his inertial separator inlet to vary widely:

1. The separation of very light particles will not be affected substantially by varying the total airflow since these particles follow the air streamlines.

2. The trajectories of intermediate and heavy particles will be affected by the varying airflow only in regions in which the air is normally trying to turn the particles. If this attempted turning occurs mainly in the bellmouth region, as is expected, an increase in the airflow will probably help separation by accelerating the incoming particles more directly toward the trap. In this case the design obviously should be biased toward the lower airflows expected, since higher airflow will tend to improve efficiency.

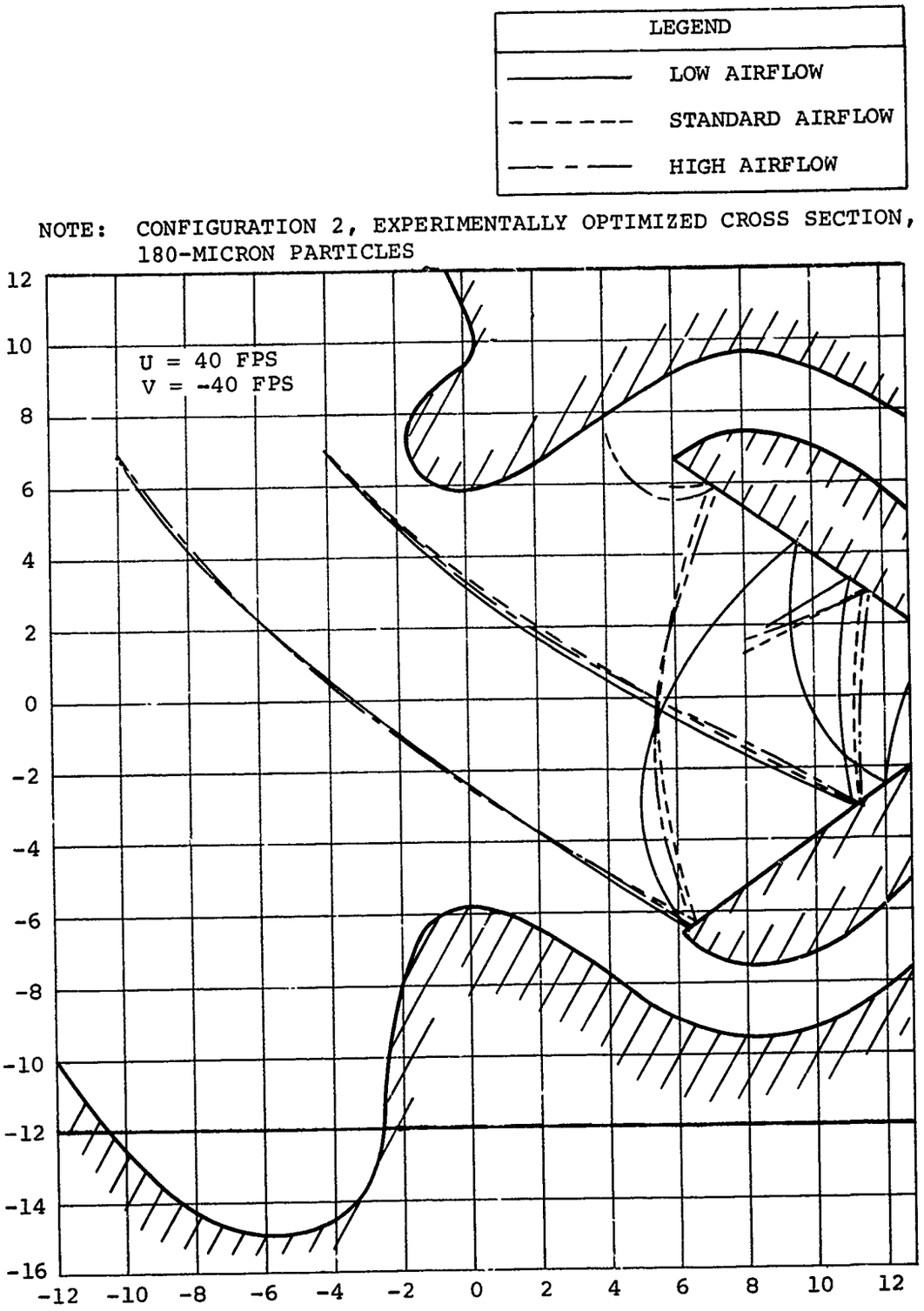

Figure 70. Effect of Varying Total Airflow on 180-Micron Particles With Downwash

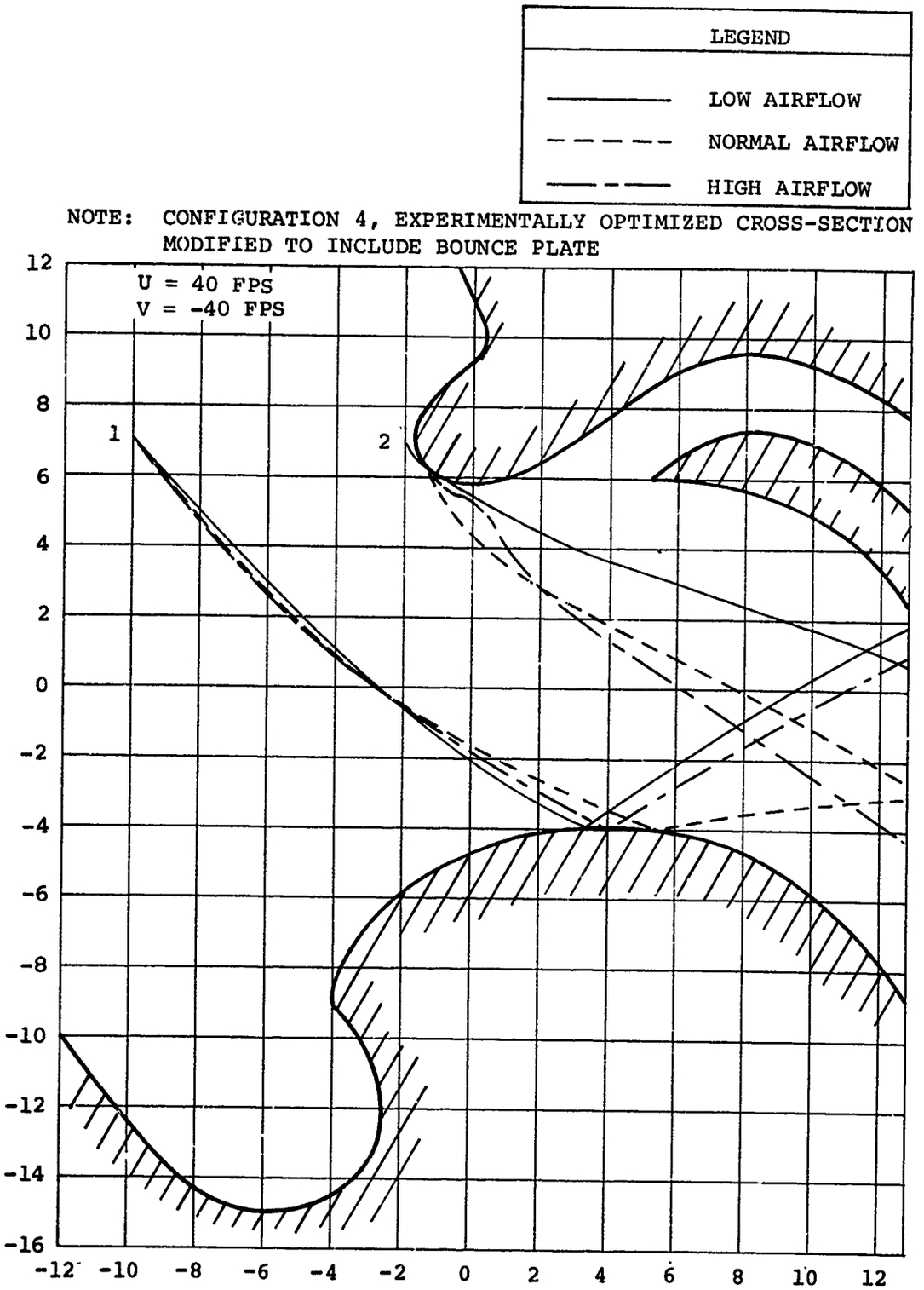

Figure 71. Effect of Varying Total Airflow on 180-Micron Particles With Downwash and Bounce Plate

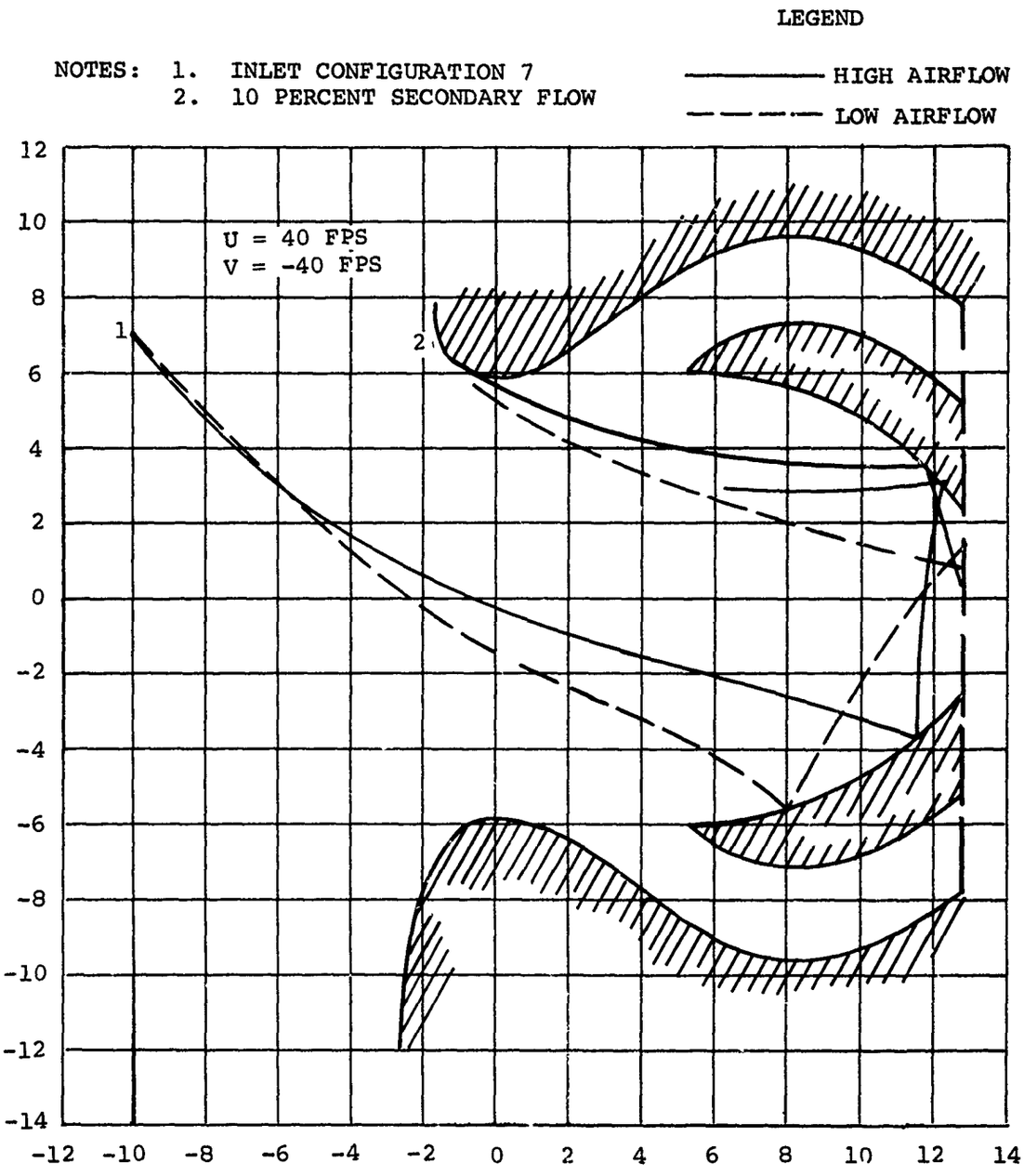

Figure 72. Effect of Varying Total Airflow on 180-Micron Particles With No Downwash

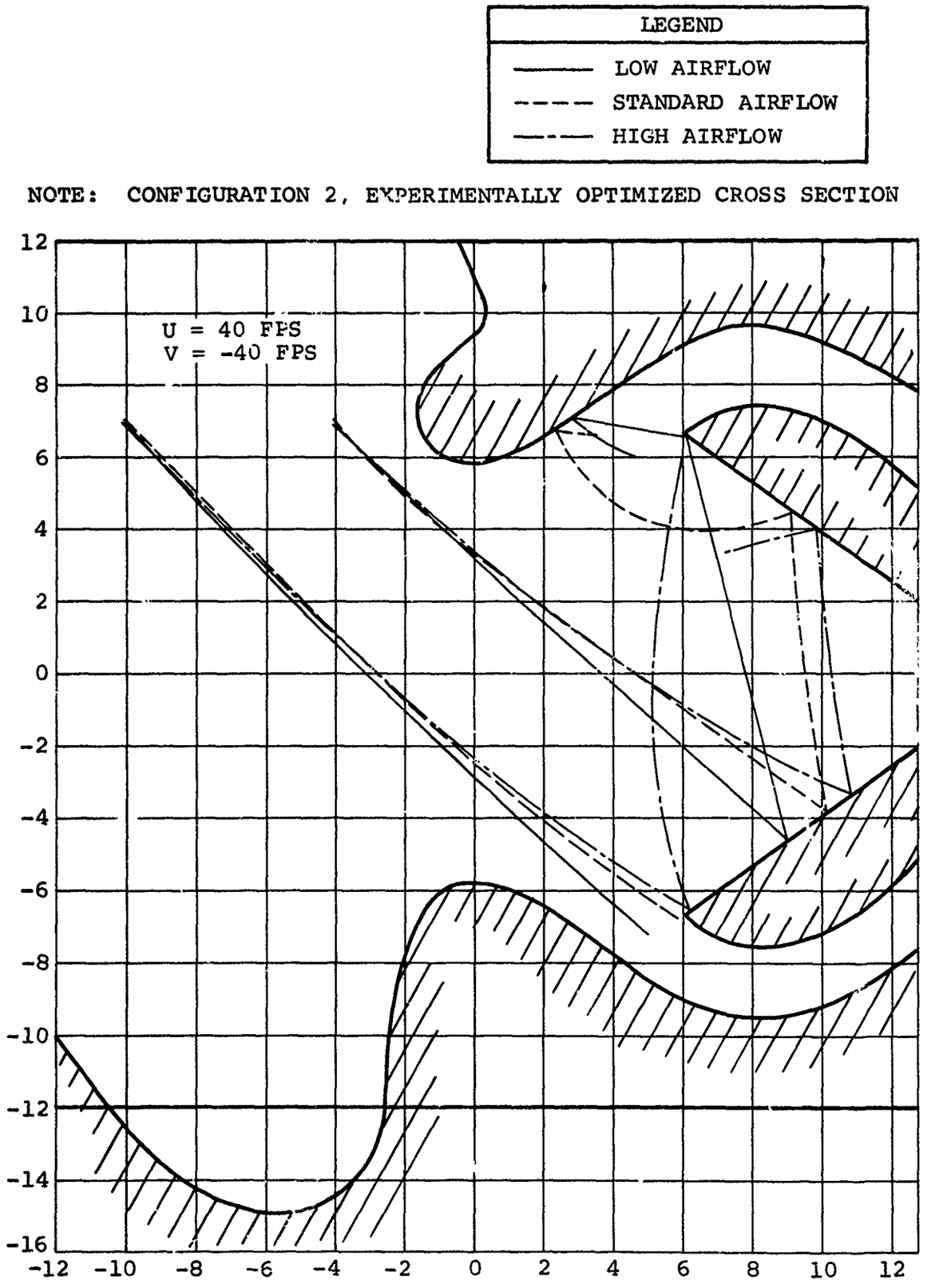

Figure 73 Effect of Varying Total Airflow on 800-Micron Particles With Downwash

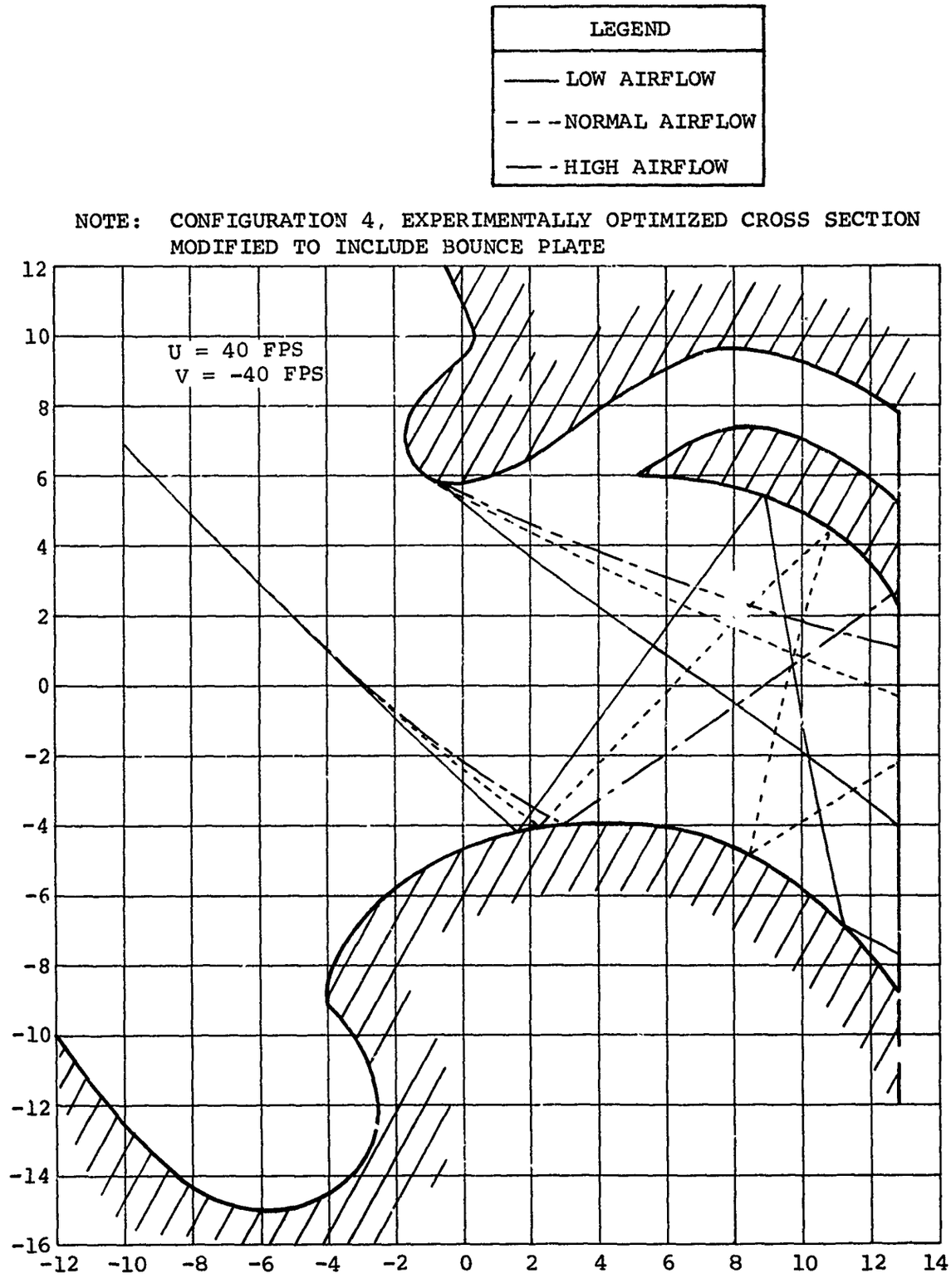

Figure 74. Effect of Varying Total Airflow on 800-Micron Particles With Downwash and Bounce Plate

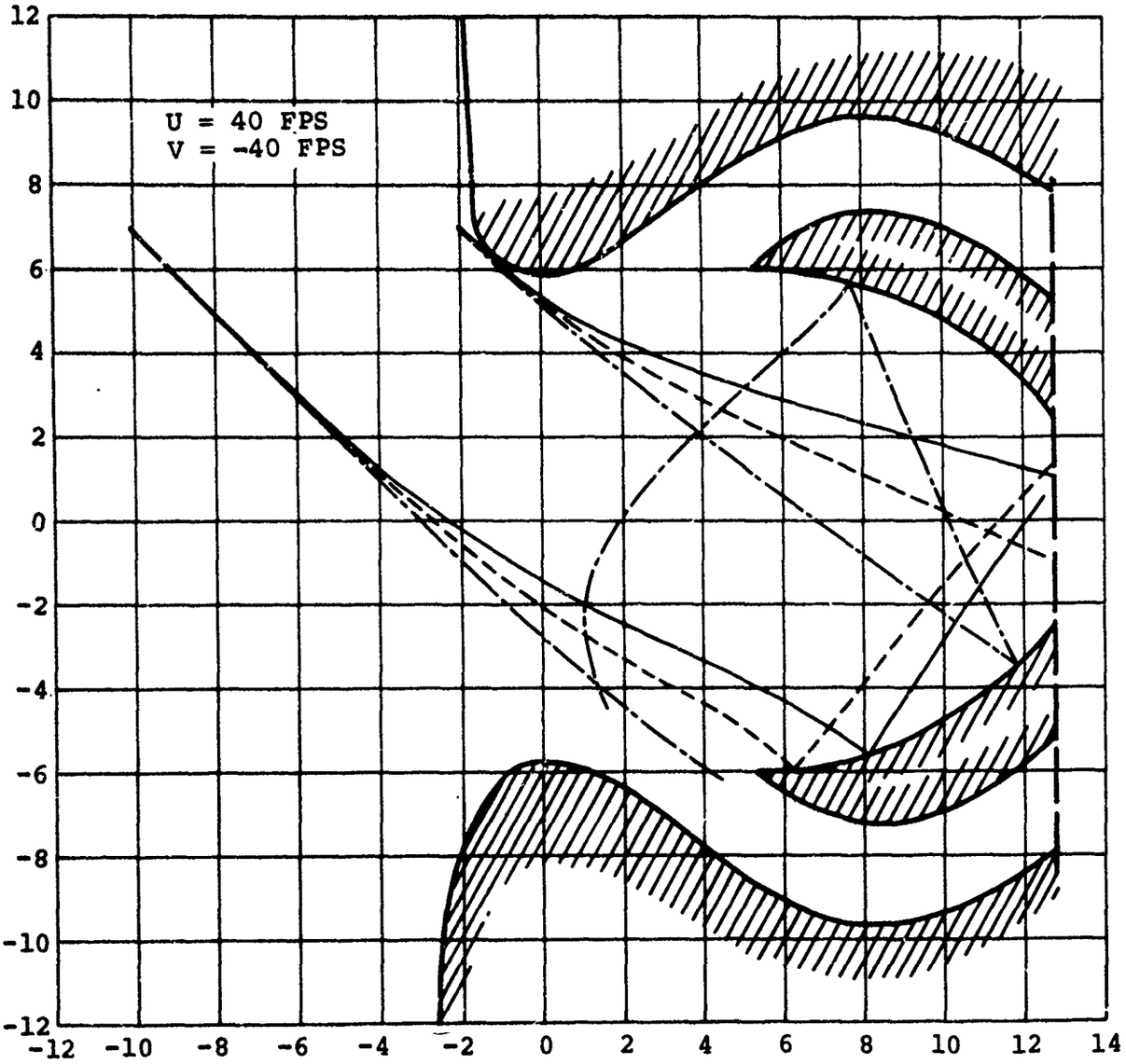

LEGEND	
———	HIGH AIRFLOW
- - - - - -	STANDARD AIRFLOW
——·——·——	LOW AIRFLOW

NOTES:

1. INLET CONFIGURATION 7
2. 10 PERCENT SECONDARY FLOW

Figure 75. Effect of Varying Total Airflow on 800-Micron Particles with No Downwash

3. Variations in the airflow will undoubtedly cause great changes in the bounce patterns, and the variable airflow inlet must therefore be designed to be as insensitive as possible to bounce. One way to do this is to orient a large proportion of the trap inner surface parallel to the inlet axis. This is a good rule in any case, since it will increase the tendency of the particles incident at all airflows to rebound in the downstream direction.

PARTICLE SPECIFIC GRAVITY EFFECTS

Little work was done toward determining the effects of particle density on individual particle trajectories. It was felt that an inlet designed to operate efficiently for a wide range of particle diameters or for a wide range of airflows would operate efficiently for a range of particle densities. The following explanation shows that this is a logical assumption. If we ignore gravitational effects, the particle trajectories are determined by the simple equations:

$$\text{Drag force} = F_{Drag} = \text{mass}_{particle} \times \text{acceleration}_{particle},$$

where F_{Drag} is also approximately proportional to the product of the particle surface area and a function of the relative velocity of the particle:

$$F_{Drag} \approx K \times f(V) \times A.$$

If the particle diameter is reduced by a factor of two for a given specific gravity, the mass decreases by a factor of eight and the drag diminishes by a factor of four. Thus the acceleration of the smaller particle for the same ΔV is approximately twice the acceleration of the original particle. If the particle density is decreased by a factor of two, the drag force remains constant but the mass decreases by a factor of two. Thus, again, the acceleration of the particle may be expected to be double that of the original particle for the same ΔV. A 100-micron particle with a specific gravity of 1.0 would then be expected to have a trajectory very similar to that of a 50-micron particle with a specific gravity of 2.0.

The trajectories plotted in Figure 76 illustrate the effect of varying the particle density by factors of two and four in one particular inlet. It can be easily seen that the effect is very similar to that of varying the particle diameter as shown in Figure 61. Figures 77 and 78 show that the density effect is quite small for small particles. The 70-micron sand and 70-micron salt water spray particles have very similar

NOTES: 1. CONFIGURATION 4, EXPERIMENTALLY OPTIMIZED CROSS SECTION MODIFIED TO INCLUDE BOUNCE PLATE

2. NORMAL AIRFLOW

3. 800-MICRON PARTICLE SIZE

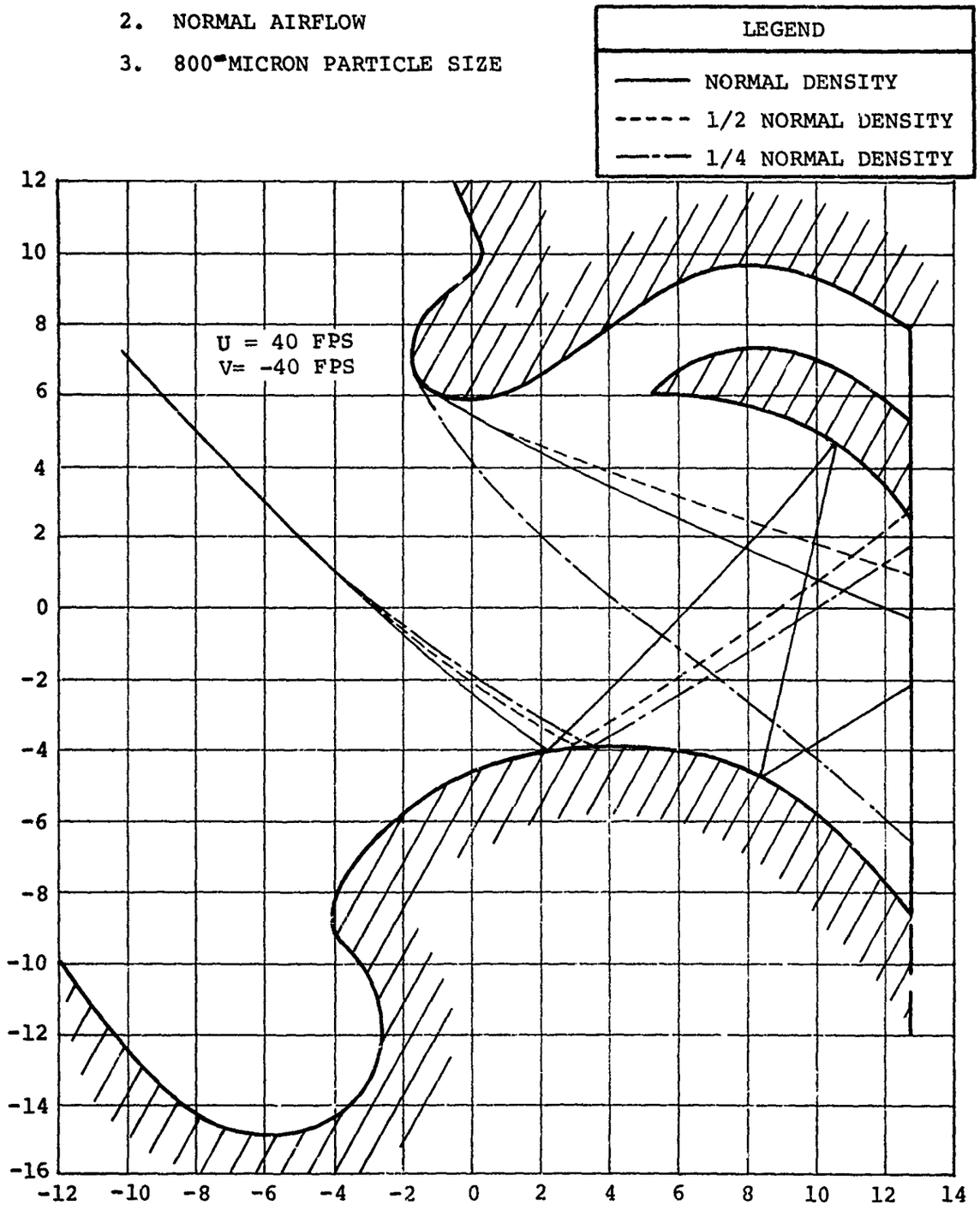

Figure 76. Effect of Varying Particle Specific Gravity

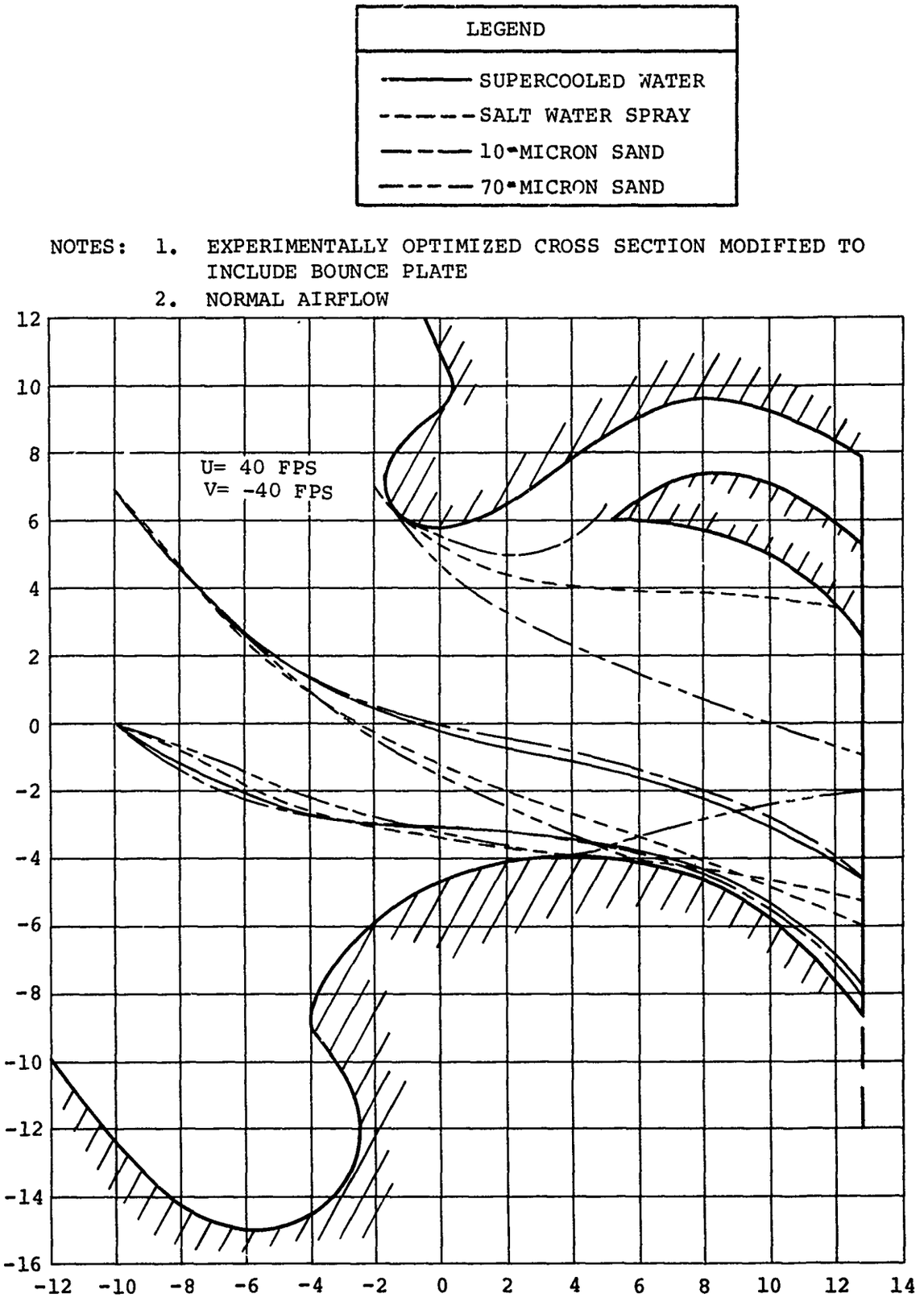

Figure 77. Comparison of Water Droplet and Small Particle Trajectories for Inlet Configuration 4

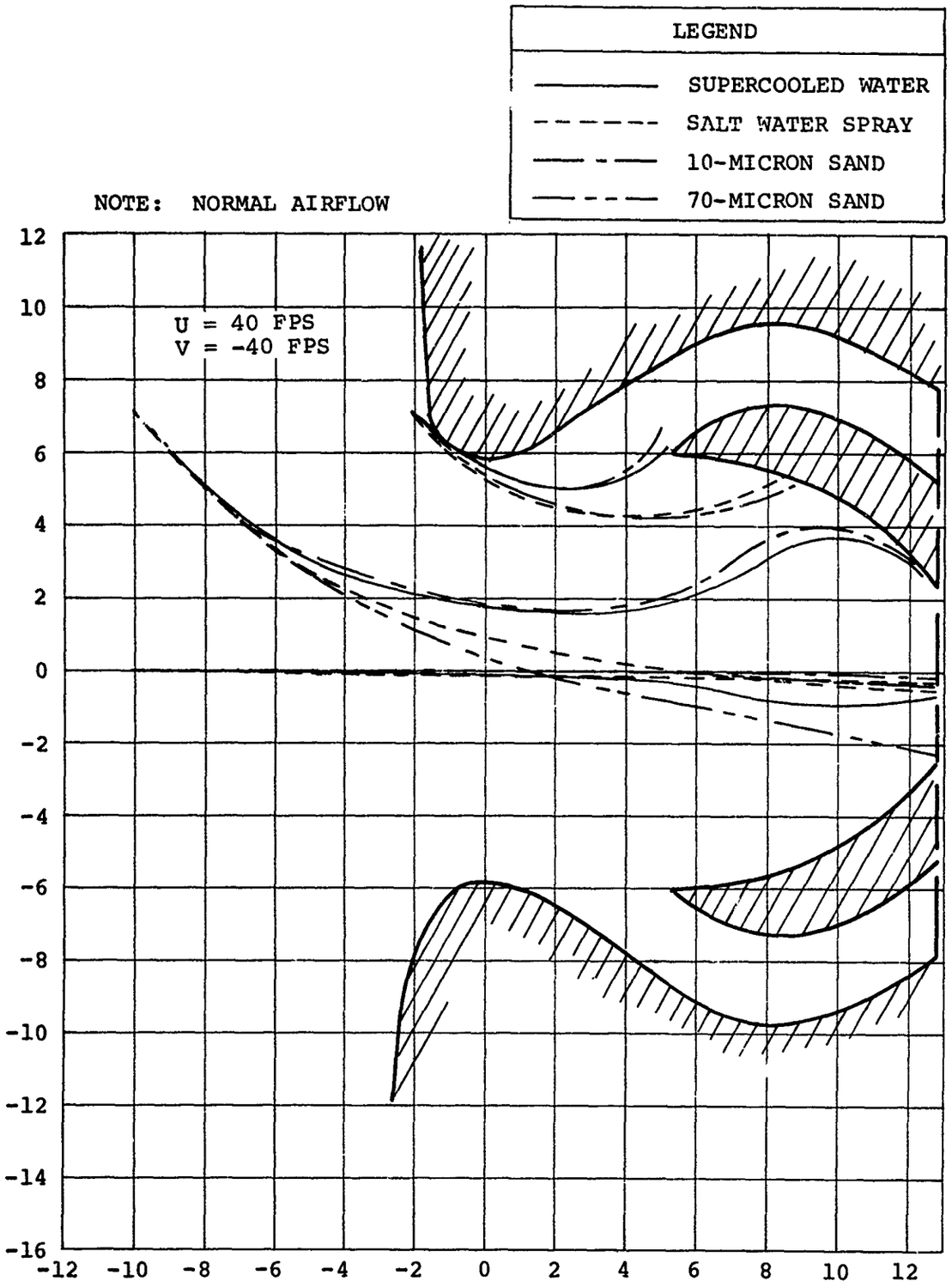

Figure 78. Comparison of Water Droplet and Small Particle Trajectories for Inlet Configuration 7

trajectories, as do the 10-micron sand and the 20-micron supercooled water particles. All these particles follow paths very close to the streamlines of the airflow pattern, which has been shown to be typical of very small particles.

Since the total variation in the specific gravity of particles collected by an inertial separator inlet is not likely to be greater than a factor of four, an appropriate way for the designer to provide for particle specific gravity variation is to allow for somewhat more than a factor of four variation in particle diameter alone, while designing for the most likely particle specific gravity and diameter. An alternative method would be to determine the range of particle masses which must be allowed for, to choose an appropriate mean or most likely specific gravity, and to calculate the range of equivalent diameters which must then be considered at the chosen specific gravity. A design which is efficient at the upper and lower limits of this diameter range should then be adequately efficient for all combinations of diameter and specific gravity likely to be encountered.

DOWNWASH AND NO-DOWNWASH EFFECTS

Figures 79 through 81 illustrate the comparison between downwash and no-downwash flow entering a symmetrical inlet, for the three characteristic particle sizes, 10, 180, and 800 microns. The curves are presented for a 5-percent secondary flow inlet; virtually the same results are obtained for 10-percent secondary flow. It is obvious from these figures that a symmetrical separator must not be expected to operate efficiently in a skewed airflow. A slight extension of this statement should be helpful in the design of three-dimensional inlets: the airflow pattern should be axisymmetrical in any plane in which the inlet cross section is axisymmetrical. An example of a design based on this principle is the type E inlet described in this report. This inlet is designed for axisymmetrical airflow in the horizontal plane and for skewed airflow in the vertical plane.

It must be emphasized here that the approach which led to the type E inlet is not exactly correct for three-dimensional inlets, since particle trajectories will not always lie in axial planes (i.e., planes containing the axis of the inlet) and since the airflow pattern presupposed by the approach is not the one actually occurring in a three-dimensional flow field. In spite of this inherent inaccuracy, the consideration of inlet airflow in horizontal and vertical planes as separate cases does appear to produce results in good agreement with experiment.

PARTICLE AND WALL RESILIENCE EFFECTS

Figure 82 illustrates the effect of varying the coefficient of restitution for the particle/wall collision within the trap. It is evident that the less resilient the wall, the less likely the particle is to rebound in an undesirable direction (i.e., upstream). Any surfaces on which particles impinge should be as nonresilient as possible. This applies equally to surfaces specifically designed for particle collisions, such as the bounce plate in inlet type C.

Examination of all the data obtained in this study reveals that a particle is almost never bounced back upstream after only one collision; at least two collisions are needed in nearly every instance. Thus all the trap surfaces should be designed to remove as much energy as possible from the incident particle at the first collision. This will enable the secondary airflow to control the rebounding particle easily and will make the probability of a second collision low. The task of the designer, when considering resiliency effects, is to determine the approximate coefficients of restitution for collisions between the design particles and the proposed trap materials, and to choose that material with the lowest coefficient, provided that it meets other design criteria.

NOTES: 1. INLET CONFIGURATION 6
2. NORMAL AIRFLOW

LEGEND	
———	DOWNWASH
– – – –	NO DOWNWASH

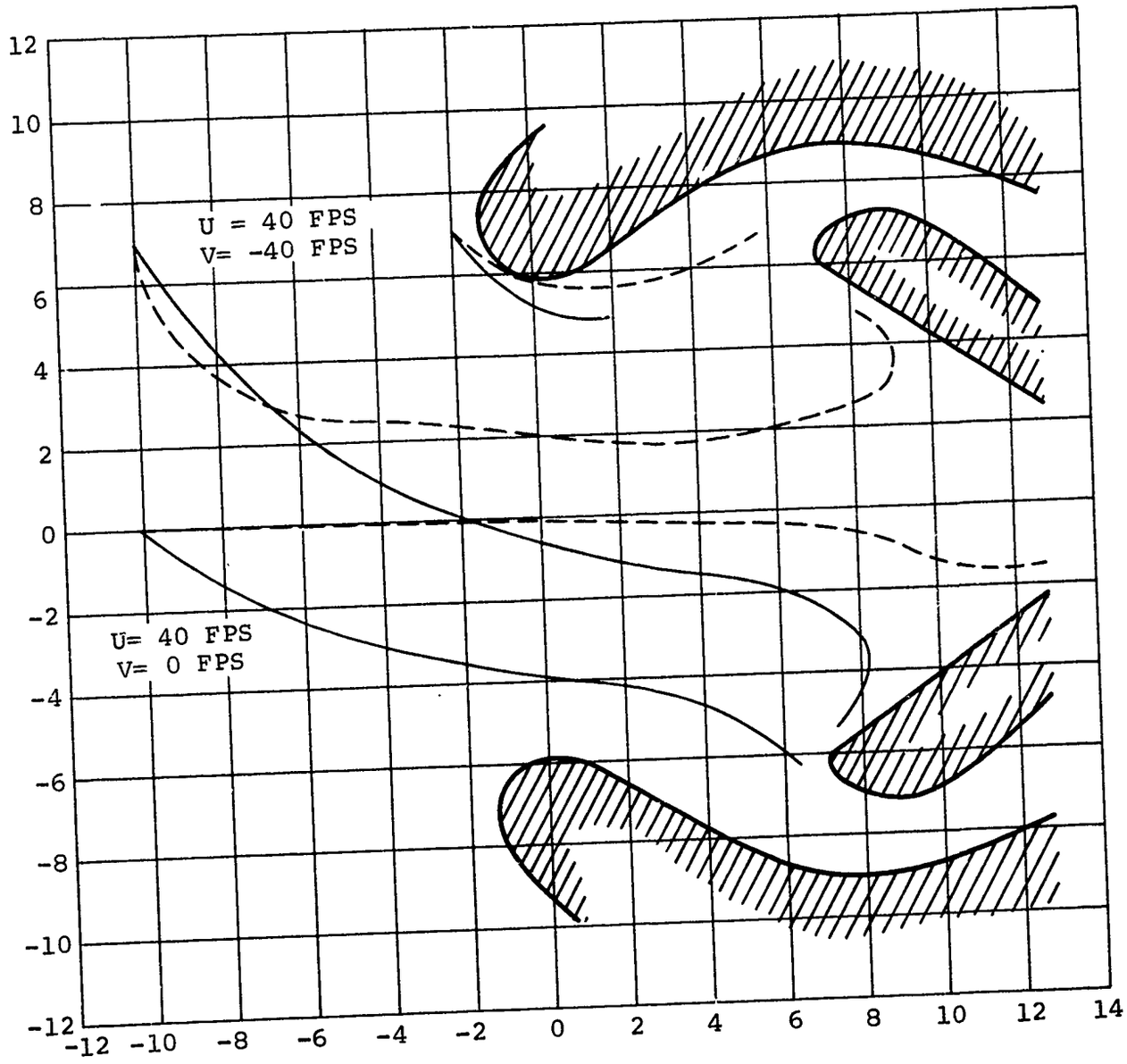

Figure 79. Effect of Downwash on Trajectories of 10-Micron Particles

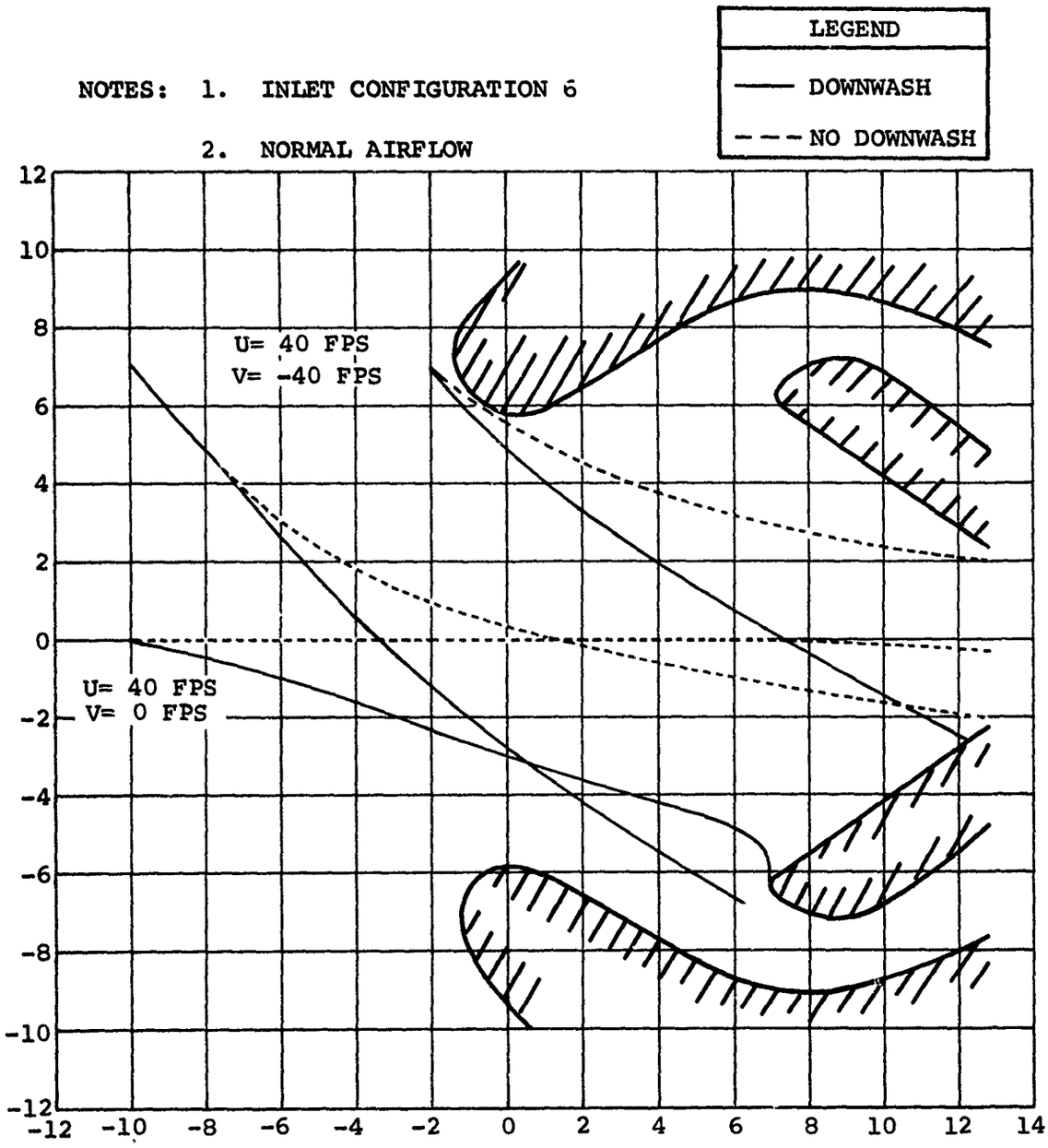

Figure 80. Effect of Downwash on Trajectories of 180-Micron Particles

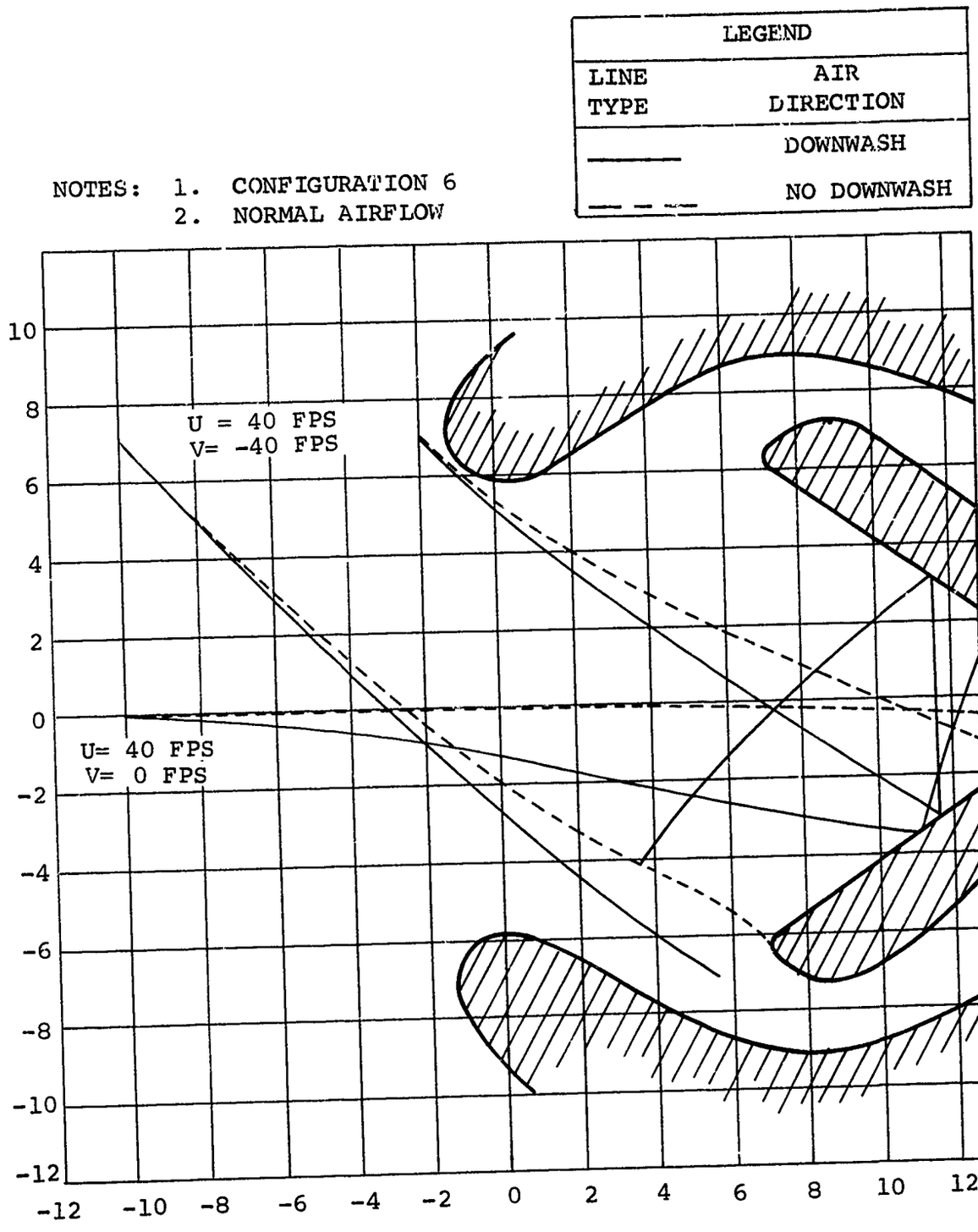

Figure 81. Effect of Downwash on Particle Trajectories of 800-Micron Sand

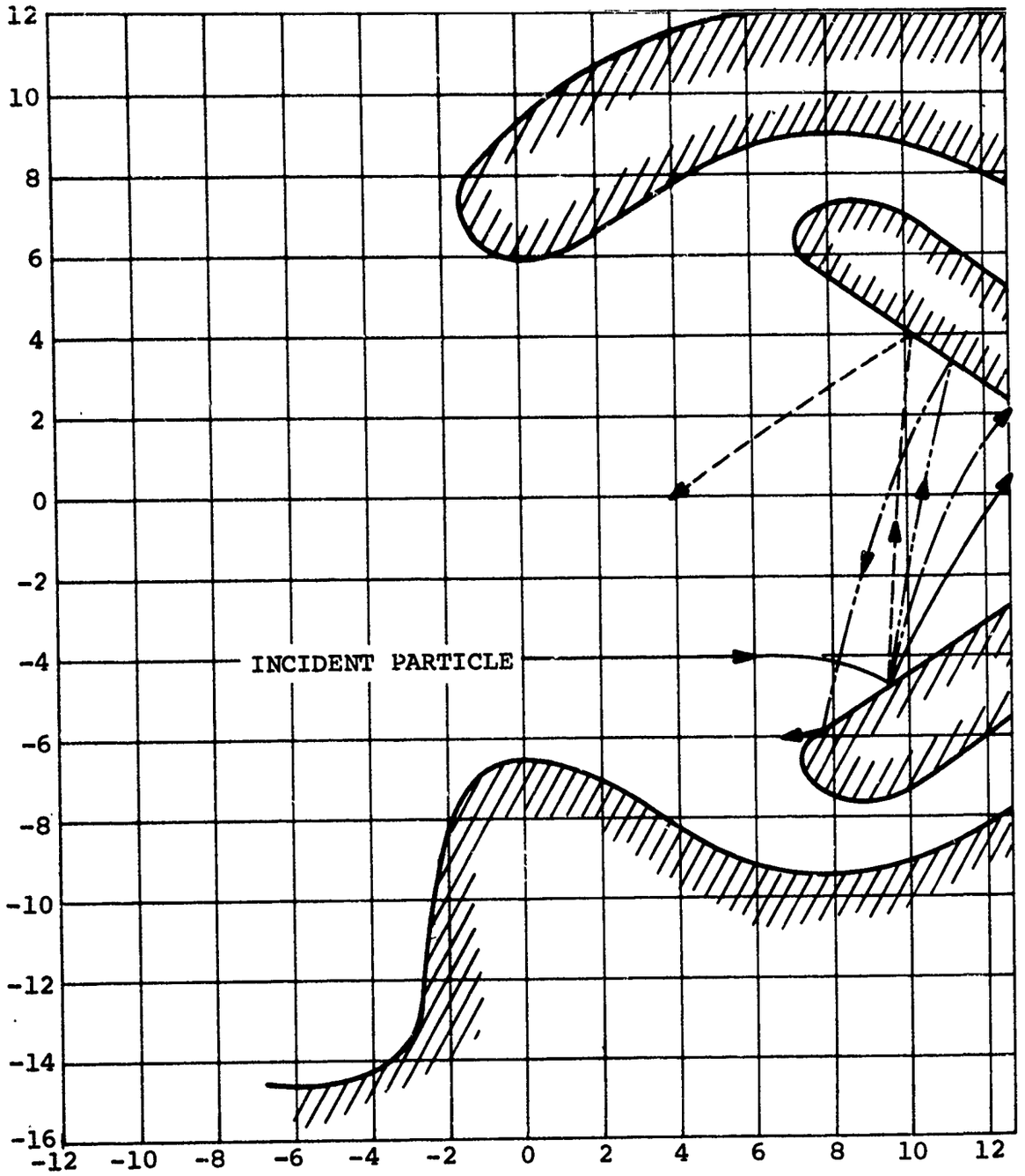

LEGEND	
LINE TYPE	COEFFICIENT OF RESTITUTION
————	0.40
—·—·—	0.60
—··—··—	0.80
- - - - -	1.00

NOTES:

1. CONFIGURATION 1
2. BASIC INLET CROSS SECTION
3. 180-MICRON PARTICLE
4. INITIAL VELOCITY = 40 FPS

Figure 82. Effect of Particle/Wall Resilience on Rebounding Particles

PARAMETERS FOR FUTURE INLET DESIGN - ASW AND DESERT OPERATIONS

The previous section has considered in a general way, the parameters which will influence the design of an inertial separator inlet. Inlet design for specified missions such as ASW or desert operation will involve consideration of exactly the same parameters discussed previously. The parameters to which most attention will be directed will vary with the application, however.

In a helicopter intended for general use, separator design must deal with a wide range of particle parameters. The design task is made somewhat easier if the mission is specified and limited, as it is in ASW or desert warfare helicopters. In either case the particle specific gravity and the particle resilience essentially will become constants. The range of particle sizes expected can also be more clearly defined, the effects of particle ingestion on the powerplant can be predicted, and the necessary separation efficiency over various regions of the particle size range can be specified. The two extreme environments involved in ASW and desert operations thus present difficult but quite clearly defined problems to the particle separator designer.

The nature of the environment characteristic of ASW operations has been described in Reference 9. The discussion below is based largely on this reference, on additional information from Reference 2, and on the results of the present investigation.

The environment seen by the ASW gas turbine inlet is a function of several variables, among which are: (1) vehicle configuration, (2) vehicle motion, (3) slipstream characteristics, and (4) sea state. The first of these variables refers mainly to the location and shielding of the inlets. Two principles should be applied in general: (1) as much of the bulk of the vehicle as possible should be put between the inlet and the surface of the water, and (2) the inlet should be as high above the surface as feasible. An inlet location atop the fuselage meets both of these requirements in most cases.

In the particular case of the helicopter, an engine location atop the fuselage also provides a simple solution to mechanical problems of shafting, transmissions, and so forth. However, it appears that the effect of the third variable listed, slipstream characteristics, can modify the top-of-the-fuselage requirement for helicopter inlets. On helicopters, inlets located directly in the rotor downwash, high on, but outboard of the fuselage proper appear to ingest less foreign matter than those directly on top of the fuselage. This is evidently because the downwash past the inlet acts as a simple inertial

separator when the fuselage is not present to turn or bounce the particles more directly into the inlet. In the case of ducted-fan aircraft or other VTOL's, this slipstream sweeping effect is not present and the fuselage top inlet location is the optimum.

The effect of the second variable listed, the vehicle motion, is closely tied to the method by which the ASW mission is to be performed. If the vehicle is to spend most of its time in hover, rather than in takeoff and landing, the spray seen by the inlets will be largely that entrained from the water surface by the recirculating rotor downwash. The drop size in this type of spray is characteristically rather small, approximately 80 microns or less. The size decreases as hover altitude increases, and above an altitude of 35 feet, little or no spray is observed at the inlets.

If the vehicle is to perform the ASW mission by executing a large number of water landings and takeoffs or by remaining on the surface for long periods of time, the character of the spray seen by the inlets changes radically and becomes largely a function of the fourth named variable, the sea state. The spray near the surface of the water is caused by the interaction of wind and waves, and for sea states of 5 or higher, it can consist of large amounts of water in the form of large drops and sheets. This spray frequently contains quantities of water great enough to cause immediate engine flameout, if ingested. The design of an aerodynamic-inertial separator of the type described in this report is complicated by the quantity of water involved, the widely varying nature of the slipstream, and the fact that engine airflow will vary from zero to takeoff values. Conversely, the relatively large amount of blockage of the direct inlet flow path characteristic of this type of separator is likely to provide a fairly high degree of engine protection from spray, particularly at low airflows.

Regarding the effect of the slipstream on the environment seen by the inlets, it has been observed that multiple slipstreams impinging on a liquid surface will tend to entrain more spray than the equivalent single slipstream (References 3 and 10). The region of the surface in which this entrainment is most pronounced is near the stagnation point between two slipstreams. In this region a highly turbulent and unstable, but predominantly upward flow exists, which tends to carry large quantities of spray particles to higher than normal altitudes. For this reason, care must be exercised to keep engine inlets away from the areas of the airplane in which multiple slipstreams converge.

Assuming that the inlet location has been determined on a given ASW vehicle, the following observations may be made as to the parameters which will influence actual inlet design: (1) particle sizes encountered may vary quite widely from less than 10 microns to over 1000 microns, (2) particle speci-fic gravity will be constant, (3) airflow will be relatively constant at maximum power if the proposed mission involves prolonged hovering; if the mission involves actual landings, the airflow will vary over a much wider range, (4) particle resilience is effectively zero. This last observation on resilience is perhaps the most important of the four. It implies that an inertial separator intended specifically for ASW can be designed with little attention given to particle bounce. Orientation of the trap surfaces is then not as critical as it is when separating solid particles.

In view of this, the principal objectives in achieving a modification of the inertial separator design for use in spray should be as follows: (1) droplets should not be allowed to strike an inlet surface upstream of a primary air intake, (2) trap surfaces which can be struck by droplets should be swept by high velocity secondary air to force the liquid film formed on the surfaces to flow downstream into the trap, (3) adequate drains must be provided in both secondary and primary systems to allow the large masses of water which may be ingested to run off without damage to the separator function, and (4) separator structure must be strong enough to withstand the impact loading of large masses of water. For design purposes, the first objective implies strong focusing action in the bellmouth, and the second implies a rapidly converging trap, which will produce rapidly accelerating secondary air to draw the impinging water drop-lets downstream.

Desert operations present different problems in separator inlet design. Missions probably will involve a large number of take-off and landing cycles as well as prolonged hover. This implies that the inlet often will be placed in highly contaminated environments while undergoing a transient type of operation, making it difficult to predict or design for a specific particle concentration or airflow. In general, the inlet must be designed for quite a wide range of particle izes for three reasons: (1) For a given ground particle size distribution, the inlet will see varying size distributions as the vehicle altitude, disc loading, and engine airflow are varied. (2) At a given station the particle size distribution at the inlet will vary as the activity of other vehicles in the immediate neighborhood varies, (for example two helicopters hovering side by side over sand will each see a higher concentration of airborne foreign material than either would

see by itself, Reference 10). (3) At given engine airflow and vehicle altitude, the particle concentration will vary with the ground particle size distribution existing in the region of downwash impingement.

The inability of the downwash to entrain very heavy particles will tend to even out partially this last variation; nevertheless, the ground particle size variation may be so pronounced as to affect substantially the entrained size distribution. For example, References 10 and 11 list four different particle size distributions for the Yuma Proving Grounds. The mean particle size in these distributions ranges from approximately 100 microns to approximately 400 microns. As shown previously particles of these two diameters would behave quite differently from each other when entrained in an airstream.

As in the case of ASW operations, the particle specific gravity (density) will not be a variable in the inlet design, once an appropriate value has been determined for the operations in question. The particle resiliency will cause difficulty since it is likely to be both high and variable. This tends to make particle capture by ricochet a risky procedure since bounces will be unpredictable and very difficult to control. For this reason the inlet design should involve careful focusing of the incident particles before they enter the trap; moreover orientation of trap surfaces should be such that ricocheting particles tend to continue to move downstream, and the inlet wall material should have the lowest practical resilience.

The designs studied in this report have an average air velocity at the throat of about 210 feet per second. This is probably an appropriate velocity for design, as it achieves reasonable focusing of the particles with reasonable turning (and consesequent low pressure loss) in the primary air. Allowance should be made, of course, for the maximum and minimum flow rates expected, with the inlet design biased toward the minimum.

Most of the particle size distribution data presently available indicate that desert sand has a mean particle diameter between 100 and 250 microns, the size range on the ground being from zero to 800 microns. Flight samples will tend to have more small particles and fewer large particles than ground samples, so that design should be aimed at the lower half of the 100- to 250-micron range. A specific gravity of approximately 2.3 (rock) was used for the sand particles in this study and is probably an appropriate design value for desert operations. If more exact information becomes available on variations in the specific gravity of the particles to be encountered, the methods outlined in the previous section should be followed to convert this variation to an effective diameter variation at constant

specific gravity.

A combination of focusing action in the bellmouth and the inevitable bouncing of particles, which will take place in the trap, will produce localized wear patterns on the trap surfaces. The trajectory plots for moderately sized particles in configuration 4, Figures 32 through 42 show the typical impingement patterns which may be expected. Bench tests of inlets at Boeing have produced very similar patterns. Consideration of possible erosion damage also should influence selection of material for the trap structure.

The bounce method of particle separation is not recommended unless no other suitable design alternative exists. One such alternative which should be considered is that of the symmetrical inlet oriented so that it sees a no-downwash airflow in all flight conditions. This inlet, for the particle size range most likely to be seen in desert operations can be developed for a separation efficiency virtually equal to that of the bounce-plate inlet. According to the present study, for instance, the former will attain 97 percent separation while the latter will have 100 percent separation at sand particle sizes of 70 to 400 microns. The symmetrical inlet has a great advantage. Most particles never contact a trap surface until they are deep within the secondary flow ductwork and they cannot then bounce back upstream.

The symmetrical inlet has the disadvantage of being oriented almost parallel to the incoming air stream in order to attain reasonable separation efficiency. For example, separation in the theore-tical inlet under study dropped from 97 to 46 percent when the air entered at approximately 30 degrees with respect to the inlet axis. The symmetrical inlet then, must be located somewhere on the aircraft where the direction of the airflow will not vary with the operating condition, and must be carefully oriented in alignment with this airstream. This requirement may cause difficulty, of course, if it is desired to obtain useful ram effect from the inlet at high forward speeds. This would imply a need for a forward-facing inlet. Unfortunately, a forward-facing inlet is not appropriate for separation in hover operations, especially if it is situated in a strong downwash region. Providing an alternate straight-through inlet or bypass is the most expedient solution for this problem. It should be noted that the same problem and the same solution are common to most of the other separator designs in which ram effect is desired in forward flight together with good particle separation in hover.

The fairly dense and resilient particles to be encountered in desert operations require a swirl separator which does not depend chiefly on particle bounce for its operation, and which, by design or by location, is insensitive to the direction and magnitude of the incoming airflow. The separation efficiency of the inlet must be high, 90 percent or more, to provide adequate long-term protection against erosion in the engine. An equivalent of the extremely high concentrations of foreign material which can be experienced momentarily by an inlet on an ASW vehicle (due to wave/spray impingement) is not likely to occur in desert operations. Therefore, the separator need not be designed with provision for draining off large masses of material in a very short time.

CONCLUSIONS AND RECOMMENDATIONS

CONCLUSIONS

1. Gas-turbine-powered helicopters and VTOL aircraft operating in areas of dust or water spray require a means of eliminating foreign material from the air ingested by the engine. To a certain extent, this can be accomplished by careful location and orientation of the inlet to place it in an area shielded by the fuselage; however, most severe environments will require some form of particle separator in the inlet design. The separators which appear best suited for present and imminent aircraft are: (1) the full-barrier filter, (2) separators being developed by the engine manufacturers, (3) the vortex tube separator, and (4) the Boeing inertial separator. Each of these has certain advantages which must be evaluated for each particular intended application.

2. Inertial separators similar to the Boeing type are amenable to analysis by the methods employed in this study. These methods include simulation of the air velocity field in the inlet by two-dimensional electrical analog methods, and simulation of particles entrained in the inlet air by a digital computer program for trajectory calculation. The methods are strictly applicable only to two-dimensional inlets for a variety of theoretical and practical reasons, but good approximations to the behavior of three-dimensional inlets can be obtained if an awareness of the differences between the two cases is maintained. In this study, the values of estimated separation efficiency for the type E (three-dimensional) inlet fell within 6 percent of the values obtained from bench tests of the same type inlet. The characteristics of the curves of separation efficiency versus particle size, and separation efficiency versus airflow, were also similar in the analytical and experimental cases, as were the particle impingement patterns. Therefore, the present study is therefore considered a valid analysis of the characteristics of the Boeing inertial separator. The methods of this study, as presently constructed, cannot be applied to inlets which depend mainly on tangential swirl to effect particle separation.

3. Alternate analytical methods are available which may improve the simulation of the three-dimensional axisymmetrical duct with the airflow entering axially. These methods would involve either the use of an electrolytic analog tank or the iterative solution of the three-dimensional, axisymmetrical Laplace equation, to calculate the airflow velocities throughout the inlet. The present type of particle trajectory calculation would still apply. There is no three-dimensional method known at present by

which the flow field in skewed airflow or in an asymmetrical inlet can be calculated from potential theory. Thus, the present analysis of inlets with downwash, with a bounce plate, or with both, is not easily improved upon by the application of methods based upon potential flow theories.

4. The analytical results of this study indicate the following:

   a. An inlet with a bounce plate and 10-percent secondary flow will achieve a separation efficiency of 90 percent or greater in downwash for virtually all sand particle diameters from 0 to 800 microns.

   b. A symmetrical, no-bounce-plate inlet oriented parallel to the entering airflow and with 10-percent secondary flow will achieve the same separation efficiency as the bounce plate inlet. With only 5-percent secondary flow, the separation efficiency of the symmetrical inlet falls substantially below that of the bounce plate inlet.

   c. The symmetrical inlets are useless in a downwash flow field, achieving at best an efficiency of approximately 50 percent.

   d. An increase in inlet length coupled with a decrease in bellmouth area and an increase in primary flow area will provide better focusing of the particles on the trap in the symmetrical inlet, and will thus tend to increas separation efficiency.

   e. An inlet, configuration 4, has been identified and optimized for a downwash flow field. This is the flow field seen by inlets mounted on the top of the typical helicopter fuselage in the vicinity of the rotor.

   f. An inlet, configuration 7, has been identified and optimized for a no-downwash flow field. This is the flow field seen by an inlet mounted far forward or under the fuselage of a helicopter or far away from the fans in a ducted fan-type vehicle.

   g. The inlets designed were optimized for #70 sand (mean particle size approximately 180 microns) at an airflow of approximately 12.8 pounds per second. The optimum particle size is largely determined by the throat velocity, which is approximately 210 feet per second for the two configurations used above.

5. The effects of several parameters on separation efficiency were determined to be as follows:

   a. Percent trap flow: An increase in percent trap flow generally is accompanied by an increase in efficiency. The improvement is a function of particle size, however, and is greater for the smaller particles.

   b. Total airflow: A decrease in separation efficiency occurs at airflows higher or lower than the design value. Type C (the inlet with the bounceplate), however, was found very insensitive to total airflow. Higher airflow than the design value is generally better than lower airflow.

   c. Individual particle density: There is no simple effect due to density, but the lighter particles are usually more difficult to trap. Once the lightest particles have entered the trap, however, they are more easily controlled by the secondary airflow and have less tendency to bounce out into the primary flow region. Variation in particle density can be allowed for in inlet design by considering equivalent variation in particle diameter.

   d. Presence or absence of downwash: Downwash is extremely detrimental to separator efficiency. In the case of the symmetrical separators, the efficiency is reduced by almost half when run with downwash.

   e. Particle diameter: This is a parameter with very complex effects. Small particles less than 100 microns are difficult to trap because they tend to follow the air streamlines very closely within little inertial effect. Large particles greater than 200 microns are difficult to trap because they may bounce within the inlet. Generally, the smallest particles are those most likely to be ingested by the engine, on a numerical, but not necessarily a weight basis.

   f. Elasticity of the particle-wall collision: The more resilient the particle or the wall (or both), the greater is the difficulty in separating any particles that are not drawn directly into the trap. Every additional bounce taken by a particle within the inlet increases its chances of entering the primary flow area and of being ingested by the engine.

   g. Particle initial position and velocity: These affect calculated separation efficiency and particle trajectories in very complex ways. No general rules can be drawn. A wide variety of initial positions and velocities must be studied for each configuration.

6. It was determined that the very low resilience of the particles encountered in a salt water spray environment makes design of a separator for an ASW helicopter a matter of focusing the particles, thereby forcing them into the trap, where they will have little tendency to bounce. In the case of desert operations it was determined that the wide range of airflow and particle masses likely to be encountered, together with the relatively high resiliency of the particles, make it necessary to control the particles carefully even after they have entered the trap. This implies either a bounce plate type inlet (for locations with downwash) or a highly focusing symmetrical inlet directly facing the prevailing flow. In both cases, inner trap contours should be designed to promote particle bounce in the downstream direction.

7. It was concluded that the main obstacle to successful separator design is the tendency for large, heavy particles to bounce within the inlet. If this tendency can be controlled by use of low resiliency materials or eliminated by careful separator design to avoid collisions, the high inertia of these particles will make them relatively easy to trap, since they are quite insensitive to sudden turns in the air stream.

RECOMMENDATIONS:

1. Additional experimental data are needed for correlation with these analytical results. If enough analytical and experimental data on exactly the same inlet could be compared, a more consistent and reliable relationship between the two types of results could be derived. A large amount of initial separator design work could then be based on analytical data, and much expensive trial and error experimentation could be eliminated.

2. Additional analytical work, based on the present methods, would be useful in obtaining data for a wider variety of actual inlet types. The present methods can be extended to cover virtually all separator inlets in which the flow is 2-dimensional, and may be used as a close approximation to any inlet in which the flow is axisymmetrical and three-dimensional, but containing negligible swirl.

3. There are two difficulties which should be eliminated in using this study as a design method:

   a. The time necessary to produce and reduce the air velocity data from an electrical analog plot is excessive. The original setup of the inlet cross section on the analog board, the plotting of the equipotential lines,

the measurement of the spacing and orientation of these lines, and the computation of air velocities, all must be done by hand. Experience has shown that digital computation of the flow field would be preferable to the analog method used. Elimination of the hand work associated with the analog method would be the major advantage of digital computation. The method would involve an iterative solution of a Laplace differential equation with the boundary conditions established by the particular inlet being studied. Input would consist mainly of coordinates describing the inlet surface, and output would consist of an table of velocity versus position in the inlet. Using this method, minor changes in the cross section of an inlet and changes in the downwash pattern entering a given inlet could be made almost instantaneously without the tedious effort required at present to compute the velocities in the modified flow field. The relative merit of the inlet modifications could then be evaluated immediately, and an optimized airflow pattern through a given inlet could be determined much more rapidly than at present.

b. The conversion of the coordinate output of the particle trajectory computer program to actual plotted trajectories is also an extremely time consuming process when done by hand. It is recommended that, in future studies of this type, the computer program be modified to provide for output consisting of plotted trajectories. A further step would be a provision in the program to allow the computer to automatically calculate each trajectory to the point where it is possible to determine whether or not the particle has been trapped. The computer could then calculate separation efficiencies for various particle types, running time per trajectory would be reduced, and it would be possible to work with particle distributions involving a much greater number of initial positions and velocities. This procedure should improve estimates of separation efficiency.

Once the two obstacles identified above have been removed, it would be possible to provide an integrated digital computer program for the optimized design of an inertial inlet. Input would be a description of the inlet cross section being prepared, while output would be the separation efficiency of the inlet for various specified particle types. Intermediate results such as plotted inlet cross section, streamline pattern through the inlet (to evaluate pressure loss), and typical particle trajectories could be displayed, as calculated, on a cathode ray tube. The designer, observing the output, would then

be able to modify the inlet design immediately to achieve a separator optimized for the particles and flow conditions desired.

The foregoing recommendation is aimed at formulation of a separator inlet design method, to be based on the computer program used in this study by addition of: (a) a different method of calculating air velocities in the inlet, and (b) additional input and output options to enable the designer to observe the effect of changes in the configuration as they are made. In conjunction with the additional experimental-analytical correlation work recommended in (1) and (2), this method should provide useful and accurate design data for the inertial separator inlet.

LIST OF REFERENCES

1. SWIRL INLET PARAMETRIC STUDY - PHASE III: SECOND QUARTERLY PROGRESS REPORT, The Boeing Company, Vertol Division, Bureau of Weapons Contract NOw 66-0562-c, 30 November 1966.

2. SALT WATER INGESTION BY GAS TURBINE ENGINES, T. F. Stirgwolt, General Electric Company, U. S. Naval Air Test Station Conference on Environmental Effects on Aircraft Propulsion, June 22 & 23, 1961, Trenton, New Jersey.

3. DOWNWASH TESTS OF THE X-22 DUCTED FAN TANDEM VTOL RESEARCH AIRCRAFT CONFIGURATIONS TO EVALUATE THE OPTIMUM ENGINE INLET LOCATIONS, Kellett Aircraft Corporation, Bureau of Weapons Contract NOw 64-0439-f, 30 December 1965.

4. DEVELOPMENT OF SWIRL TYPE TURBINE ENGINE FOREIGN PARTICLE SEPARATOR, The Boeing Company, Vertol Division, Bureau of Weapons Contract NOw 62-0814-c, 13 September 1963.

5. MODEL T55-L-11 GAS TURBINE ENGINE INFORMATION, Technical Brochure No. 1214.25, Lycoming Division, AVCO Corporation, Stratford, Connecticut.

6. INSTRUCTION MANUAL IM24-1, MODEL 241A ANALOG FIELD PLOTTER, Sunshine Scientific Instrument Co., Philadelphia, Pa.

7. AN EMPIRICAL METHOD PERMITTING RAPID DETERMINATION OF THE AREA, RATE, AND DISTRIBUTION OF WATER-DROP IMPINGEMENT ON AN AIRFOIL OF ARBITRARY SECTION AT SUBSONIC SPEEDS, N. R. Bergrun, NACA TN2476, September 1951.

8. SWIRL INLET PARAMETRIC STUDY - PHASE III: SIXTH QUARTERLY REPORT, The Boeing Company, Vertol Division, Bureau of Weapons Contract NOw 66-0562-c, 14 December 1967.

9. ENGINE/AIRFRAME INTERFACE CONSIDERATION FOR FUTURE OPEN-OCEAN ASW AIRCRAFT, G. G. Ward, Ling-Temco-Vought Aeronautical Corporation, Proceedings of the Seventh Annual National Conference on Environmental Effects on Aircraft and Propulsion Systems, September 25 - 27, 1967, Princeton, New Jersey.

10. EVALUATION OF THE DUST CLOUD GENERATED BY HELICOPTER ROTOR BLADE DOWNWASH, S. H. Rodgers, MSA Research Corporation, Proceedings of the Seventh Annual National Conference on Environmental Effects on Aircraft and Propulsion Systems, September 25 - 27, 1967, Princeton, New Jersey.

11. T63 ENGINE - LIGHT OBSERVATION HELICOPTER SAND AND DUST SAMPLING TESTS, conducted for U. S. Army LOH Field Project Office under contracts P.O. 23-204-05-0632T and P.O. 23-204-05-06303T, Allison Division, General Motors Corporation, Indianapolis, Indiana.

UNCLASSIFIED

Security Classification

DOCUMENT CONTROL DATA - R&D

(Security classification of title, body of abstract and indexing annotation must be entered when the overall report is classified)

1 ORIGINATING ACTIVITY (Corporate author)

The Boeing Company, Vertol Division
Philadelphia, Pennsylvania 19142

2a. REPORT SECURITY CLASSIFICATION
Unclassified

2b GROUP
NA

3 REPORT TITLE

A Parametric Study of Swirl Inlet Particle Separators

4. DESCRIPTIVE NOTES (Type of report and inclusive dates)
Phase III, Final Report

5 AUTHOR(S) (Last name, first name, initial)
Darling, Richard

6 REPORT DATE	7a TOTAL NO. OF PAGES	7b NO. OF REFS
February 1968		

8a CONTRACT OR GRANT NO.	9a. ORIGINATOR'S REPORT NUMBER(S)
NOw 66-0562c b. PROJECT NO.	D8-0911
c.	9b OTHER REPORT NO(S) (Any other numbers that may be assigned this report)
d.	NA

10 AVAILABILITY/LIMITATION NOTICES

~~Qualified requesters may obtain copies of this report directly~~ from DDC

THIS DOCUMENT IS SUBJECT TO SPECIAL EXPORT CONTROLS AND EACH TRANSMITTAL TO FOREIGN GOVERNMENTS OR FOREIGN NATIONALS MAY BE MADE ONLY WITH THE PRIOR APPROVAL OF DEPARTMENT OF THE NAVAL AIR SYSTEMS COMMAND

11. SUPPLEMENTARY NOTES	12. SPONSORING MILITARY ACTIVITY
	Naval Air Systems Command, Department of the Navy, Washington, D.C.

13 ABSTRACT

Helicopter turbine engines suffer extensive internal damage from the effects of foreign particles carried into the engine in the intake airstream. Many types of intake filters have already been designed to cope with this problem; however, none is entirely satisfactory. This report describes the investigation of this problem with the goal of producing an inlet particle separator which would be the optimum design for the problem; the resultant design must have high filtration efficiency, low airflow losses, and basic simplicity of concept. The study involved the two-dimensional simulation of the three-dimensional ingestion of particles by an actual inlet. This simulation was performed by using a two-dimensional, electrified inlet configuration in conjunction with a comprehensive computer program. Seven basic inlets were simulated, along with variations of several of the inlets. Various types of particles were represented in the simulation. The two basic trajectory influences were represented by airflow with and without helicopter rotor downwash. Complete procedural steps are given, along with a detailed account of the test results. Positive conclusions and recommendations are given at the end of the report.

DD FORM 1 JAN 64 1473

UNCLASSIFIED

Security Classification

14. KEY WORDS	LINK A		LINK B		LINK C	
	ROLE	WT	ROLE	WT	ROLE	WT
PARAMETRIC STUDY						
SWIRL INLET PARTICLE SEPARATORS						
TWO-DIMENSIONAL SIMULATION						
SEVEN INLET CONFIGURATIONS						
FOUR TYPES OF PARTICLES						
AIRFLOW WITHOUT DOWNWASH						
AIRFLOW WITH DOWNWASH						
PRIMARY FLOW						
SECONDARY FLOW						
BOUNCE PLATE						
INERTIAL SEPARATOR						

INSTRUCTIONS

1. ORIGINATING ACTIVITY: Enter the name and address of the contractor, subcontractor, grantee, Department of Defense activity or other organization *(corporate author)* issuing the report.

2a. REPORT SECURITY CLASSIFICATION: Enter the overall security classification of the report. Indicate whether "Restricted Data" is included. Marking is to be in accordance with appropriate security regulations.

2b. GROUP: Automatic downgrading is specified in DoD Directive 5200.10 and Armed Forces Industrial Manual. Enter the group number. Also, when applicable, show that optional markings have been used for Group 3 and Group 4 as authorized.

3. REPORT TITLE: Enter the complete report title in all capital letters. Titles in all cases should be unclassified. If a meaningful title cannot be selected without classification, show title classification in all capitals in parenthesis immediately following the title.

4. DESCRIPTIVE NOTES: If appropriate, enter the type of report, e.g., interim, progress, summary, annual, or final. Give the inclusive dates when a specific reporting period is covered.

5. AUTHOR(S): Enter the name(s) of author(s) as shown on or in the report. Enter last name, first name, middle initial. If military, show rank and branch of service. The name of the principal author is an absolute minimum requirement.

6. REPORT DATE: Enter the date of the report as day, month, year; or month, year. If more than one date appears on the report, use date of publication.

7a. TOTAL NUMBER OF PAGES: The total page count should follow normal pagination procedures, i.e., enter the number of pages containing information.

7b. NUMBER OF REFERENCES: Enter the total number of references cited in the report.

8a. CONTRACT OR GRANT NUMBER: If appropriate, enter the applicable number of the contract or grant under which the report was written.

8b, 8c, & 8d. PROJECT NUMBER: Enter the appropriate military department identification, such as project number, subproject number, system numbers, task number, etc.

9a. ORIGINATOR'S REPORT NUMBER(S): Enter the official report number by which the document will be identified and controlled by the originating activity. This number must be unique to this report.

9b. OTHER REPORT NUMBER(S): If the report has been assigned any other report numbers *(either by the originator or by the sponsor)*, also enter this number(s).

10. AVAILABILITY/LIMITATION NOTICES: Enter any limitations on further dissemination of the report, other than those imposed by security classification, using standard statements such as:

(1) "Qualified requesters may obtain copies of this report from DDC."

(2) "Foreign announcement and dissemination of this report by DDC is not authorized."

(3) "U. S. Government agencies may obtain copies of this report directly from DDC. Other qualified DDC users shall request through _____."

(4) "U. S. military agencies may obtain copies of this report directly from DDC. Other qualified users shall request through _____."

(5) "All distribution of this report is controlled. Qualified DDC users shall request through _____."

If the report has been furnished to the Office of Technical Services, Department of Commerce, for sale to the public, indicate this fact and enter the price, if known.

11. SUPPLEMENTARY NOTES: Use for additional explanatory notes.

12. SPONSORING MILITARY ACTIVITY: Enter the name of the departmental project office or laboratory sponsoring *(paying for)* the research and development. Include address.

13. ABSTRACT: Enter an abstract giving a brief and factual summary of the document indicative of the report, even though it may also appear elsewhere in the body of the technical report. If additional space is required, a continuation sheet shall be attached.

It is highly desirable that the abstract of classified reports be unclassified. Each paragraph of the abstract shall end with an indication of the military security classification of the information in the paragraph, represented as *(TS), (S), (C), or (U)*

There is no limitation on the length of the abstract. However, the suggested length is from 150 to 225 words.

14. KEY WORDS: Key words are technically meaningful terms or short phrases that characterize a report and may be used as index entries for cataloging the report. Key words must be selected so that no security classification is required. Identifiers, such as equipment model designation, trade name, military project code name, geographic location, may be used as key words but will be followed by an indication of technical context. The assignment of links, rules, and weights is optional.